(1)

AFIT/GSO/ENS/88D-4

USE OF COMMERCIAL SATELLITE IMAGERY FOR SURVEILLANCE OF THE CANADIAN NORTH BY THE CANADIAN ARMED FORCES

THESIS

Robert Chekan, B.Sc.
Major, CAF

AFIT/GSO/ENS/88D-4

AFIT/GSO/ENS/88D-4

USE OF COMMERCIAL SATELLITE IMAGERY FOR SURVEILLANCE OF THE CANADIAN NORTH BY THE CANADIAN ARMED FORCES

THESIS

Presented to the Faculty of the School of Engineering

of the Air Force Institute of Technology

Air University

In Partial Fulfillment of the

Requirement for the Degree of

Master of Science in Space Operations

Robert Chekan, B.Sc.

Major, CAF

November 1988

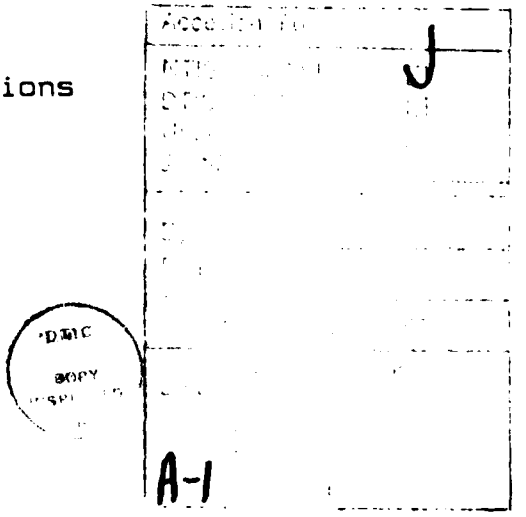

Approved for public release; distribution unlimited

Acknowledgements

A thesis is a remarkable undertaking. I could not have completed this work without the help of the faculty, my friends, and my family.

First I thank my thesis advisor, LtCol Jim Robinson. Your guidance and the freedom you extended to me throughout this research are much appreciated.

Second I thank LtCol Howard Evans who is both an inspiration and a gifted teacher. Much of the credit for the problem solving contained in this thesis is yours. I shall never forget you.

To my friends, how could I have survived without you? I thank Maj Mike Delpinto for ferreting out the many articles you sent my way. I thank Flt Lt Wayne Gale and Capt Alan Sterns for the support, the encouragement, and the constructive criticism you gave me throughout this research.

Last, and most of all, I thank my wife [redacted] who has held our family together and still found time to listen to me explain my latest triumph or defeat. You're the greatest.

Table of Contents

List of Figures

List of Tables

Abstract

This thesis examines the utility of commercial satellite-acquired imagery for the surveillance of the Canadian North. Analytical performance models are developed for visible and thermal wavelength sensors. These models form the basis for evaluation of an individual sensor's potential contribution to surveillance. The mission of surveillance is sectioned into five separate missions. For each mission, sensor system evaluation algorithms, which combine individual sensor's probabilities of detection and tracking, are proposed and optimization techniques identified. Sample algorithms, using a representative target set, are provided for each mission. Analysis shows that the selection of specific sensors is mission and situation specific.

USE OF COMMERCIAL SATELLITE IMAGERY FOR SURVEILLANCE OF THE CANADIAN NORTH BY THE CANADIAN ARMED FORCES

I. Introduction

Background

The first civilian satellite built to observe the earth was the National Aeronautics and Space Administration's (NASA) Earth Resources Technology Satellite launched in 1972. That satellite was later renamed the Land Satellite (Landsat-1) and was the forerunner of a series of remote sensing satellites built and flown by NASA. In 1985 the Landsat system was transferred from NASA to the Earth Observation Satellite Company (EOSAT): a private company formed to market Landsat to the world. The remote sensing of the Earth had become a commercial enterprise.

Interest in providing satellite sensed data for profit is growing. Systeme Probatoire d'Observation de la Terre, or SPOT, joined EOSAT in the remote sensing marketplace in 1986 with the launch of its first satellite, SPOT-1. The following year, in 1987, the Soviet Union began selling photographs taken from its satellites through a commercial organization known as Sojuzkarta. In the near future other

nations plan to build, fly, and market their own systems. Among them are Japan, Canada, India, and a consortium of European nations which participate in the European Space Agency (ESA).

Not only will there be more systems available in the 1990s, but the resolution of the data the systems will provide will be improved. For example, Landsat 5 carries a sensor that achieves a ground resolution of 30 meters. A similar sensor on Landsat 6 will achieve a ground resolution of 15 meters (72:360).

As the resolution of the imaging sensors increases, so does the potential for use of the data by the military for surveillance and reconnaissance. At present SPOT can provide images having a ground resolution of 10 meters. This resolution applies irrespective of whether SPOT is looking at wheat fields or military installations. While military intelligence gathering satellites provide better resolution than does SPOT, there is sufficient detail available on SPOT images to reveal information of military value such as the existence of facilities and tracks made by the gathering of vehicles (21:5). "SPOT's implications are profound because it blurs the distinction between civilian and military observation from space in direct proportion to the clarity of its imagery" (10:326).

Although the trends toward more and better data are clear, the specific military value of data from commercial systems is difficult to ascertain -- difficult since the value of available information is largely determined by comparing it to the information required for a specific mission which can be hard to identify, and difficult since the information requirements for the diversity of modern military missions are equally diverse.

Although there are many responsibilities entrusted to the military, the primary mission of any nation's armed forces is the establishment and enforcement of control over national territory, airspace, and territorial waters. This requires information on the current situation within territorial boundaries, and on potential threats to the nation.

Notwithstanding the fact that the enforcement of sovereignty is a common mission of all militaries and that this requires similar types of information, the magnitude of the task is significantly different for different militaries. Perhaps the military most challenged by this mission is the Canadian Armed Forces (CAF). Canada is the second largest country in the world, covering 9,920,330 square kilometers. Moreover, approximately 90% of its territory is isolated and bears no permanent settlements (13:3). Yet the vast stretches of the Canadian North offer

economic and scientific wealth, and occupy a region of significant strategic importance between the United States and the Soviet Union.

The Canadian North is large and it must be controlled. To attempt to exercise control through permanent stationing of forces throughout the area would be impractical. In contrast, it is reasonable to maintain surveillance of the Canadian North so that forces may be assigned as required.

The task of maintaining surveillance in the arctic is itself a formidable one. However, it is possible that commercial satellite imaging systems may be able to provide data of sufficient quality to support this mission. Therefore, it is appropriate to assess the value of such data in terms of its ability to provide useful surveillance information about the Canadian North to the CAF. Moreover, the imminent proliferation of commercial satellite imaging systems makes this a good time to conduct this assessment.

Problem Statement

In that the Canadian Armed Forces (CAF) requires information concerning current situations and potential threats in the Canadian North, and in that surveillance information derived from satellite imaging sensors will be available from commercial firms, the problem is to determine the value of commercial satellite images to the CAF and to develop a system use strategy for the purchase of images.

Research Questions

The following questions are addressed in this research:

(1) What commercial satellite imaging systems will be potential suppliers for surveillance and reconnaissance data during the 1990s?

(2) What will the system's capabilities be for these potential suppliers? Analysis of system performance will include consideration of system responsiveness and coverage, and will investigate the minimum target size detectable by the system's sensors.

(3) How can commercial satellite images be evaluated?

(4) Can weather satellites detect and track targets of interest?

(5) Will commercial systems require cuing, and will they provide cuing for other reconnaissance resources?

(6) Will a combination of several systems outperform a single system?

(7) How good would an alternate system have to be before it outperforms the best mix of available commercial satellite imaging systems?

(8) How much information on Canadian military activity in the arctic will be available to commercial satellite surveillance data customers?

Scope

The complete assessment of the value of satellite imagery for any application involves the broad areas discussed in the next chapter. However, analysis of all of these areas for detection and tracking of targets in the Canadian North is beyond the scope of this research. Instead, this research concentrates on the development of algorithms which calculate imaging systems' probabilities of detection and tracking targets of interest, on the system wide optimization of these probabilities, and on the validation of the algorithms which are developed.

This is an unclassified thesis. Representative, rather than actual, targets will be used to analyze systems' capabilities.

Assumptions

Simplifying assumptions may be necessary to complete analytical calculations to determine systems' capabilities.

Also, although information could be made available to the CAF from allied military reconnaissance sources, such sources will not be considered as alternative collection options. It is assumed that the CAF is conducting unilateral operations, and for this reason foreign military reconnaissance is either not requested or unavailable.

Research Applications

Although the analysis presented in this thesis is specific to the surveillance of Northern Canada, the algorithms developed in this research could be applied to determine the surveillance value of commercial satellite images of any location.

II. Current Literature

Organization

Many factors are involved in determining the military value of images produced by commercial satellite systems. The problem is that many of the factors are dependent upon each other. For example, the quality of an image and its price are directly related; the better the quality, the higher the price.

To present a coherent picture of these factors, it is helpful to break up this circle of dependencies and discuss segments as if they were independent. In this way the factors contributing to the military value of images produced by commercial satellite systems can be discussed under broad headings. Four such headings are:

(1) the quality of the image;

(2) the timeliness of the image;

(3) the cost of extracting useful information from the image; and

(4) the availability of the image.

The Quality of the Image

The first major factor to consider in determining image value is the quality of the image. System capabilities are commonly reported in terms of resolution. The problem is that there are several types of resolution which can be

identified for satellite systems, and some of those have a variety of measures available. As a result, "Users do not understand the significance of resolution figures quoted, and for many applications significantly overestimate capability" (69:2). To be of practical value, figures given should include the conditions under which the resolution was achieved and can be expected in future. For example, a high resolution system that is pointing at the ocean may not reveal very much, yet the systems capabilities are not at fault. In contrast, the conditions can be chosen to show the system's best capabilities.

A more structured approach to assessing a system's capabilities is to break that system down into its constituent parts and to handle the parts separately. This sectioning accomplishes two things: it reduces the complexity of the analysis to a manageable level, and it highlights the actual conditions under which the system is being assessed. In this regard remote sensing models commonly consist of three elements: the scene model, or that which is being looked at, the model representing the medium through which electro-magnetic energy travels from the scene to the sensor, and the sensor model (68:123).

Scene Modeling. The scene model is made up of the description of the features within the field of view of a

sensor. These features can be fully described by their spatial, temporal, and spectral characteristics.

Spatial characteristics describe the physical dimensions of features and where they are in the scene. Colwell writes that the spatial composition of a scene can range from simple to complex, and has vegetation, soil, geological, hydrological, and geographical components (19:81). Notwithstanding this complexity, the scene should be described as completely as possible since the actual resolution achieved by a system is strongly scene dependent (50:4).

The temporal characteristics of a scene describe how the scene changes over time and are strongly research dependent. For example, if remote sensing imagery is to be used to map stable geological formations, the scene can be characterized as displaying little change through time. In contrast, using imagery to track drift ice involves a scene that changes continuously through time. Colwell emphasizes this point since the temporal characteristics of a scene will determine whether one requires a single look at an area, or whether images are required frequently (19:86).

The third set of characteristics of a scene model describes the spectral properties of features in the scene. Spectral here refers to the electro-magnetic spectrum. In effect the features within the field of view of the sensor

reflect and emit radiant energy. They reflect energy according to their reflectivity, and emit energy according to their temperature and emissivity.

In addition to energy reflected and emitted by objects in the scene, a third factor should be included during spectral analysis, that of the transmitting medium which lies between the scene and the sensor. Clearly this medium is also in the field of view of the sensor. Therefore, its reflectivity and emittance must be taken into consideration (5:1264).

Atmospheric Modeling. The second element of a remote sensing model represents the medium between the scene and the sensor. For satellite remote sensors that medium is the Earth's atmosphere.

The atmosphere interacts with electro-magnetic radiation in a variety of ways. However, the two most important of these interactions are scattering and absorption. These interactions are important since they do not affect all wavelengths of radiation equally. For example, "windows" exist for some wavelengths. These are specific regions of the spectrum for which the atmosphere is essentially transparent (11:34). On the other hand, there are wavelengths that are strongly attenuated. As a result the distance travelled through the atmosphere by the electro-magnetic energy is important.

In addition to accounting for scattering and absorption, an atmospheric model should consider obscuring phenomena such as clouds, and whether the obscuration is rare or persistent (19:86).

Sensor Modeling. The third element of a remote sensing model is the sensor model. Although imaging sensors on board commercial satellites can be complex in design and operation, they can nonetheless be placed into two general design categories: radiometers, and synthetic aperture radars. This first section of sensor modelling considerations briefly explains the operating principles and how resolutions are determined for each sensor category. The second section shows trends in sensor systems. For a review of current and planned sensor suites, see Appendix A.

Radiometers. A radiometer focuses radiant energy from everything within its field of view onto a detector array. This "image" is then preserved directly on film or is converted into a digital signal for subsequent transmission to a receiving site. In the case of digital signals, an image is produced by lining up the individual picture elements, or pixels, a process which in effect reconstructs the original scene, square by square (33:25).

If the detector array is film, the problem remains as to how to transport the information contained on the film back to the Earth. To do this, the film is either scanned

by a second sensor and the information converted into a digital signal as described above, or a canister containing the film is jettisoned from the satellite and recovered on Earth.

Radiometer Resolution. Radiometer resolution is described by Jensen as being characterized under four general headings: spectral, radiometric, temporal, and spatial (41:4).

The spectral resolution of a radiometer identifies the portions of the electro-magnetic spectrum to which the instrument is sensitive. Commonly imaging radiometers are sensitive to visible and near infrared radiation. For example, the High Resolution Visible (HRV) radiometers operating on the SPOT satellite collect visible wavelength radiation in four channels or bands, .5-.59 μm, .61-.68 μm, .79-.89 μm, and .51-.73 μm (20:495). This defines the spectral resolution of the HRV.

The radiometric resolution of a sensor is its ability to record many levels of brightness in its images (11:224). Although this concept can be applied to film it is more important in systems that digitize their information for transmission to Earth. In such systems, levels of brightness are recorded as discrete values only. Depending on the system there are typically 64, 128, or 256 values for brightness available for each pixel. While 64 levels of

brightness may appear to limit the system only slightly, this limitation nonetheless introduces errors in the image.

A system's temporal resolution is a measure of how often it images a given area of interest (41:5). Full discussion of temporal resolution is presented in the review of image timeliness.

The final measure of resolution, spatial resolution, is both the most important for consideration and the most complex for discussion. The complexity arises not in the concept, since spatial resolution is basically a measure of the smallest linear separation between two objects that can be resolved (41:4). The complexity arises since there are four different ways to determine and report spatial resolution (69:3).

While each of the four ways carries its own advantages and disadvantages, they all share one limitation. That limitation is that their ability to resolve objects is calculated for objects that are equally intense and distinct from the background. In fact a system's resolution is maximized under such conditions. Under conditions of moderate contrast, actual resolutions can be expected to be considerably less (69:8).

One way to calculate spatial resolution is to consider only the geometry of the system. By this method, the instantaneous field of view (IFOV) is determined by taking

the product of the range to the target and the detector size, and dividing this product by the focal length of the optics. This equation is shown below.

$$IFOV = \frac{Rd}{f} \qquad (1)$$

Where IFOV = instantaneous field of view
R = range to target surface
d = individual detector size
f = focal length

This calculates the nominal ground resolution cell, or the area seen by a single detector in the array. If two objects in the scene fall within a single ground resolution cell, the sensor will record a single target, so the objects will not be resolved.

The problem with IFOV calculations is that there are several factors which degrade this ideal capability. Fusco and Hsu have reported that actual Landsat Thematic Mapper (TM) data spatial resolution is between 40 and 50 meters, in contrast to the 30 meter IFOV (30:161). They attribute the difference to non-sensor factors including geometric re-sampling and atmospheric effects. Watkins and Thormodsgard report similar effective instantaneous fields of view (EIFOV) and attribute the degradation to the sensor optics. However, they argue that correction for the optics can

restore the actual resolution to values very near those predicted by the IFOV (71:225).

Again, contrast must be considered. The contrast ratio is defined as the ratio of maximum irradiance received in an image to the minimum irradiance received (64:206). Jasani reports that in a scene in which the contrast ratio is 2:1, the actual spatial resolution achieved is approximately 2.0 to 2.4 times the IFOV. It is not until the contrast ratio reaches 1000:1 that this factor is reduced to 1.4 times the IFOV (39:10).

Synthetic Aperture Radar. In contrast to a passive radiometer, which relies on detection of electromagnetic radiation originating from an external source, synthetic aperture radars (SAR) are active devices which send out pulses of energy and build an image based on the energy reflected from the scene. The advantage of a SAR is that it can acquire surface imagery anytime of the day or night irrespective of the surface solar irradiance or cloud cover (26:641).

The basic principles for SARs are similar to those of conventional radars and directly affect SAR resolution.

SAR Resolution. Radars determine the range to a target by timing how long a pulse takes to return to the antenna. It is important to note that the pulse of energy that is being sent out does not go out instantaneously, but

requires time to send. As a result, a return received at a time, T1, may be energy contained in the initial part of the pulse that was reflected from a maximum range, energy contained in the last part of the pulse that was reflected by a nearby feature in the scene, or some combination of time and distance in between these extremes. Thus the range resolution is determined by the time it takes to send the pulse, or pulse length of the outgoing signal. Equation 2 shows the relationship between pulse length and range resolution (29:182).

$$\text{delta } R = \frac{c\,\tau}{2\,\sin(\emptyset)} \qquad (2)$$

Where delta R = range resolution
c = speed of light
τ = pulse length
$\emptyset$ = depression angle

The bearing to a target, or azimuth, is determined by recording the direction in which the antenna is pointing at the time of the return of the energy. The problem is that all of the energy that is sent out is not found on a line drawn normal to the center of the antenna, but is distributed around that line. The better the concentration of the energy, the finer is the beam, and the greater is the azimuthal resolution of the radar.

Two things control a radar's azimuthal resolution: it is directly proportional to the wavelength of the energy sent out, and inversely proportional to the diameter of the radar antenna (33:29).

$$Ra = \frac{.7\ S\ \lambda}{D} \qquad (3)$$

Where Ra = width of the beam
S = slant range to the target
λ = wavelength of radar
D = diameter of the antenna

To improve Ra, two options exist: to increase the size of the antenna, or to decrease the wavelength of the radar. There are practical limitations to each of these options (33:30). However, it is possible to emulate the performance of an antenna larger than the actual antenna. This is accomplished by illuminating a target with more than one pulse of radar energy as the aircraft or spacecraft travels along its track, and storing the amplitude and phase of the returns from each pulse. These returns can then be combined to provide azimuthal resolution equal to that achievable by an antenna as long as the full path flown by the platform while the target was being illuminated. In the limit this resolution is not dependent upon range to the target (33:30). This is true because of the geometry involved. As

the range increases, the length of the synthetic aperture also increases since the target will be illuminated sooner and for a longer period of time. At its best the finest azimuthal resolution of a SAR is half the length of the actual aperture of the radar (33:30).

$$Ra = \frac{L}{2} \qquad (4)$$

Where Ra = azimuthal resolution
L = length of the actual radar aperture

This best resolution is not always sought since it maximizes the processing required for imaging, which in turn decreases the number of images that can be acquired. In practice only a portion of the available path is used.

Sensor Trends. The first important trend in sensors is that there will be more commercial sensors flying in the future. By the mid-1990s images may be available from eight or more systems. Planned imaging satellites are described in Appendix A, and shown in Figure 1.

A second important trend in sensors is that in spite of speculation that higher resolution sensors will be employed on platforms in the 1990s, published plans are to orbit sensors with resolutions similar to those that are available now. For example, Landsat reports a spatial resolution of

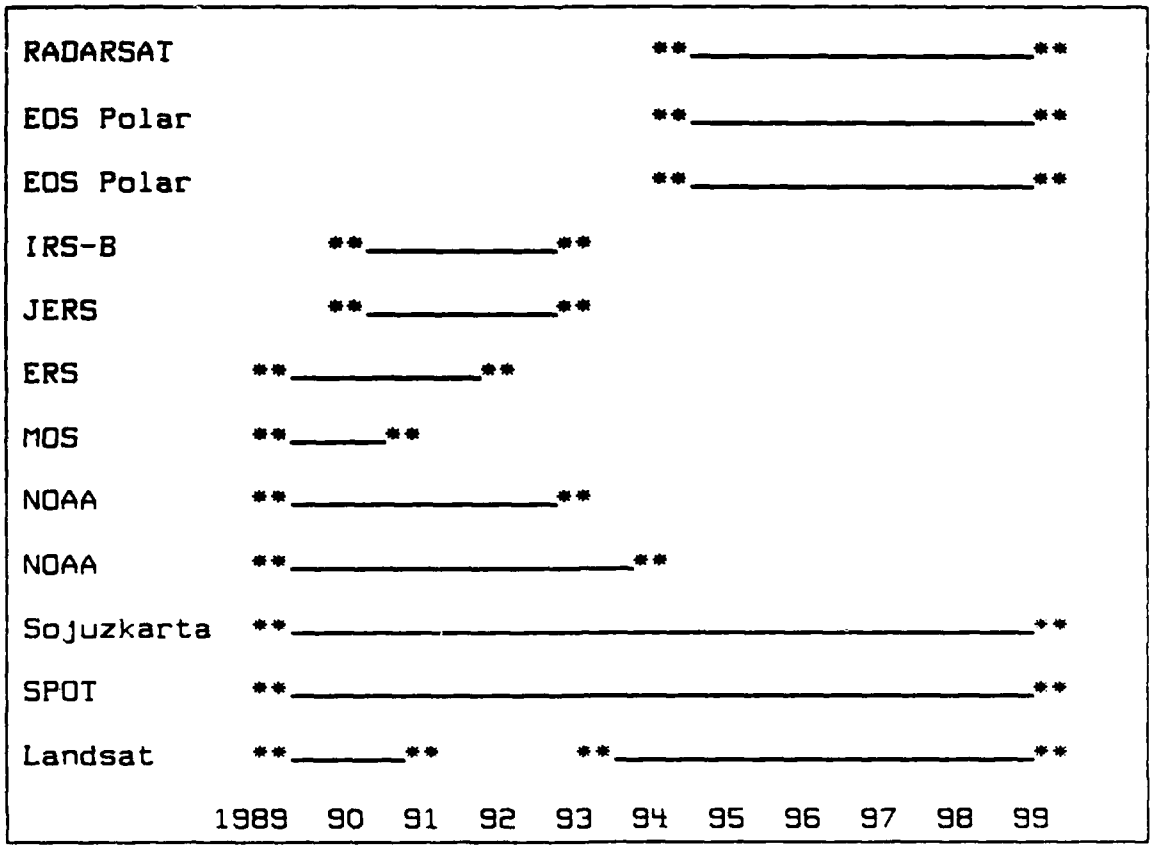

Figure 1. Commercial Satellite Imaging Systems

30 meters for its thematic mapper. SPOT's radiometers yield a 10 meter spatial resolution when operating in the panchromatic, or across all color, mode. Sojuzkarta, the Soviet Union's marketing agency for satellite acquired images, boasts an average of 5 meter spatial resolution for its highest resolution photographs (43:358).

A third important trend in sensors is that there will be more SARs in the future. The first civilian SAR was SEASAT, launched in 1978. Since then several SARs have been flown on the shuttle. By the mid-1990s there may be three

imaging SARs, one each on the Canadian radar satellite (RADARSAT), the European Space Agency's Earth resources satellite (ERS-2), and the follow-on to the Japanese Earth resources satellite (JERS-1).

Summary of Image Quality

In summary, image quality depends on the scene, the atmosphere, and the sensor. The variety of components contributing to the overall quality of the image is shown in Figure 2.

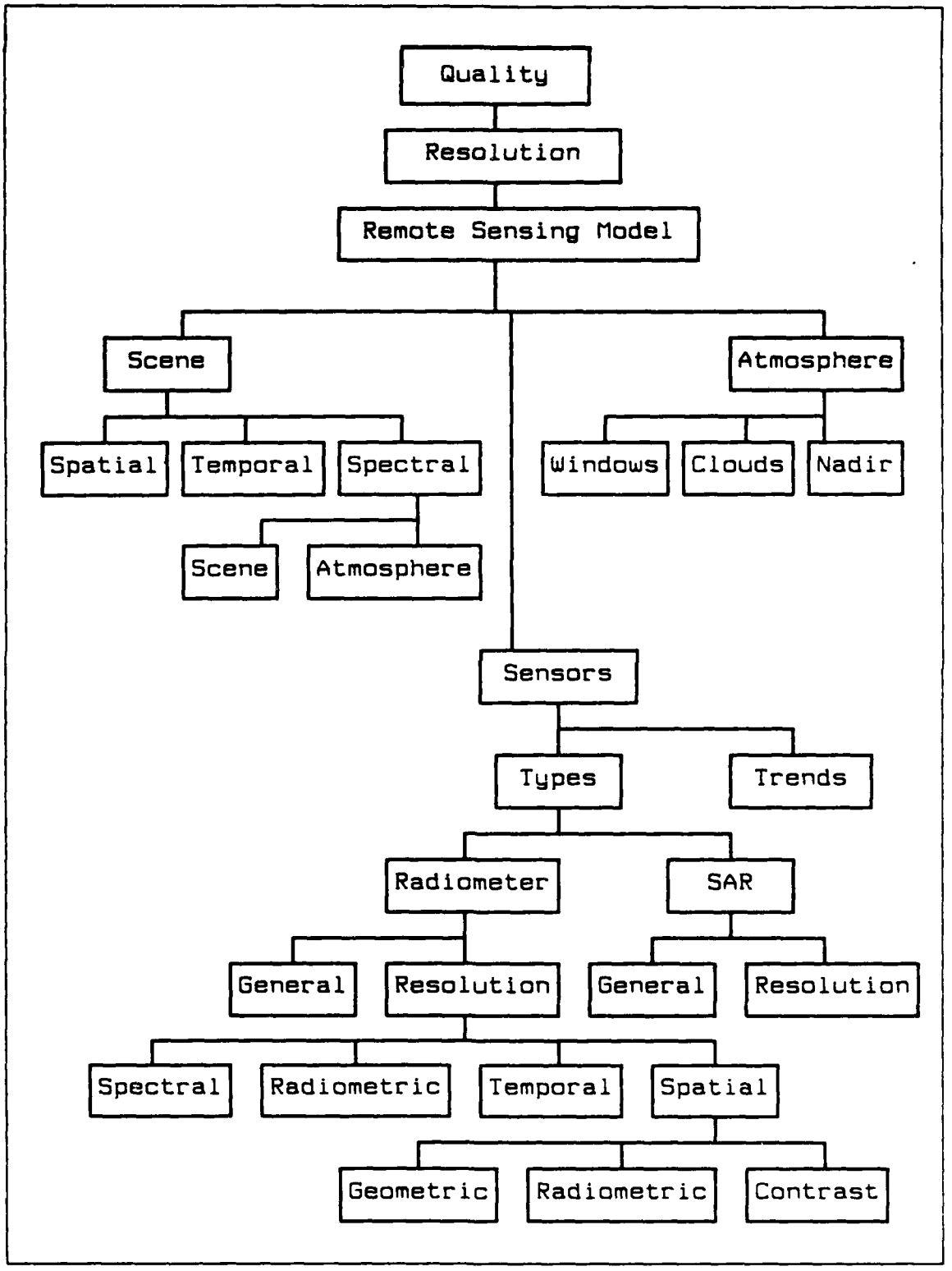

Figure 2. Components Contributing to Image Quality

The Timeliness of the Image

The second major factor to be considered in determining image utility is the timeliness with which the image is received. Not surprisingly timeliness can be divided into several parts: the time it takes a system to acquire the image, the time it takes to relay that image to the Earth, and the time it takes to process and deliver the image.

Image Acquisition. The time it takes a system to acquire an image of a specific target depends on how quickly the system can be tasked to provide the image, and on how quickly the system can respond to the tasking and position a sensor within range of the target.

Tasking a system can take time, particularly if an exchange of documents and contracts is required prior to acceptance of the tasking. Once the tasking is accepted, additional time may be needed to re-program the sensor.

System responsiveness to a tasking is determined by the sensors on board and the orbit of the satellite. Considering the sensors first, the primary feature which governs responsiveness is whether the sensor is fixed or able to be pointed. For example, the HRVs on SPOT can collect data from up to 27 degrees either side of the satellite ground trace. This reduces the maximum time to re-visit a target from 26 to 5 days (20:496).

The satellite's orbit is also important in assessing responsiveness. Harris points out that there is a tradeoff involved between the spatial and temporal resolutions of a system (33:49). This occurs since higher resolution for a fixed detector array requires a lower altitude. Selection of a lower altitude means that the sensor will see a smaller area, or swath, on each pass. If a smaller swath is observed on each pass, it will take longer to image the entire surface of interest, and in turn it will take longer to re-visit a specific area.

Relay Time. The time it takes to relay the image to Earth depends on the system strategy for that relay. Three relay strategies are common: direct transmission, delayed transmission, and hard copy recovery.

Direct transmission is possible if the sensor produces a digital signal representing the image and is in range of either a relay platform or a ground receiving station. The delay introduced by this strategy is measured in fractions of a second and is not significant overall.

Delayed transmission is used if the image can be stored electronically and if the sensor is not in range of either a ground station or a relay satellite. The delay introduced by this strategy is measured in minutes since typical orbit periods for imaging satellites are about 100 minutes.

To recover a hard copy of the image on Earth is the most time consuming strategy of the three. This involves de-orbiting a film canister and can introduce delays measured in months.

Processing Time. The time required to process data depends on the information needed from it. Processing options and their costs are presented in the following discussion.

Summary of Image Timeliness

The components that contribute to the time it takes to receive an image are summarized in Figure 3.

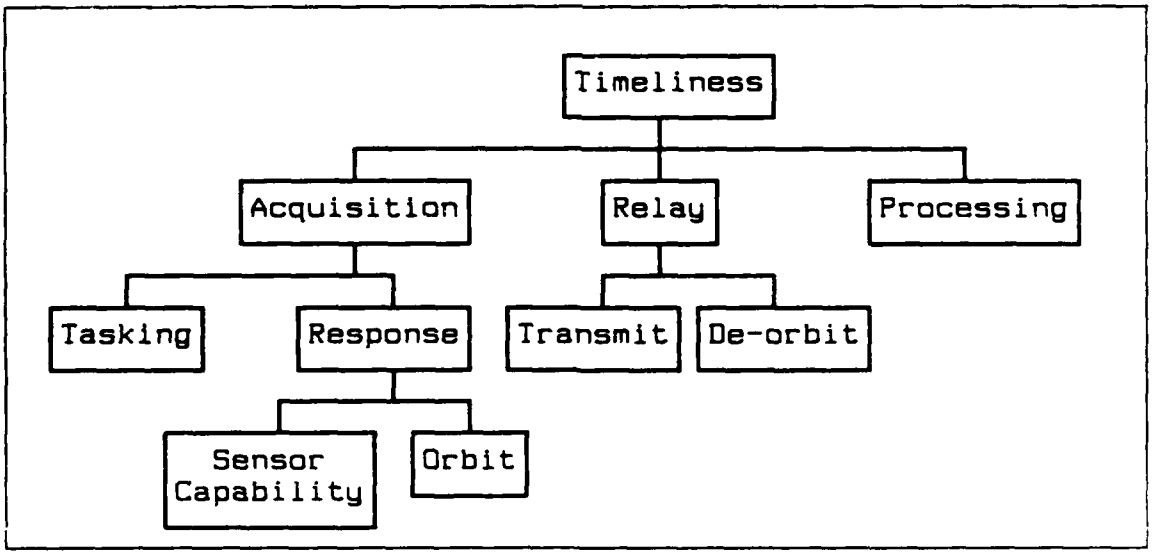

Figure 3. Components Contributing to Image Timeliness

The Cost of Extracting Useful Information from the Image

The third major factor to consider in determining image utility is the cost of extracting useful information from the image. This section of the literature review defines useful information, the data processing options that are available to assist in information extraction, and the cost in time and money of those data processing options.

Useful Information. The usefulness of information can be determined by comparing the information available to that required. As noted earlier, the information required is determined by the specific mission. Here that mission is surveillance.

Surveillance is defined in general terms as watch keeping. For the military, to effect surveillance is to detect, identify, and track objects of interest. As a consequence of this definition, for information to have surveillance value, it must contribute to the detection, identification, or tracking of objects of interest.

Objects of Interest. Objects of interest are easily defined. In writing on the requirements for real time information, Allen points out that if information is needed in real time, it must be because the situation is changing. If the situation is changing, the objects of interest must be moving. Based on this logic, he proffers a list of targets which includes tanks, trucks, missiles, guns,

troops, ships, boats, and aircraft (2:145). A similar definition of objects of interest in the Canadian North has been made by a Canadian Government interdepartmental task force. Their report defines fishing boats, survey parties on land or ice, base camps on land or ice, drift stations on ice, and all ships as objects of interest (14:112-123).

Detection. The first task in surveillance is to find, or detect an object of interest. Campbell defines detection as determining the presence or absence of features (11:87). However, this definition closely resembles the definition of identification. To prevent confusion in this analysis, detection is used to mean finding differences in the scene. In contrast, identification is used to mean determining what caused those differences.

Finding differences in a scene can be approached in two ways. The first way is to analyze a single scene to find features that are distinct from the background. This is detection based on the spatial characteristics of the scene. The second way is to look for changes in two or more images of the same scene taken at different times. This is change detection based on the temporal characteristics of the scene (41:234).

Detection may not be a straightforward task. Hord writes that resolution and detection are not the same thing. For example, a radar may detect an object much smaller than

its ground resolution cell if the object reflects sufficient energy back to the antenna (35:39). Similarly, a small bright source may send out sufficient energy to raise the overall response of a passive detector, and thus be detected. In each case, "sufficient energy" is determined by the amount of signal, or energy from the scene, and the amount of the noise, which is the current generated in the detector by everything but the scene being imaged. If the signal-to-noise ratio is high enough, approximately 3:1 or better, the target can be considered detectable (29:12).

Change detection involves the comparison of two images of a scene. This comparison can be made before or after feature identification and classification have been done. If a comparison is made before classification, two techniques are common: image differencing and image ratioing. In image differencing, the first image is subtracted from the second and a constant brightness is added back in to accommodate negative values. In image ratioing the brightness value for each pixel at time 1 is divided by its brightness value at time 2. For both of these algorithms the interpreter must decide what the threshold level is above which a pixel is considered to have changed (41:234-254).

Identification. Although detection of an anomaly is an important part of surveillance, the heart of the mission is

identifying the cause of the anomaly. In civilian applications the task of identifying features is referred to as classification, and necessarily preceeds the counting, measuring, and delineation of features (11:87). Very often this is accomplished by investigating small portions of the scene in situ, selecting typical objects which can be easily located in the satellite image, and then comparing elements in the image to the reference objects whose distribution of characteristics is known (68:128). The other option is to build a "Canopy" model based on radiative transfer theory. Such models are usually validated by comparing predicted and actual values of reflected and emitted radiation (68:130).

The issue of resolution re-appears at this point. Some authors argue that identification requires higher resolution than does detection (24:50). Others report that too high a resolution can cause errors in classification if the IFOV captures individual differences within a population (19:115). When this occurs some members of the population could be classified incorrectly.

Although seemingly otherwise, these two approaches are in agreement. This is true since authors interested in small feature identification are united in their insistence on the requirement for high resolution systems, while low resolution systems are supported by authors interested in large scale land use classification studies. Colwell

confirms that selection of a high or low resolution system depends on the specific study being conducted (19:117).

Specific to small feature identification, it is important to consider the interplay of resolution and identification. Jasani provides a very good discussion and illustration of this interplay (39:11-16). In short, the better the resolution the more specific the identification.

Jensen states that for identification the spatial resolution of a system should be less than half the smallest dimension of the feature. Even at that he cautions that identification is not guaranteed if the feature has the same spectral response as does its background (41:5). Representative spatial resolutions required to detect and identify common military targets are provided by Jasani and are reproduced in Table 1. However, Doyle cautions that the origin of the numbers is unclear and the contrast conditions in the scene unreported (24:50).

Tracking. To track an object is to maintain a record of where that object has been. Although it is often given as the third task in surveillance, tracking does not necessarily follow identification. In fact, tracking of unidentified objects is a common occurrence in any surveillance system, and often occupies the time between detection and identification of the object.

Table 1. Surveillance Resolution Required (meters)

Objects	Detection	Identification	Description
Aircraft	4.6	1.5	0.15
Airports	6.0	4.6	0.3
Ports/Harbors	30.5	15.0	3.0
Bridges	6.0	4.6	0.9
Ships	7.6	4.6	0.3
Subs on Surface	30.5	6.0	0.9
Troops	6.0	2.0	0.3

Source: (39:15)

Whether or not identification has occurred is important since the tracking of identified and unidentified objects can be considerably different. Tracking of identified objects can be through periodic contact with them, with the frequency of contact depending on the importance of the object and the object's relative velocity in the scene. In contrast, tracking of unidentified objects requires contact often enough to ensure that the same object is being detected each time a contact is made. Again, the object's velocity relative to the fixed elements in the scene will affect the frequency of detections required.

Data Processing. Having defined useful information, the information on hand can be evaluated through comparison. This is straightforward except for one thing; the information on hand is not static--it can be processed to

facilitate information extraction. For convenience, processing is divided into three categories: pre-processing, image enhancement, and image classification.

Pre-Processing. Pre-processing is also referred to as image rectification and restoration, and is commonly undertaken by the system prior to delivery of the image to the customer. Pre-processing seeks to accomplish three things: to correct for geometric distortions, to correct for radiometric distortions, and to eliminate noise (48:611).

Geometric distortions in the image are the result of both systematic and non-systematic effects. Systematic effects include panoramic distortions, the distortion introduced by the motion of the sensor as it passes over the scene, and the distortion introduced by the motion of the scene itself due to the rotation of the Earth. Systematic distortions are well understood and predictable, and can be corrected by using appropriate algorithms. In contrast, non-systematic distortions, such as small changes in the platform's altitude or attitude (41:102), are not predictable. However, non-systematic distortions can be corrected by cross-referencing the image to well-known ground points (48:614).

Radiometric distortions arise as a result of differences in scene irradiation and errors in the sensor operation (11:245). To correct for differences in scene

irradiation, the relative position of the sun is determined and the brightnesses recorded are adjusted or normalized in each image acquired. In contrast, sensor performance is modelled radiometrically both before flight and during flight so that a standard correction can be applied to all images. Prior to launch, sensor performance is determined by irradiating the detector array with a uniform light source. The responses of individual detectors are recorded and used to correct subsequent images. Similarly, during flight, absolute calibration of sensors can be determined by presenting a standard target to the sensor. For example, in March 1986, the HRV cameras on SPOT-1 were aimed at a test ground site at White Sands, New Mexico. Comparison of the brightnesses recorded by the HRVs to those recorded by the ground site and an helicopter borne radiometer provided data for absolute calibration (6:66-76).

Noise, as noted earlier, is false information that is inserted into the image either by unwanted photons or by the sensor's electronics. An important source of unwanted photons is atmospheric scattering and absorption. An approximation of these effects, and therefore correction for them, is possible since near infrared radiation is not strongly scattered or absorbed by the atmosphere (41:97). In the sensor's electronics, although noise is random, individual detectors may report characteristic levels of

noise. A comparison of the responses of detectors and their neighbors can identify individual differences (11:277).

Image Enhancement. The goal of image enhancement is to increase the visual distinction between features in a scene. Therefore, image enhancement carries with it the implication that information extraction is to be completed manually, using the human eye as the final sensor. There are four general techniques used to effect image enhancement: contrast manipulation, spatial feature manipulation, edge enhancement, and multi-imaging manipulation.

Contrast manipulation involves the selective display of only those pixels that have specific values of brightness. Two examples of contrast manipulation are grey level thresholding and level splicing. In grey level thresholding the analyst specifies that only pixels having a brightness value higher than a threshold value will be displayed. In level splicing the analyst selects brightness groupings and specifies that all pixels having brightness levels within the group's range will be displayed as having the same brightness (48:627).

The spatial frequency of an image is defined as "the number of changes in brightness value per unit distance for any particular part of the image" (41:138). In spatial feature manipulation a filter is used to emphasize some

features and de-emphasize others based on their frequency of occurrence. For example, one low pass filter algorithm averages the brightness values for a three-by-three block of pixels and replaces the center pixel brightness value with that average. In contrast, a high pass filter subtracts the low pass filtered brightness value from the original brightness value. The effect is that low pass filters preserve details which occur infrequently in the image but reduce the display of high frequency features, while high pass filters accomplish the opposite (48:637).

The third general technique used in image enhancement is edge enhancement. Edge enhancement operations sharpen the edges of some features by comparing neighboring pixels and adjusting the brightness values in these pixels once a threshold of difference has been reached (11:282). The threshold is specified by the analyst. This produces greater contrast for the eye and can make features more prominent and easier to analyze (41:144).

The last general technique for image enhancement discussed here is multi-image manipulation. Multi-image manipulation does not involve comparison of two images of the same scene taken at different times. It refers to the comparison of the simultaneous response of one spectral band of the radiometer to another (48:650). This comparison is made by dividing the brightness recorded in one band by that

recorded in the other, pixel by pixel, throughout the image. Thus the ratio of one band response to the other is obtained. Although selection of the bands for comparison is largely trial and error, ratioing has been useful in reducing differences caused by topography, shadows, and seasonal variations in surface irradiation (41:135).

Image Classification. Image classification, as defined earlier, is the identification of features in a scene. Automated image classification is the identification of scene features using pattern recognition rules that compare the features in a scene to a reference set of spatial and spectral characteristics (48:688).

Cost. The extraction of useful information from an image begins with receipt of the image and may require use of the techniques described above. Clearly, once an image has been processed sufficiently to allow for information extraction, the processing need not be continued. At that point the cost of the information, in both money and time, can be determined.

The information cost in dollars is dependent upon both the specific system tasked to provide the image, and the data processing techniques that may have been used to extract the information. Taken together these costs should be evaluated using normal standards of cost effectiveness and in full consideration of the alternatives (15:47).

The information cost in time is again system and processing dependent. However, it is taking less and less time to process images. In the extreme, five hours of operation of a SAR on a shuttle flight required one year of analysis (40:14). In contrast, the ESA ERS-1 SAR plans to be able to provide fast delivery data within three hours of scene irradiation (25:537). Moreover, Bernstein predicts that near-real-time distribution of information will be available in the future because of on-board processing (7:74).

Summary

In summary, useful information is information that is needed to detect, identify, and track objects of interest. Such information may be embedded in an image and require further processing to be extracted. Overall, the processing of data contributes to its value but also increases both the time required to extract the information and the cost. The elements contributing to the cost of extracting information are summarized in Figure 4.

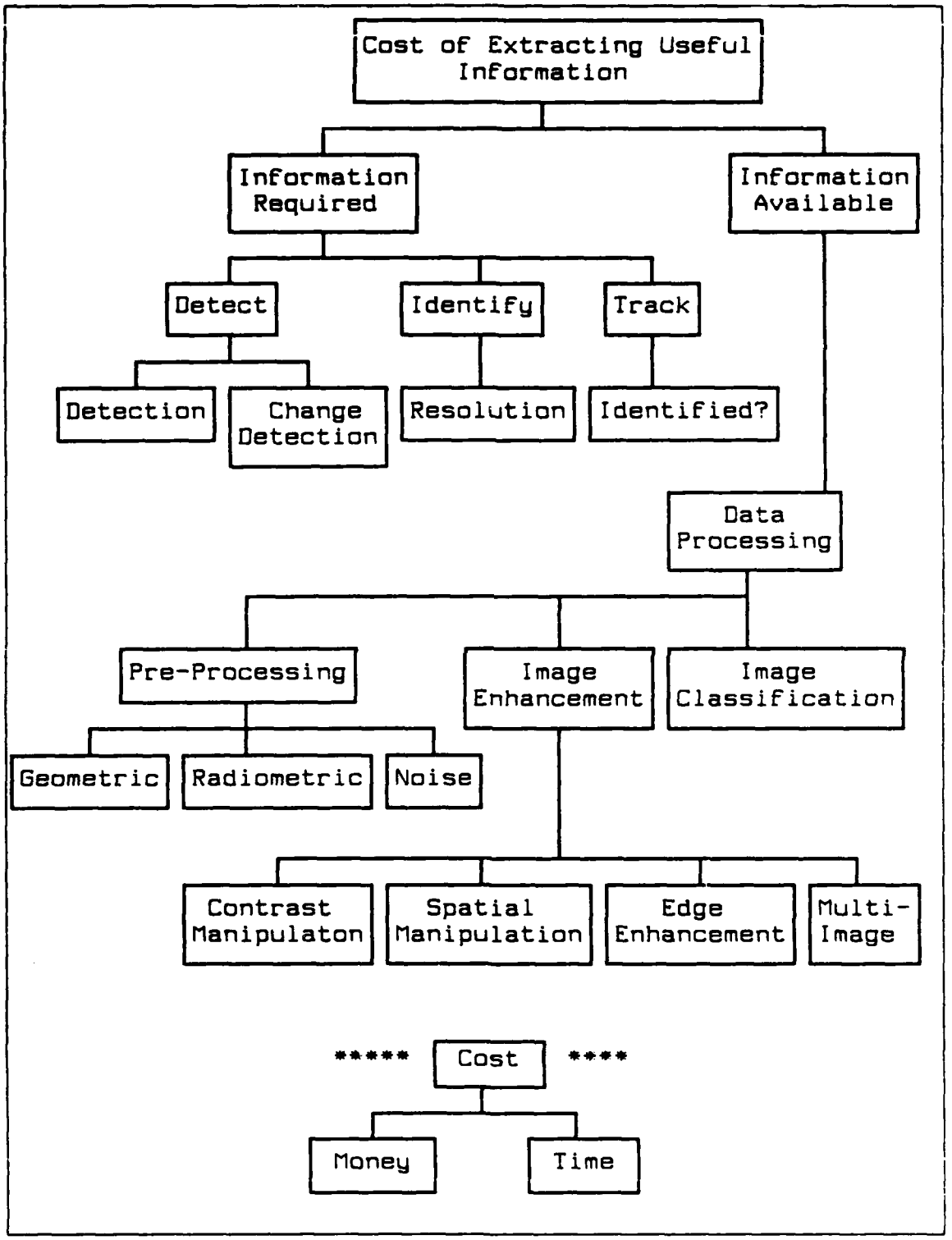

Figure 4. Components Contributing to the Cost of Extracting Useful Information

The Availability of the Image

"The passage of a satellite from the space above one country to that above another requires no visa, and technology has made obsolete the concept of complete national privacy" (54:35). However, there are many things that could restrict the availability of images. Thus the fourth major factor to consider in determining the utility of images is the availability of those images.

First is the issue of national security. McElroy writes that one reason for the early support of weather satellite data was that their relatively coarse resolution aroused no concerns about national security. However, concern is increasing as resolution improves and systems become good enough to monitor military formations and movements (54:35,38).

Second is the issue of access. Given that data has been gathered and information extracted from it, who should have access to this information? A resolution adopted by the United Nations General Assembly in January, 1987, provides guidelines for access that include the promotion of co-operation and mandatory passage of information to affected states in the case of impending natural disasters. However, the resolution does not address two situations of concern to many developing nations: that information of military or economic value could receive wide distribution

(40:15), or that system access could be restricted due to military alliances (54:35).

Third is the issue of cost. Notwithstanding the provisions of the United Nations resolution mentioned above, which calls for availability at reasonable cost, it is possible that only affluent nations will be able to afford satellite-acquired remote sensing information (54:36).

Fourth is the issue of denial. Denial of access to a system's data could occur because of changes made unilaterally by the owner, or through total shut down of a system should it be economically inviable (54:36). In either situation, an investment such as a ground receiving station could be rendered useless.

Fifth is the issue of risk to the sensor. Sloup notes that since the military reconnaissance satellites used by the superpowers are considerably more powerful than are current remote sensing satellites, that superpower interest will likely be in keeping track of what others learn through such data (66:80). Given the inherent vulnerability of satellite sensors (67:58), and given that laser interference with satellites is possible and may have already occurred (10:281), intentional dazzling of commercial imaging satellites is possible.

Sixth is the issue of how many of the projected systems will actually be launched. Jasani and Creasey state that

current data processing and telecommunications markets are barely sufficient to support the cost of the current range of products (40:15). Future systems that will rely on commercial income may not find a market.

Seventh is the issue of legalities. Sloup notes that customary law has established that space reconnaissance is legal as long as it relates to self-defense (66:79). However, several authors suggest that while this is true of passive sensors, there is an element of intrusion involved in active sensors and that this issue has yet to be resolved (61:25, 54:38).

Eighth is the issue of delay, for it may be sufficient to delay provision of information to invalidate it. "For perishable data, delay is as bad as denial" (54:35).

Summary

The issues contributing to the availability of satellite images are summarized in Figure 5.

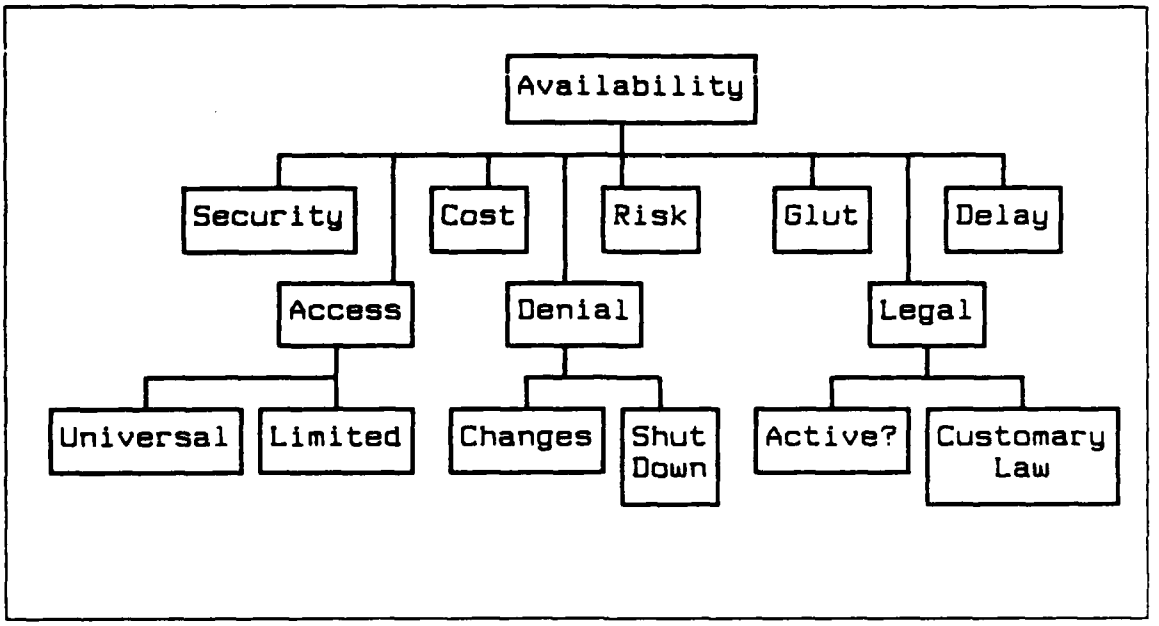

Figure 5. Components Contributing to Image Availability

III. Methodology

The review of current literature shows the many components involved in the evaluation of remote sensing imagery. Although an in-depth analysis of all of these areas is necessary to fully evaluate satellite imagery, it is not possible in the time available to complete this research. For this reason, this analysis is limited to the evaluation of commercial satellite systems' abilities to detect and track objects of interest.

Sensor Performance Evaluation

The first question to resolve is whether a sensor can distinguish an object of interest from its background. Thus, Chapter IV develops a method to determine the probability that a sensor will detect a target.

Algorithm Development

The second question to resolve is how does the sensor compare to others that are available. Since all the systems sell their information, the evaluation of their relative worth is based on the information they can provide and on the cost of that information. Thus, Chapter V develops algorithms to compare systems' costs and information performances and identifies techniques to select the best mix of sensors from those that are available.

Analysis

The third question to resolve is whether the algorithms that are developed are valid. Although the quality of any analysis depends on how good the database is, developing actual models using representative targets is a way to investigate the face validity of the algorithms proposed in Chapter V. Therefore, Chapter VI tests the optimization algorithms by building example analyses.

IV. Sensor Performance Evaluation

General

Whether a sensor distinguishes a target from its background depends on the sensor, the target, and the background. In simple terms, it is all a matter of energy since it is the collection of the energy which elicits the response (signal) from the sensor. Current satellite-borne sensors distinguish a target from its background, or detect a target, by collecting the visible wavelength energy that the target reflects, or by collecting the infrared wavelength energy that the target emits. Since reflection and emission are different phenomena, separate analysis is required to determine target detection probabilities for visible and thermal wavelength sensors.

Each evaluation of sensor performance begins with analysis of the sensor under ideal conditions. Ideal conditions means that the target is fully in view of a single detector in the sensor's detector array. Additional complexity is added to the analysis once the ideal case has been completed.

Although visible and thermal wavelength sensors are different, they share several performance degrading phenomena. For example, both are prevented from imaging a target on the ground if there are clouds in the target area.

Since this is true, a single discussion of how cloud cover is accounted for in an analysis is enough. For this reason the discussion of common degrading phenomena is presented after that which describes the evaluation of sensors under ideal conditions, and only once.

In short, the topics covered in this chapter are:

(1) Visible Sensor Analysis -- Ideal Conditions;

(2) Thermal Sensor Analysis -- Ideal Conditions;

(3) Non-Ideal Considerations; and

(4) Obscuring Phenomena.

Visible Sensor Analysis - Ideal Conditions

Visible sensors are sensitive to radiation in the visible wavelength band, which is approximately .4 -.7 μm. Assuming that the target itself is not a source of visible light, detection of a target depends on the collection of solar energy reflected by the target. Since the target and its background receive the same solar irradiance, they will reflect different amounts of energy to the sensor if their reflectances are different. If this difference is large enough, the target is detected.

An implicit definition has been made here which is important for the remainder of this analysis. It is that "detection" is used to mean the distinction of the target from its background in the spatial domain.

One measure of a visible wavelength sensor's sensitivity is its noise equivalent reflectance difference, or NERD. This is the difference between the target and background reflectances which is just detectable given the target entirely fills a ground resolution cell, the target and background cells are receiving equal irradiance, and there is no atmospheric attenuation between the scene and the sensor. The NERD corresponds to a signal-to-noise ratio of 1 under conditions of minimum scene irradiance (62:405).

Detection depends on target size and reflectance difference with respect to the background. A target which is at least as large as the sensor's ground resolution cell, and having a reflectance difference of the sensor's NERD or more will be detected under ideal conditions. Similarly, a smaller target having a large enough reflectance difference will also be detected. The threshold for detection is that combination of target size and reflectance difference which just corresponds to the sensor's NERD.

The relationship for threshold detection is geometric and is derived by comparing a ground cell that contains a target to one that does not.

In Figure 6 the total energy per second, or power, reflected from cell A is the product of the solar irradiance, the background reflectance, and the cell area.

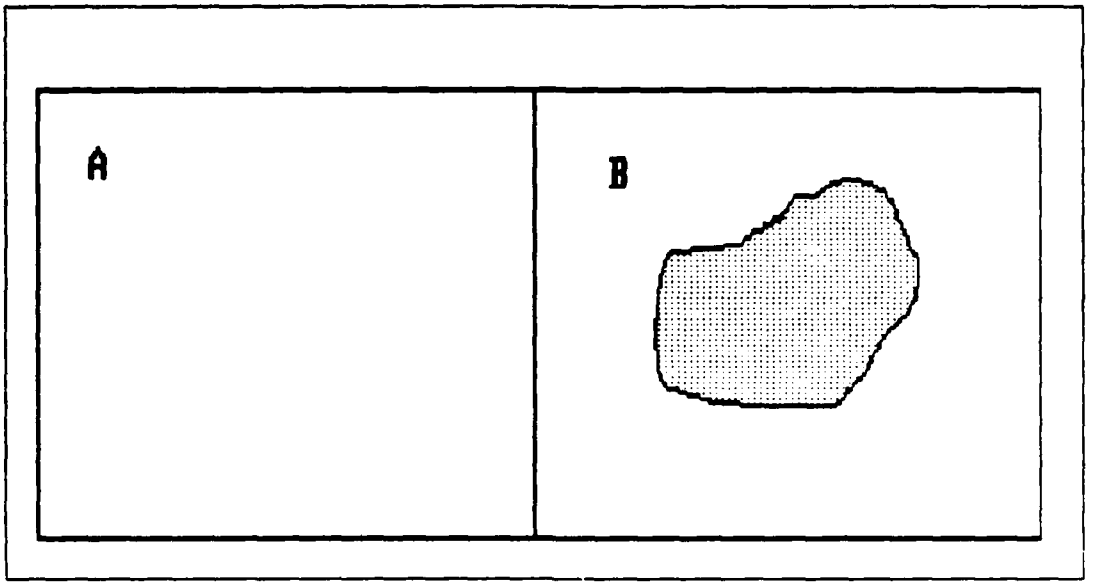

Figure 6. Ground Cells for Comparison

$$\Phi_a = E_s R_b A_c \qquad (5)$$

Where Φ_a = power reflected from cell A
E_s = solar irradiance
R_b = background reflectance
A_c = area of ground resolution cell

The total power reflected from cell B is:

$$\Phi_b = E_s(R_b A_b + R_t A_t) \qquad (6)$$

Where Φ_b = power reflected from cell B
A_b = area of background not obscured by target
R_t = target reflectance
A_t = target area

Detection occurs when the absolute value of $\blacksquare_a - \blacksquare_b$ exceeds the threshold as specified by the NERD, or when:

$$\left| \frac{R_t A_t + R_b A_b}{A_c} - R_b \right| \geq \text{NERD} \qquad (7)$$

Where NERD = noise equivalent reflectance difference

In the limiting case, threshold detection occurs when the left side of equation 7 is equal to the NERD. When this is true the minimum target area which results in detection can be expressed as a function of the reflectance between the target and the background.

$$A_t = \left| \frac{A_c \ \text{NERD}}{R_t - R_b} \right| \qquad (8)$$

This general relationship still assumes a clear atmosphere. In fact, the atmosphere attenuates some of the power reflected by the scene. This has the effect of reducing the effective sensitivity of the sensor. That is, the effective NERD to be used is:

$$\text{ENERD} = \frac{\text{NERD}}{\tau_a} \qquad (9)$$

Where ENERD = Effective NERD
τ_a = atmospheric transmission

Combining equations 8 and 9, the target size for threshold detection is given by:

$$A_t = \left| \frac{A_c \ NERD}{(R_t - R_b)\ \tau_a} \right| \qquad (10)$$

Using this relationship threshold detection curves can be plotted. A typical plot is shown in Figure 7. Targets falling above the threshold detection line will be detected; those falling below will not.

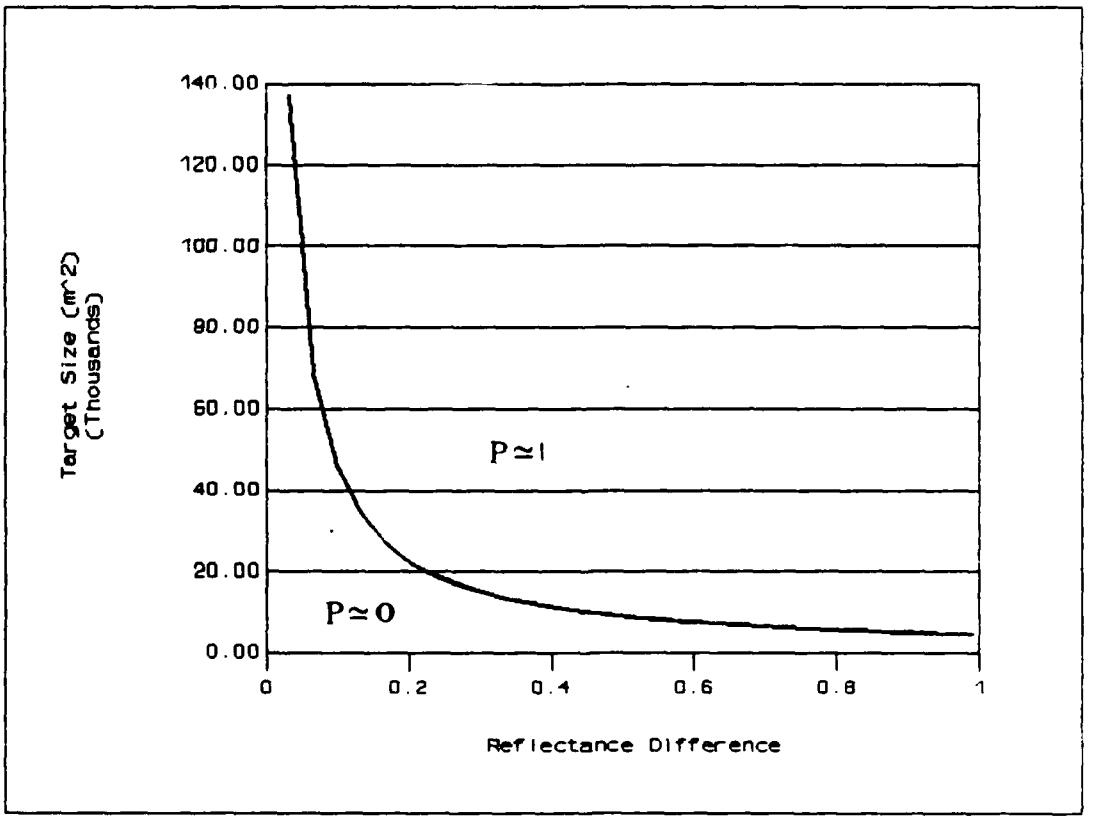

Figure 7. Generic Threshold Detection Curve

This analysis makes assumptions. They are:

(1) Backgrounds and targets are Lambertian;

(2) Background and target reflectances are uniform throughout the bandpass of the sensor;

(3) Atmospheric transmission is uniform across the bandpass of the sensor;

(4) Sensor response is linear throughout the bandpass of the sensor;

(5) The target is not moving with respect to the background; and

(6) The target falls in a single ground resolution cell.

Thermal Sensor Analysis - Ideal Conditions

Thermal detection of targets depends not on the energy reflected by a target but by the energy emitted by the target. Every object warmer than 0°K radiates energy. The amount of energy radiated is not uniform across all wavelengths and is a function of its temperature. For a blackbody the energy each second, or power, per square meter per unit wavelength interval radiated is given by the Planck function (29:7).

$$M_\lambda(\lambda,T) = \frac{3.74 \times 10^8}{\lambda^5(\exp(1.44 \times 10^4/\lambda T) - 1)} \quad \frac{W}{m^2\ \mu m} \qquad (11)$$

Where λ = wavelength in μm
T = temperature (°K)

The power emitted by an object is distributed across all wavelengths. Figure 8 shows the spectral blackbody power per square meter, or exitance, as a function of

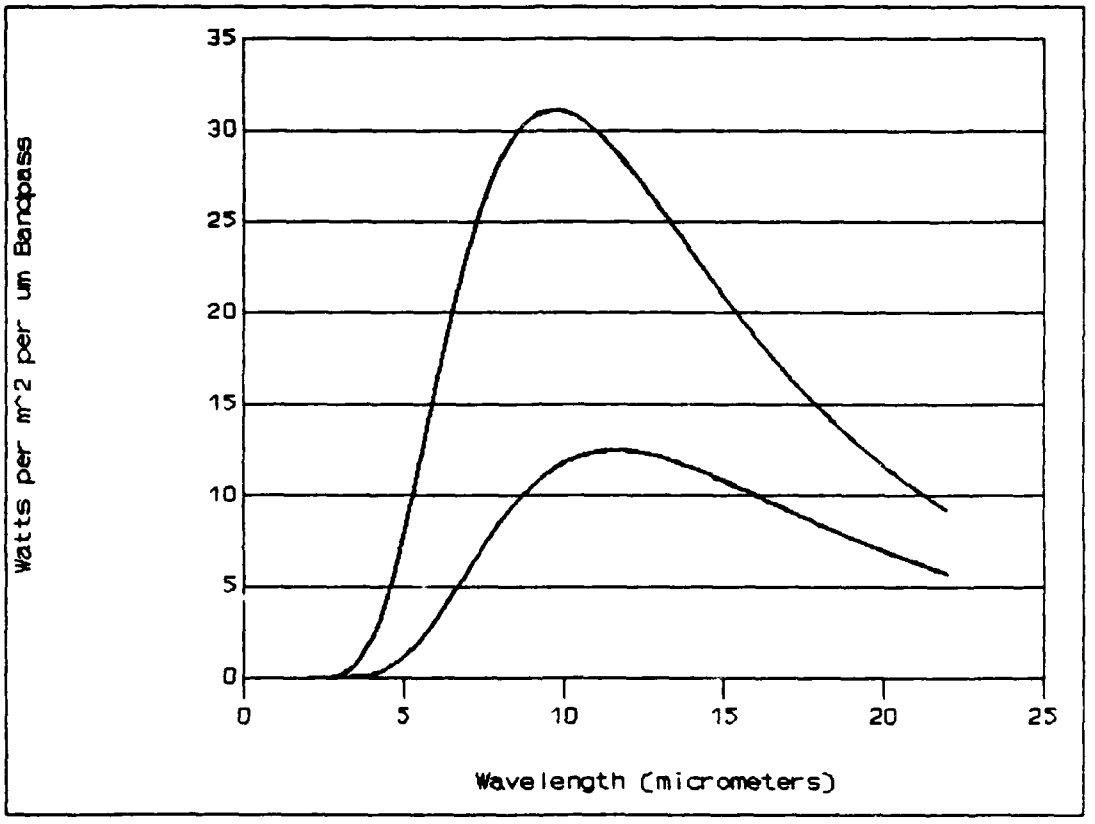

Figure 8. Blackbody Exitance Curves for Objects at 300°K (top) and 250°K (bottom)

wavelength for two objects, one at 300°K, and one at 250°K.

Since exitance is wavelength dependent, and since a sensor responds only to a portion of the electro-magnetic spectrum, the power output in a specific spectral bandpass is required for analysis. This is calculated by

integrating the Planck function over the wavelength interval for which the sensor is sensitive.

$$M(T) = \int_{\lambda 1}^{\lambda 2} M_{\lambda}(\lambda, T)\, d\lambda \qquad (12)$$

The total power emitted by an object in a specific bandpass is then:

$$\Phi_{o} = M(T) \epsilon A_{o} \qquad (13)$$

Where ϵ = object emissivity
A_o = surface area of the object

Given that the sensor response is linear, a ground cell containing a target will be detected (that is, register a different output current) if the sensor receives a sufficiently different amount of power from that cell as compared to a cell in which no target is located. One measure of how much power is sufficient for detection refers to the source of the power difference, temperature, and is the noise equivalent temperature difference, or NETD. This is the minimum temperature difference between cells which is just detectable by a sensor, given that the cells are at a uniform temperature and the background or reference temperature is a specific value. For example, the Landsat 5 TM thermal band is reported to have a NETD of .5°K at 300°K background temperature (64:498).

One problem in using the NETD as a measure of sensor sensitivity is that the conversion to sensor sensitivity for other background temperatures is not direct. However, the approximate NETD for other background temperatures can be derived based on the elements which contribute to the signal-to-noise ratio.

In general the signal to noise ratio for a sensor operating in the linear response portion of its response curve is determined by considering the arrival rate of photons at the focal plane, and on the sensor's electronics.

Signal output from the sensor is dependent upon the arrival of photons. The relationship is (29:225):

$$i_s = (\#\ \text{photons/unit time})K_1 \qquad (14)$$

Where i_s = signal current
$\#_{photons}$ = number of photons incident
K_1 = constant (charge per electron times the quantum efficiency of the detector)

Detector noise results from inherent detector characteristics such as sampling rate noise, dark current, and shot noise. Dark current is the current which flows in the detector when its field of view is dark. Shot noise is associated with the random arrival of photons. In simplified form detector noise is given by equation 15.

$$i_n = [(\text{shot noise})^2 + \sum(\text{all other sources})^2]^{.5} \quad (15)$$

Where i_n = noise current

Shot noise is calculated by:

$$i_{shot} = [(i_m\, e)/\tau]^{.5} \quad (16)$$

Where i_m = average signal
e = charge on one electron
τ = detector integration time

Combining these equations:

$$\frac{S}{N} = \frac{(\#\ \text{photons}^*)K_1}{[((\#\ \text{photons}^*)K_1 e/\tau)^2 + (\text{other sources})^2]^{.5}} \quad (17)$$

* per unit time

As a result of this relationship S/N behaves differently as a function of the arrival rate of photons. If few photons are received, then the total noise is dominated by other sources and shot noise can be discarded from analysis. Conversely, if many photons are received shot noise dominates and other sources of noise can be discarded from analysis.

This gives rise to three distinct portions of the S/N verses number of incident photons curve. Below a specific arrival rate, the curve is linear. This is the portion in

which shot noise can be discarded and total noise is effectively constant. Above a specific arrival rate, shot noise dominates and S/N increases as the square root of the arrival rate. Between these tails, shot and inherent noise are important. This relationship is shown in Figure 9. In the figure, area 1 is the region which behaves linearly.

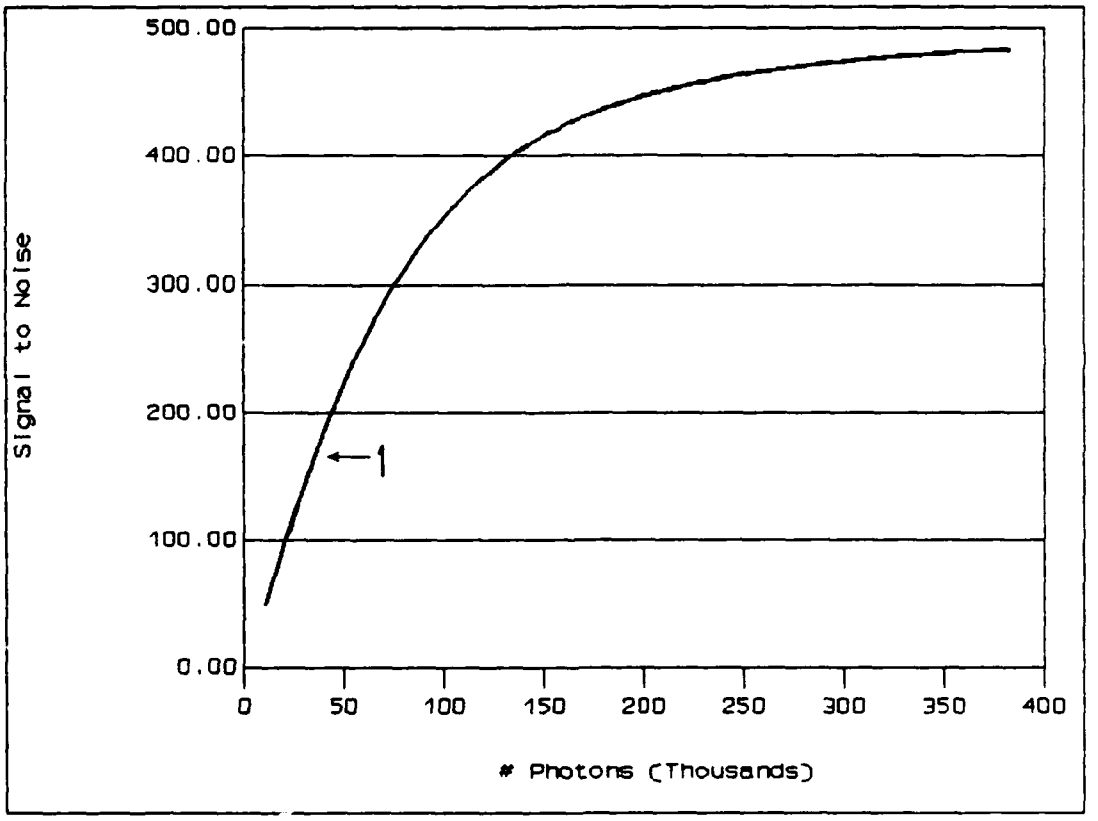

Figure 9. Representative Signal to Noise Curve

As noted earlier, NETDs are reported for a specific temperature, one which is in the linear response portion of the curve. For the thermal sensor, this temperature

corresponds to a specific number of incident photons. As shown in Figure 9, arrival of fewer photons than the number equivalent to the NETD should result in a linear response by the sensor. In this region of sensor response (area 1) inherent noise dominates and can be assumed to be reasonably constant. Since the noise is approximately constant, and since the NETD identifies threshold S/N for detection, the signal required for threshold detection remains approximately constant in this region.

From the previous discussion, NETD can be considered in terms of numbers of photons. It can also represent a specific power difference. That is, an NETD of 2°K @ 300°K is equivalent to:

$$NEPD = \Phi(302°K) - \Phi(300°K) \qquad (18)$$

Where NEPD = noise equivalent power difference
$\Phi(302°K)$ = power received in sensor bandpass from object filling the field of view at 302°K
$\Phi(300°K)$ = power received in sensor bandpass from object filling the field of view at 300°K

In the linear response portion of the curve, when referencing a background cell that is at a lower temperature than the NETD, if the power difference between two cells differs by more than the NEPD, the sensor will register a different response. If that difference is caused by the target, then the sensor has detected the target.

Using the NEPD derived above it is possible to generate threshold detection curves for thermal sensors. As in the derivation of visible wavelength sensor detection curves, the analysis begins by considering two ground cells, one that contains a target and one that does not. This is shown in Figure 10.

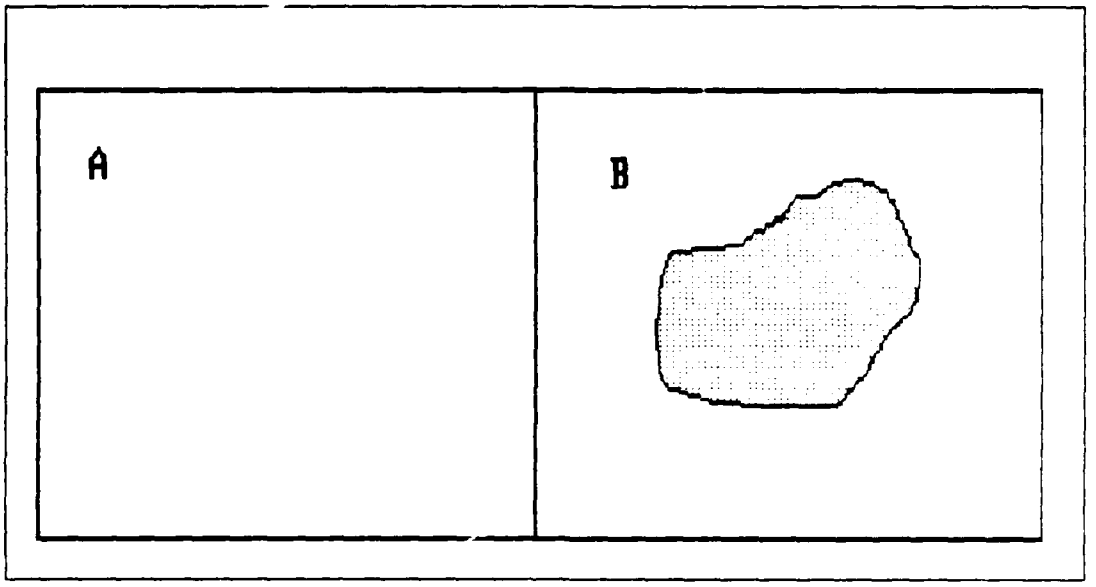

Figure 10. Ground Cells for Comparison

The power emitted in the sensor bandpass by cell A is:

$$\Phi_A = M_b(T_b)A_c\epsilon_b \qquad (19)$$

Where $M_b(T_b)$ = spectral exitance for the cell at temperature T_b in the sensor bandpass
A_c = area of the cell
ϵ_b = emissivity of the background

The power emitted in the sensor bandpass by cell B is:

$$\Phi_B = M_t(T_t)A_t\epsilon_t + M_b(T_b)A_r\epsilon_b \qquad (20)$$

Where $M_t(T_t)$ = spectral exitance for the target at temperature T_t in the sensor bandpass
A_t = area of the target
ϵ_t = emissivity of the background
A_r = area of background not obscured by the target

Detection occurs when the absolute value of $\Phi_A - \Phi_B$ is greater than or equal to the NEPD, or:

$$\left| M_b(T_b)A_c\epsilon_b - M_t(T_t)A_t\epsilon_t - M_b(T_b)A_r\epsilon_b \right| \geq \text{NEPD} \qquad (21)$$

The target size for threshold detection is:

$$A_t = \frac{\text{NEPD}}{\left| M_b(T_b)\epsilon_b - M_t(T_t)\epsilon_t \right|} \qquad (22)$$

Again the atmospheric attenuation must be considered.

$$\text{ENEPD} = \frac{\text{NEPD}}{\tau_a} \qquad (23)$$

Where ENEPD = effective NEPD
τ_a = atmospheric transmission

Therefore threshold detection is calculated using:

$$A_t = \frac{\text{NEPD}/\tau_a}{\left| M_b(T_b)\epsilon_b - M_t(T_t)\epsilon_t \right|} \qquad (24)$$

Using this relationship, threshold detection curves as a function of target exitance can be plotted. Once again a combination of target size and exitance which falls below the threshold line will mean that the sensor will not see the target against the background. However, unlike the curves plotted for the visible wavelength sensors, thermal threshold detection curves are both sensor and situation specific and cannot be generalized for all targets in all situations. For example, the emissivity of the target will shift the curve up or down the exitance axis. This is shown in Figure 11 in which the detection curves for three target emissivities are plotted. Because of this variability, thermal detection curves apply only for the situation for which they were generated.

Non-Ideal Considerations

The detection curves developed to this point are valid for targets which are completely contained in a single ground resolution cell. However, a target may fall in the junction of several cells. When this happens, a target which is larger than the threshold detection size may not be detected since it could present a small enough profile to each individual detector to escape detection.

In the extreme case, a target could be equally shared by four ground resolution cells. In this situation, the minimum actual target size needed to guarantee threshold

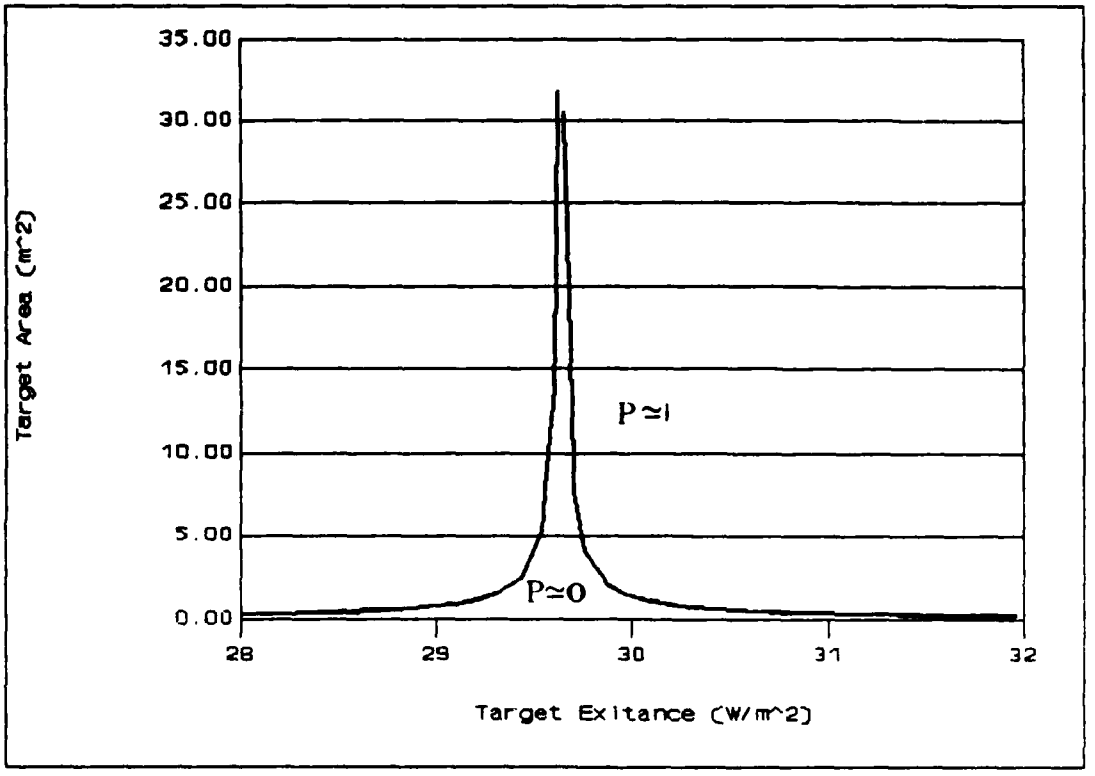

Figure 11. Threshold Detection Curves for Several Target Emissivities

detection is four times the size of the target under ideal conditions.

A second complication is encountered when there are gaps between detectors in the focal plane of the sensor as shown in Figure 12. Again the effect is to increase the size of the target which would always trigger detection. The actual target size for threshold detection in all cases is calculated using equation 25.

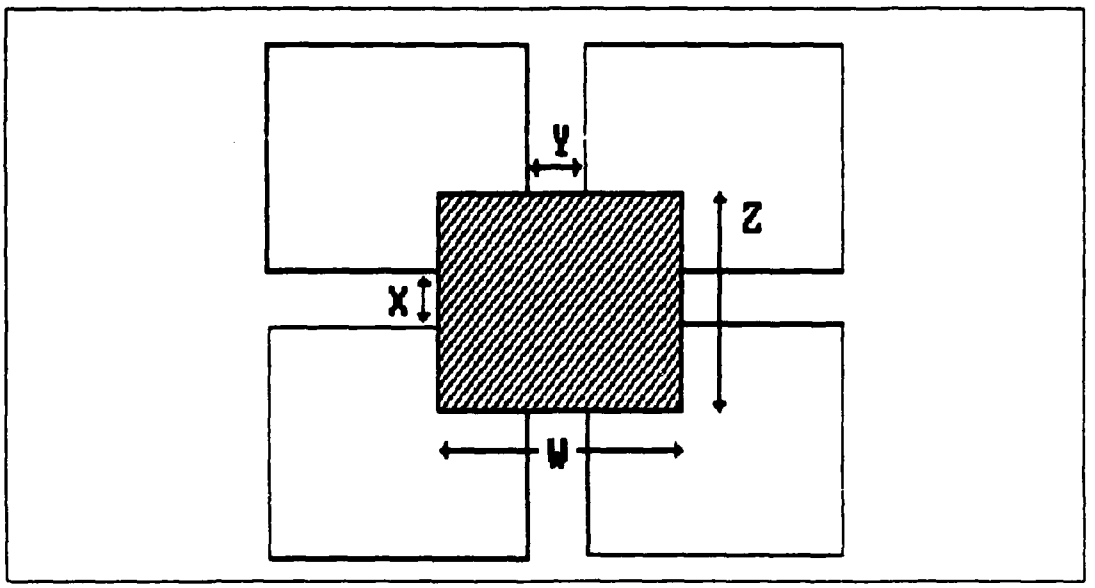

Figure 12. Target Overlapping Gaps in Detector Array

$$A_{th} = 4A_{ti} + 2X(A_{ti})^{.5} + 2Y(A_{ti})^{.5} + XY \qquad (25)$$

Where A_{th} = target size for threshold detection
A_{ti} = target size for threshold detection under ideal conditions
X,Y = gaps between detectors

Finally it is possible that a sensor could detect a target under ideal conditions, but will not if the target overlaps several pixels. Detection of the target now becomes stochastic. The probability that the target will be detected can be approximated by considering the size of the target and the size of the threshold detection target.

The probability of detecting the target is one if enough of the target falls in the active sensing portion of a single detector in the detector array. The probability

that enough of the target will fall in the active portion of the detector is calculated geometrically.

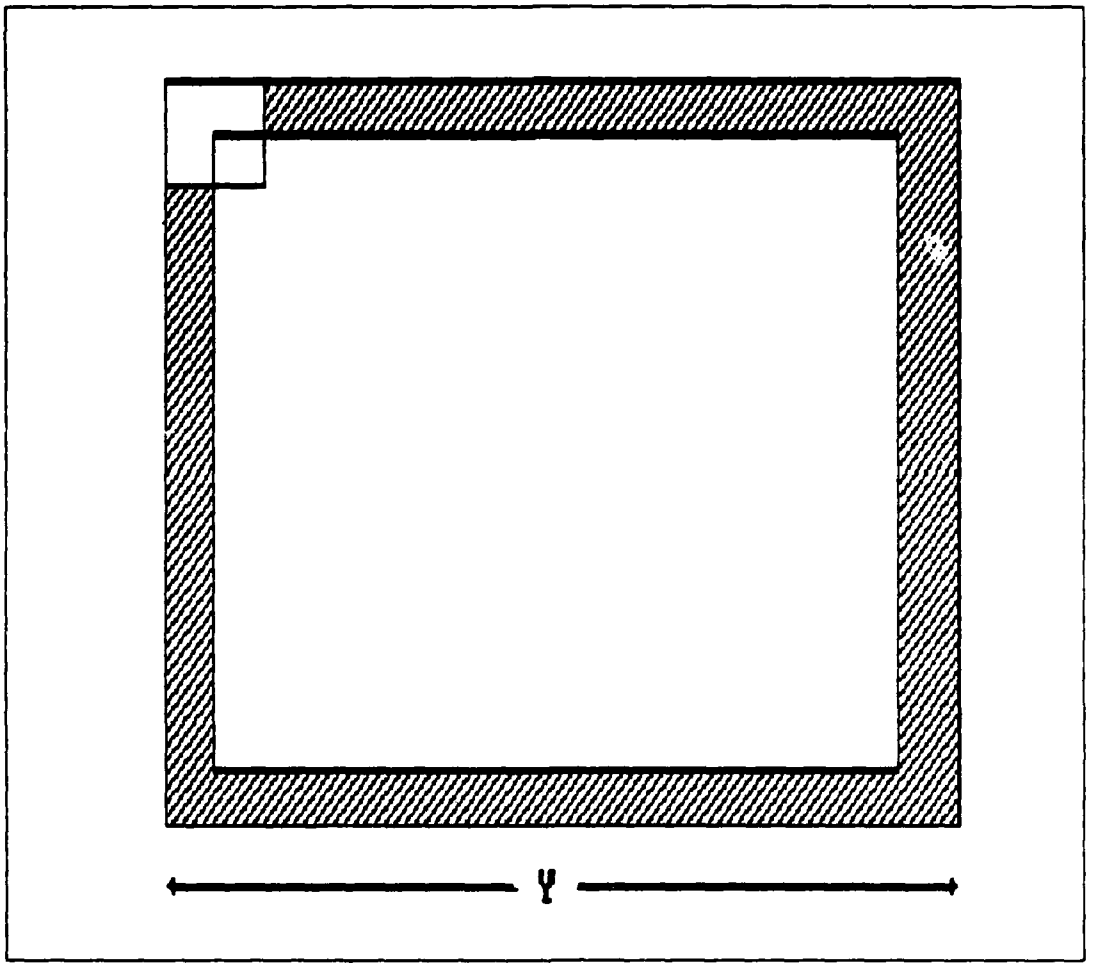

Figure 13. General Detection Probability Geometry

Consider Figure 13. For the target to be detected the center of the target must fall within the active area of the detector. If the target falls on the edges of the detector or the gaps between detectors such that the target area remaining on the active detector is less than the threshold

target size for detection, the target is not detected. In that the center of the target is equally likely to fall anywhere in the detector array, the probability that the target will be detected is the area that would result in detection divided by the total area.

$$P_{det} = \frac{A_{det}}{A_{tot}} \qquad (26)$$

Where P_{det} = probability of detection
A_{det} = area which results in detection
A_{tot} = area total

The total area in which the center of a target could fall is the size of a single detector plus half the area of the gaps which surround individual detectors. Considering square detectors with equal gaps on all sides, the total area is:

$$A_{tot} = (W+d)^2 \qquad (27)$$

Where W = length of one side of detector
d = gap between detectors

Again the geometry is used to solve the area in which the target will be detected. In Figure 14:

(1) X is the center point of the gaps in the detector array;
(2) Z is the center of the target which could lie anywhere along the diagonal line; and
(3) a is the dimension of one side of the area of the target which lies on the active portion of the detector.

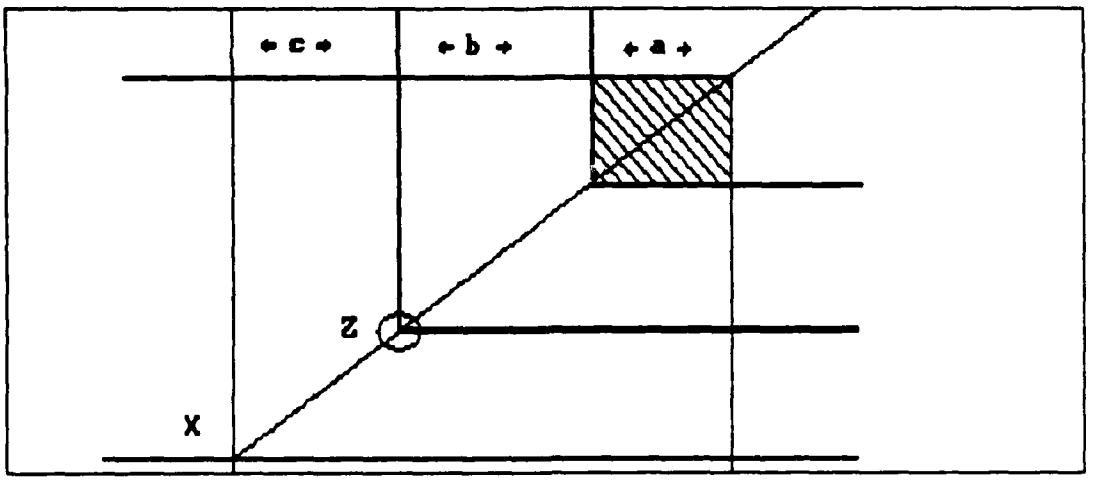

Figure 14. Target Gap Overlap and Detection Probability

From this (b+c) is equal to half the gap between detectors. For detection, the area remaining in view of the detector (a^2) must equal or exceed the threshold detection size under ideal conditions (A_{ti}). Also, the target size is equal to four times the square of size $(a+b)^2$. Solving for b:

$$b = \frac{(A_t)^{.5}}{2} - (A_{ti})^{.5} \qquad (28)$$

The area in which the center of the target may fall and still result in detection is then:

$$A_{det} = (w+2b)^2 \qquad (29)$$

Obscuring Phenomena

Having considered the internal complications which occur because of the physical layout of the detector array, it is time to consider complicating factors which are outside the sensor. Such factors have the effect of obscuring the sensor. In general two major types of obscuring phenomena are found in the Canadian arctic: darkness and cloud cover.

Darkness. Darkness is predictable and is a function of latitude and time of year. Of interest are the local sidereal times that the sun rises and sets at a given latitude. Since the orbits for imaging satellites are sun-synchronous, they overfly the same latitude at the same local sidereal time each pass (only the longitude changes). As a result the time when the satellite is overhead a given latitude is predictable. If the satellite is overhead during darkness, and if the sensors on board require sunlight for target irradiation, the obscuration by darkness is complete and the probability of detection is reduced to zero. On the other hand, if the satellite flies over the target while the target is being irradiated by the sun the obscuration by darkness is zero.

Although there are times when the sun has risen but is not yet high enough in the sky to provide enough irradiation of the ground for imaging, this analysis assumes there is no

middle ground. If the sun is up the target can be imaged. Therefore the irradiation factor, I_{fac}, can only take on the values zero or one.

The time of sunrise and sunset is determined by considering the right ascension and declination of the sun, and the latitude of the observer (4:A12). The formula is:

$$LST = .99727(\alpha \pm \cos^{-1}(-\tan\emptyset \tan\pi)) \quad (30)$$

Where LST = local sidereal time
α = right ascension
$\emptyset$ = latitude of observation
π = declination

Table 2. Local Sidereal Times for Sunrise and Sunset

	60°N		70°N		80°N	
	Rise	Set	Rise	Set	Rise	Set
Jan 23	0835	1549	1048	1337	////	////
Feb 22	0721	1707	0805	1624	////	////
Mar 23	0553	1822	0545	1830	//**	**//
Apr 22	0423	1935	0320	2040	****	****
May 22	0307	2048	****	****	****	****
Jun 21	0236	2128	****	****	****	****
Jul 21	0316	2056	****	****	****	****
Aug 23	0433	1930	0335	2027	****	****
Sep 22	0544	1800	0540	1803	//**	**//
Oct 22	0657	1631	0744	1544	////	////
Nov 21	0813	1519	1036	1256	////	////
Dec 21	0902	1454	////	////	////	////

//// - 24 hour darkness
**** - 24 hour sunshine

The times of local sidereal sunrises and sunsets are published annually in the Astronomical Almanac. Although there is some variation, the approximate time of sunrise for a given date at a given latitude is the same year to year. For this reason, it is reasonable to use the almanac's times of sunrise and sunset throughout the analysis period. However, the almanac only provides times for latitudes up to and including 66°N. To determine local sidereal times for sunrise and sunset at latitudes not listed in the almanac, the formula shown in equation 30 was used. The times for sunrise and sunset are given in Table 2.

Determination of the local sidereal time of satellite passage over a given latitude requires orbital analysis. Since an imaging satellite flies in a circular orbit, its ground speed is constant throughout its orbit. If the orbit is inclined at 90°, the time taken to travel between any two latitudes is calculated using equation 31.

$$T_{lat} = ((\beta_1 - \beta_2)/360)T_{per} \qquad (31)$$

Where T_{lat} = time to travel between the latitudes
$\beta_{1,2}$ = first, second latitude
T_{per} = orbital period of the satellite

A satellite in an orbit at any other inclination has more ground to cover before it reaches the latitude of

interest. This distance is calculated by considering both the latitude of interest and the orbit inclination. Since the satellite's ground speed is constant, the time to travel between the equator and the latitude of interest becomes:

$$T_{lat} = \sin^{-1}\left\{\frac{\sin(Lat)}{\sin(i)}\right\} \frac{T_{per}}{360^{\circ}} \qquad (32)$$

Where Lat = latitude of interest

Having worked out the time for passage between the equator and a given latitude, the local sidereal time the satellite passes over this latitude is its equatorial crossing plus or minus the transit time. The plus or minus is assigned depending on whether the satellite is ascending or descending at time of equatorial crossing.

Armed with the local sidereal times for sunrise, sunset, and satellite passage overhead, the rule for assigning the irradiation factor is:

$$I_{fac} = 1 \quad \text{If } t_{sr} \leq t_{pass} \leq t_{ss} \qquad (33)$$

$$I_{fac} = 0 \quad \text{Otherwise}$$

Where t_{sr} = time of sunrise
t_{pass} = time of satellite passage
t_{ss} = time of sunset

Cloud Cover. In contrast to the predictability of darkness, analysis of the second obscuring phenomenon, clouds, is stochastic. For those sensors which will suffer obscuration, the obscuration is taken to be complete when clouds are present. Therefore, the information needed is the probability that there will be cloud cover in the target area. Once this is found, the probability of getting an image of the target area considering the cloud cover is given in equation 34.

$$P_{obscl} = (1-P_{cloud}) \tag{34}$$

Where P_{obscl} = probability of observation considering clouds
P_{cloud} = probability of cloud cover

Conclusion

In summary this analysis shows that the overall probability of detecting a target, given that it is in the field of view, is the sensor's detection capability under ideal conditions modified to include the complications of array geometry and external obscurations.

The obscuring phenomena of interest for visible wavelength sensors are clouds and darkness. Thus for visible wavelength sensors, the expression for P_{det*}, which

is the probability of detection in a single image considering obscuring phenomena, is:

$$P_{det*} = P_{det} I_{fac}^{(1-P_{cloud})} \tag{35}$$

The obscuring phenomenon of interest for thermal sensors is cloud cover. Thus for thermal sensors the expression for P_{det*} is given by:

$$P_{det*} = P_{det}^{(1-P_{cloud})} \tag{36}$$

V. Algorithm Development

General

The second question to resolve is how a sensor compares to the other sensors which are available. Although individual comparisons are interesting, it is more important to be able to compare all the sensors in terms of their contribution to the mission at hand. Conceptually there is a system of commercial sensors. The goal of this chapter is to develop the rules for optimization of the system's performance through selection of the sensor or mix of sensors which provides the greatest mission accomplishment.

Sensor comparisons are based on the individual sensor detection capabilities as discussed in Chapter IV. However, the previous chapter only shows how a single sensor's probability of target detection can be calculated given that the target is in the field of view of the sensor. How likely is the target to be in the field of view? The answer is that it depends on the mission and on the sensor. For this reason this chapter builds mission specific algorithms that are used to assess the system performance.

Detection

The first mission in surveillance is detection. However, detection itself can be broken into two distinct

missions. The first mission is cued detection. Can the system of available sensors detect a target given the system knows where to look? Information from a source suggests that a target may be at a location. The measure of performance for cued detection is the probability that the system will image the target and confirm or deny its presence. The second mission is non-cued detection. Can the system detect a target if it does not know where to look? In non-cued detection, the system is tested as a wide area surveillance tool. The measure of performance for non-cued detection is the probability that the system will detect a target given that the target is in the area of interest but the location is unknown.

Phenomenologically cued detection is a subset of non-cued detection. Thus, non-cued detection is the more demanding of the two detection missions. For this reason the algorithm to calculate the probability that the system will detect a target under non-cued conditions is developed first.

Non-Cued Detection Algorithm -- Stationary Targets

In general, non-cued detection is pursued over an extended period of time during which many images of the total area of interest could be acquired. Given that the images that are acquired do not overlap and that the target is not moving, the probability of detecting the presence of

a target in the area of interest depends on the probability that the target will be detected in a single image, the size of one image as compared to the total area in which the target could be, and on the number of images acquired. The relationship for a given sensor is given in equation 37.

$$P_{dot} = \frac{A_{one} N_{im} P_{det*}}{A_{int}} \quad (37)$$

Where P_{dot} = probability of detection over time
A_{one} = area of a single image
N_{im} = number of images acquired
P_{det*} = probability of detection in single image
A_{int} = total area of interest

The number of images that are acquired will depend on the time the target remains in the area of interest.

$$N_{im} = N_{ut} T_{tav} \quad (38)$$

Where N_{ut} = # images taken per unit time
T_{tav} = time target is in the area

Also the maximum number of images taken in a given unit of time will be constrained by the cost of the images, or:

$$N_{ut} = \frac{B_{\$}}{C_{si}} \quad (39)$$

Where $B_{\$}$ = budget per unit time
C_{si} = cost of a single image

Folding equations 37, 38 and 39 together yields a general expression for the probability of detection over time of stationary targets given that all images acquired are non-overlapping.

$$P_{dot} = \frac{A_{one} B_{\$} T_{tav} P_{det*}}{A_{int} C_{si}} \qquad (40)$$

Optimization Non-Cued Detection -- Stationary Targets

Equation 37 gives the probability of non-cued detection of stationary targets for individual sensors. To identify the best sensor or sensors to use in a given situation requires an optimization methodology.

For convenience, equation 37 can be rewritten in the general form:

$$P_{dot} = N_{im} P_{dot1} \qquad (41)$$

Where $$P_{dot1} = \frac{A_{one} P_{det*}}{A_{int}}$$

If there is more than one sensor available, the expression for overall probability of detection is the linear combination of each sensor's individual P_{dot1} times the number of images acquired from that sensor. This combination is given in equation 42.

$$P_{dsys} = \sum_{i=1}^{n} (N_{im})_i (P_{dot1})_i \qquad (42)$$

Where P_{dsys} = overall probability of detection
n = number of sensors available
$(N_{im})_i$ = number of images acquired from sensor i
$(P_{dot1})_i$ = probability of detection in a single image from sensor i

Equation 42 is counter-intuitive. However, this result is important and must be accepted for the subsequent analysis to have any merit. By way of example, consider the situation of a checkerboard with a single checker placed on a square at random. A player is blindfolded and given the task of finding the checker. He searches for the checker by asking that a third party look at a number of specific squares and tell him if the checker is in any of the squares. The restriction on the number of squares a player may choose is that each request costs him money and he has only a restricted budget available. The last rule is that the checker is not moved during the game so that revisiting a square does the player no good. The game begins.

The task of finding a stationary target using satellite imagery of an area of interest is the checkerboard game scaled up to the dimensions of the area of interest. The total areas of interest are the 64 squares of the checkerboard and the 7,000,000 square kilometers in Northern Canada. Picking one square is analagous to contracting for

one image. The probability of finding the checker is one (1) given the player request that the square holding the checker be looked at. The probability that the player will request the correct square is N/64 where N is the number of requests made at the start of the game. Thus the probability of finding the checker increases linearly with the number of trials taken. Similarly the probability of finding a stationary target in Northern Canada increases linearly with the number of images contracted. In each case the probability of success is maximized at the point that all 64 squares are chosen or all the territory is imaged. Beyond this point both the analogy and the analysis break down. Therefore, for the linear analysis which follows to be valid, the restriction of non-overlapping images must be honored.

The first constraint on P_{dsys} is that there is an upper limit to the number of images that can be acquired as constrained by the available budget. That is:

$$B_{\$} \geq \sum_{i=1}^{n} C_i (N_{im})_i \qquad (43)$$

Where C_i = cost of one image from sensor i

The second constraint limits the number of images that can be provided by the sensors. Since the sensors are restricted to providing non-overlapping images, once the

entire area of interest has been imaged further acquisition is terminated. This constraint takes the form:

$$A_{tot} \geq \sum (N_{im})_i (A_{one})_i \qquad (44)$$

Where $(A_{one})_i$ = area of one image taken by sensor i

The third constraint is actually a family of constraints; those that restrict the maximum number of images that can be acquired from a specific sensor in a specific period of time. These constraints take the form:

$$0 \leq (N_{im})_i \leq K_i \qquad (45)$$

Where K_i = maximum number of images that can be acquired from sensor i in the period

The fourth constraint requires explanation. The goal of non-cued detection of stationary targets is to achieve a uniform probability of detecting targets throughout the entire area of interest. However, the area of interest is not uniform. The non-uniformity occurs since there are regions within the area of interest that are more easily imaged than others because of darkness and a difference in the probability of cloud cover. As the model stands now any optimization methodology would select areas to image that would return the highest individual P_{det*} at the expense of

coverage of lower P_{det*} areas. To enforce a uniform probability of detection throughout the area of interest, areas of common obscuration phenomena must be identified, and constraints added which specify that each unique area must achieve the same P_{dsys}.

Having built the expression to be maximized, and having identified the series of constraints which must be met, the task of optimizing the selection of sensors remains. One method which will solve the combination of equations above is linear programming (49:72). This can be accomplished using equation 42 as the objective function to be maximized and equations 43, 44, and 45 plus those specifying equal P_{dsys} for each unique area as the constraints. This yields the maximum probability of detection given a specified budget. A second option is to specify a minimum acceptable P_{dsys} for equation 42 and write the linear program using equation 43 as the objective function to be minimized. This would solve for the minimum cost to achieve a constrained probability of detection.

A problem arises in that the value for P_{dot1} changes as a function of the time of year, type of target, and location of the target. Because of this, care must be taken to explicitly define what is to be maximized. In its largest scale the analysis could produce a maximum probability of detection of all target types located in all possible

locations throughout the entire year. Analysis at this scale is impractical if the numbers of sensors, target types, locations, and distinct times of year are large. In such a situation either simplifying assumptions are required, or subsets of the large linear programme can be analyzed.

In using these algorithms, one final caveat is appropriate. The situation could arise that complete imaging of an area results in a probability of target detection below that specified by operational requirements. For the system to yield a higher probability of detection, multiple imaging of the area of interest would be required. That is, sensors would have to be tasked to image areas more than once. This would have the effect of increasing the probability of detection for those areas that were imaged more than once. Multiple imaging of areas is discussed in the next section of this chapter.

Non-Cued Detection Algorithm -- Moving Targets

If a target is moving in relation to the background, acquiring an image of a specific ground cell at time t1 does not absolve the detection system from having to re-image that area at any other time in order to see what is there. The probability of detecting the presence of a target in the area of interest again depends upon the probability that the target will be detected in a single image and upon the

number of images acquired. However, in contrast to the case of stationary targets, the relationship between the number of images acquired and the overall probability of detection is not linear.

The first case to consider is the situation where a single sensor is tasked to provide multiple images of the area of interest. Such a situation would occur if the sensor performance in detecting a specific target was dominant in relation to other available sensors. Defining a detection to be a success, the probability of success (detection) in a single image is P_{dot1}. Then the probability of X successes in N trials (images acquired) is binomially distributed (21:98). For example, the probability of at least one success as a function of the number of trials using a probability of success of .1 is shown in Figure 15.

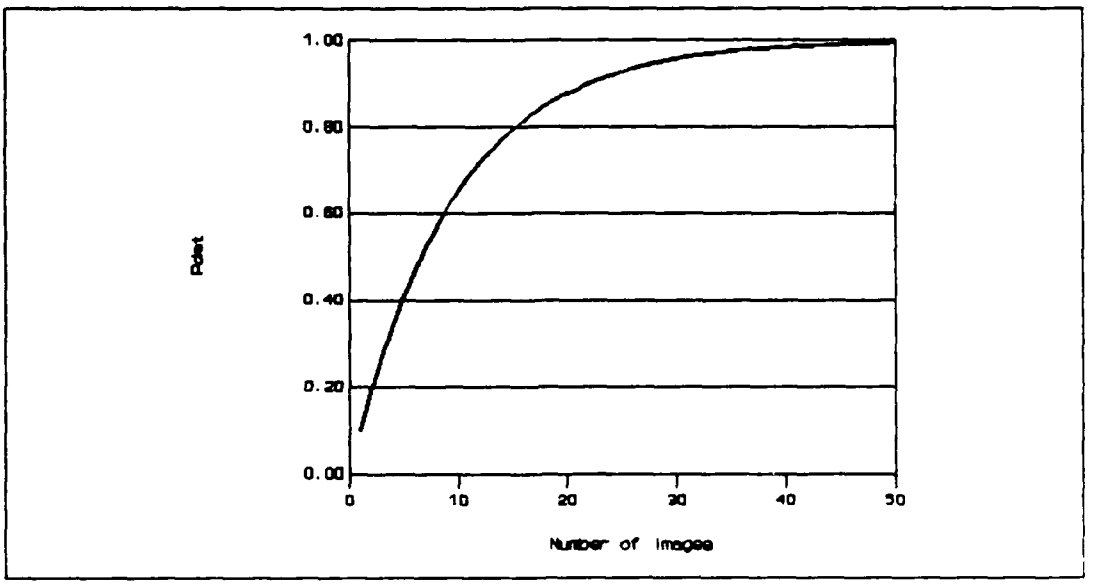

Figure 15. Probability of Detection vs Number of Trials for P(Success)=.1

The second case to consider is the situation where a variety of sensors are used to provide an image of the area of interest. One method to calculate the combined probability of detection is by buiding a probability tree based on the individual sensor's probability of target detection for a single image, P_{dot1}.

Two hypothetical sensors can illustrate this procedure. Given their respective P_{dot1}s are .7 and .6, the probability tree which results from acquiring one image from each sensor is shown in Figure 16. Because the goal of multiple imaging is to achieve an acceptable probability of at least one detection, the outcome of primary importance is the one which shows "no detection" throughout. The probability of

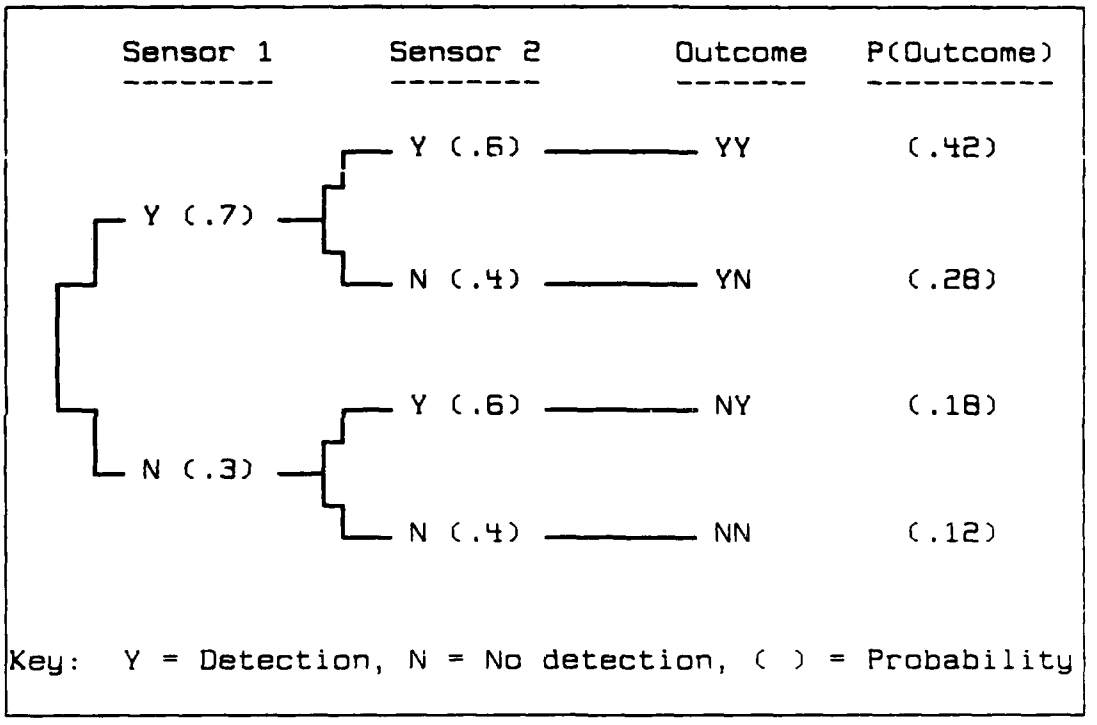

Figure 16. Example Probability Tree for Two Sensors

at least one detection is equal to one (1) minus the probability of no detections throughout.

$$P_{d \geq 1} = 1 - P_{nodet} \quad (46)$$

Where $P_{d \geq 1}$ = probability of at least one detection
P_{nodet} = probability of no detection throughout

The probability of the no detection throughout outcome is the product of the individual probabilities of no detection for each image acquired. This is because, as shown in the figure, there is always one all negative

outcome irrespective of the number of images acquired. All other combinations contain at least one detection. Each sensor's individual probability of no detection is one (1) minus the probability of detection for a single image, P_{dot1}. Equation 47 provides the expression for the probability of at least one detection in a series of images acquired from a variety of sensors.

$$P_{d\geq 1} = 1-((1-P_{dot11})^{x1}(1-P_{dot12})^{x2}\ldots(1-P_{dot1n})^{xn}) \quad (47)$$

Where
- P_{dot11} = probability of detection for a single image from sensor 1
- P_{dot12} = probability of detection for a single image from sensor 2
- P_{dot1n} = probability of detection for a single image from sensor n
- x1 = number of images acquired from sensor 1
- x2 = number of images acquired from sensor 2
- xn = number of images acquired from sensor n

This relationship holds for both cases discussed above since the selection of multiple images from a single sensor is a subset of the general case.

Optimization Non-Cued Detection -- Moving Target

As is the case for stationary target detection optimization, moving target detection optimization can be approached from two perspectives. The goal is either to

maximize the $P_{d\geq 1}$ subject to the constraints of budget and image availability, or to minimize cost subject to the constraints of an acceptable $P_{d\geq 1}$ and image availability. However, since equation 47 is non-linear, linear programming cannot be used directly to solve this model.

The probability of at least one detection can be maximized through a variety of non-linear programming techniques. In its general form equation 47 is the objective function to be maximized, and equations 43, and 45 make up the constraints.

To minimize the cost involved in achieving an acceptable $P_{d\geq 1}$, again non-linear programming techniques could be used. In this case equation 43 becomes the objective function to be minimized, and equations 45 and 47 become the constraints.

In either case the non-uniformity of the area of interest must be accounted for. This will generate additional constraints to enforce an uniform $P_{d\geq 1}$ for each unique region within the area of interest.

Cued Detection Algorithm -- Stationary Targets

Cued detection of stationary targets is very similar to non-cued detection of moving targets. Again the probability of detecting the presence of a target depends on the probability that the target will be detected in a single

image and the number of images acquired. Again the logic of multiple imaging of an area applies. However, a major difference occurs in the size of the area of interest. In cued detection of a stationary target a single location is imaged. This effectively reduces the area of interest to the area of a single image from the sensor. Thus the probability of detection by an individual sensor which applies is the raw probability of detection amended to include appropriate obscuring factors, or P_{det*}. The equation for calculating the probability of at least one detection becomes:

$$P_{d\geq 1} = 1-\{(1-P_{det*1})^{x1}(1-P_{det*2})^{x2}\ldots(1-P_{det*n})^{xn}\} \quad (48)$$

Where $P_{det*1,2,\ldots,n}$ = probability of detection in one image from sensor 1,2,...,n

Optimization Cued Detection -- Stationary Targets

As in non-cued detection of moving targets, the optimization methodology used to optimize cued detection of stationary targets depends on whether the $P_{d\geq 1}$ is to be maximized or the cost is to be minimized. Again a variety of techniques is available to accomplish this optimization.

Cued Detection Algorithm -- Moving Targets

Cued detection of moving targets is an alias for tracking. Therefore, the algorithm developed in this section to assess a sensor's capability to detect moving targets when cued is actually a measure of the sensor's ability to track a target. Similarly, the probability that a sensor will detect the target is equivalent to its probability of tracking the target.

There are two broad tracking categories. First, a sensor may be tasked to establish a second contact with a target. In this case, the first contact has occurred and constitutes the cueing information. Second, a sensor may be tasked to locate a target for which at least two contacts have been established. In this case, the task may be simplified since some prediction of the target location is possible.

Second Contact. Given that the first contact, or cue information, is accurate, the probability that a system will detect a target depends on the sensor's single image probability of detection, the size of the image, the position of the first contact, the velocity of the target, and upon the responsiveness of the sensor. Consistent with an approach of simple first, complex second, the analysis begins with consideration of fixed sensors.

Sensors Fixed at Nadir. The general situation of sensor swath and target area overlap is shown in Figure 17. In the figure, X is the position of the target at time t_1, Z is the subsatellite point at time t_2 when the satellite crosses the latitude of initial target detection and the sensor is within range of the possible target area.

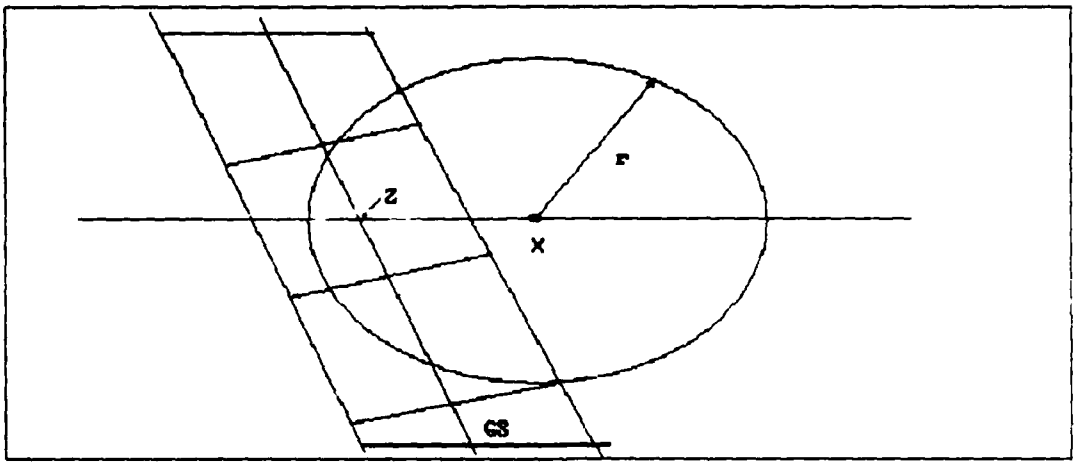

Figure 17. Sensor Swath Overlap of Possible Target Area

The possible target area is enclosed in the circle of radius r, where r is equal to the distance that the target could have moved if it were travelling at top speed for the period $t_2 - t_1$. The diagonal swath is the territory that the sensor could image on the current pass.

If the ground swath overlaps the possible target area, and if the target is equally likely to be anywhere in the possible target area, then the probability that the sensor will detect the target on this pass is given in equation 49.

$$P_{track} = P_{trkcon}P_{det*} \quad (49)$$

Where P_{track} = probability sensor will track target on this pass
P_{trkcon} = the ratio of the area imaged which could contain the target to the area which could contain the target

In the limiting case the sensor's swath just touches the area in which the target could be. This is shown in

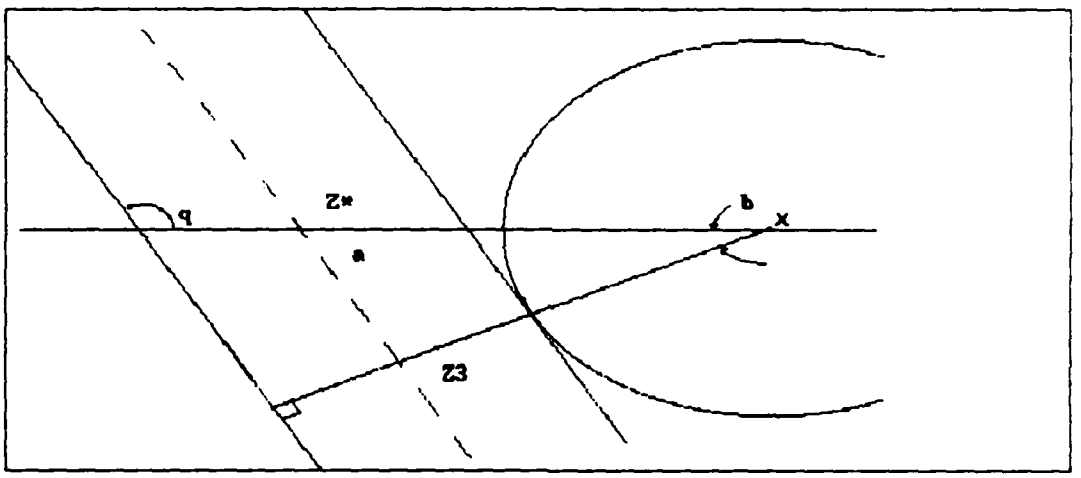

Figure 18. Sensor Swath Edge Tangential to Possible Target Area

Figure 18. At time t_3, when the sensor is overhead point Z3, the distance between Z3 and X is given in equation 50.

$$(Z3 - X) = (t_3 - t_1)s + S_w/2 \quad (50)$$

Where S_w = width of the sensor's ground resolution cell
s = target speed

Angle (a) is equal to 180° minus the local crossing angle (q). The local crossing angle is a function of the orbit inclination and the latitude of interest. The formulas for determining the local crossing angle are contained in Appendix E. The distance between Z* and X is:

$$(Z^* - X) = \frac{(t_3 - t_1)s + S_w/2}{\sin(a)} \qquad (51)$$

This distance can be converted to the equivalent number of degrees of longitude. Assuming a spherical Earth, the circumference of a specific parallel of latitude is given by the expression:

$$Cir_L = 2\pi R_e \cos(L) \qquad (52)$$

Where Cir_L = circumference at latitude L
R_e = radius of the Earth
L = latitude

The number of degrees of longitude equivalent to the distance (Z* - X) is then:

$$\ell = \frac{Z^* - X}{Cir_L} (360°) \qquad (53)$$

The equivalent degrees of longitude is used to determine whether the sensor's swath and the possible target area overlap. If at time t_2 the subsatellite longitude is

within the threshold boundaries (±) of the initial target longitude, the sensor swath and possible target area will overlap. The relationship between the threshold longitude for overlap and (t_3-t_1) is linear and is shown for 60°N

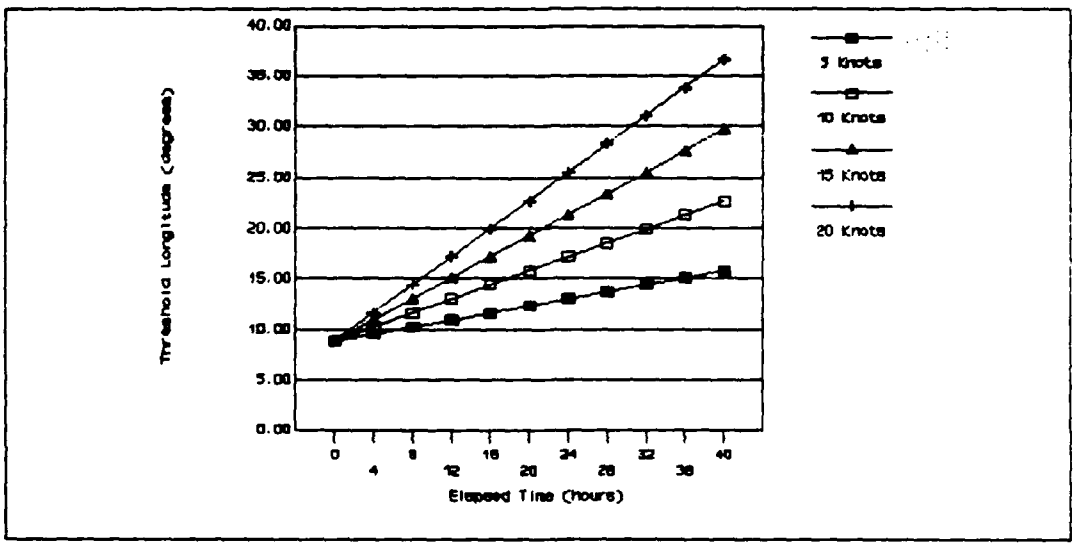

Figure 19. Threshold Longitude vs Elapsed Time

latitude and the Landsat 5 swath in Figure 19. Curves plotted for Landsat 5 and SPOT 1 are provided in Appendix E.

Having determined that there will be overlap at time t_2, the question remains as to how much area is overlapped. This overlap will depend on the size of the sensor swath and the size of the possible target area. The general situation of overlap is shown in Figure 20. Since the longitude of

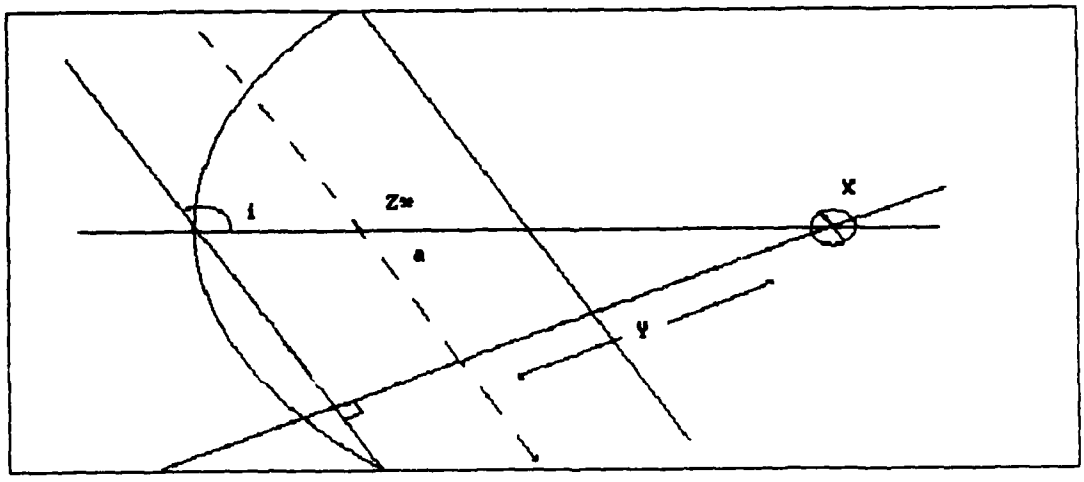

Figure 20. Sensor Swath Overlapping Possible Target Area

the subsatellite point Z* is known, the distance (Z* - X) can be determined using:

$$(Z^* - X) = \frac{(l_* - l_X)\ Cir_L}{360^\circ} \qquad (54)$$

Where l_* = longitude of Z*
l_X = longitude of initial contact

Once (Z* - X) is known, the distance Y is:

$$Y = (Z^* - X) \sin(a) \qquad (55)$$

Once Y is known the area of the swath can be determined geometrically. Two situations can exist. First, Y may be less than half the swath width of the sensor, in which case

the swath stradles the initial target location. Second, Y may be greater than or equal to half the swath width of the sensor, in which case the swath falls in only one half of the circle.

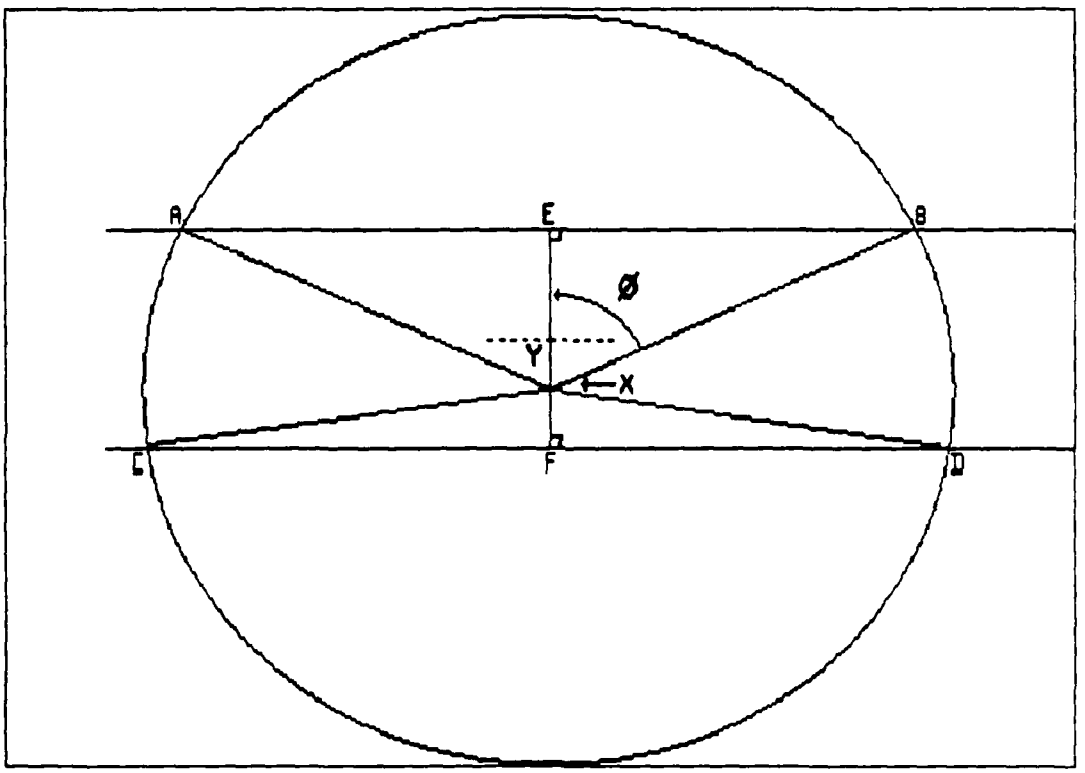

Figure 21. Geometry for Swath Overlapping Center of Possible Target Area

Figure 21 shows the geometry which results when Y is less than half the sensor's swath width. In this case the area of the circle which is overlapped by the swath is given in equation 56.

$$A_{SWC} = A_{cir} - (S_{XAB} - A_{XAB}) - (S_{XCD} - A_{XCD}) \quad (56)$$

Where A_{SWC} = area of swath overlap in circle
A_{cir} = area of the circle
S_{XAB} = area of sector XAB
A_{XAB} = area of triangle XAB
S_{XCD} = area of sector XCD
A_{XCD} = area of triangle XCD

The angle (Ø) is calculated using:

$$\cos(Ø) = \frac{Y + S_w/2}{t_d s} \quad (57)$$

Where $t_d = t_2 - t_1$

The angle FXD, (ß) is:

$$\cos(ß) = \frac{S_w/2 - Y}{t_d s} \quad (58)$$

The area of sector XAB is:

$$S_{XAB} = \frac{2Ø}{360} (\pi t_d^2 s^2) \quad (59)$$

The area of triangle XAB is:

$$A_{XAB} = (S_w/2 + Y)^2 \tan(Ø) \quad (60)$$

The area of sector XCD is:

$$S_{XCD} = \frac{2\beta}{360} (\pi t_d^2 s^2) \qquad (61)$$

The area of triangle XCD is:

$$A_{XCD} = (S_w/2 - Y)^2 \tan(\beta) \qquad (62)$$

The analysis for determining the area of overlap when the swath overlaps the initial contact point is not quite complete. There are two special situations that require additional consideration.

First, the situation could arise that the subsatellite point of the sensor's next crossing of the initial contact latitude exactly corresponds to the initial detection point. This is shown in Figure 22. In this case the P_{trkcon} remains at unity until the possible target area exceeds

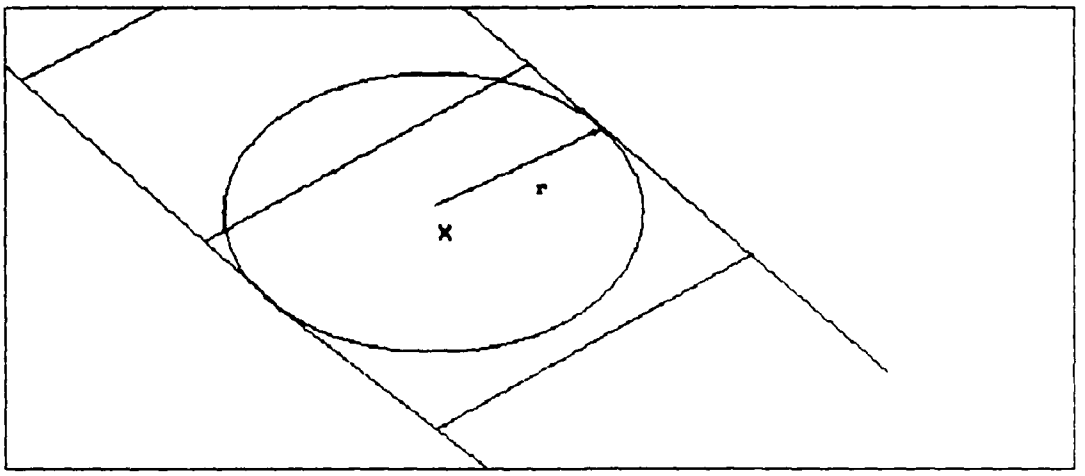

Figure 22. Geometry for Sub-Satellite Point Exactly Over Initial Target Location

the size of the swath width. Therefore when equation 63 is true the P_{trkcon} is assigned a value of 1.

$$t_d s - S_W/2 \leq 0 \tag{63}$$

Second, in the situation that the sensor's swath contains the initial contact point, there is a period of time when the possible target area does not fully extend through the sensor's swath. This is shown in Figure 23. For any t_d less than the time required to travel to the edge

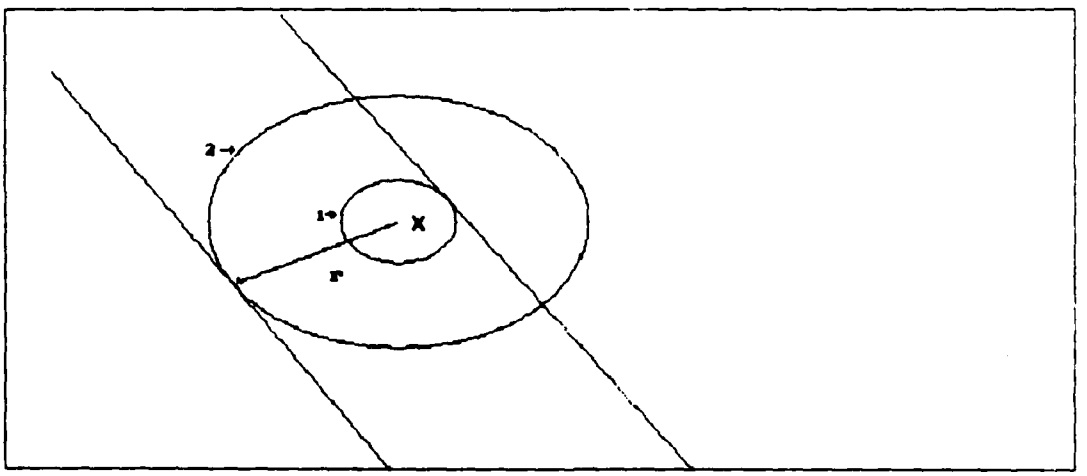

Figure 23. Geometry for Swath Overlapping Initial Target Location

of circle 1, the P_{trkcon} must be 1. For the period it takes to transit from circle 1 to circle 2, the formula for overlap is given in equation 64.

$$A_{SWC} = A_{cir} - (S_{XCD} - A_{XCD}) \tag{64}$$

Figure 24 shows the geometry which results when Y is greater than half the sensor's swath width. In this case the area of the circle which is overlapped by the swath is:

$$A_{SWC} = S_{XDC} - A_{XDC} - [S_{XAB} - A_{XAB}] \quad (65)$$

Where S_{XDC} = area of sector XDC
A_{XDC} = area of triangle XDC
S_{XAB} = area of sector XAB
A_{XAB} = area of triangle XAB

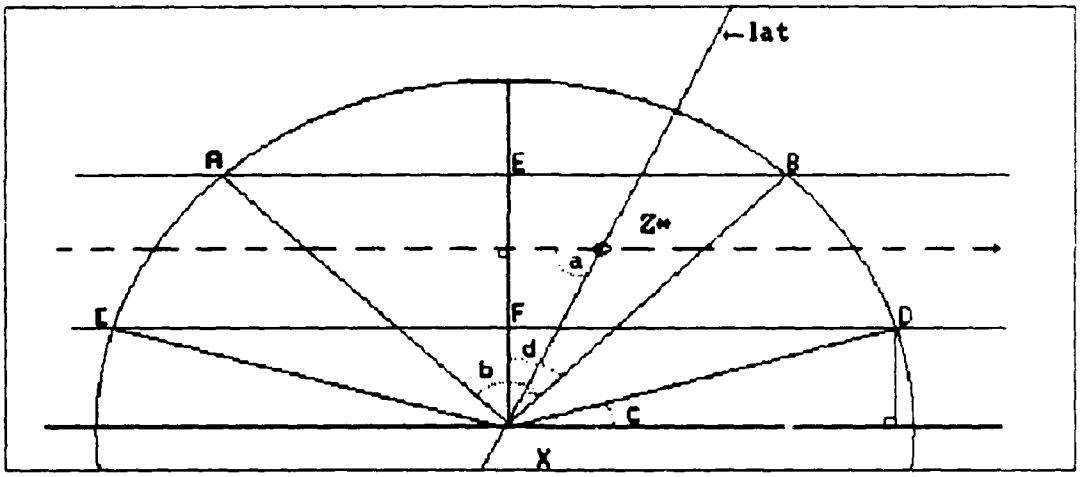

Figure 24. Geometry for Swath Not Overlapping Center of Possible Target Area

The angle (c) is calculated using:

$$\sin(c) = \frac{Y - S_W/2}{t_d s} \quad (66)$$

The area of sector XDC is then:

$$S_{XDC} = \frac{2(90^\circ - c)}{360^\circ} (\pi t_d^2 s^2) \quad (67)$$

The area of triangle XDC is:

$$A_{XDC} = \cos(c) t_d s (Y - S_w/2) \quad (68)$$

The angle (d) is:

$$\cos(d) = \frac{Y + S_w/2}{t_d s} \quad (69)$$

The area of sector XAB is:

$$S_{XAB} = \frac{2d}{360^\circ} (\pi t_d^2 s^2) \quad (70)$$

The area of triangle XAB is:

$$A_{XAB} = (Y + S_w/2) t_d s \sin(d) \quad (71)$$

Pointable Sensors. All of the geometry to this point in the analysis is used to calculate the overlap of the sensor swath and target area for a sensor which looks only directly below itself. How does this change in the case of satellites that can point their sensors at targets which are offset from the satellite ground trace?

The geometry for a pointable sensor's overlap with a target area is shown in Figure 25. The first difference in this analysis as compared to fixed sensor analysis is the value of the distance Y. This distance is again calculated using equations 55 and 56. However since Y is equal to the distance from the ground trace to the initial target location, in the threshold case it is the distance off track the sensor is pointing (Z-S*) plus half the swath width of the sensor plus the target speed times the elapsed time (r).

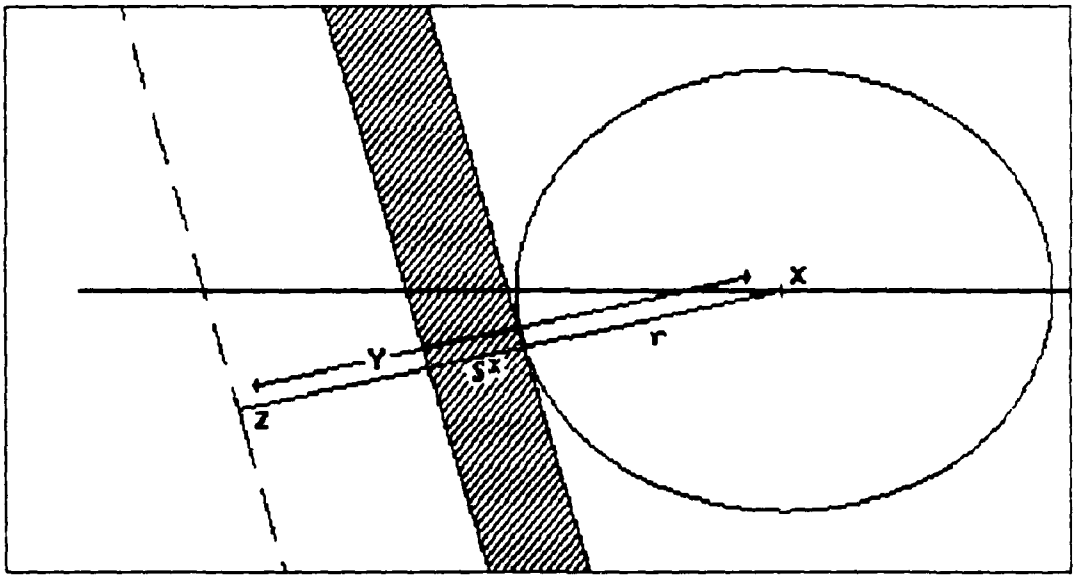

Figure 25. Pointable Sensor Threshold Overlap

Again the swath may or may not overlap the point of initial target detection. In the case of swath overlap with the point X, the distance Y will be less than the distance (Z-S*) plus half of the swath width of the sensor. This is

shown in Figure 26. In the figure the distance d2 is equal to (Z-S*) plus half the swath width minus Y.

$$d2 = (Z-S^*) + S_W/2 - Y \qquad (72)$$

The distance d1 is Y minus (Z-S*) plus half the swath width. Using these distances the area of the swath overlap with the target area can be calculated using equations 56 through 64.

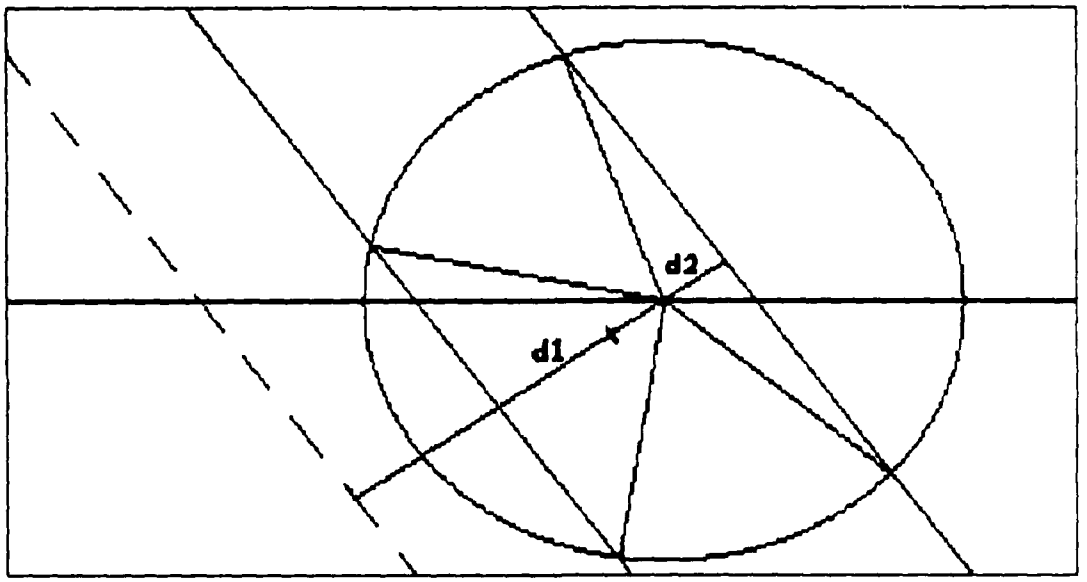

Figure 26. Geometry for Pointable Sensor Swath Overlap

If the sensor's swath does not overlap the initial target location, the swath overlap geometry is shown in Figure 24. In this case the distance XF is calculated by subtracting the distance (Z-S*) and half the swath width from the distance Y. Thereafter the calculations for overlap follow those developed in equations 65 through 71.

Conditional Tracking Probability Calculation. All of the geometry shown so far contributes one half of the information needed to determine the conditional tracking probability. The second half is just the total possible target area, A_{pos}. It is:

$$A_{pos} = \pi t_d^2 s^2 \tag{73}$$

Finally, an expression for the probability of tracking, conditional on the sensor seeing the target, can be written.

$$P_{trkcon} = \frac{A_{SWC}}{A_{pos}} \tag{74}$$

The P_{trkcon} is sensor specific. Defining the sensor's response time, t_d, to be the elapsed time between the initial target contact and the time of sensor crossing of last known target latitude, the P_{trkcon} can be plotted against sensor response time. The general form of the curve is shown in Figure 27, which is made using the Landsat 5 swath, an initial target latitude of 60°N, and target speed of 5 Knots.

Not only does the P_{trkcon} decreases rapidly as the possible target area increases, but also more images are required to achieve the P_{trkcon}. The relationship between the equivalent number of images required to achieve the maximum P_{trkcon} and response time is shown in Figure 28.

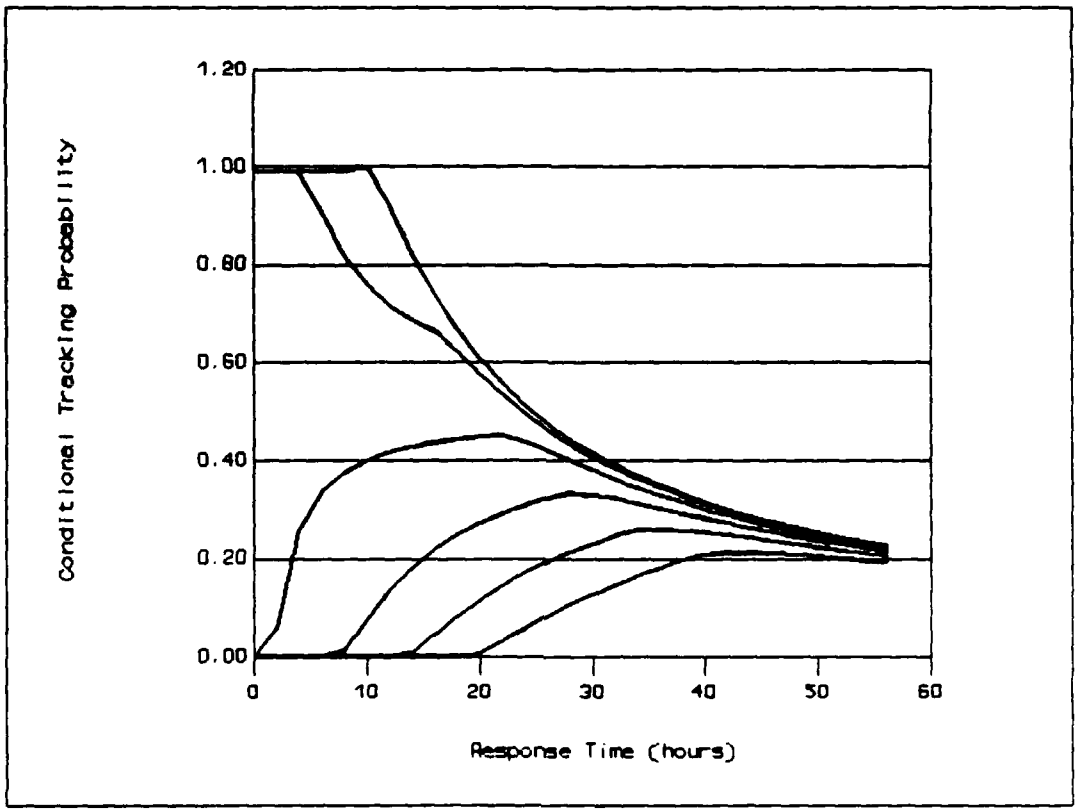

Figure 27. Conditional Tracking Probability verses Response Time
(Top to bottom are 0,1,2,3,4,5° Longitude Displacement)

Figure 27 shows the conditional tracking probability for a single sensor, a single target speed, and a single initial target detection latitude. There are many combinations of these variables. Nonetheless, comparative plots of conditional tracking probabilities can be used as a first check to determine if a given sensor could provide an acceptable response. For this reason conditional tracking curves for Landsat 5 and SPOT 1 are included in Appendix F.

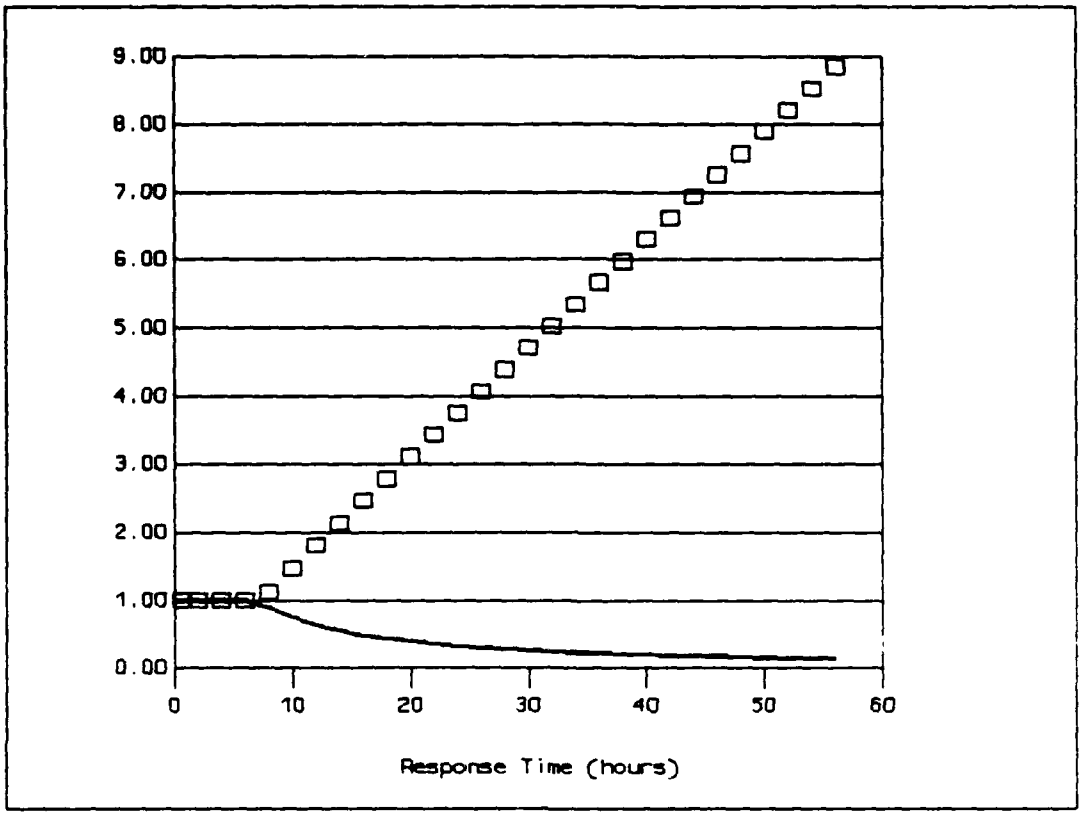

Figure 28. Conditional Tracking Probability and Equivalent Number of Images vs Response Time

The P_{trkcon} calculated above, when divided by the equivalent number of images required to achieve it, is a measure of the conditional probability of tracking in a single image, or:

$$P_{tim} = \frac{P_{trkcon}}{E_{qim}} \tag{75}$$

Where P_{tim} = conditional tracking probability per equivalent image
E_{qim} = equivalent number of images

It is the P_{tim}, when multiplied by the P_{det*} that gives the probability of tracking the target in a single image, or P_{track1}:

$$P_{track1} = P_{tim}P_{det*} \tag{76}$$

Optimization Tracking Algorithm -- Second Contact

The algorithm chosen to optimize the probability of tracking a target depends on whether overlapping or non-overlapping images are available.

In the case of non-overlapping images, P_{track} can be maximized using linear programming. The objective function to be maximized is given in equation 77.

$$\sum_{i=1}^{n} (N_{im})_i P_{tracki} \tag{77}$$

Subject to the constraint set:

$$\sum_{i=1}^{n} (N_{im})_i C_i \leq B_{\$} \tag{78}$$

$$0 \leq x_i \leq K_i \tag{79}$$

Where K_i = maximum number of images available from sensor i

If there is overlapping coverage, the optimization becomes untidy. The untidiness occurs since the objective function must account for areas of single and overlapping

coverage. An example of overlapping swaths is shown in Figure 29.

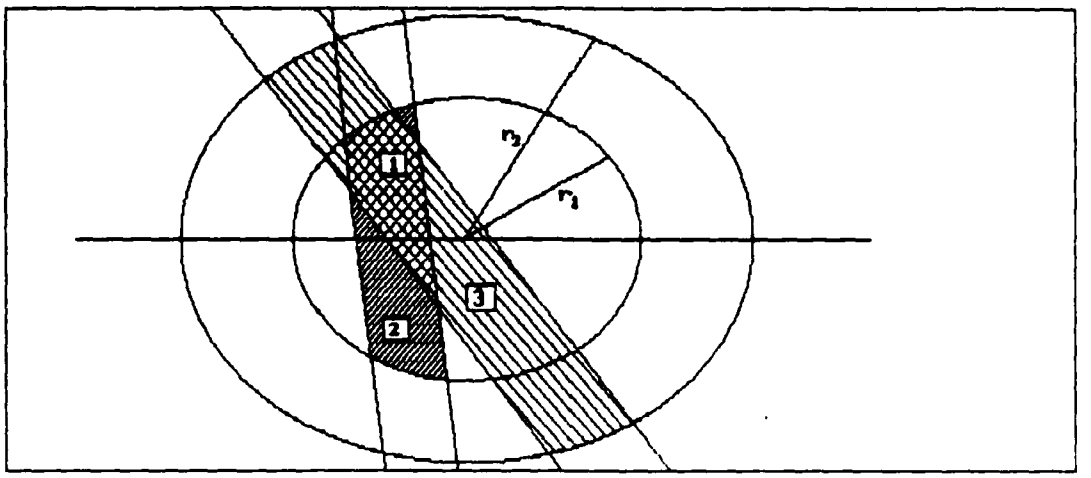

Figure 29. Overlapping Swath Coverage Geometry

In the figure, Sensor A passes overhead at time t1, Sensor B passes overhead sometime later at time t2. The areas of single and double coverage depend on the swath widths of the sensors, the sensors' inclinations, and the time of each of the sensor's passages overhead.

The areas in which only a single sensor provides coverage behave linearly--that is, their contribution to overall tracking probability provided by images acquired in these areas will increase linearly as a function of the number of images. Given complete overlap of multiple imaged areas, their contribution to the overall P_{track} will be non-linear. However, since in a given situation the individual P_{track} values will be known, and since only one image from

each sensor can be taken of an area on the ground in a single pass, the combined $P_{track1+2}$ is fixed and is:

$$P_{track1+2} = 1-((1-P_{track1})(1-P_{track2})) \quad (80)$$

Since $P_{track1+2}$ is a fixed value it also contributes to the objective function linearly. Therefore optimization for overlapping coverage, assuming the overlap is complete, can be accomplished through linear programming. The form of the objective function to be maximized is:

$$P_{track} = x_1P_{track1} + x_2P_{track2} + x_{1+2}P_{track1+2} \quad (81)$$

Where $x_{1,2}$ = number of non-overlaping images acquired from sensors 1,2
x_{1+2} = number of overlapping images taken

The constraint set is:

$$x_1C_1 + x_2C_2 + x_{1+2}(C_1+C_2) \leq B_\$ \quad (82)$$

$$x_1 \leq E_{qim1}(\text{Area Single Coverage 1/Total Swath 1}) \quad (83)$$

$$x_2 \leq E_{qim2}(\text{Area Single Coverage 2/Total Swath 2})$$

$$x_{1+2} \leq E_{qim1}(\text{Area Double Coverage/Total Swath Double})$$

In practice single area coverage will be exhausted prior to the acquisition of overlapping images. This is true since a combined image yields a $P_{track1+2}$ which is

lower than the sum of its components in all cases, but which costs the same as the individual images.

Tracking Algorithm -- Follow-on Contacts

Once a target's position is plotted for two points in time, its location at any subsequent time can be predicted. Assuming the target's velocity remains constant, the task of establishing follow-on contacts reduces to cued detection and the algorithms developed for cued detection of stationary targets can be applied. The only glitch that remains is determining if and when the sensor will overfly the target.

The question of simultaneous target location and sensor swath overlap can be broken into two constituent parts; how soon will the target penetrate a specific ground swath, and how long will the target take to traverse the swath. With these two pieces of information, it is possible to determine whether the satellite will overfly the target on a given pass. That is, a window of opportunity for imaging during a specific pass can be determined.

The first piece of information to determine is how soon a target will penetrate a specific ground swath. Figure 30 illustrates the geometry. The shortest path to the swath is perpendicular to the inclination of the sensor's orbit. This distance is given by equation 84.

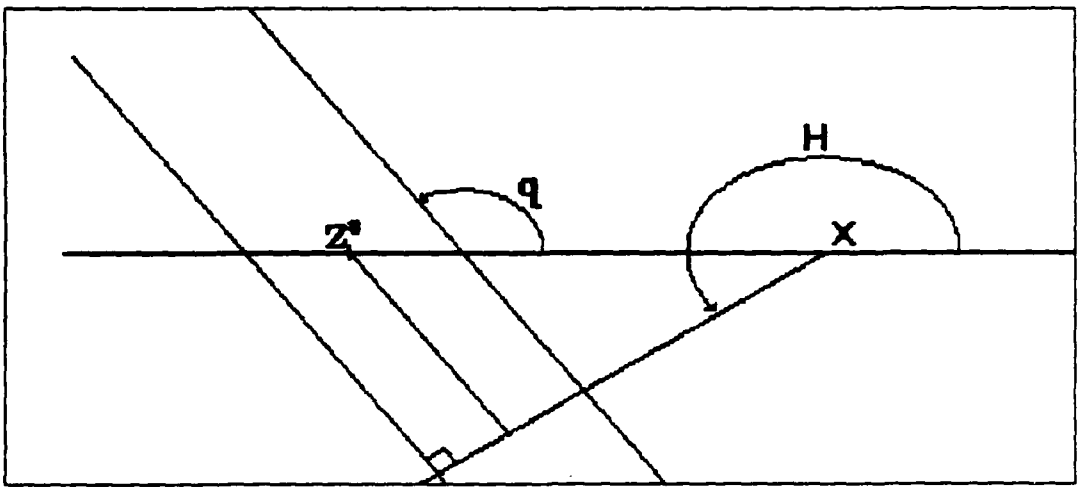

Figure 30. Swath Penetration Geometry

$$D_{sh} = \sin(a)\,\ell^{\circ}(F) - S_w/2 \qquad (84)$$

Where D_{sh} = shortest path
F = # km per degree longitude at latitude

The distance to the swath increases as the target heading varies from the perpendicular. The distance to the swath for any angle other than the perpendicular is determined by dividing the shortest distance by the cosine of the angle between the target heading (H) and the perpendicular. Therefore, the distance to the swath is:

$$D = \frac{\sin(a)\,\ell^{\circ}(F) - S_w/2}{\cos(H-i-90)} \qquad (85)$$

A negative result for D indicates that the target is heading away from the swath. This would occur if the target were heading East and the sensor's swath under consideration were West of the target's last known position.

Once the distance from the target's last known position to the swath is calculated, the time it takes to transit this distance is just the distance divided by the target's speed. This provides the first piece of information needed for the imaging window.

The second piece of information needed for the imaging window is the time it will take the target to transit a swath. The geometry of swath transit is also shown in Figure 30. The difference is that the shortest distance in this case is the swath width itself. Using the swath width as the numerator in equation 85, swath transit times for a given target speed can be worked out.

Optimization Tracking Algorithm -- Follow-on Contacts

If the above analysis yields several imaging opportunities, the task remains to optimize the selection of sensors. A complexity arises since the value of the target being tracked will dictate the frequency with which track updates will be required. At one extreme, a low value target may not require tracking. At the other extreme a high value target may require continuous track updates.

Once again two distinct approaches can be taken to optimize selection of sensors. If the goal is to maximize the probability of at least one detection of the target, the objective function becomes:

$$P_{d\geq 1} = 1 - P_{nodet} \tag{86}$$

Where $P_{nodet} = \prod(1-P_{det*ij})$
P_{det*ij} = single image detection probability for sensor i on pass j

And the constraint set is:

$$\sum(N_{im})_i C_i \leq B_s \tag{87}$$

$$0 \leq (N_{im})_i \leq K_i \tag{88}$$

Where K_i = maximum number of images available from sensor i

Once again there are a variety of non-linear programming alternatives which can optimize the objective function subject to the constraint set.

Summary

In summary, this chapter has answered the second question. That is, the selection of sensors from those available is accomplished by optimizing the performance of the system of sensors. The system performances are measured in terms of its probabilities of detecting or tracking

targets. Therefore, the selection of imagery from a specific sensor depends on how large its contribution to the overall system's probabilities of detection and tracking is in comparison to the options which are available.

VI. Analysis

General

The third question to resolve is how valid are the algorithms which have been developed in Chapter V.? As with all models, the quality of the output will depend on the quality of the input. Nonetheless there is value in developing the algorithms for specific situations since this will afford face validity to the methodology itself. Thus, this analysis chapter presents an example formulation in each mission area.

Example Analyses

At the start of an analysis the analyst must specify the mission, the target(s) of interest and the time frame for consideration. Based on the target of interest and the mission, the area of interest can be defined. Based on this area and the time frame of the analysis, all possible backgrounds can be described in spatial, spectral, and temporal terms. Similarly, all targets can be described in these three domains. Next, the possible sensors can be selected based on the time frame of the analysis.

Using this database, the analysis begins. The first question to be answered is whether the sensor will detect the target against the background under ideal conditions.

This requires analysis of each sensor with every possible target and background combination. For visible wavelength sensors, equation 10 is used. If the actual target area is larger than the threshold target area, the target can be detected by the sensor. For quick reference Appendix C contains threshold detection curves for various sensors. Similarly, equation 24 is used to determine if a thermal wavelength sensor can detect a target under ideal conditions.

Comparing actual target areas to threshold target areas returns a P_{det} of one (1) in the case of detection, or zero (0) in the case of no detection. At this point in the analysis, all target, background, and sensor combinations which return a P_{det} of 0 are discarded.

To this point the steps required are common for all the missions. They form a checklist of actions which begin every analysis. In contrast, subsequent analysis depends on the mission under consideration. To continue this example it is assumed that the mission is non-cued detection of stationary targets.

The next step in the analysis is to determine the P_{det} considering detector array geometry. This is accomplished using equations 27, 28, and 29. It is this value of Pdet which is carried into the rest of the analysis.

The analysis continues with the partitioning of the target area into areas of common obscuration. Once this is done, the P_{det*} for each combination of sensor, target, background, and location can be determined using equations 35 and 36. If the irradiation factor for a combination is zero (0), this combination is discarded.

Having determined the P_{det*} values for the surviving combinations, the next task in the analysis is to work out the corresponding P_{dot1} value for each, using equation 41. The area of interest here is the area of common obscuration.

At this point the linear program can be written. In this example, the objective function to be maximized is equation 42, and the constraint set is furnished by equations 43, 44, and 45, and by specifying each area must return the same P_{dsys}. Solving the linear program gives the P_{dsys} achievable for the budget specified.

Appendix H provides checklists for analysis start and for each mission.

The remainder of this chapter contains example analyses using the representative target set described in Appendix D. Each mission area is analyzed. Sources of data are enclosed in parentheses.

First Analysis: Non-Cued Detection of Stationary Targets

START -- Checklist 1

1. Mission: Non-cued detection of stationary targets

   Target: Survey Parties

   Time frame: Month of January

2. Area of interest: 60°W - 142°W, 60°N - 83°N

3. Possible background(s): Snow (Ref:18)

4. Background characteristics:

   Spatial - Elevation ≤ 1000 meters (Ref:12)

   Spectral - Reflectance 0.9 (16:7)

   - Emissivity (10-12 μm) .985 (16:7)

   Temporal - No change in time frame

5. Target characteristics: (Appendix D)

   Spatial - Vehicles up to 50 m^2

   Spectral - Reflectance 0.12

   - Emissivity .92, 1/4 surface area 2°K warmer than ambient

   Temporal - No change in time frame

6. Sensors available: NOAA AVHRR

   Landsat 5 MSS, TM

   SPOT 1 HRV

   Sojuzkarta*

   * Not considered due to the delay in receipt of the image

7. P_{det} calculation:

   Visible - $(R_t - R_b) = .78$

Table 3. Visible Sensor First Analysis

Sensor	$A_{ti}(m^2)$	P_{det}
AVHRR	1800 (Fig. C17)	0
MSS	67 (Fig. C7)	0
TM	10 (Fig. C5)	1
HRV	1 (Fig. C1)	1

Thermal - Target exitance 28.8 W/m^2

Table 4. Thermal Sensor First Analysis

Sensor	$A_{ti}(m^2)$	P_{det}
TM Band 6	1 (Fig. G4)	1

8. Surviving options: Landsat TM Band 1,3 or 4

Landsat TM Band 6

SPOT HRV

9. End checklist 1

Checklist 2: Non-Cued Detection of Stationary Targets

1. Landsat 5 and SPOT 1 detector arrays are staggered, and there are effectively no gaps in the detector array. Thus if $A_t \geq 4*A_{ti}$, P_{det} remains at one (1). For all surviving sensors this is true.

2. Partition area of interest: The two considerations are darkness and cloud cover since both thermal and visible sensors have survived to this point.

Darkness -

A. Period of satellites - Landsat 5 is 98.9 minutes
- SPOT 1 is 101.5 minutes

B. Using equations 32, 33 and the local sidereal times of sunrise and sunset, the time each sensor passes overhead a given latitude can be worked out and a value for I_{fac} determined. Table 5 contains these values.

Table 5. I_{fac} Determination

Latitude	Landsat T_{lat}	I_{fac}	SPOT T_{lat}	I_{fac}
0	0945		1030	
60	0928	1	1013	1
62	0928	1	1012	1
64	0927	1	1012	1
66	0927	0	1011	1
68	0926	0	1011	1
70	0926	0	1010	0
72	0925	0	1010	0

Cloud cover -

Cloud cover data is taken from Reference 18. Superimposing the areas of darkness and cloud cover yields six distinct areas of common obscuration. These are shown in Figure 31.

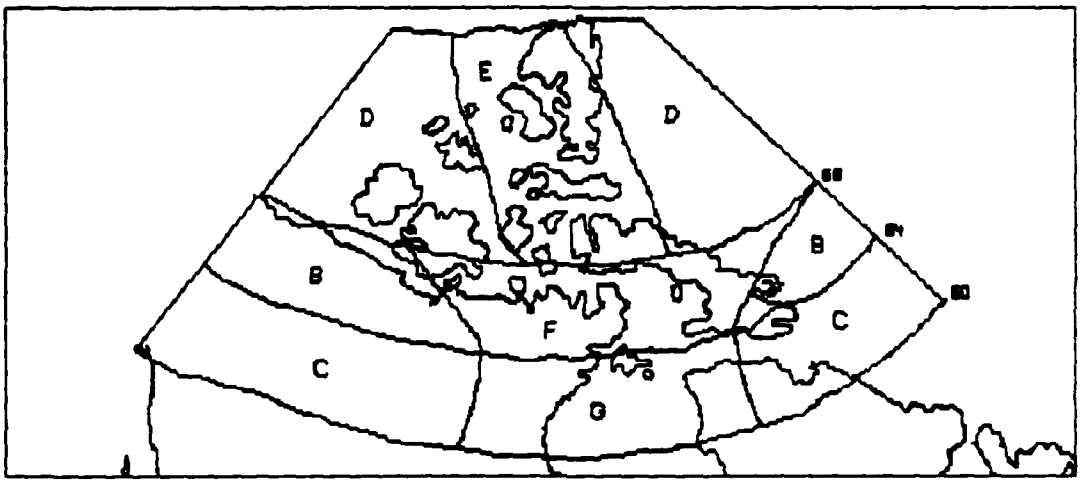

Figure 31. First Analysis Areas of Common Obscuration

3/4/5. P_{det*} , P_{dot1} calculation:

A. Approximate areas of each of these regions are shown in Table 6.

Table 6. Areas of Regions of Common Obscuration
First Analysis

Region	Area (km^2)
B	805450
C	1278040
D	3017460
E	691380
F	845500
G	627450

B. Table 7 contains the values for P_{det*} and P_{dot1} for each region.

Table 7. First Analysis P_{det*} and P_{dot1}

Region	P_{cloud}	Sensor	P_{det*}	P_{dot1}
B	.6	LT	.4	1.88E-3
		HRV	.4	1.98E-4
C	.6	LT	.4	1.88E-3
		LV	.4	1.88E-3
		HRV	.4	1.98E-4
D	.5	LT	.5	2.36E-3
E	.4	LT	.6	2.83E-3
F	.5	LT	.5	2.36E-3
		HRV	.5	2.48E-4
G	.5	LT	.5	2.36E-3
		LV	.5	2.36E-3
		HRV	.5	2.48E-4

Legend : LT - Landsat 5 Band 6
LV - Landsat 5 Band 3
HRV - SPOT 1

6. The goal of this analysis is to maximize the system wide probability of detection given a total of $1,000,000.00 for the time frame under analysis.

7. A. Since Landsat 5 Band 6 and Band 3 sensors return the same probability of detection and cost the same, where both are available only Band 3 is carried forward for analysis. Using equation 42 as the template the objective function is given in equation 89.

$$P_{dsys} = 1.88E\text{-}3\ X1 + 1.88E\text{-}3\ X2 + 2.36E\text{-}3\ X3 + 2.83E\text{-}3\ X4 + 2.36E\text{-}3\ X5 + 2.36E\text{-}3\ X6 + 1.98E\text{-}4\ X7 + 1.98E\text{-}4\ X8 + 2.48E\text{-}4\ X9 + 2.48\ E\text{-}4\ X10 \quad (89)$$

Where X1 = # images taken by Landsat in region B
X2 = # images taken by Landsat in region C
X3 = # images taken by Landsat in region D
X4 = # images taken by Landsat in region E
X5 = # images taken by Landsat in region F
X6 = # images taken by Landsat in region G
X7 = # images taken by SPOT in region B
X8 = # images taken by SPOT in region C
X9 = # images taken by SPOT in region F
X10 = # images taken by SPOT in region G

7. B. The cost of a Landsat TM image is $4,600.00. The cost of a SPOT image is $1000.00 (43:357). Using equation 43 as the template the cost constraint is:

$$4600\ X1 + 4600\ X2 + 4600\ X3 + 4600\ X4 + 4600\ X5 + 4600\ X6 + 1000\ X7 + 1000\ X8 + 1000\ X9 + 1000\ X10 \leq 1000000 \quad (90)$$

7. C. Using equation 44 as the template, the restriction on overlapping images is:

$$34225\ X1 + 3600\ X7 \leq 805450 \quad (91)$$

$$34225\ X2 + 3600\ X8 \leq 1278040 \quad (92)$$

$$34225\ X3 \leq 3017460 \quad (93)$$

$$34225\ X4 \leq 691380 \quad (94)$$

$$34225\ X5 + 3600\ X9 \leq 845500 \quad (95)$$

$$34225\ X6 + 3600\ X10 \leq 627450 \quad (96)$$

7. D. The final set of constraints restrict the probabilities of detection within each region to be within a

specified range of each other. This prevents domination of one region of clear weather at the expense of coverage in harder-to-image regions. To do this the area of the region is used to specify a local P_{dot1} and this figure is used to balance the regions.

$$1.7E\text{-}2\ X1 + 1.8E\text{-}3\ X7 - 1.07E\text{-}2 - 1.13E\text{-}3 \leq .1 \quad (97)$$

$$1.7E\text{-}2\ X1 + 1.8E\text{-}3\ X7 - 1.07E\text{-}2 - 1.13E\text{-}3 \geq -.1 \quad (98)$$

$$1.7E\text{-}2\ X1 + 1.8E\text{-}3\ X7 - 5.67E\text{-}3\ X3 \leq .1 \quad (99)$$

$$1.7E\text{-}2\ X1 + 1.8E\text{-}3\ X7 - 5.67E\text{-}3\ X3 \geq -.1 \quad (100)$$

$$1.7E\text{-}2\ X1 + 1.8E\text{-}3\ X7 - 2.97E\text{-}4\ X4 \leq .1 \quad (101)$$

$$1.7E\text{-}2\ X1 + 1.8E\text{-}3\ X7 - 2.97E\text{-}4\ X4 \geq -.1 \quad (102)$$

$$1.7E\text{-}2\ X1 + 1.8E\text{-}3\ X7 - 2.02E\text{-}2\ X5 - 2.13E\text{-}3\ X9 \leq .1 \quad (103)$$

$$1.7E\text{-}2\ X1 + 1.8E\text{-}3\ X8 - 2.02E\text{-}2\ X5 - 2.13E\text{-}3\ X10 \geq -.1 \quad (104)$$

$$1.7E\text{-}2\ X1 + 1.8E\text{-}3\ X7 - 2.73E\text{-}2\ X6 - 2.87E\text{-}3\ X10 \leq .1 \quad (105)$$

$$1.7E\text{-}2\ X1 + 1.8E\text{-}3\ X7 - 2.73E\text{-}2\ X6 - 2.87E\text{-}3\ X10 \geq -.1 \quad (106)$$

9. This linear program was solved.

Second Analysis: Non-Cued Detection of Moving Targets

START -- Checklist 1

1. Mission: Non-cued detection of moving targets

   Target: Ship

   Time frame: Month of July

2. Area of interest: Arctic waterways

   Approximately 3,000,000 km^2 (12:23)

3. Possible background(s): Water

4. Background characteristics:

   Spatial - Sea level

   Spectral - Reflectance 0.09 (16:7)

   - Emissivity (10-12 μm) 0.99 (16:7)

   Temporal - No change in time frame

5. Target characteristics: (Appendix D)

   Spatial - 121 x 15 meters

   Spectral - Reflectance 0.85

   - Emissivity 0.74, 1/10 surface area 2°K warmer than ambient

   Temporal - In area of interest entire month

6. Sensors available: NOAA AVHRR

   Landsat 5 MSS, TM

   SPOT 1 HRV

7. P_{det} calculation:

   Visible - $(R_t - R_b) = 0.76$

Table 8. Visible Sensor Second Analysis

Sensor	A_{ti} (m^2)	P_{det}
AVHRR	1800 (Fig. C18)	0
MSS	67 (Fig. C8)	1
TM	8 (Fig. C6)	1
HRV	1 (Fig. C2)	1

Thermal - Target exitance 56.7 W/m^2

Table 9. Thermal Sensor Second Analysis

Sensor	A_{ti} (m^2)	P_{det}
TM Band 6	1 (Fig. G7)	1

8. Surviving options: Landsat MSS (any band)

Landsat TM Band (any band)

SPOT HRV

9. End checklist 1

Checklist 3: Non-Cued Detection of Moving Targets

1. As discussed in the first analysis, all P_{det} values remain at one (1).

2. Partition area of interest: The only consideration is cloud cover since the I_{fac} value is one (1) for both Landsat and SPOT.

Cloud cover -

Cloud cover data is taken from Reference 18. For the month of July the probability of cloud cover is approximately 0.8 throughout the area. As a result the area of interest is not partitioned.

3/4/5. P_{det*} ,P_{dot1} calculation:

Table 10 contains the values for P_{det*} and P_{dot1} for each sensor.

Table 10. Second Analysis P_{det*} and P_{dot1}

Region	P_{cloud}	Sensor	P_{det*}	P_{dot1}
Entire	.8	TM	.2	2.28E-3
		MSS	.2	2.28E-3
		HRV	.2	2.40E-4

6. The goal of this analysis is to maximize the system wide probability of detection given $100,000.00 for the time frame of the analysis.

7. A. The objective function is:

$$P_{d\geq 1} = 1 - ((1-2.28E-3)^{X1}(1-2.28E-3)^{X2}(1-2.4E-4)^{X3}) \quad (107)$$

Where X1 = number of images taken by Landsat TM
X2 = number of images taken by Landsat MSS
X3 = number of images taken by SPOT

7. B. The cost of a Landsat MSS image is $1,000.00 (43:357). Using equation 43 as the template the cost constraint is:

$$4600\ X1 + 1000\ X2 + 1000\ X3 \leq 100000 \quad (108)$$

Since the area of interest is not partitioned in this analysis, additional constraints designed to return even $P_{d\geq 1}$ values from each unique region are not necessary.

7. C. This model was not solved.

Third Analysis: Cued Detection of Stationary Targets

START -- Checklist 1

1. Mission: Cued detection of stationary targets

   Target: Survey Parties

   Time frame: Months of April, May, and June

2. Area of interest: Target location 5 (see Figure 32)
   Banks Island 123°W 73°N

   Target location 1
   Southampton Island 85°W 65°N

   Target location 4
   Axel Heiberg Island 95°W 80°N

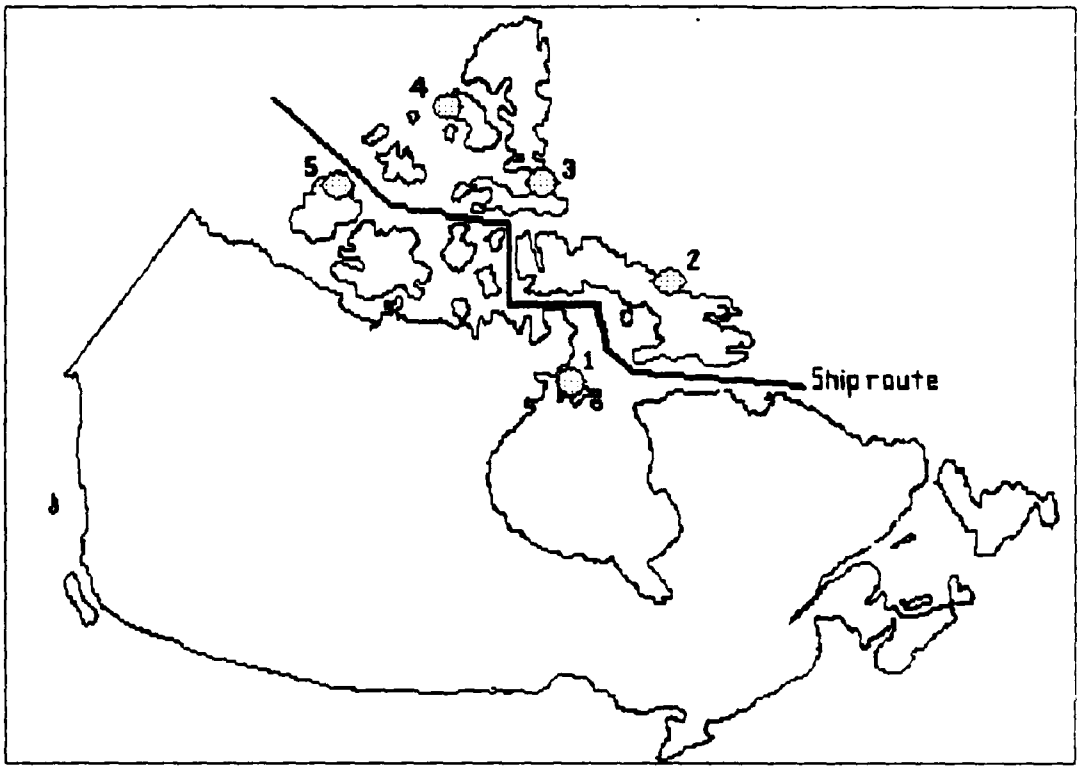

Figure 32. Fixed Target Locations and Ship Route

3. Possible background(s): Snow (Ref:18)

Ground

4. Background characteristics:

Snow -

Spatial - Elevation ≤ 1000 meters (Ref:12)

Spectral - Reflectance 0.9 (16:7)

- Emissivity (10-12 μm) .985 (16:7)

Temporal - Change in time frame to ground

Ground -

Spatial - As above

Spectral - Reflectance 0.25 (16:7)

- Emissivity (10-12 μm) 0.94 (16:7)

Temporal - No further change in time frame

5. Target characteristics: (Appendix D)

Spatial - Vehicles up to 50 m^2

Spectral - Reflectance 0.12

- Emissivity .92, 1/4 surface area 2°K warmer than ambient

Temporal - No change in time frame

6. Sensors available: NOAA AVHRR

Landsat 5 MSS, TM

SPOT 1 HRV

7. P_{det} calculation:

Visible - Background of snow, $(R_t - R_b) = .78$

- Background of ground, $(R_t - R_b) = .13$

Table 11. Visible Sensor Third Analysis

Sensor	$A_{ti}(m^2)_{Snow}$	P_{det}	$A_{ti}(m^2)_{Ground}$	P_{det}
AVHRR	1800 (Fig. C17)	0	** (Fig. C23)	0
MSS	67 (Fig. C7)	0	300 (Fig. C8)	0
TM Band 4	10 (Fig. C5)	1	25 (Fig. C6)	1
HRV	1 (Fig. C1)	1	4 (Fig. C3)	1

Thermal - Target exitance (@ 277°K) 42.8 W/m^2

Table 12. Thermal Sensor Third Analysis

Sensor	$A_{ti}(m^2)_{Snow}$	P_{det}	$A_{ti}(m^2)_{Ground}$	P_{det}
TM Band 6	1 (Fig. G5)	1	1 (Fig. G2)	1

8. Surviving options: Landsat TM Band 4

Landsat TM Band 6

SPOT HRV

9. End checklist 1

Checklist 4: Cued Detection of Stationary Targets

1. Table 13 shows the number of opportunities each satellite has in the 3 month period of interest.

Table 13. Imaging Opportunities

Target	Landsat 5	SPOT 1
Axel Heiberg	41	174
Banks	25	110
Southampton	8	73

2. P_{det} calculation:

P_{det} for TM Band 4 is 0.81

3. P_{det*} calculation:

Only cloud cover will obscure the target locations during the time frame of the analysis. Table 14 shows the results of P_{det*} for each target and sensor calculation.

Table 14. Third Analysis P_{det*}

Target	Month	P_{cloud}	Sensor	P_{det}	P_{det*}
Axel Heiberg	April	0.5	TM Band 4	1.0	0.5
			HRV	1.0	0.5*
			TM Band 6	1.0	0.5*
	May	0.7	TM Band 4	1.0	0.3
			HRV	1.0	0.3*
			TM Band 6	1.0	0.3*
	June	0.8	TM Band 4	0.81	0.16
			HRV	1.0	0.2
			TM Band 6	1.0	0.2
Banks	April	0.5	TM Band 4	1.0	0.5
			HRV	1.0	0.5*
			TM Band 6	1.0	0.5*
	May	0.75	TM Band 4	1.0	0.25
			HRV	1.0	0.25*
			TM Band 6	1.0	0.25*
	June	0.8	TM Band 4	0.81	0.16
			HRV	1.0	0.2
			TM Band 6	1.0	0.2
Southampton	April	0.6	TM Band 4	1.0	0.4
			HRV	1.0	0.4*
			TM Band 6	1.0	0.4*
	May	0.8	TM Band 4	1.0	0.2
			HRV	1.0	0.2*
			TM Band 6	1.0	0.2*
	June	0.8	TM Band 4	0.81	0.16
			HRV	1.0	0.2
			TM Band 6	1.0	0.2

* Discarded from further analysis since the same P_{det*} is available from the same sensor for the same cost.

4. The goal of this analysis is to maximize the probability of detection of targets given $10000.00 for the time frame of the analysis.

5. A. The objective function is:

$$P_{d\geq 1} = 1 - ((.5)^{x1}(.5)^{x2}(.7)^{x3}(.7)^{x4}(.84)^{x5}(.8)^{x6} \quad (109)$$
$$(.8)^{x7}(.5)^{x8}(.5)^{x9}(.75)^{x10}(.75)^{x11}$$
$$(.84)^{x12}(.8)^{x13}(.8)^{x14}(.6)^{x15}(.6)^{x16}$$
$$(.8)^{x17}(.8)^{x18}(.84)^{x19}(.8)^{x20}(.8)^{x21})$$

Where x1 = # TM Band 4 images taken of target 4 in April
x2 = # HRV images taken of target 4 in April
x3 = # TM Band 4 images taken of target 4 in May
x4 = # HRV images taken of target 4 in May
x5 = # TM Band 4 images taken of target 4 in June
x6 = # HRV images taken of target 4 in May
x7 = # TM Band 6 images taken of target 4 in June
x8 = # TM Band 4 images taken of target 5 in April
x9 = # HRV images taken of target 5 in April
x10 = # TM Band 4 images taken of target 5 in May
x11 = # HRV images taken of target 5 in May
x12 = # TM Band 4 images taken of target 5 in June
x13 = # HRV images taken of target 5 in June
x14 = # TM Band 6 images taken of target 5 in June
x15 = # TM Band 4 images taken of target 1 in April
x16 = # HRV images taken of target 1 in April
x17 = # TM Band 4 images taken of target 1 in May
x18 = # HRV images taken of target 1 in May
x19 = # TM Band 4 images taken of target 1 in June
x20 = # HRV images taken of target 1 in June
x21 = # TM Band 6 images taken of target 1 in June

5. B. The cost constraint is:

$$4600\,x1 + 1000\,x2 + 4600\,x3 + 1000\,x4 + 4600\,x5 \quad (110)$$
$$+ 1000\,x6 + 4600\,x7 + 4600\,x8 + 1000\,x9$$
$$+ 4600\,x10 + 1000\,x11 + 4600\,x12 + 1000\,x13$$
$$+ 4600\,x14 + 4600\,x15 + 1000\,x16 + 4600\,x17$$
$$+ 1000\,x18 + 4600\,x19 + 1000\,x20 + 4600\,x21 \leq 10000$$

5. C. The image availability constraints are:

$$x1 + x3 + x5 + x7 \leq 41 \quad (111)$$

$$x2 + x4 + x6 \leq 174 \quad (112)$$

$$x8 + x10 + x12 + x14 \leq 25 \quad (113)$$

$$x9 + x11 + x13 \leq 110 \quad (114)$$

$$x15 + x17 + x19 + x21 \leq 8 \quad (115)$$

$$x16 + x18 + x20 \leq 73 \quad (116)$$

5. D. This model was not solved.

Note: If operations dictate the requirement that the system deliver an equal probability of detection for each target, additional constraints must be written. These constraints would be similar in both form and effect as those written to ensure areas of common obscuration returned equal probabilities of detection in earlier analysis.

Fourth Analysis: Second Contact

START -- Checklist 1

1. Mission: Second Contact

   Target: Ship

   Time frame: Month of August

2. Area of interest: Arctic waterways

   Approximately 3,000,000 km^2 (13:23)

3. Possible background(s): Water

4. Background characteristics:

   Spatial - Sea level

   Spectral - Reflectance 0.09 (16:7)

   - Emissivity (10-12 μm) 0.99 (16:7)

   Temporal - No change in time frame

5. Target characteristics: (Appendix D)

   Spatial - 121 x 15 meters

   Spectral - Reflectance 0.85

   - Emissivity 0.74, 1/10 surface area 2°K warmer than ambient

   Temporal - Ship's top speed 10 Knots

6. Sensors available: NOAA AVHRR

   Landsat 5 MSS, TM

   SPOT 1 HRV

7. P_{det} calculation:

   Visible - $(R_t - R_b) = 0.76$

Table 15. Visible Sensor Fourth Analysis

Sensor	$A_{ti}(m^2)$	P_{det}
AVHRR	1800 (Fig. C18)	0
MSS	67 (Fig. C8)	1
TM	8 (Fig. C6)	1
HRV	1 (Fig. C2)	1

Thermal - Target exitance 56.7 W/m^2

Table 16. Thermal Sensor Fourth Analysis

Sensor	$A_{ti}(m^2)$	P_{det}
TM Band 6	1 (Fig. G7)	1

8. Surviving options: Landsat MSS (any band)

Landsat TM Band (any band)

SPOT HRV

9. End checklist 1

Checklist 5: Second Contact

1. The first step in this analysis would normally be supplied from the sensor's owners. To show the model formulation it is assumed that the initial contact with the target is 130°W 75°N, and that the position of Landsat 5 is 80°W 75°N and the position of SPOT 1 is 70°W 75°N five (5) hours after the initial contact with the target.

2. The Landsat 5 swath overlaps the possible target area in 8.3 hours as it crosses 75°N latitude at 129.5°W longitude.

SPOT has two opportunities to image the possible target area within 10 hours. The first occurs in eight (8) hours at 75°N 121°W. The second occurs in 10 hours at 75°N 146°W.

3. The P_{det} remains at one (1) for all imaging opportunities.

4,5,6,7,8. Since Landsat MSS imagery is less expensive than TM imagery but equal in P_{det}, only MSS imagery is considered in the rest of this analysis. Empirical weather data is used to determine P_{det*}. P_{trkcon} values are found in Appendix F. The P_{tim} is calculated based on the size of the possible target area and the P_{trkcon}. Table 17 contains the results for these calculations.

Table 17. Second Contact Calculations Summary

Opportunity	P_{det*}	P_{trkcon}	P_{tim}	P_{track1}
Landsat MSS	0.2	0.68	0.34	6.8E-2
SPOT(1st)	0.2	0.5	0.045	9.0E-3
SPOT(2nd)	0.2	0.12	0.03	6.0E-3

9. The available swaths could overlap. However, it is assumed that the sensors will be restricted to imaging separate areas to provide the broadest coverage possible.

9. A. The goal of this analysis is to maximize P_{track} given a budget of $10,000.00.

9. B. The objective function is:

$$P_{track} = 6.8E\text{-}2\ X1 + 9.0E\text{-}3\ X2 + 6.0E\text{-}3\ X3 \qquad (117)$$

Where X1 = # images taken by Landsat
X2 = # images taken by SPOT on first pass
X3 = # images taken by SPOT on second pass

The cost constraint is:

$$4600\ X1 + 1000\ X2 + 1000\ X3 \leq 10000 \qquad (118)$$

The image availability constraints are:

$$0 \leq X1 \leq 2 \qquad (119)$$

$$0 \leq X2 \leq 11 \qquad (120)$$

$$0 \leq X3 \leq 4 \qquad (121)$$

9. D. This linear program was not solved.

Fifth Analysis: Follow-on Contact

START -- Checklist 1

1. Mission: Second Contact

   Target: Ship

   Time frame: June, Duration of the voyage

2. Area of interest: Ship's Route which begins at 60°N 60°W and proceeds Northwest until the ship has cleared the area. The ship's route is shown in Figure 32.

3. Possible background(s): Water

4. Background characteristics:

   Spatial - Sea level

   Spectral - Reflectance 0.09 (16:7)

   - Emissivity (10-12 μm) 0.99 (16:7)

   Temporal - No change in time frame

5. Target characteristics: (Appendix D)

   Spatial - 121 x 15 meters

   Spectral - Reflectance 0.85

   - Emissivity 0.74, 1/10 surface area 2°K warmer than ambient

   Temporal - Ship's top speed 10 Knots

6. Sensors available: NOAA AVHRR

   Landsat 5 MSS, TM

   SPOT 1 HRV

7. P_{det} calculation:

   Visible - $(R_t - R_b) = 0.76$

Table 18. Visible Sensor Fifth Analysis

Sensor	$A_{ti}(m^2)$	P_{det}
AVHRR	1800 (Fig. C18)	0
MSS	67 (Fig. C8)	1
TM	8 (Fig. C6)	1
HRV	1 (Fig. C2)	1

Thermal - Target exitance 56.7 W/m^2

Table 19. Thermal Sensor Fifth Analysis

Sensor	$A_{ti}(m^2)$	P_{det}
TM Band 6	1 (Fig. G7)	1

8. Surviving options: Landsat MSS (any band)
Landsat TM Band (any band)
SPOT HRV

9. End checklist 1

Checklist 6: Follow-On Contact

1,2,3 A. The total time for the voyage is approximately 250 hours.

B. Given an initial Landsat 5 location of 110°W 60°N, and a SPOT location of 90°W 60°N at the start of the ship's voyage (arbitrary for demonstration purposes), there will be five (5) imaging opportunities during the voyage. These are shown in Figure 33.

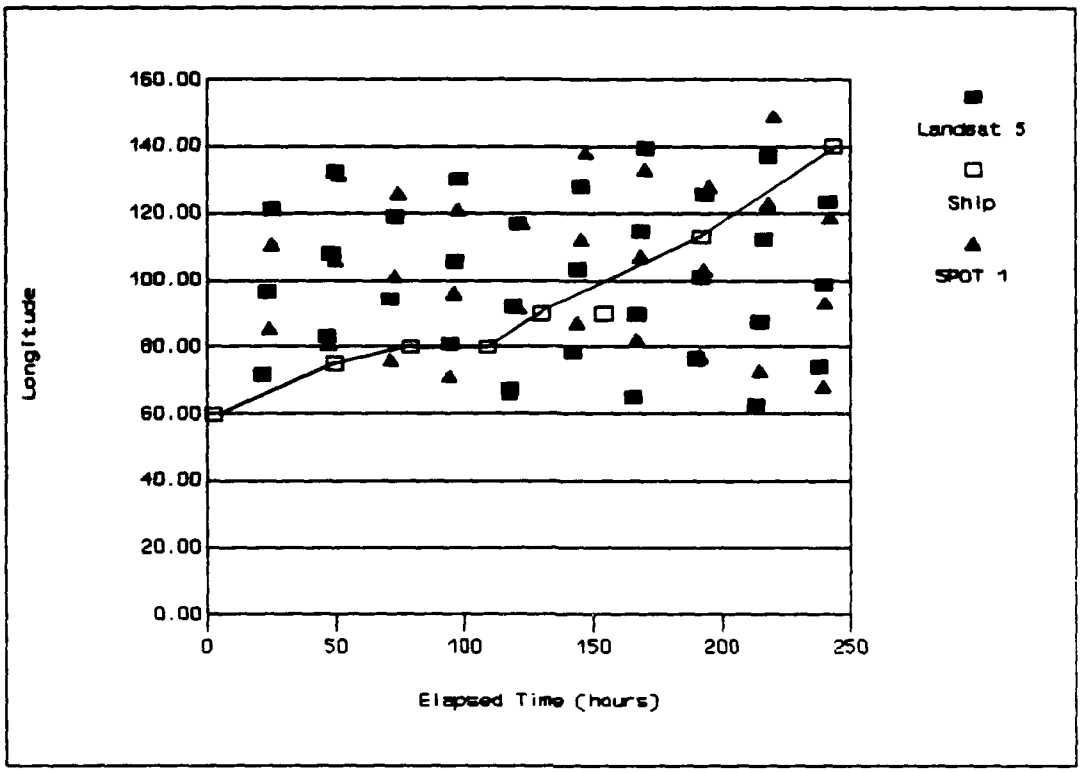

Figure 33. Scatter Plot of Imaging Opportunities

4. The imaging opportunities and P_{det*} values are summarized in Table 20.

Table 20. Imaging Opportunities

Time(hours)	Sensor	P_{cloud}	P_{det*}
47	SPOT	0.8	0.2
71	SPOT	0.8	0.2
94	Landsat	0.8	0.2
144	SPOT	0.8	0.2
218	SPOT	0.8	0.2

5. $P_{d\geq 1}$ is to be maximized in this example. The available budget is $2,000.00. Therefore the objective function is:

$$P_{d\geq 1} = 1-((.8)^{X1}(.8)^{X2}(.8)^{X3}(.8)^{X4}(.8)^{X5}) \qquad (122)$$

Where X1 = number of images taken by SPOT on its first opportunity
X2 = number of images taken by SPOT on its second opportunity
X3 = number of images taken on the Landsat pass
X4 = number of images taken by SPOT on its third opportunity
X5 = number of images taken by SPOT on its fourth opportunity

The cost constraint is:

$$1000\,X1 + 1000\,X2 + 1000\,X3 + 1000\,X4 + 1000\,X5 \leq 2000 \qquad (123)$$

The image availability constraint is that each sensor can provide only one image of the expected ship location on each pass.

6. This model was not solved.

VII. Conclusions and Recommendations for Further Research

General

Satellite remote sensing of the Earth for any purpose is a complex process involving the scene, the atmosphere, and the sensor. Equally complex is the task of evaluating the images that are available from remote sensing satellites. The sensor evaluation procedures and surveillance mission evaluation algorithms developed in this research consider only a small part of the entire process.

As a result of the narrow focus taken in this research some questions can be answered while others remain. Therefore this concluding section of this report separates conclusions into two categories. The first category is hard conclusions, those that are defendable. These conclusions are presented in the section which addresses the research questions posed in Chapter 1. The second category is soft conclusions, those that are observations on the interaction of satellites and surveillance. These observations are presented in their own section.

The final section of this chapter presents some areas which could be investigated by follow-on research.

Discussion of Research Questions

What satellite imaging systems will be available?

The United States, Europe (ESA), India, Japan, Canada, the Soviet Union, and France plan to sell satellite acquired imagery in the 1990s. Additional sources of satellite acquired imagery may include Chinasat, Mediasat, Bressex, and a Soviet digital imaging system.

What will the system's capabilities be for these suppliers?

The minimum target size that can be detected by a visible wavelength sensor is determined by the sensor's ground resolution cell (A_c), the sensor's noise equivalent reflectance difference (NERD), the atmospheric transmission (τ_a), the reflectance of the target (R_t), and the reflectance of the background (R_b).

$$A_t = \frac{A_c \, (NERD/\tau_a)}{| R_t - R_b |} \qquad (124)$$

The minimum target that can be detected by a thermal wavelength sensor is determined by the sensor's noise equivalent power difference (NEPD), the atmospheric transmission (τ_a), the background exitance ($M_b(T_b)$), the emissivity of the background (ϵ_b), the target exitance ($M_t(T_t)$), and the target emissivity (ϵ_t).

$$A_t = \frac{NEPD/\tau_a}{| M_b(T_b)\epsilon_b - M_t(T_t)\epsilon_t |} \qquad (125)$$

Analysis of visible and thermal sensors must consider the detector array geometry and its affect on the probability of target detection. For both types of sensor the probability of target detection is the ratio of the area in which the target could fall and be detected (A_{det}) to the total area in which the target could fall (A_{tot}).

$$P_{det} = A_{det}/A_{tot} \qquad (126)$$

How can commercial satellite images be evaluated?

Commercial satellite images can be evaluated by comparing the information they provide to the information required, and by considering the cost of the information they provide. The specific algorithms used for sensor evaluation against a mission requirement are mission specific and can be optimized using linear and non-linear optimization techniques.

For non-cued detection of stationary targets the system wide probability of detecting a target is given below in equation 127.

$$P_{dsys} = \sum_{i=1}^{n} (N_{im})_i \ (P_{dot1})_i \qquad (127)$$

Where P_{dsys} = system wide probability of detection
$(N_{im})_i$ = # of images taken by sensor i
$(P_{dot1})_i$ = probability of target detection in area of interest in a single image from sensor i

For non-cued detection of moving targets the system wide probability of at least one target detection is:

$$P_{d\geq 1} = 1 - \left(\prod_{i=1}^{n} (1-P_{dot1i})^{xi} \right) \qquad (128)$$

Where $P_{d\geq 1}$ = system wide probability of at least one detection
P_{dot1i} = probability of target detection in area of interest in a single image from sensor i
xi = # of images taken by sensor i

For cued detection of stationary targets the system wide probability of at least one target detection is:

$$P_{d\geq 1} = 1 - \left(\prod_{i=1}^{n} (1-P_{det*i})^{xi} \right) \qquad (129)$$

Where P_{det*i} = probability of target detection in a single image from sensor i

For second contact on moving targets the system wide probability of tracking is given in equation 130.

$$P_{track} = \sum_{i=1}^{n} (N_{im})_i \; P_{track1i} \qquad (130)$$

Where P_{track} = system wide probability of tracking
$P_{track1i}$ = probability of tracking the target in a single image from sensor i

This relationship holds for overlapping and non-overlapping images by considering overlapping images to be available from a separate sensor having a P_{track1} derived from the P_{track1} of the sensors involved.

For follow-on contact the system wide probability of at least one detection is:

$$P_{d\geq 1} = 1 - \left(\prod_{i=1}^{n} \prod_{j=1}^{m} (1-P_{det*ij}) \right) \qquad (131)$$

Where P_{det*ij} = probability of detection in image j of sensor i

For all missions the constraint set is:

$$\sum_{i=1}^{n} (N_{im})_i \; C_i \leq B_{\$} \qquad (132)$$

Where C_i = cost of one image from sensor i
$B_{\$}$ = budget available in the time frame

$$0 \leq (N_{im})_i \leq K_i \qquad (133)$$

Where K_i = maximum number of images available from sensor i in the time frame

For non-cued detection, additional constraints are required to ensure that more easily imaged areas within the

area of interest are not selected over areas that are more difficult to image.

Can weather satellites detect and track targets of interest?

Current weather satellites cannot detect or track objects of interest in the Canadian North. This is because geosynchronous satellites do not provide images of Northern Canada, and the minimum target size for detection by the NOAA series of satellites is approximately 2000 square meters.

Will commercial systems require cuing?

The decision on whether to use commercial imaging sensors as cues is economic. The system wide probability of detection is limited to a maximum which corresponds to the probability that there are clear skies in the target area. To achieve the maximum probability of detection the entire area of interest would have to be imaged. Assuming that the price per image remains constant irrespective of the number of images acquired, the cost of imaging the entire area is $212,000.00 if Landsat MSS imagery is used. The cost of imaging the entire area is $976,000.00 if Landsat TM imagery is used. The cost of imaging the entire area is $2,000,000.00 if SPOT imagery is used. If this imaging were undertaken in August the system wide probability of detecting a target located somewhere in the target area

would be approximately 0.2 due to the likelihood of clouds. Imaging of the entire area would take Landsat 16 days. It would take SPOT 5 days.

If cued, Landsat 5 and SPOT 1 sensors will detect targets of interest in Northern Canada with a probability in a single image equal to the probability of clear skies in the target area. Since the probability of clear skies varies both spatially and temporally, the specific location will influence the number of images to be acquired to return an acceptable probability of at least one detection.

Will a combination of sensors outperform a single sensor?

The question of sensor or system dominance can be decided in general terms for each mission. This is discussed in more detail in the observations section of this chapter.

Could an alternative system outperform commercial sensors?

An alternative system would have to outperform the combination of sensors available from commercial sources. Therefore it would have to return larger system wide probabilities of detection and tracking for the same cost, or would have to return equal system wide probabilities of detection and tracking for less cost than the commercial systems.

Can commercial systems detect Canadian military activity?

Canadian military vehicles and ships, if they have similar characteristics to those used in this analysis, can be detected and tracked by current commercial satellite sensors.

Observations

The sixth research question asks whether a mix of sensors performs better than does a single sensor. The short answer is that it depends on the mission. A brief discussion of each mission explains this point.

In non-cued detection the goal is wide area surveillance. A comparison of sensors is possible through their respective P_{dot1} and costs. The P_{dot1} is given by equation 134.

$$P_{dot1} = \frac{A_{one} P_{det*}}{A_{int}} \qquad (134)$$

Where A_{one} = area of a single image from the sensor
A_{int} = area of interest

Given competing sensors have equal P_{det*}, and since the area of interest is the same for each sensor, a sensor producing a larger image will be favored over one which produces a smaller image. The solution of the linear program developed in the first analysis shows the domination

of SPOT by Landsat for the wide area surveillance mission. These results are shown in Table 21.

Table 21. Summary of First Analysis Results

Sensor/Area	# Images
Landsat/B	23.8
Landsat/C	38.2
Landsat/D	88.2
Landsat/E	17.0
Landsat/F	25.0
Landsat/G	18.5
SPOT /B	0.0
SPOT /C	0.0
SPOT /F	0.0
SPOT /G	0.0

The explanation for this domination is the cost of the imagery. Landsat TM imagery covers territory at a cost of $0.13 each square kilometer. SPOT HRV covers territory at a cost of $0.28 each square kilometer.

In cued detection of stationary targets the size of the image is not important in the selection of the sensor. This is true since sensor performance is compared using individual P_{det*} which does not consider the relative sizes of the swath and area of interest. In this analysis the P_{det*} is established for Landsat and SPOT as the probability of there being clear weather in the target area. The two

factors which are important in sensor selection are the cost of the sensor and the responsiveness of the sensor. For high value targets it may be necessary to confirm or deny its presence as quickly as possible. In this situation the selection of a sensor will be driven by the ability of the sensor to image an area before a competitor.

Selection of a sensor for second contact with a target again depends on the situation. The preferred option will provide the highest P_{trkcon} of those available. An interesting outcome of the analysis is that pointable sensors provide slightly higher P_{trkcon} values if their ground trace does not overfly the initial target location directly. This is shown in Figure 34. The reason this is true is that the sensor's swath, and thus the area it can cover, is slightly larger off nadir.

Finally, attempting to acquire follow-on contacts with targets favors pointable sensors. The selection of one sensor over another is again situation dependent since several imaging opportunities may be present for each sensor. The final selection from the available opportunities will depend on the value of the target and the requirement to monitor the target as frequently as its value demands.

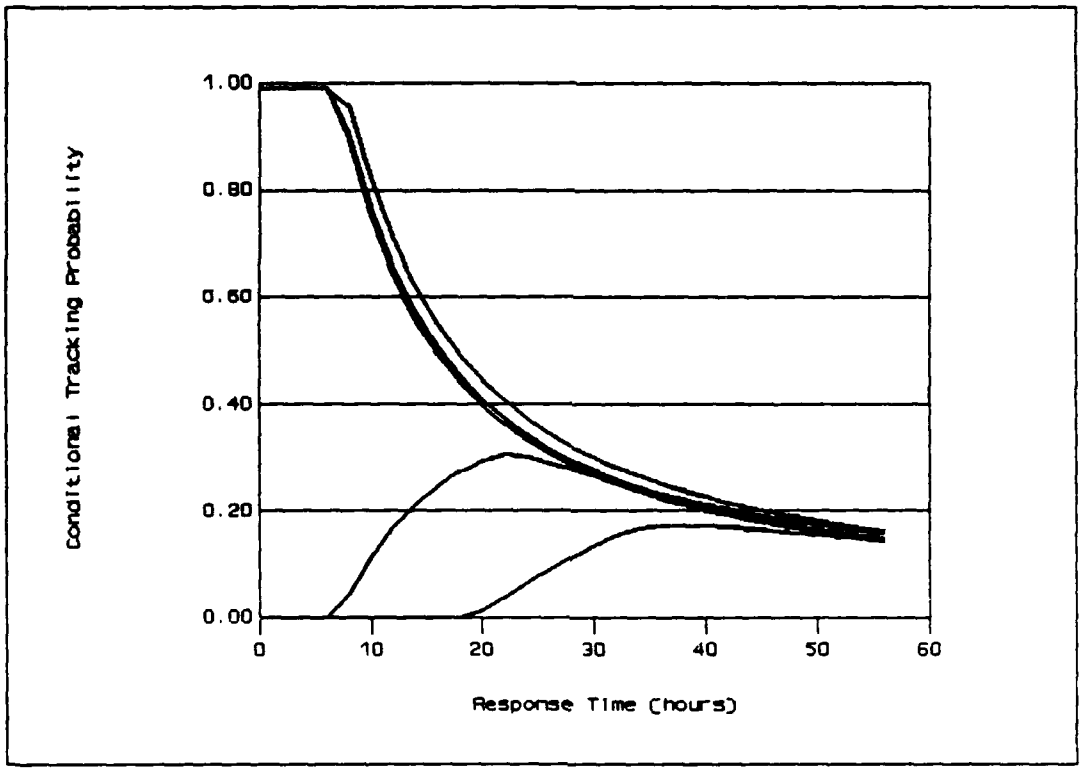

Figure 34. SPOT 1 Conditional Tracking Probability
60°N Latitude, 5 Knots
(Top to bottom are 8,4,0,10,12° Longitude Displacement)

Recommendations

Detection throughout this research refers to distinguishing a target from its background in the spatial domain. It is also possible to approach detection in the temporal domain. This requires prior information on the area of interest and the development of algorithms to separate out evidence of change over time. Follow-on research could address the problem of detection in the

temporal domain and investigate the data storage and processing which would be required to accomplish such detection.

This research assumes that the timeliness and availability of images is ideal. Given that these factors are not necessarily ideal, how could they be evaluated in the overall determination of the worth of satellite imagery. Follow-on research could develop the algorithms to use in the evaluation of timeliness and availability and could develop an overall value algorithm for satellite acquired imagery.

The third mission of surveillance is identification. What is involved in this mission? Should the military train photo-interpreters or develop pattern recognition algorithms to effect identification? Follow-on research could identify the infrastructure and costs involved in these options and evaluate the options against the mission requirements.

The fourth major area of research which could be pursued is the addition of active sensor evaluation criteria and investigation of the impact of active sensors in the selection of imaging sensors.

Appendix A: Sensor Description

This appendix contains a general description of imaging sensors that are either current or are planned to be launched in the 1990s. Excluded from this listing are sensors that are incapable of imaging Northern Canada, examples of which are the GOES geosynchronous weather observation satellites and the Tropical Earth Resources Satellite (TERS) which is planned to fly at 0° inclination.

There are four notable omissions from this appendix. The first is Bressex, a Brazilian shuttle-borne system. It is omitted since little information is available on this system. The other omitted systems are Chinasat, Mediasat, and a possible Soviet digital imaging system. Although these systems may be developed and become available commercially in future their current status is speculative at best.

Earth Observation System (EOS) Polar Platforms

Country of Origin	Launch Date	Orbit Parameters	Lifetime	Main Sensor
USA	1994	i = 98° H = 824 km EQX = 0900 Descending H = 824/542/705 km EQX = 1330 Ascending	10 years	Active/ Passive

Background: The EOS is sponsored by NASA and is conceived as the next major operational Earth remote sensing system. The two polar platforms will carry a variety of sensors and will in part replace the NOAA weather observation satellite.

Imaging Sensors:

Name	Band	Bandpass(μm)	GRC(m)	NERD(%)	Swath(km)
MODIS-N	1	.46-.48	500	.2-.5	1500
	2	.54-.56	500	.2-.5	
	3	.66-.68	500	.2-.5	
	4	.70-.72	500	.2-.5	
	5	.87-.89	500	.2-.5	
	6	.93-.95	500	.2-.5	
	7	.43-.44	1000		
	8	.485-.495	1000		
	9	.515-.525	1000		
	10	.56-.57	1000		
	11	.615-.625	1000		
	12	.66-.67	1000		
	13	.68-.69	1000		
	14	.76-.77	1000		
	15	.86-.87	1000		
	21	1.07-1.09	500	.2-.5	
	22	1.12-1.14	500	.2-.5	
	23	1.54-1.56	500	.2-.5	
	24	1.63-1.65	500	.2-.5	
	25	2.01-2.11	500	.2-.5	
	26	2.08-2.18	500	.2-.5	
MODIS-T	?	.40-1.04	1000		
AMRIR	1-11	VIS-NIR	500		

Name	Band	Bandpass(μm)	GRC(m)	NERD(%)	Swath(km)
TIMS	?	.40-12.5	30		
SAR	1	19MHz	25		33-100
ITIR	1	.85-.92	15		
	2-6	1.6-2.36	15		
	7-11	3.53-11.7	60		
HIRIS	?	.45-2.45	30		23

MODIS-N - Moderate Resolution Imaging Spectrometer -- Nadir (This MODIS is fixed at nadir)
MODIS-T - T is for tilt along track ± 50°
AMRIR - Advanced Medium Resolution Imaging Radiometer (Follow-on to NOAA AVHRR)
ITIR - Intermediate Thermal Infrared, proposed by Japan
HIRIS - High Resolution Imaging Spectrometer
TIMS - Thermal Imaging Spectrometer
SAR - Synthetic Aperture Radar

Other: The HIRIS will be pointable across track ± 20° and along track ± 60°, and is intended to be a targeted sensor rather than in continuous operation.

Sources: (23:77)(34:82)(17:105)(62:362)(31:371)(57:388)

European Space Agency Resources Satellite (ERS-1)

Country of Origin	Launch Date	Orbit Parameters	Lifetime	Main Sensor
ESA	1989	i = 98.5° H = 777 km C = 3 days EQX = 1030 Descending	3 years	Active

Background: ERS-1 will be the first Earth remote sensing satellite for the ESA. It is intended to be experimental and will be the forerunner for follow-on satellites. If ERS-1 is a success, ERS-2 could be launched in 1993.

Imaging Sensors:

Name	Band	Frequency	GRC(m)	Swath(km)
AMI	C	5.3 GHz	30	75

AMI - Advanced Microwave Instrument

Other: ESA plan to make fast delivery products available within three hours. A fast delivery reception facility is planned for Gatineau.

Sources: (53:70)(25:537)(32:375)

Indian Remote Sensing Satellite (IRS)

Country of Origin	Launch Date	Orbit Parameters	Lifetime	
India	?	i = 99° H = 904 km C = 22 days	3 Years	

Background: The Indian remote sensing satellites are follow-ons to the Bhaskara 1 and 2 satellites flown in the late 1970s and early 1980s. The IRS program is planned as a pre-operational space-based remote sensing system.

Imaging Sensors:

Name	Band	Bandpass(μm)	GRC(m)	NERD(%)	Swath(km)
LISS-1	1	.45-.52	72		148
	2	.52-.60			
	3	.63-.69			
	4	.76-.90			
LISS-2*	1	.45-.52	36	.5	148*
	2	.52-.59		.5	
	3	.62-.68		.35	
	4	.77-.86		.3	

LISS - Linear Imaging Self-Scanning
* There are two LISS-2 sensors, each swath is 74 km.

Other: Three levels of data products are planned. Level 1 will be corrected for radiometric errors and Earth rotation and will be delivered in three days. Level 2 will be corrected for geometric errors and will be delivered in seven days. Level 3 are referred to as precision products and will be delivered within three weeks of imaging.

Sources: (42:87)(56:615)(59:630)(60:153)

JANUS Earth Observation Satellite (JEOS)

Country of Origin	Launch Date	Orbit Parameters	Lifetime	Main Sensor
ESA		i = 98.5° H = 780 km C = 22 days EQX = 1000	4 years	Passive

Background: This is a proposed Earth remote sensing satellite that could be inserted into orbit in piggy-back fashion during an ESA launch. The goal is to produce a low cost satellite.

Imaging Sensors:

Name	Band	Bandpass(μm)	GRC(m)	NERD(%)	Swath(km)
?	1	.45-.52	30	.5	120*
	2	.52-.59		.5	
	3	.62-.68		.35	
	4	.77-.86		.3	

Source: (55:615)

Japanese Earth Resources Satellite (JERS-1)

Country of Origin	Launch Date	Orbit Parameters	Lifetime	
Japan	1990	i = 99.7° H = 568 km		

Background: In 1980 the National Space Development Agency of Japan began a research and development program for remote sensing. Both the JERS-1 and MOS-1 are products of this program.

Imaging Sensors:

Name	Band	Bandpass(μm)	GRC(m)	NERD	Swath(km)
VNR	1	.45-.52	25		150
	2	.52-.60			
	3	.63-.69			
	4	.76-.90			
SAR	Frequency	1.275 GHz	25x25		75

VNR - Visible and Near-Infrared Radiometer
SAR - Synthetic Aperture Radar

Sources: (36:611)(53:71)

Landsat 5

Country of Origin	Launch Date	Orbit Parameters	Lifetime	
USA	March 1984	i = 98° H = 705 km C = 16 days EQX = 0945 Descending	1991*	

Background: Landsat 5 is the fifth land satellite to be launched. This program was originally funded by the US government but became a commercial venture in 1985. Delays are expected for the launch of Landsat 6 so Landsat 5 is being operated below capacity in order to extend the life of the satellite.

Imaging Sensors:

Name	Band	Bandpass(μm)	GRC(m)	NERD(%)	Swath(km)
TM	1	.45-.52	30	.65	185
	2	.52-.60		.57	
	3	.63-.69		.57	
	4	.76-.90		.33	
	5	1.55-1.75		1.68	
	7	2.08-2.35		2.00	
	6	10.4-12.5	120	NETD .5°K @ 300°K	
MSS	1	.50-.60	80		
	2	.60-.70			
	3	.70-.80			
	4	.80-1.1			

TM - Thematic Mapper
MSS - Multispectral Scanner

Other: Data from Landsat satellites can be relayed through the tracking and data relay satellites (TDRS). Initial MSS processing is accomplished at the Goddard Space Flight Center (GSFC). Follow-on processing and storage is done at the Earth resources observation system data center in Sioux Falls, South Dakota. TM data can be fully processed at GSFC.

Sources: (56:356)(33:63-72)(64:498)

Landsat 6/7

Country of Origin	Launch Date	Orbit Parameters	Lifetime	
USA	1989/1991	i = 98° H = 705 km C = 16 days EQX = 0945 Descending		

Background: The future of Landsat 6 and 7 is unclear. Landsat 6 was originally scheduled for launch in 1988. Now estimates for a launch date range to 1993. Landsat 7 plans continue however funding for this platform is questionable.

Imaging Sensors:

Name	Band	Bandpass(μm)	GRC(m)	NERD(%)	Swath(km)
ETM	(7 spectral as found in Landsat 5)				
	Pan*	.50-.90	15/5*		
	M*	3.53-3.93	120		
	8*	8.20-8.75	60		
	9*	8.75-9.30	60		
	10*	10.2-11.0	60		
	11*	11.0-11.3	60		
ALS	4*	from VNIR	10		
	4*	from SWIR	20		

ETM - Enhanced Thematic Mapper, this sensor will be able to emulate the MSS found on Landsat 5
ALS - Advanced Landsat Sensor, possible for Landsat 7
VNIR - Visible and near infrared wavelengths
SWIR - Short wave infrared wavelengths
* - Under consideration

Other: EOSAT has conducted a market survey, which included potential customers from the media, to investigate the possible market for 5 meter resolution imagery. Also EOSAT has declared that TDRS will not be used to relay imagery of foreign countries in near real time. Instead such imagery will be recorded for subsequent transmission.

Sources: (72:74)(11:149)(27:73)(28:885)(33:189)

Maritime Observation Satellite (MOS-1)

Country of Origin	Launch Date	Orbit Parameters	Lifetime	
Japan	1989	i = 99° H = 908 km EQX = 1100 Descending	2 years	

Background: MOS-1 is the maritime portion of a Japanese research and development program to establish fundamental technologies for remote sensing satellites.

Imaging Sensors:

Name	Band	Bandpass(μm)	GRC(m)	NERD(%)	Swath(km)
MESSR	1	.51-.59	50		100
	2	.61-.69			
	3	.72-.80			
	4	.80-1.1			
VTIR	1	.50-.70	900		1500
	2	6.0-7.0	2700		
	3	10.5-11.5	2700		
	4	11.5-12.5	2700		

MESSR - Multispectral electronic self-scanning radiometer, there are two on MOS-1
VTIR - Visible and thermal infrared radiometer

Sources: (33:187)(53:70)(44:595)(49:18)

NOAA I/J/K/L/M

Country of Origin	Launch Date	Orbit Parameters	Lifetime	
USA	I/Oct 1988 J/Mar 1989 K/Oct 1990	i = 98.9° H = 862 km		

Background: NOAA stands for the National Oceanic and Atmospheric Administration. The satellites that bear this name are weather observation satellites. NOAA satellites are follow-ons in a continuing program which began with the launch of TIROS-1 on April 1, 1960. Typically NOAA satellites operate two at a time and provide both morning and afternoon imaging of weather systems.

Imaging Sensors:

Name	Band	Bandpass(μm)	GRC(m)	NERD(%)	Swath(km)
AVHRR	1	.58-.68	1000		3000
	2	.73-1.0			
	3a*	1.57-1.78			
	3b	3.53-3.93			
	4	10.2-11.3			
	5	11.5-12.5			

AVHRR - Advanced Very High Resolution Radiometer
* - Planned for NOAA K/L/M

Other: NOAA satellites transmit images in real time directly to users. The resolution at which those images are received depends on the ground station built. Automatic picture transmission (APT) images are received at a ground resolution of four kilometers. High resolution picture transmission (HRPT) images are received at a ground resolution of one kilometer.

Sources: (65:441)(63:52-67)(37:221)(58:3)

RADARSAT

Country of Origin	Launch Date	Orbit Parameters	Lifetime	
Canada	1994	i = 98.5° H = 792 km C = 16 days EQX = 1030 Descending	5 years	

Background: RADARSAT is Canada's first Earth observation satellite. RADARSAT is intended to be both research and operations oriented. The main sensor will be an active microwave imaging radar. Until recently the United Kingdom planned to develop a radiometer to fly with the radar, however the UK has pulled out of RADARSAT. As a result, the inclusion of a radiometer has not been finalized.

Imaging Sensors:

Name	Band	Frequency	GRC(m)	Swath(km)
SAR	C	5.3 Ghz	25(R)x28(AZ) -- 7 main	500*
			35(R)x28(AZ) -- 2 wide-swath	600
			10(R)x9(AZ) -- 5 high resolution	45

(R) = Range
(AZ)= Azimuth
* - The seven beams each have a swath of 100 km but they overlap.

Other: Ground stations for RADARSAT include Fort Churchill, Shoe Cove, Gatineau, Prince Albert, Fairbanks, and Stranraer in Scotland. Data relay will be possible through an ANIK satellite.

Sources: (53:70)(45:33)(46:561)(47:409)(1:8)

Sojuzkarta

Country of Origin	Launch Date	Orbit Parameters	Lifetime	Main Sensor
USSR	?	?	?	?

Background: Sojuzkarta is a commercial firm established by the government of the Soviet Union to sell satellite acquired imagery to the world. Few details are available on platforms, orbits, and sensors. However, Sojuzkarta provide a general description of their sensors with their order form and price list. All sensors listed below are cameras and rely on physical retrieval of film canisters to transport the film to the ground.

Imaging Sensors:

Name	Altitude (km)	Spectral Range (μm)	Resolution (m)	Swath (km x km)
KATE-200	250	.50-.60 .60-.70 .70-.90	15-30	180 x 180
MKF-6	250	.46-.52 .52-.56 .58-.62 .64-.68 .70-.74 .79-.90	20	140 x 200
KATE-140	250	.50-.70	60	270 x 270
KFA-1000	250	.57-.67 .67-.80	5-10	60 x 60

Sources: (52:1346)(65:148)

SPOT 1/2/3

Country of Origin	Launch Date	Orbit Parameters	Lifetime	
France	Feb 1986	i = 98.5° H = 832 km C = 5 days EQX = 1030 Descending	2-3 years	

Background: Systeme Probatoire d'Observation de la Terre, or SPOT began as an ESA project but changed into a French lead program involving only Sweden, Belgium, and private interests. It is currently overseen by the Centre National d'Etudes Spatial (CNES), a French government agency.

Imaging Sensors:

Name	Band	Bandpass(μm)	GRC(m)	NERD(%)	Swath(km)
HRV	xs1	.50-.59	20	.5	117*
	xs2	.61-.68	20	.5	
	xs3	.79-.89	20	.5	
	Pa	.51-.73	10	.5	

*HRV - High Resolution Visible
- There are two HRVs onboard, each with a swath of 60 km. The overlap of these HRVs results in this swath width.

Other: SPOT's HRVs can be pointed up to 27° off nadir. This contributes to the orbit repeat cycle considerably lower than any other commercial sensor. SPOT data can be received directly within 2600 km of the satellite. Ground stations include Toulouse, Kiruna (Sweden), Prince Albert, and Gatineau. However only two of the four possible data streams can be sent by the satellite. SPOT can be reprogrammed within three to eight hours for urgent requests. Follow-ons to SPOT 1 are planned. SPOT 2 and 3 are planned to be identical to SPOT 1. For SPOT 4 the goal is for complete superimposability of panchromatic and spectral channel data. Also an ocean surveillance sensor is under consideration.

Sources: (20:510)(3:3)(11:151)(8:1115)(9:143)

Appendix B: Atmospheric Transmission

This appendix contains plots of transmission verses wavelength generated by LOWTRAN 6 for summer and winter sub-arctic atmospheres (Figures B1 through B8).

The parameters used to generate the SUMMER SUB-ARCTIC and WINTER SUB-ARCTIC transmission profiles are given in Table B1.

Major causes of attenuation for specific wavelengths are provided in Table B2.

Table B1. LOWTRAN 6 Parameters Used

Name	Description	Summer Value	Winter Value
MODEL		4	5
ITYPE	Slant Path	3	3
IEMSCT	Transmittance	0	0
M1	Temp/Pressure	0	0
M2	Water Vapour	0	0
M3	Ozone	0	0
NOPRT	Normal	0	0
TBOUND	Temperature	293.0	253.0
SALB	Albedo	0	0
IHAZE	Haze	0	0
ISEASN	Season	0	0
IVULCN	Volcanic Ash	0	0
VIS	Visibility	0	0
ICIR	Cirrus Clouds	0	0
IVSA	Army VSA	0	0
RAINRT	Rain Rate	0	0
H1	Initial Altitude	0	0
H2	Tangent Altitude	0	0
ANGLE	Zenith Angle	0/27	0/27
RANGE	Path Length	1000	1000
BETA	Centred Angle	0	0
RO	Earth Radius	0	0
V1	Init Wavenumber	800	800
V2	Final Wavenumber	25000	25000
DV	Increment	5/10/50	5/10/50

Table B2. Major Attenuation Culprits

Bandpass (μm)	Attenuation Explanation
≤ 0.5	Molecular Scattering
0.71-0.73	Water
0.76	Carbon Dioxide
0.90-0.92	Water
0.93-0.95	Water
1.10-1.15	Water, Carbon Dioxide
1.30-1.50	Water, Water Continuum
1.80-1.90	Water, Water Continuum
2.50-2.90	Water, Water Continuum
3.00-3.10	Water
4.30-4.40	Carbon Dioxide
5.20-7.50	Water, Water Continuum
7.50-8.00	Water, Water Continuum
9.10-10.0	Ozone
≥ 11.00	Water Continuum

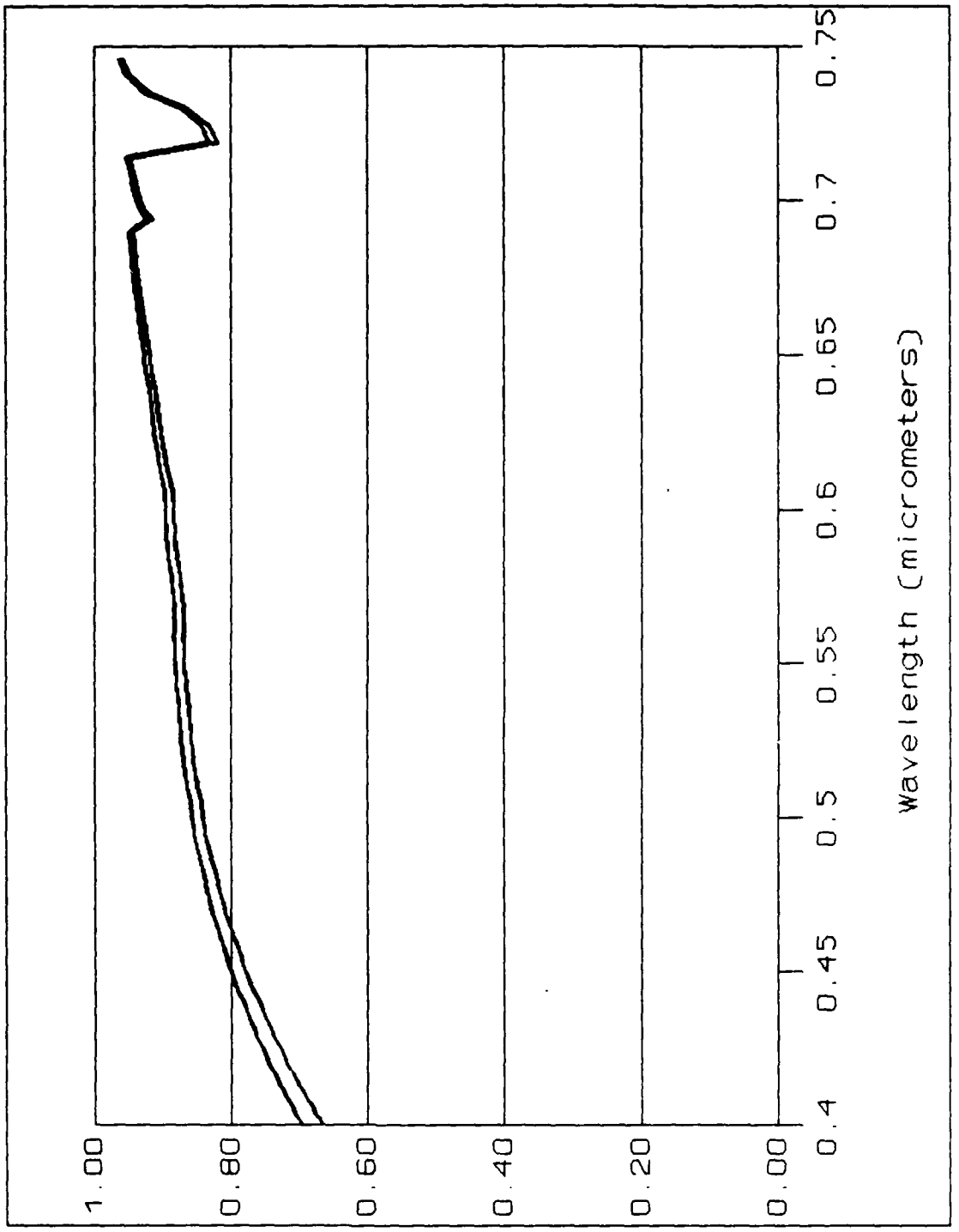

Figure B1. Sub-Arctic Summer Atmospheric Transmission
.4-.7 Micrometers
(Lower line for Zenith angle 27 degrees)

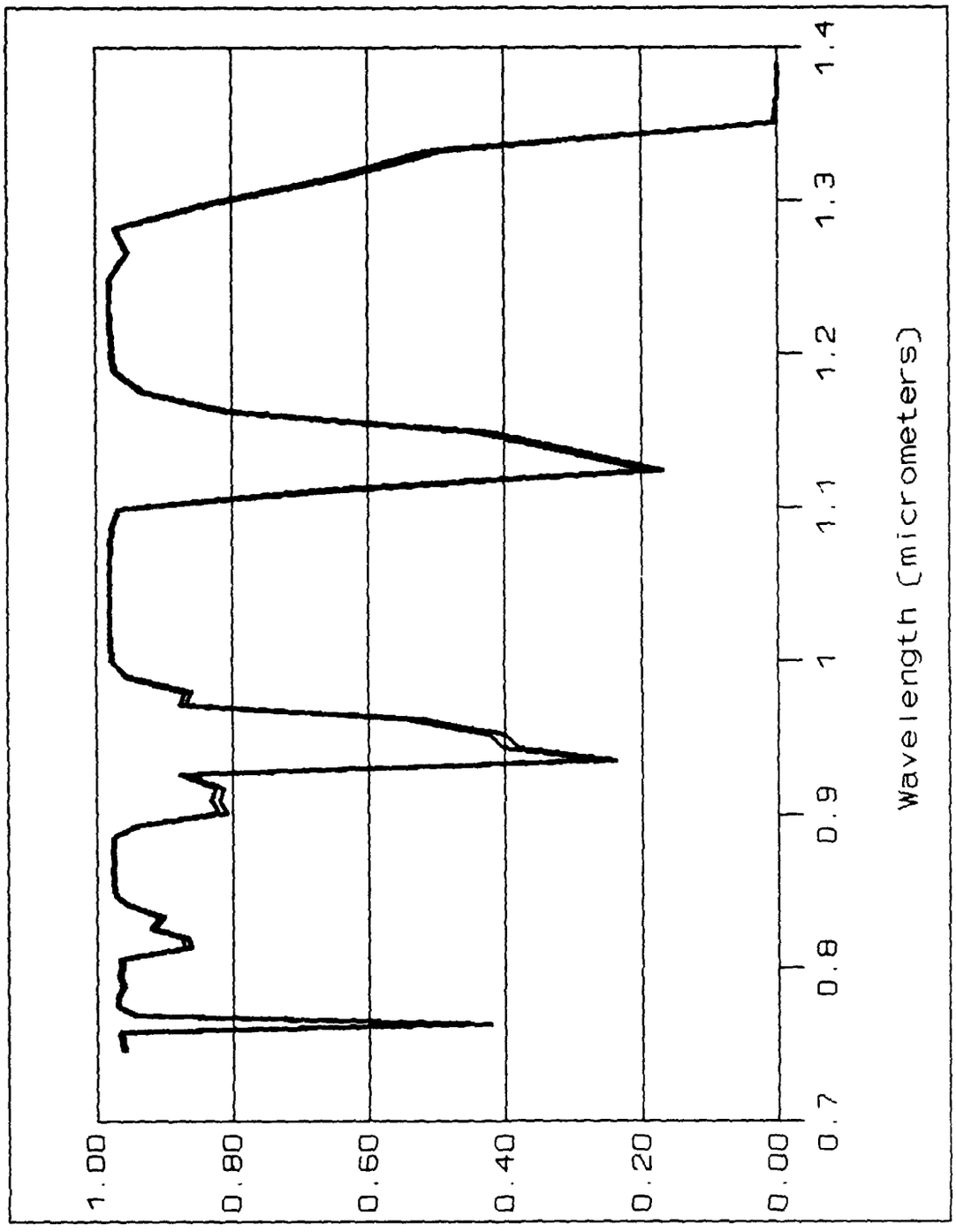

Figure B2. Sub-Arctic Summer Atmospheric Transmission
.7-1.4 Micrometers
(Lower line for Zenith angle 27 degrees)

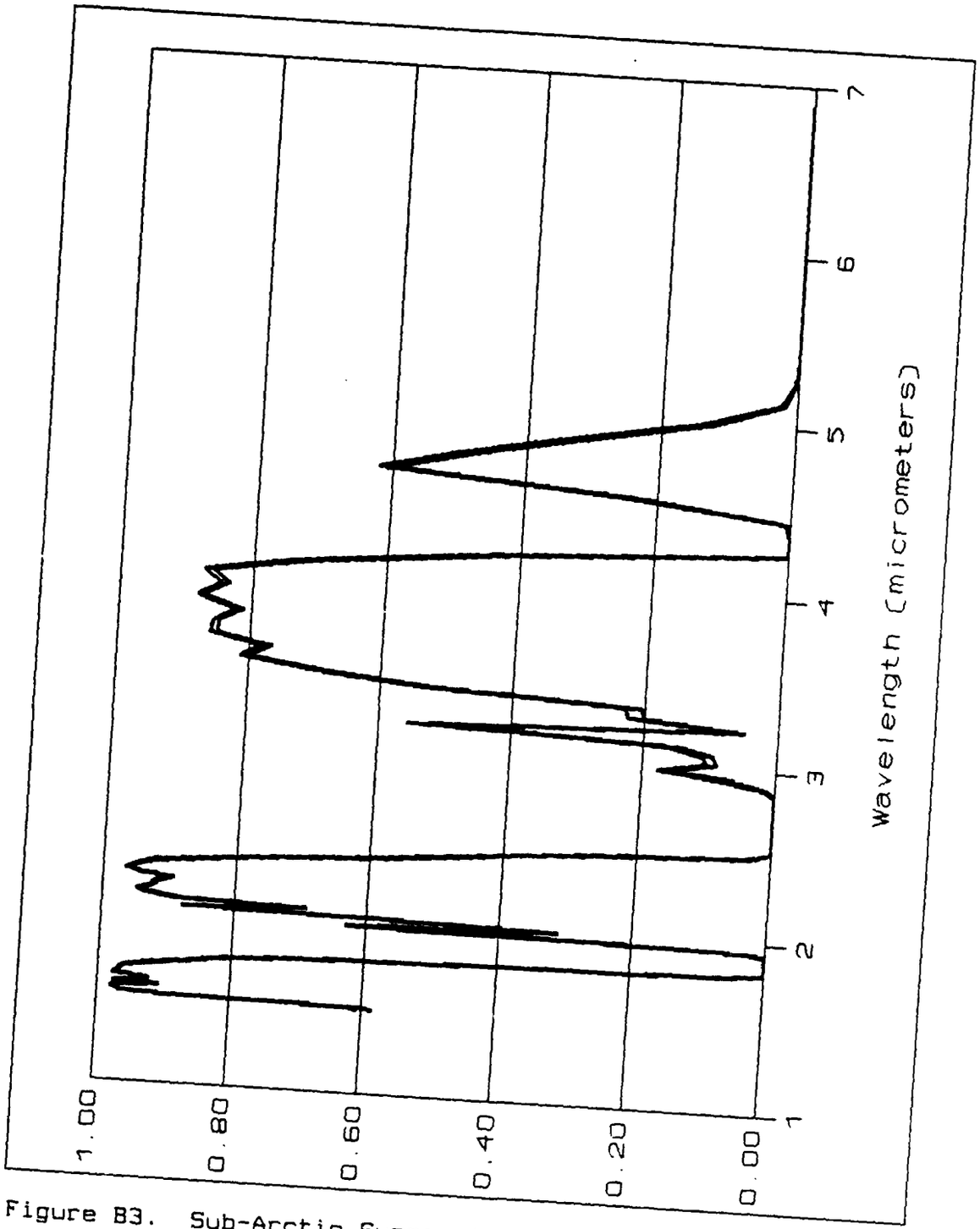

Figure B3. Sub-Arctic Summer Atmospheric Transmission
1.4-7 Micrometers
(Lower line for Zenith angle 27 degrees)

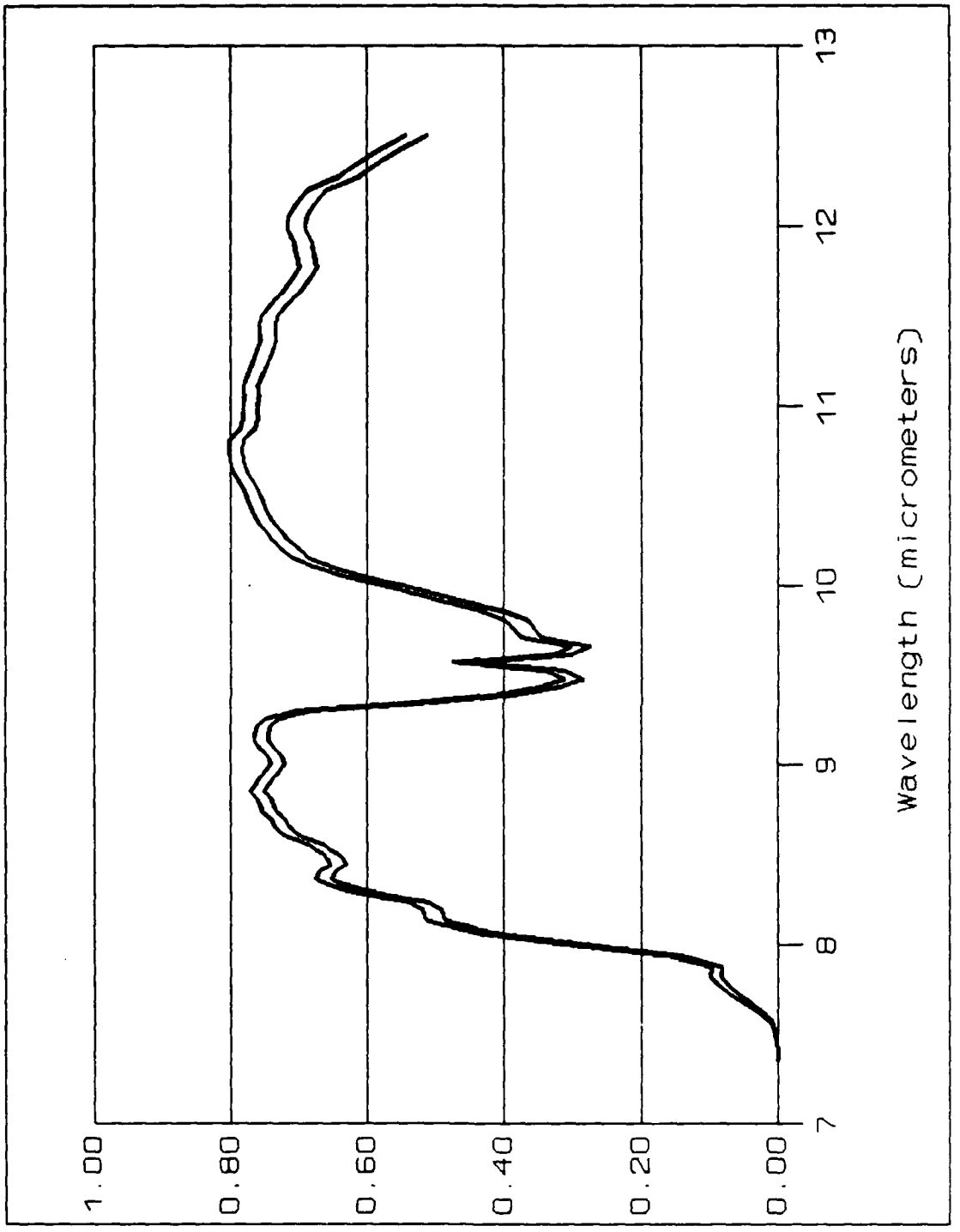

Figure B4. Sub-Arctic Summer Atmospheric Transmission
7-12.5 Micrometers
(Lower line for Zenith angle 27 degrees)

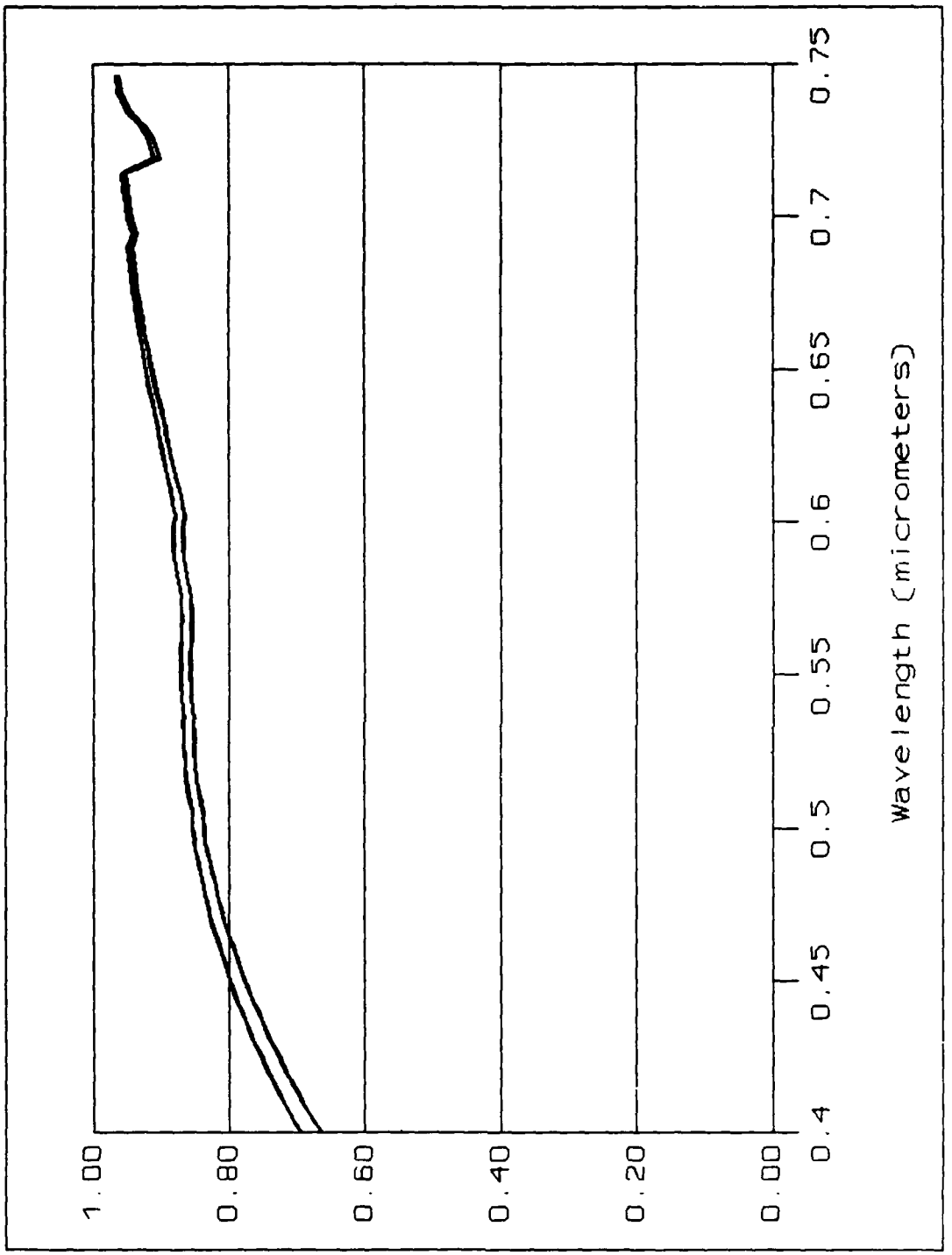

Figure B5. Sub-Arctic Winter Atmospheric Transmission
.4-.7 Micrometers
(Lower line for Zenith angle 27 degrees)

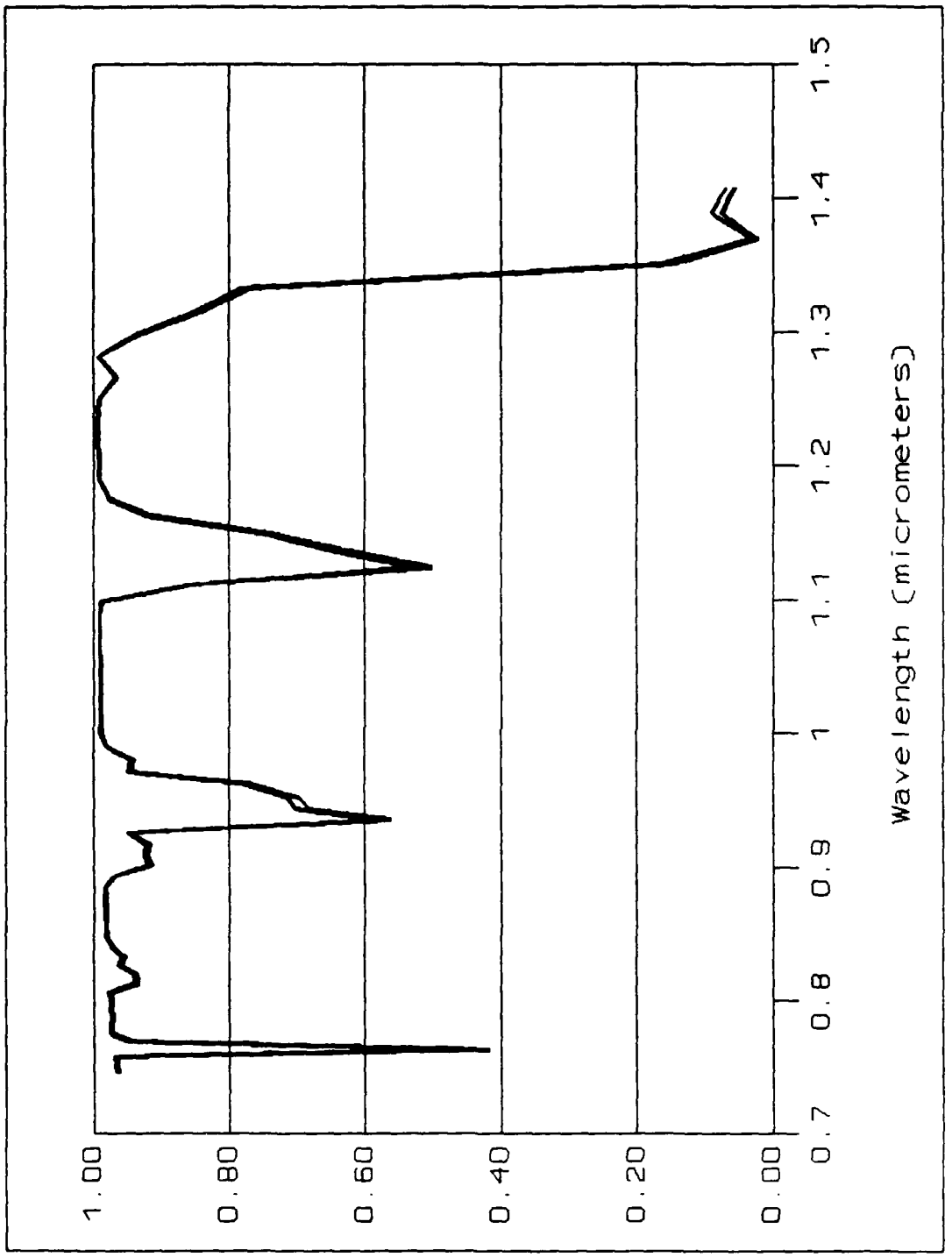

Figure B6. Sub-Arctic Winter Atmospheric Transmission
.7-1.4 Micrometers
(Lower line for Zenith angle 27 degrees)

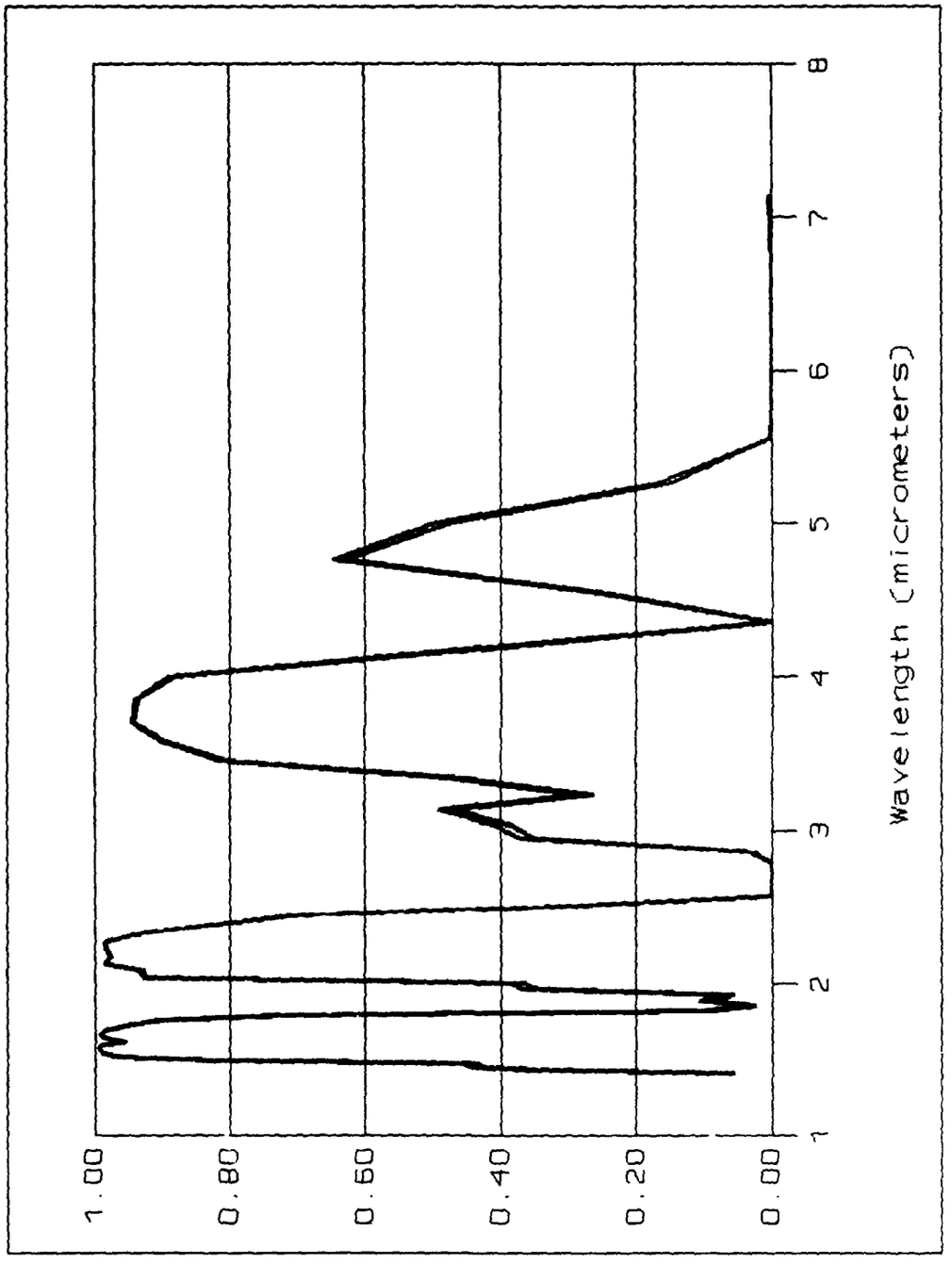

Figure B7. Sub-Arctic Winter Atmospheric Transmission
1.4-7 Micrometers
(Lower line for Zenith angle 27 degrees)

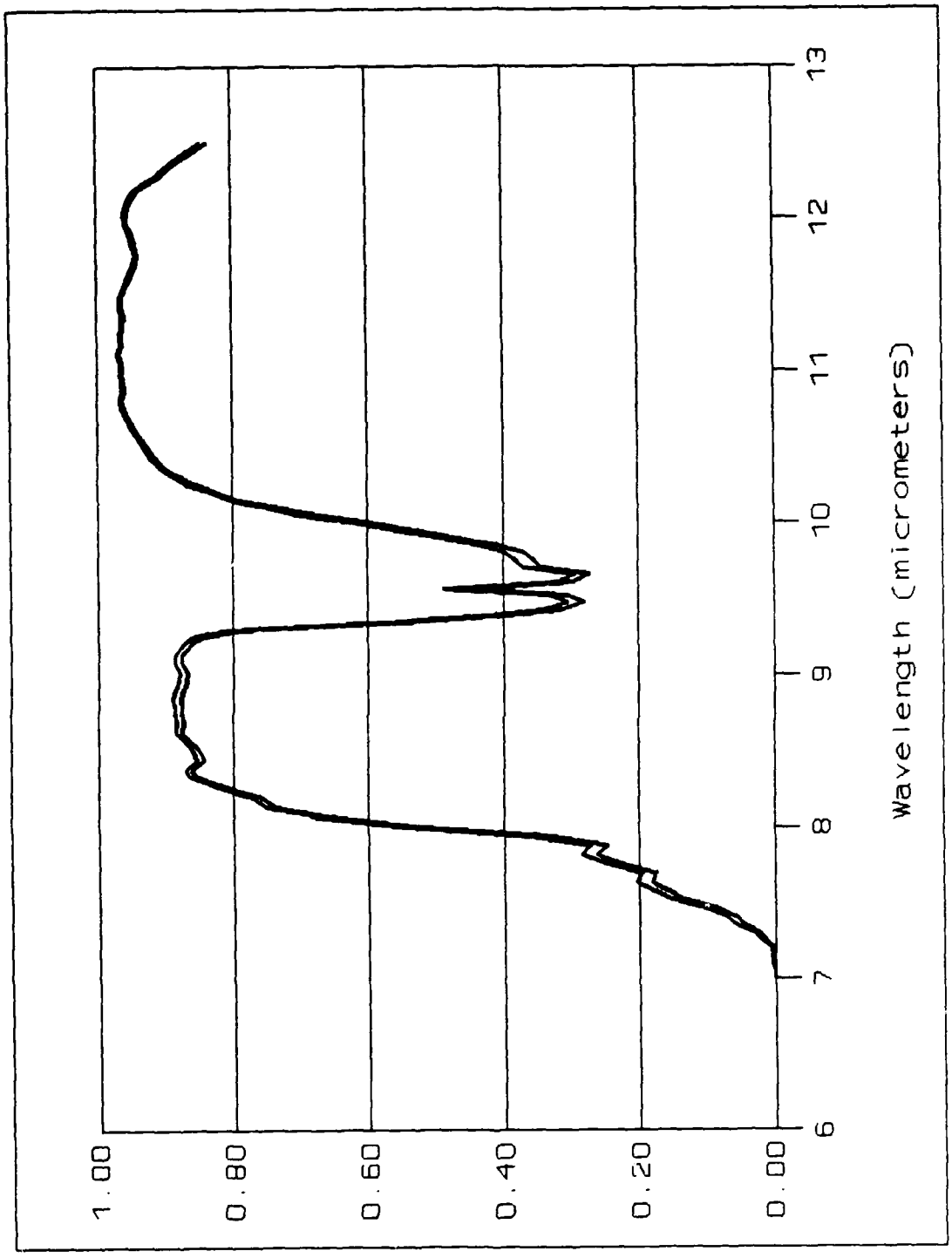

Figure B8. Sub-Arctic Winter Atmospheric Transmission
7-12.5 Micrometers
(Lower line for Zenith angle 27 degrees)

Appendix C: Visible Sensor Threshold Detection Curves

This appendix contains threshold detection curves for the visible wavelength sensors described in Appendix A.

The plotted line is generated using equation 10. Actual NERD values were used for Landsat, SPOT, and IRS sensors. For all other sensors a nominal NERD of 0.5% was used. Atmospheric transmission values were taken from the curves presented in Appendix B.

The threshold line plotted represents the boundary between detection and non-detection of the target by the sensor. If the combination of target size and reflectance difference falls on or above the threshold line the target will be detected by the sensor. If it falls below the threshold line the target will not be detected.

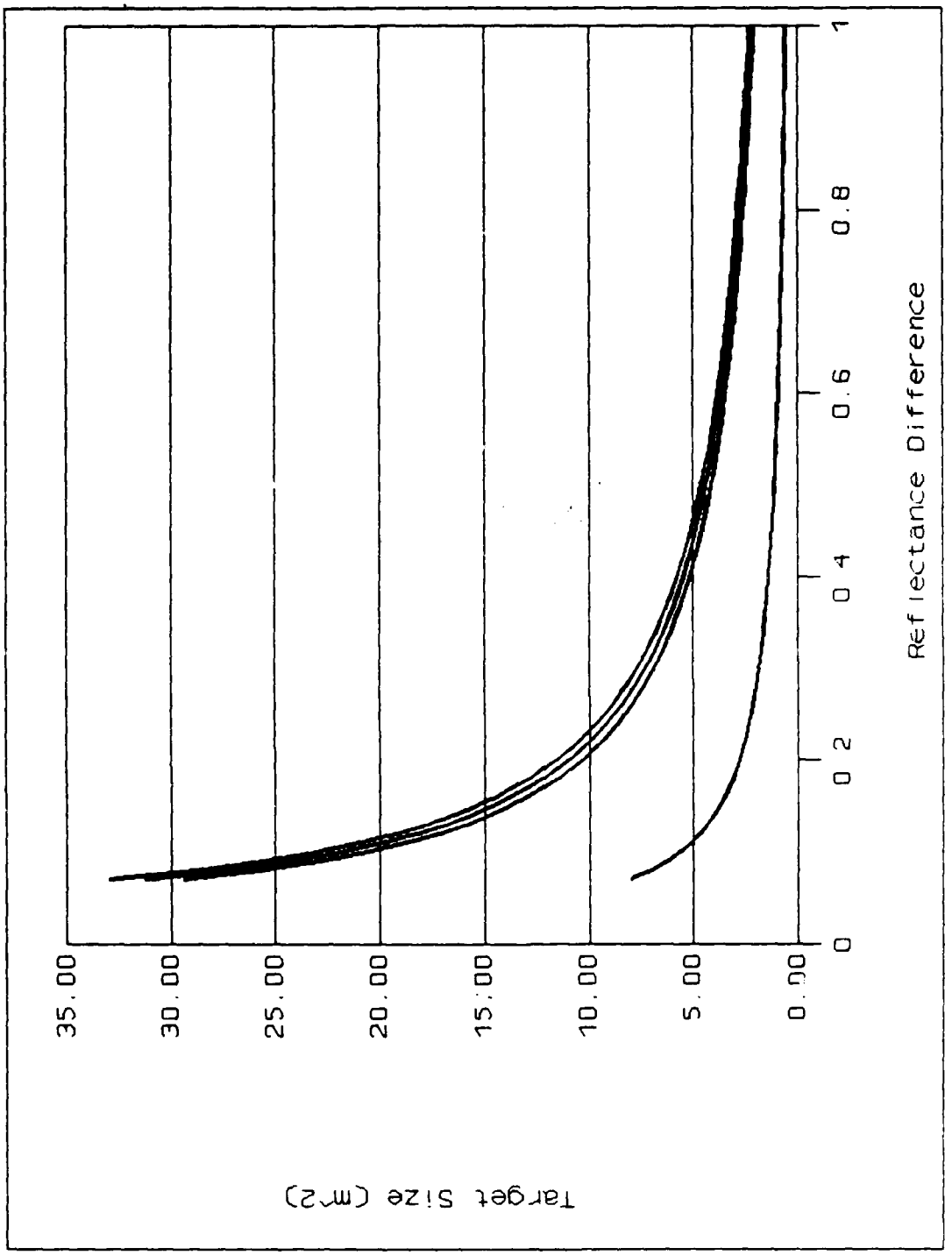

Figure C1. SPOT 3 Target Detection, Winter, Zenith 0
(Top to bottom are Xs1, Xs2, Xs3, Pa Bands)

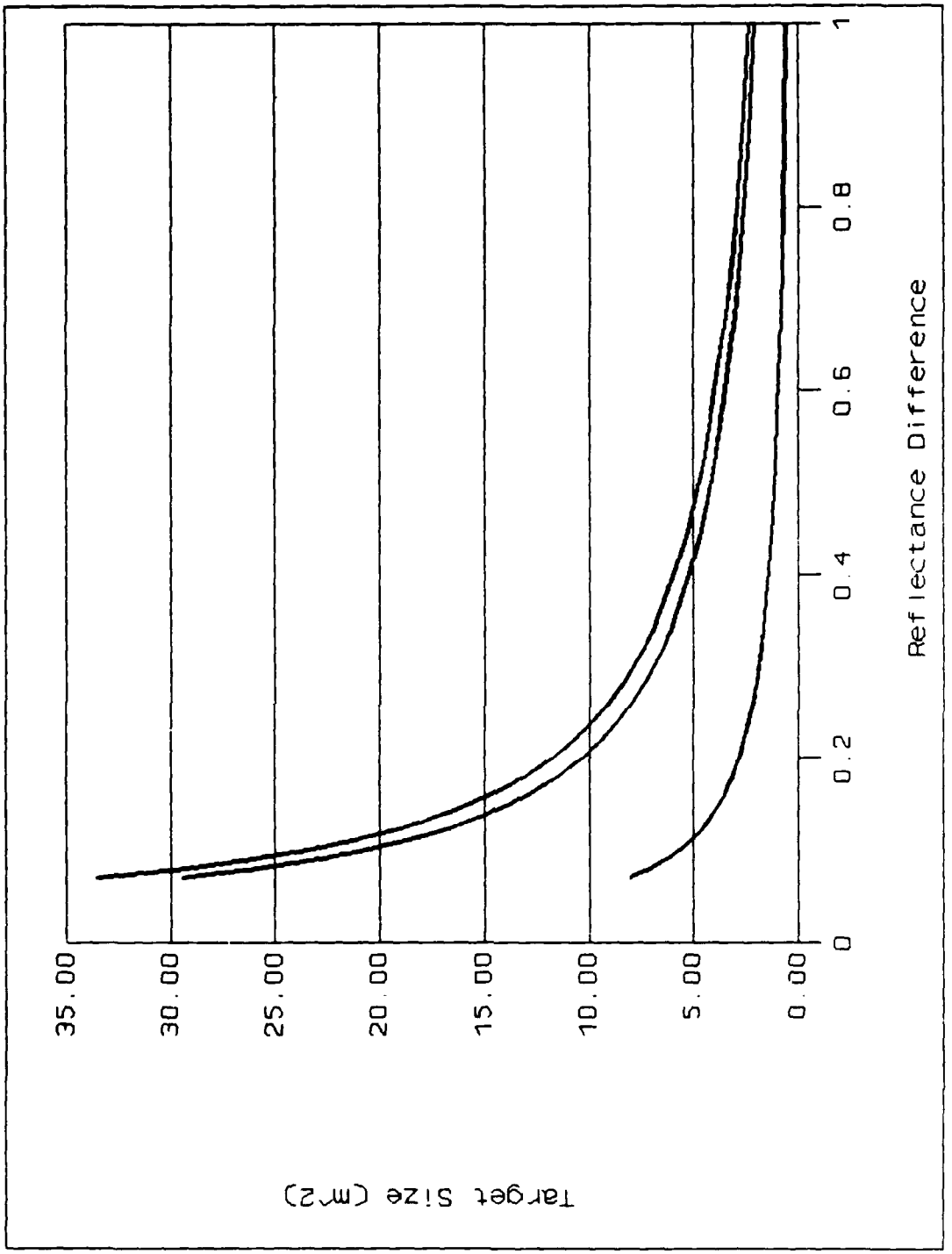

Figure C2. SPOT 4 Target Detection, Winter, Zenith 27
(Top to bottom are Xs1, SWIR, Pa Bands)

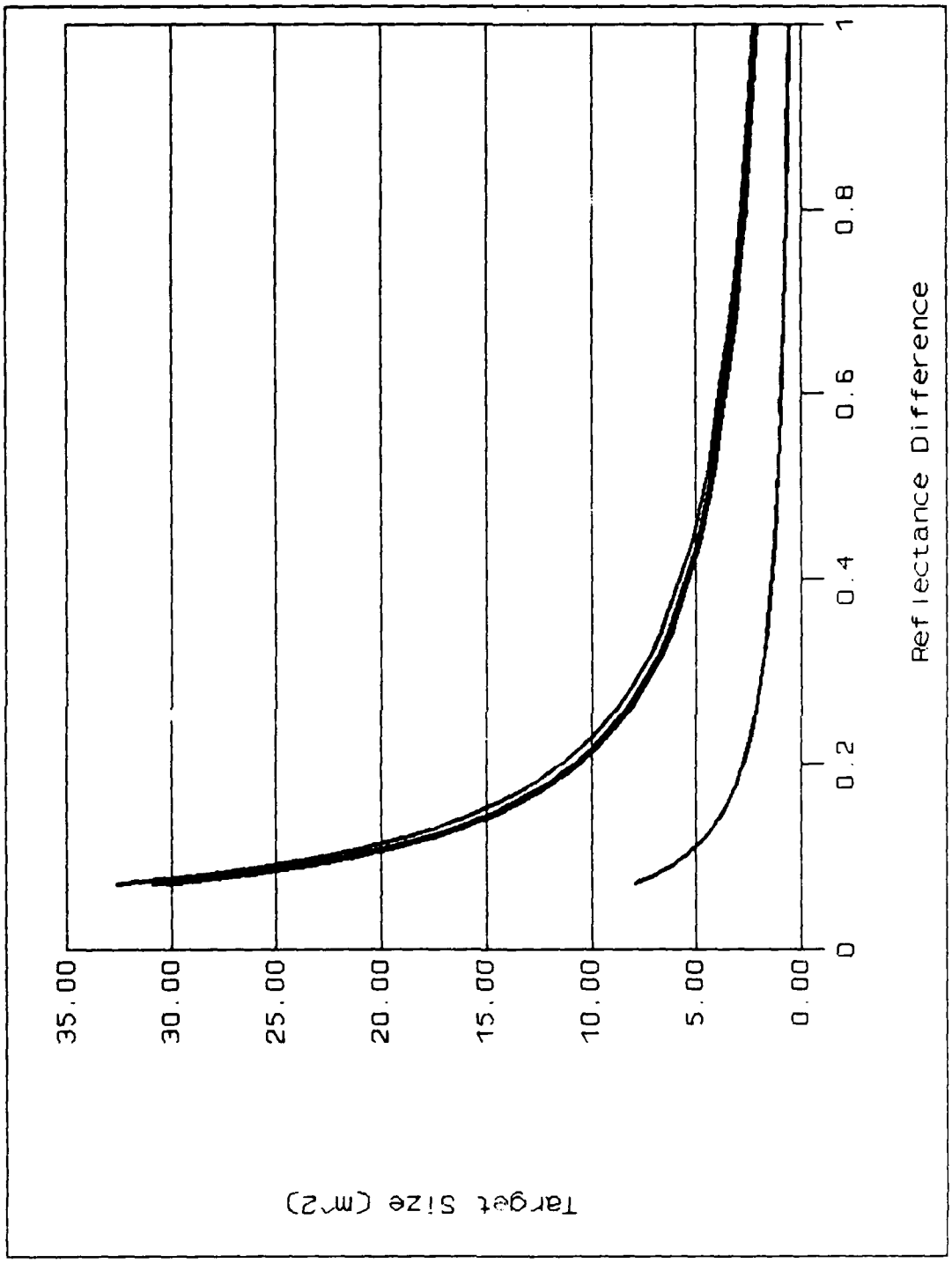

Figure C3. SPOT 3 Target Detection, Summer, Zenith 0
(Top to bottom are Xs1, Xs2, Xs3, Pa Bands)

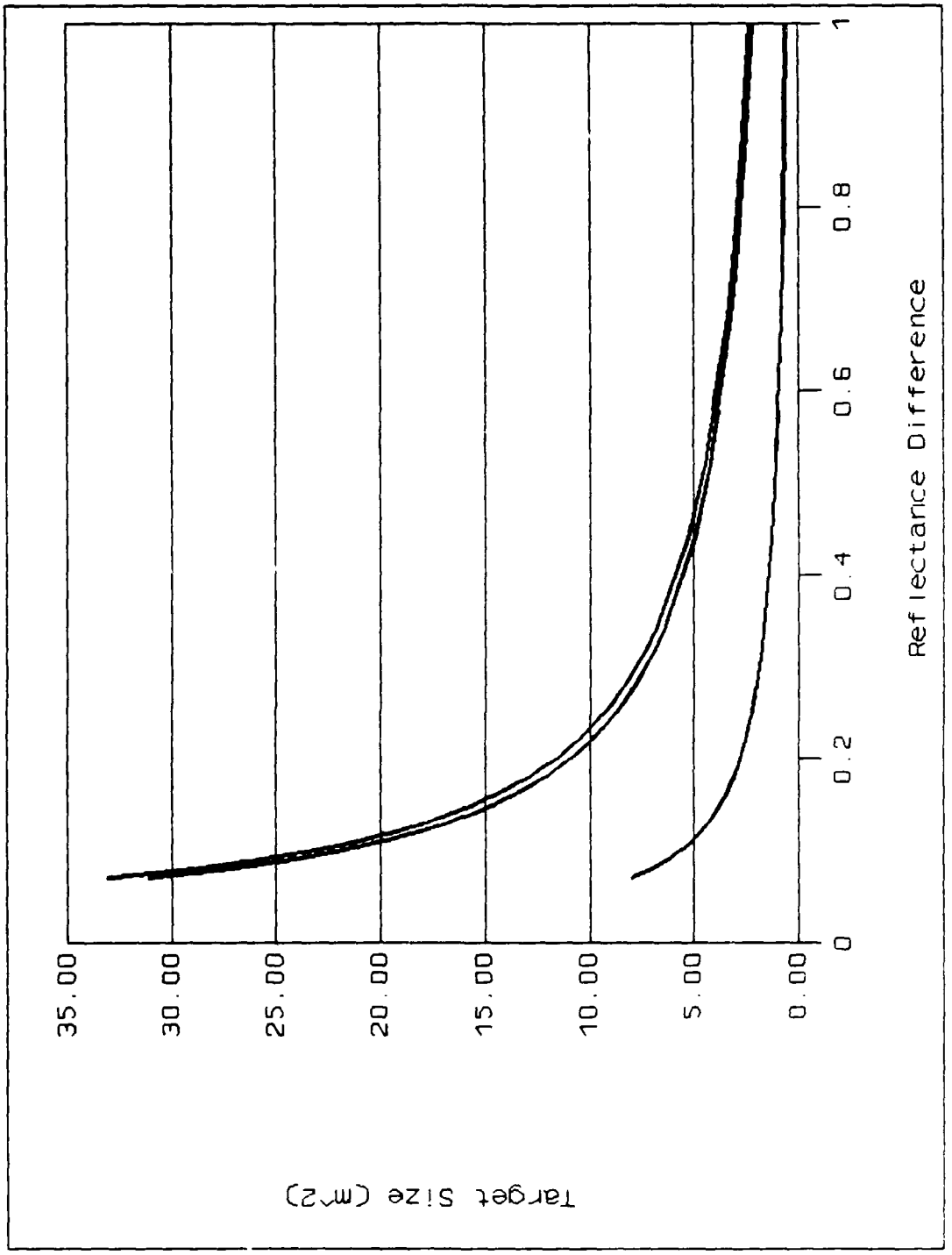

Figure C4. SPOT 4 Target Detection, Summer, Zenith 27
(Top to bottom are Xs1, SWIR, Pa Bands)

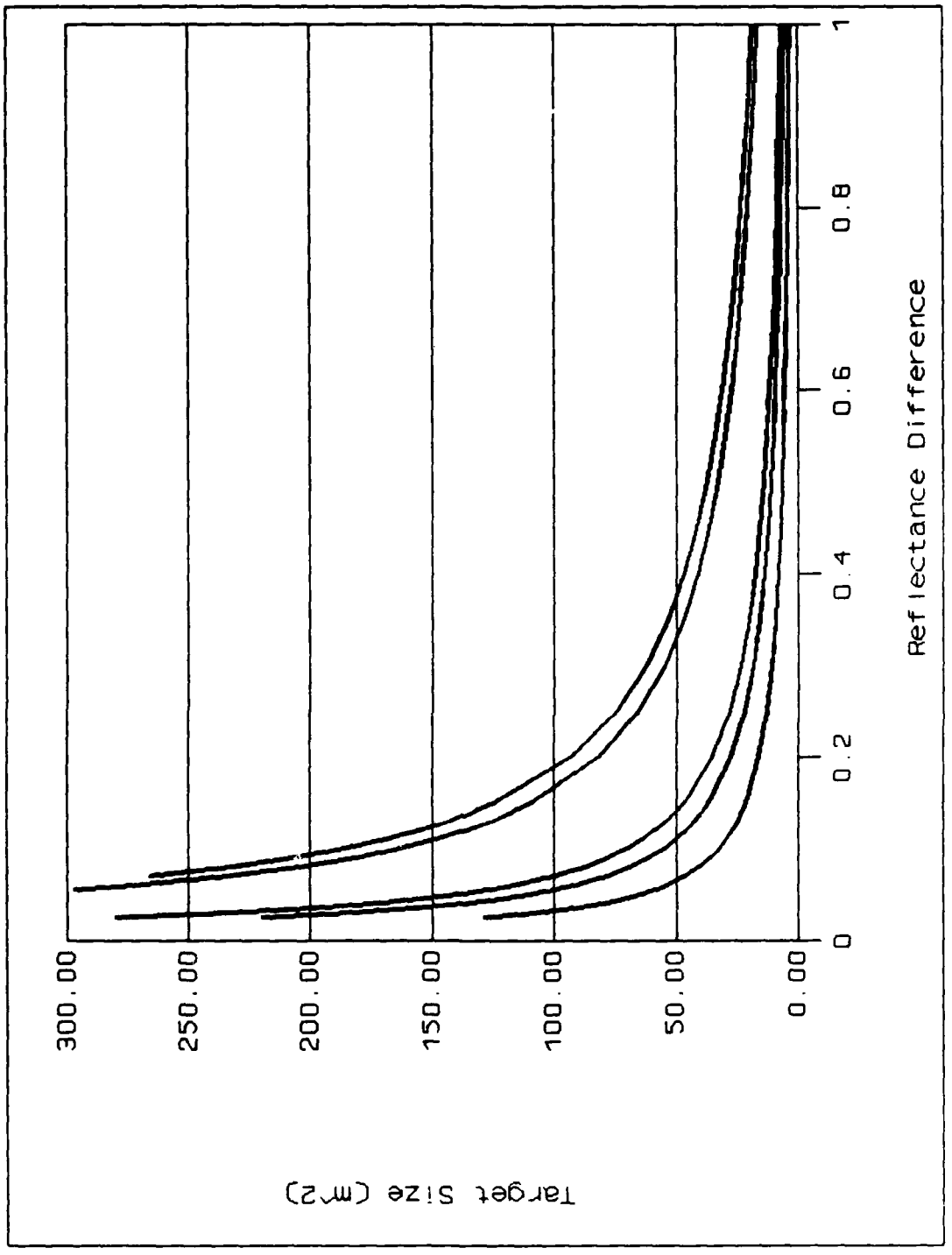

Figure C5. Landsat Thematic Mapper, Winter
(Top to bottom are Bands 7, 5, 1, 3, 4)

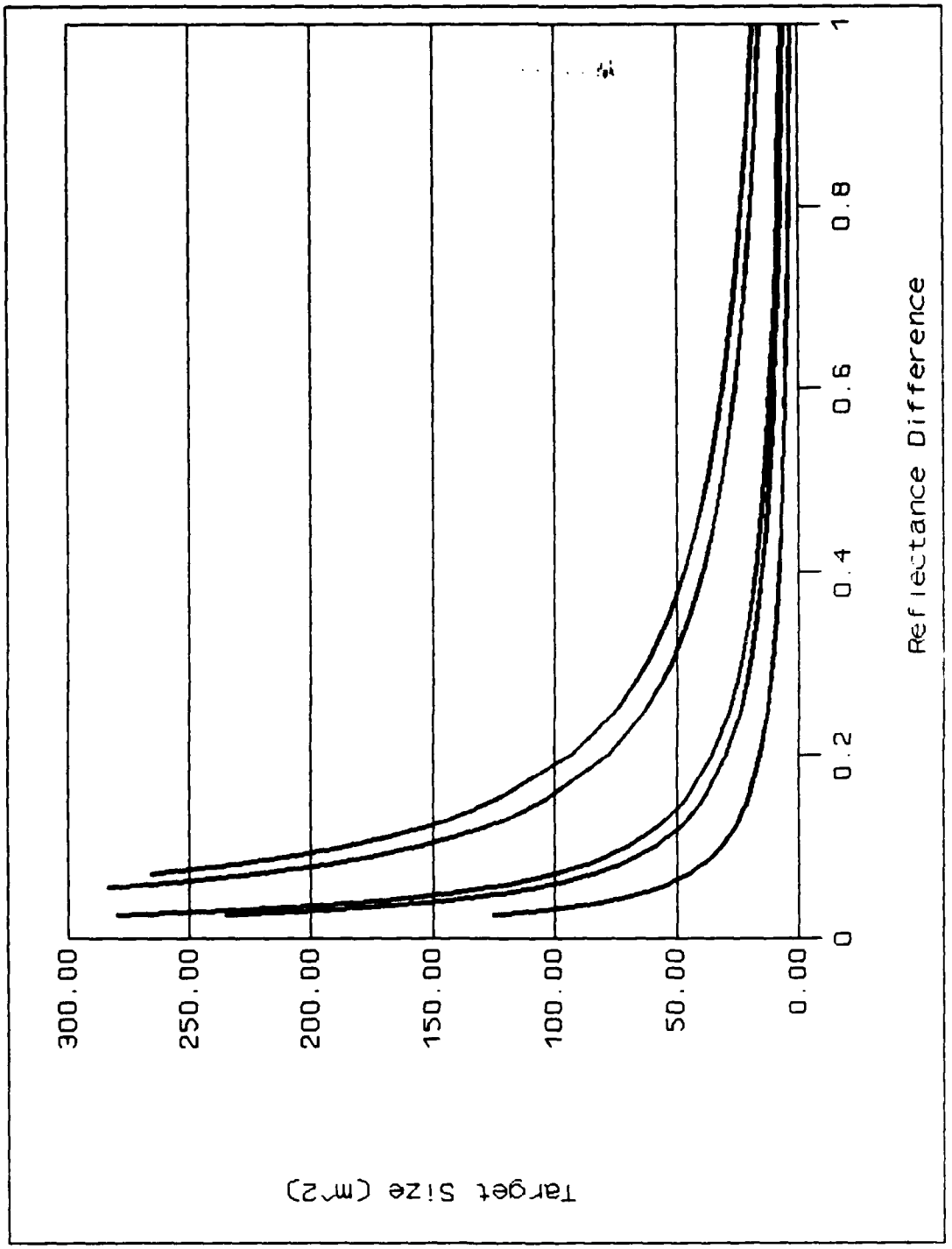

Figure C6. Landsat Thematic Mapper, Summer
(Top to bottom are Bands 7, 5, 1, 3, 4)

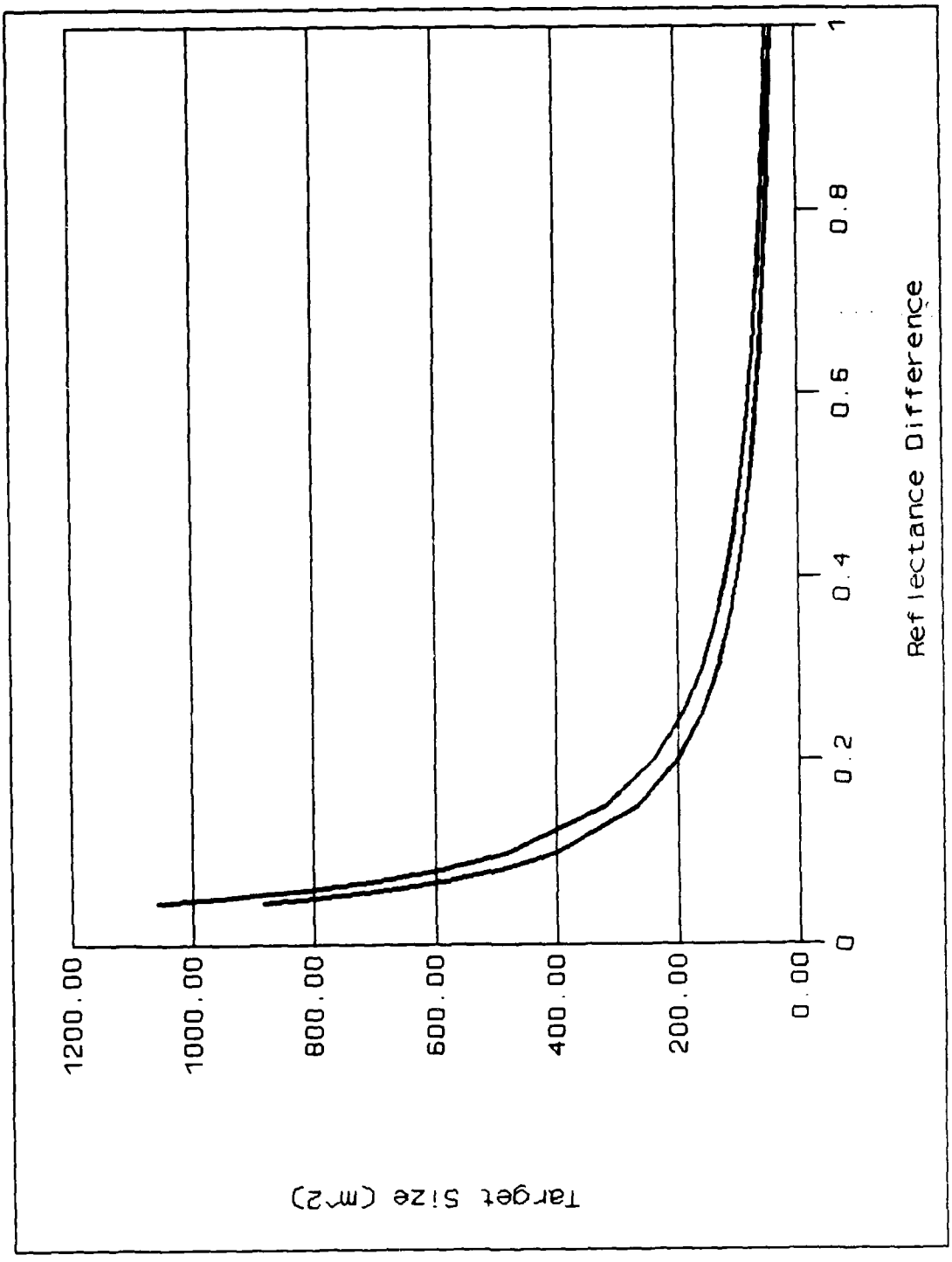

Figure C7. Landsat Multispectral Scanner, Winter
(Top curve is Band 4, bottom is Band 2)

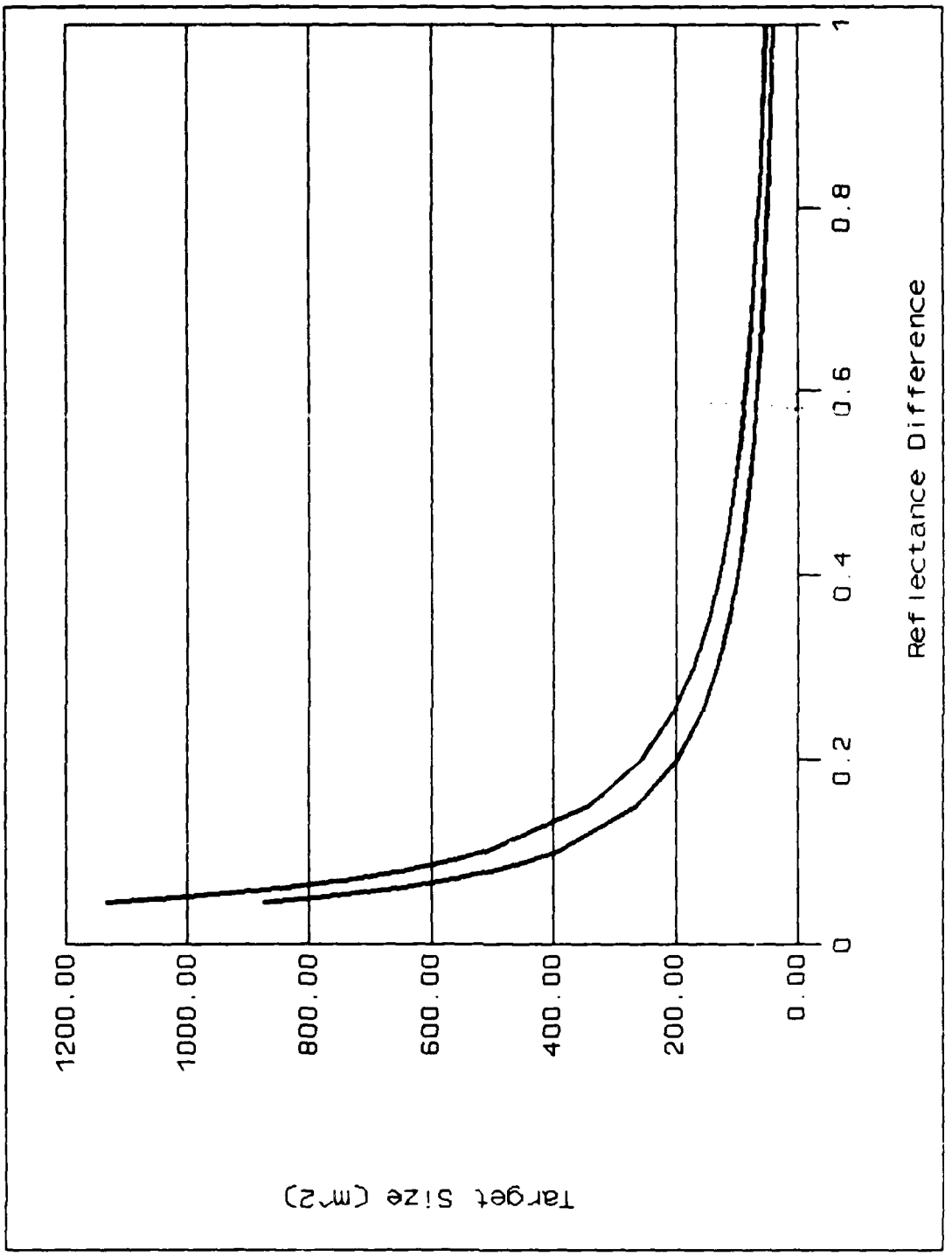

Figure C8. Landsat Multispectral Scanner, Summer
(Top curve is Band 4, bottom is Band 2)

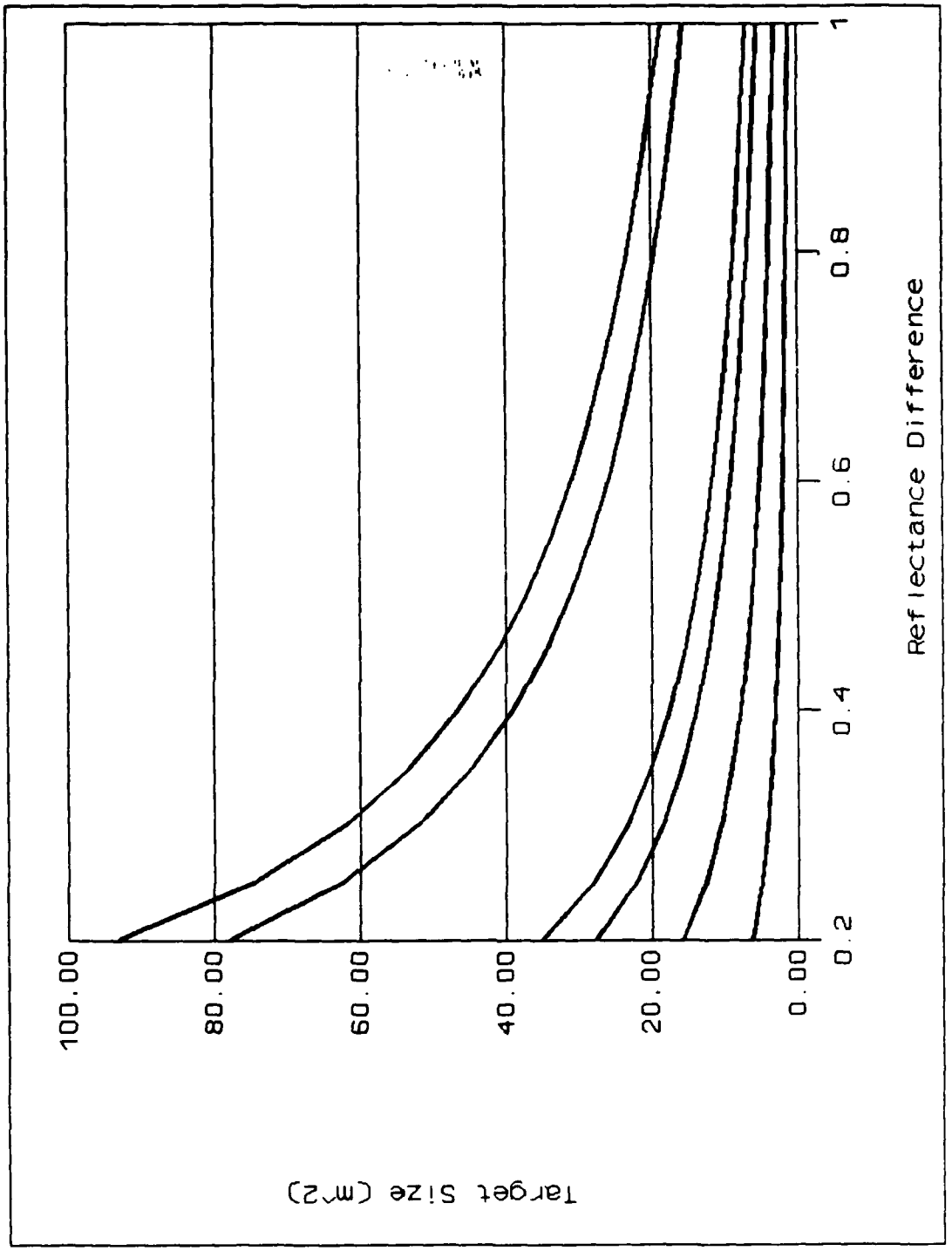

Figure C9. Landsat Enhanced Thematic Mapper, Winter
(Top to bottom are Bands 7, 5, 1, 3, 4, Pa)

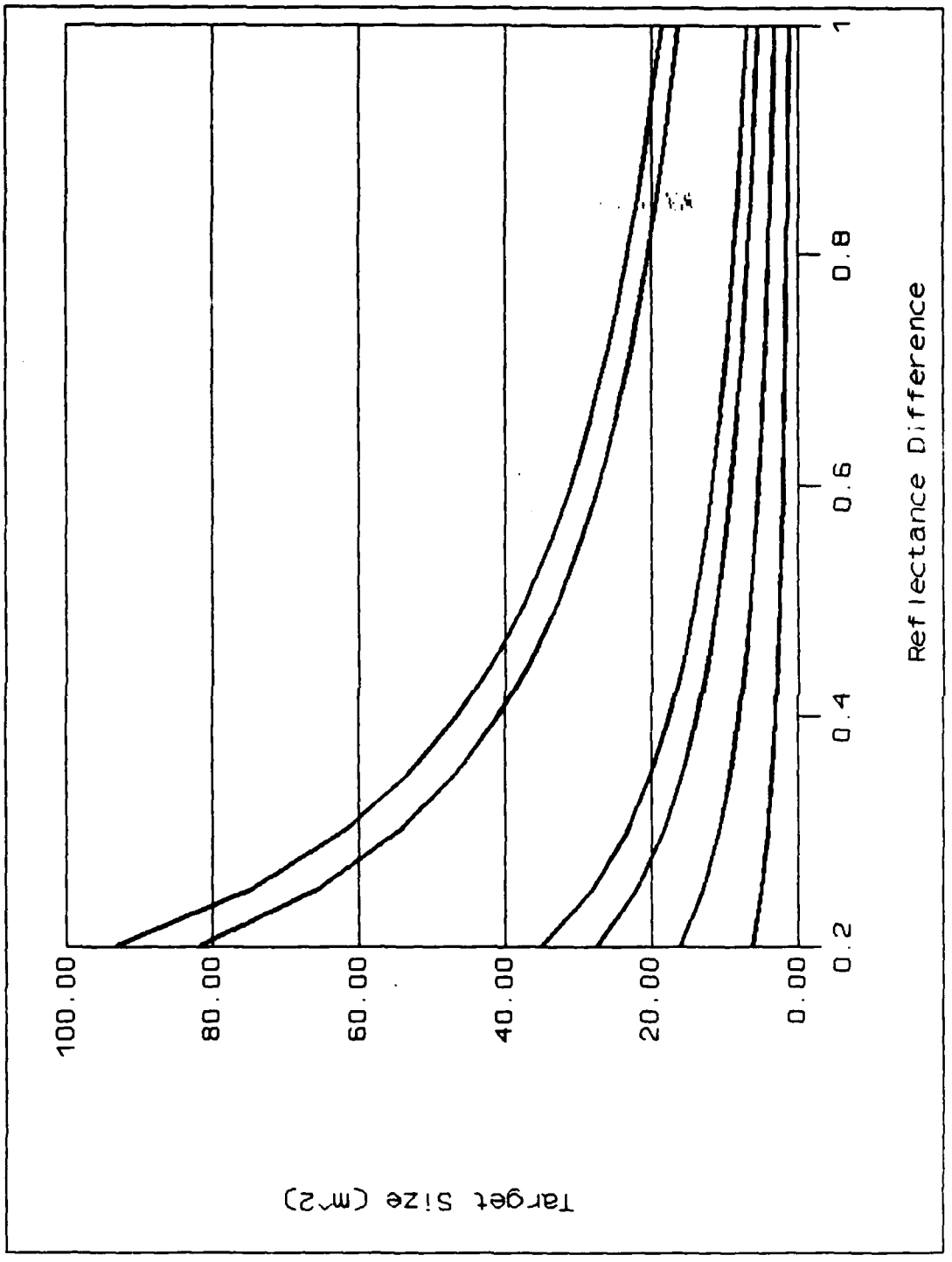

Figure C10. Landsat Enhanced Thematic Mapper, Summer
(Top to bottom are Bands 7, 5, 1, 3, 4, Pa)

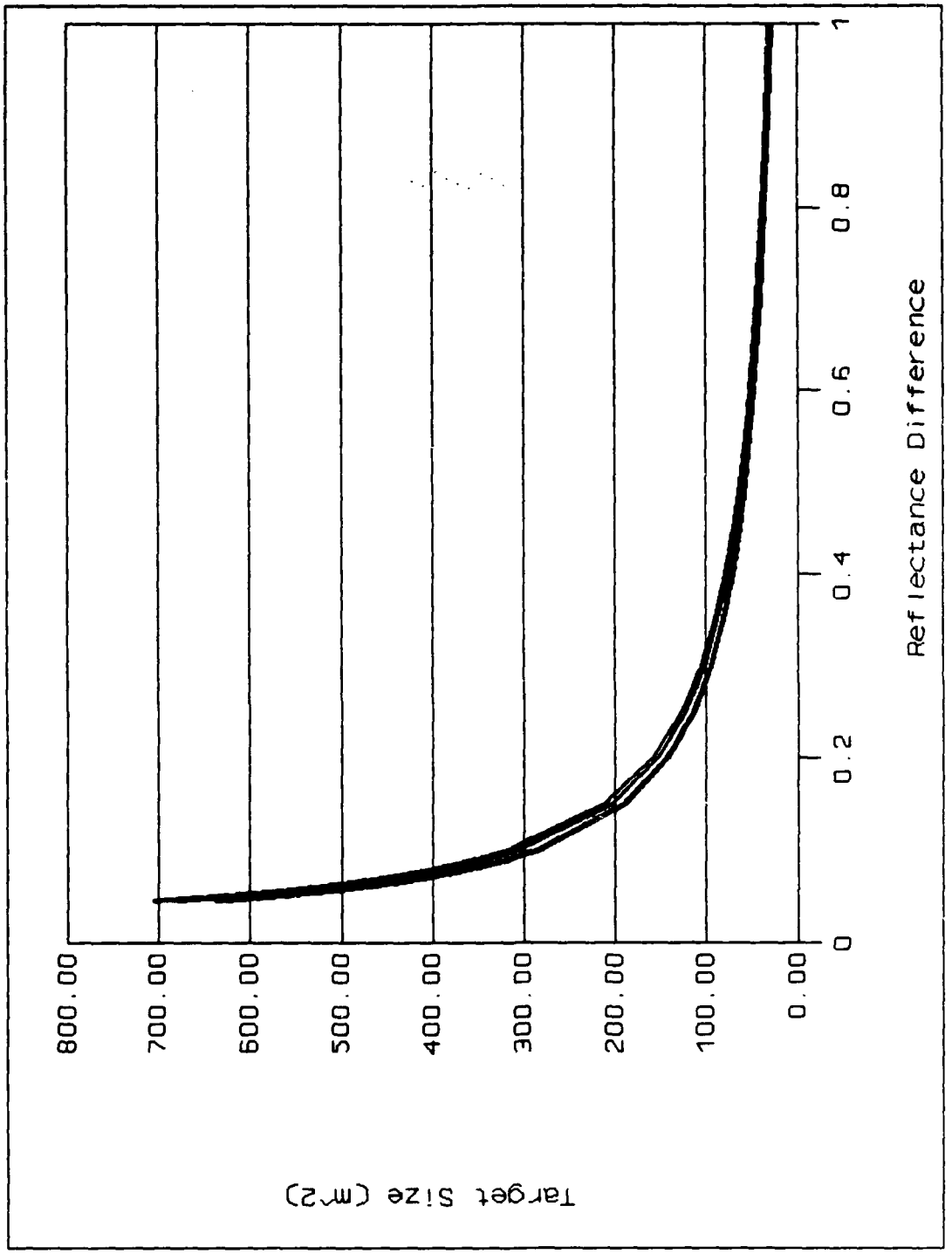

Figure C11. LISS-1, Winter
(Top to bottom are Bands 1, 2, 3, 4)

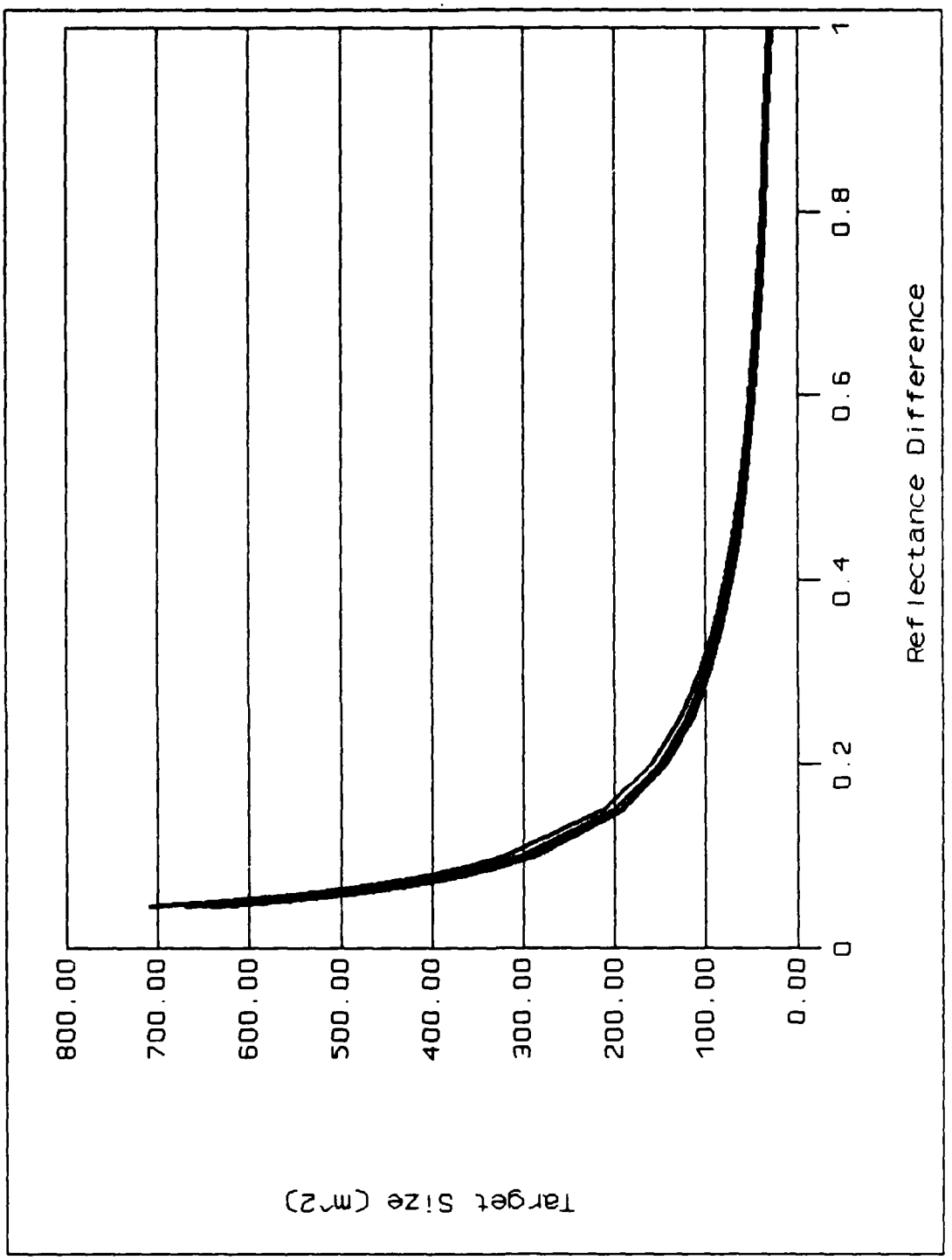

Figure C12. LISS-1, Summer
(Top to bottom are Bands 1, 2, 3, 4)

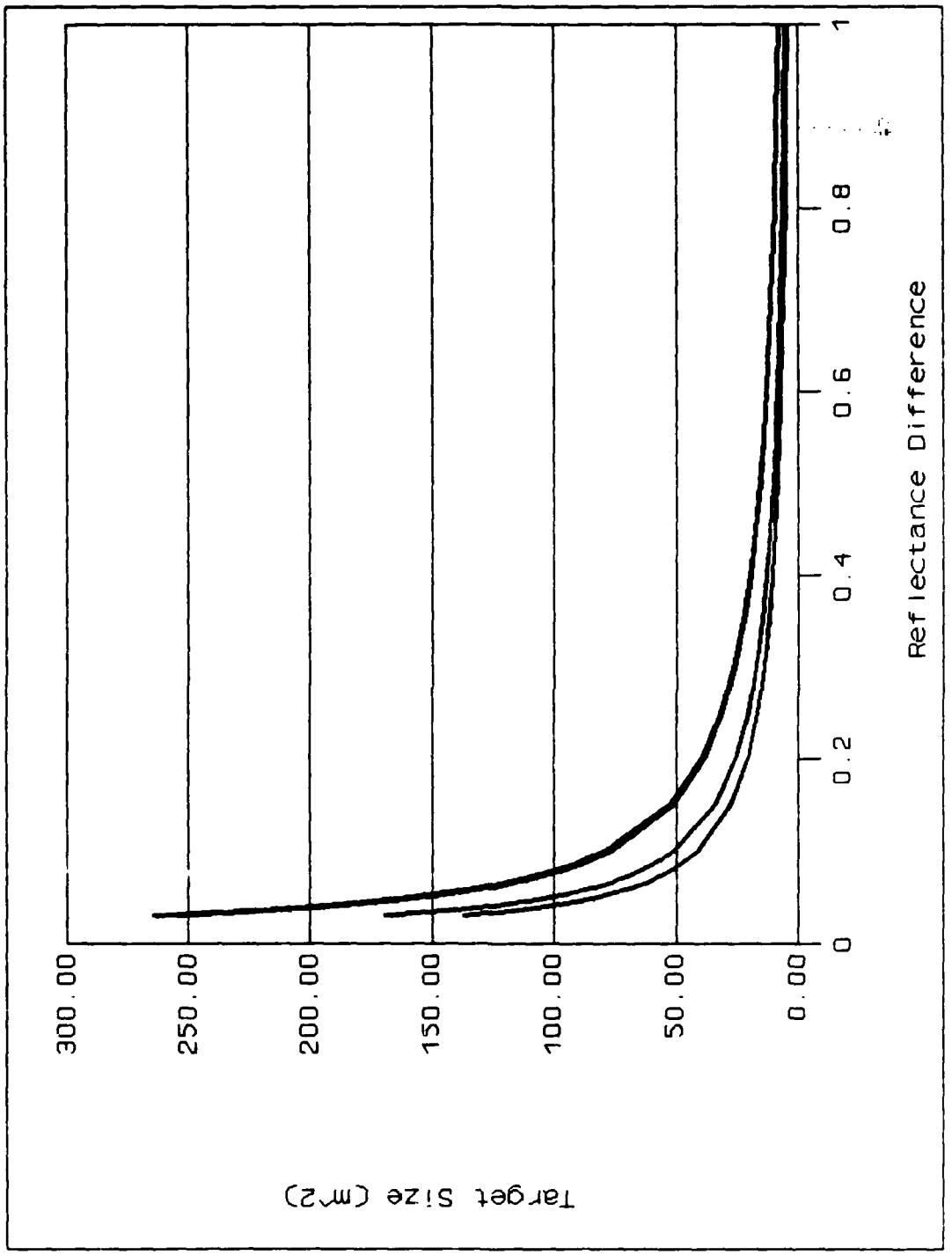

Figure C13. LISS-2, Winter
(Top to bottom are Bands 1, 2, 3, 4)

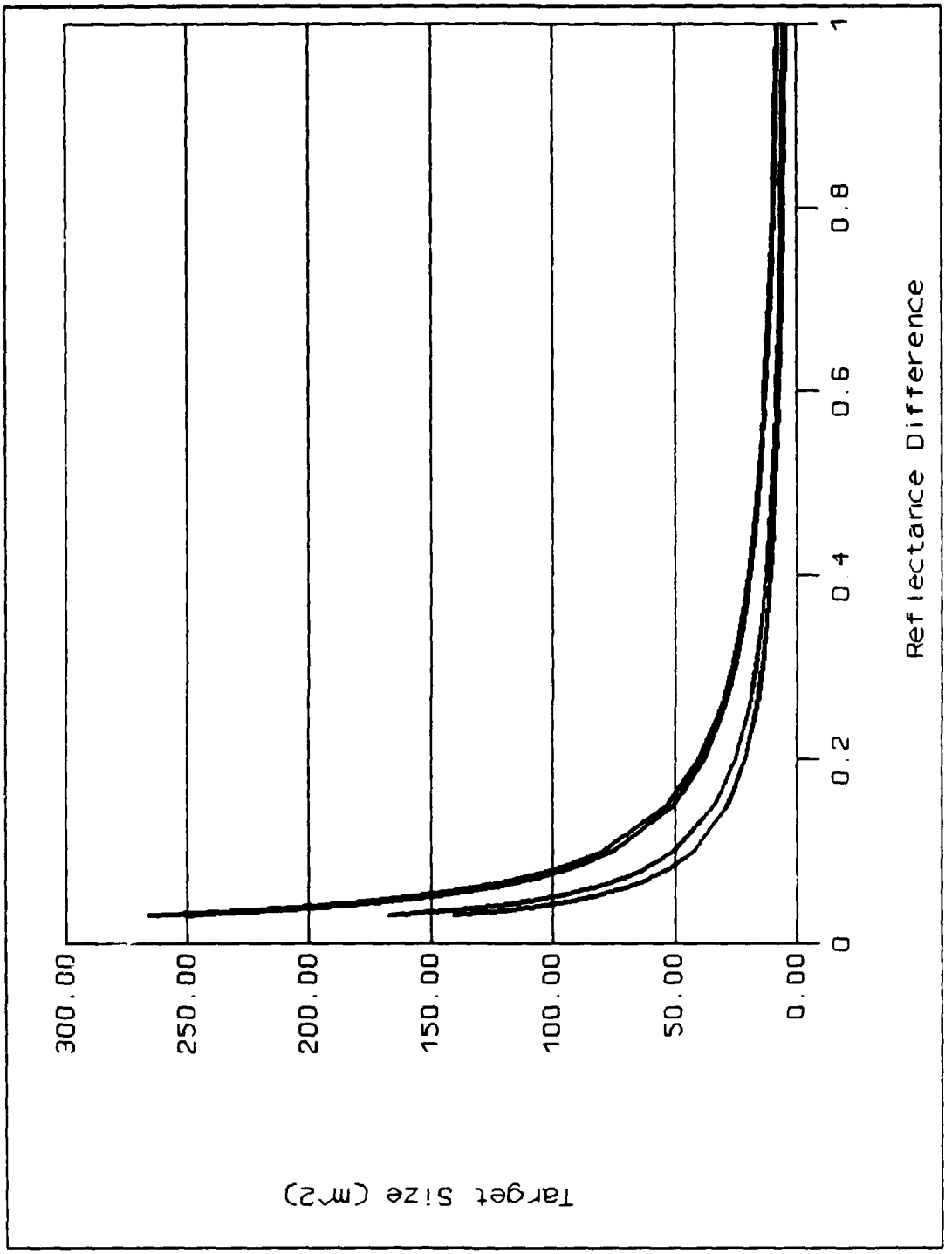

Figure C14. LISS-2, Summer
(Top to bottom are Bands 1, 2, 3, 4)

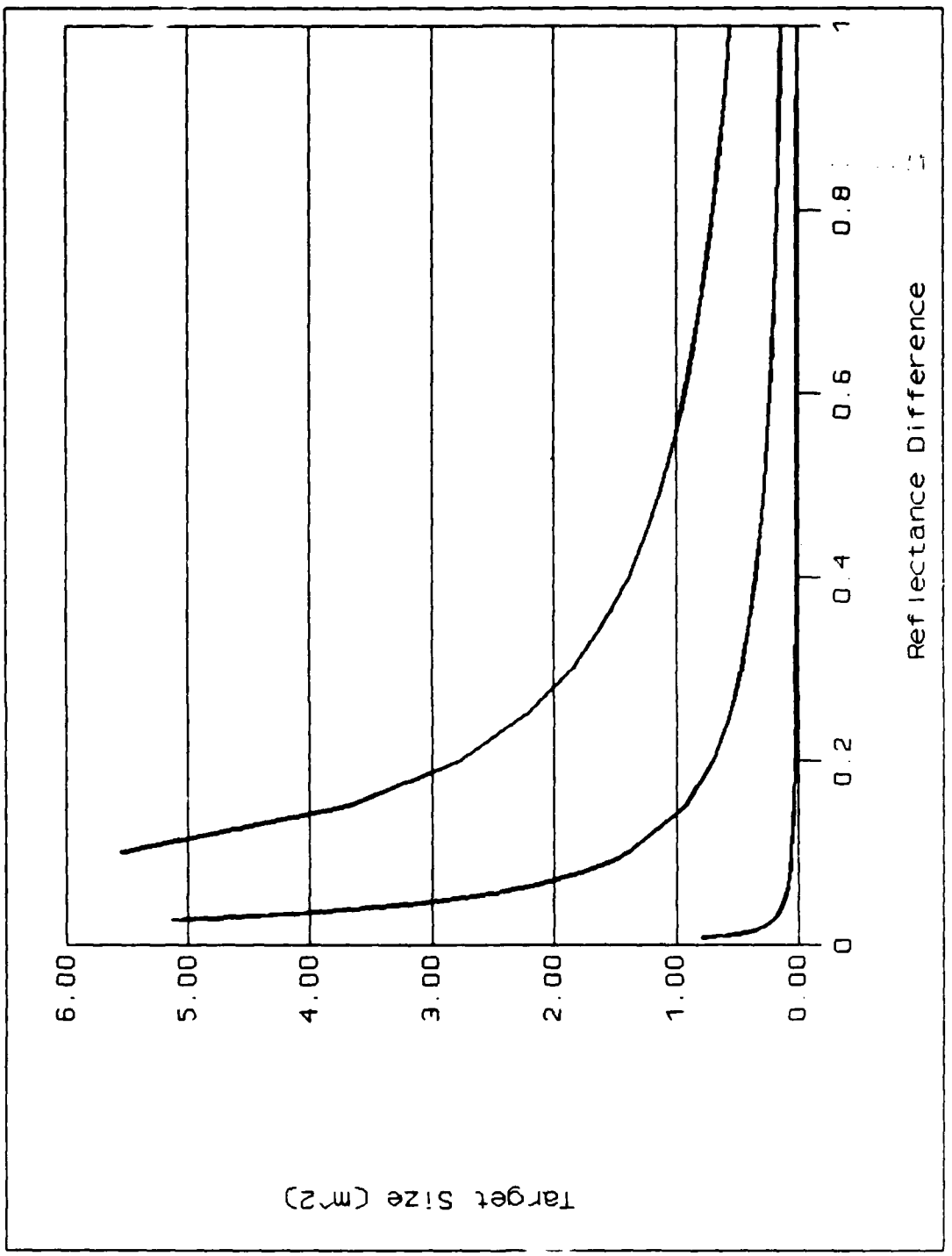

Figure C15. Hypothetical 10, 5, and 1 Meter
Ground Resolution Cell Sensors
(Top to bottom are 10, 5, and 1 meter threshold curves)

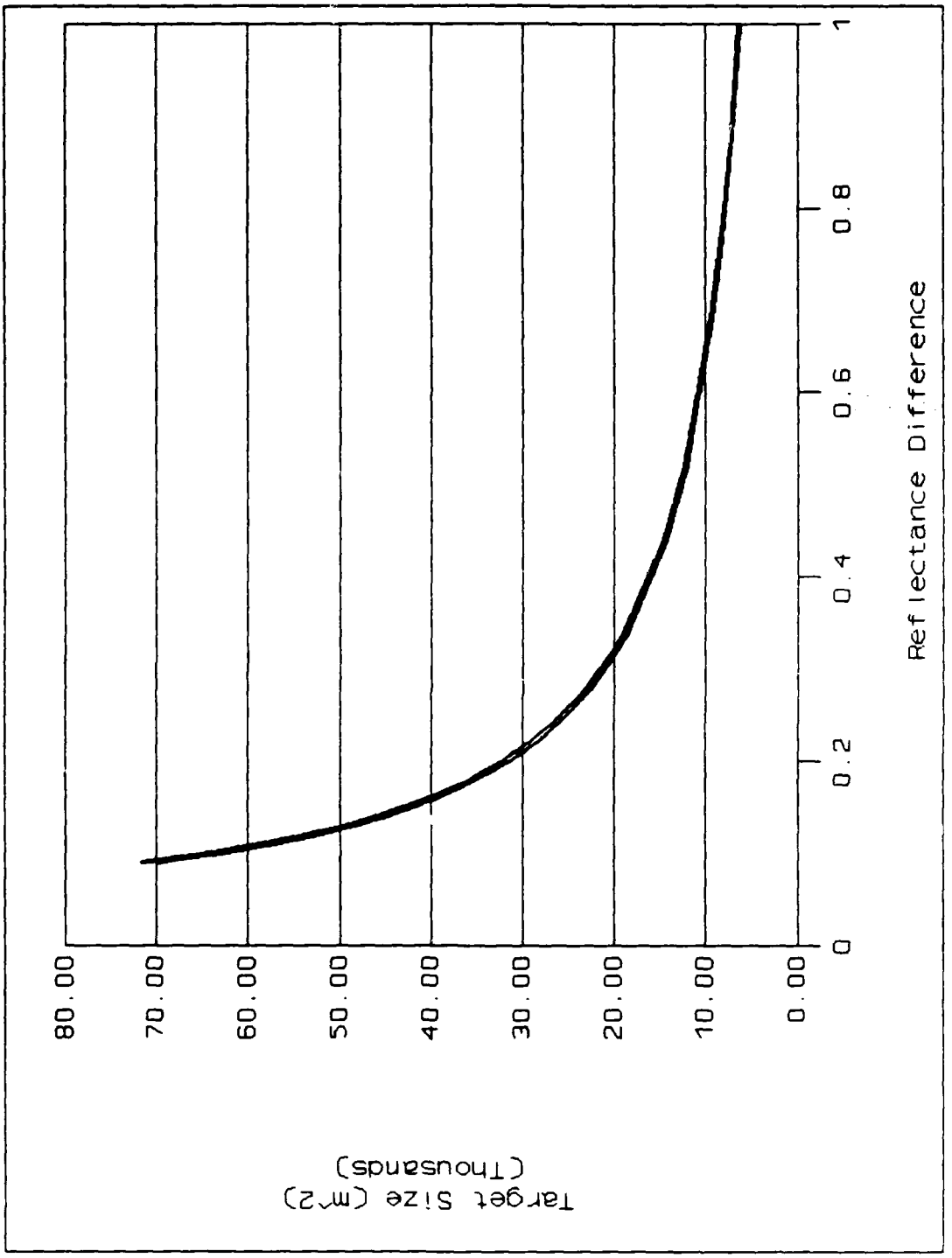

Figure C16. SPOT 4 HRV 0.43-0.47 Sensor
Summer and Winter

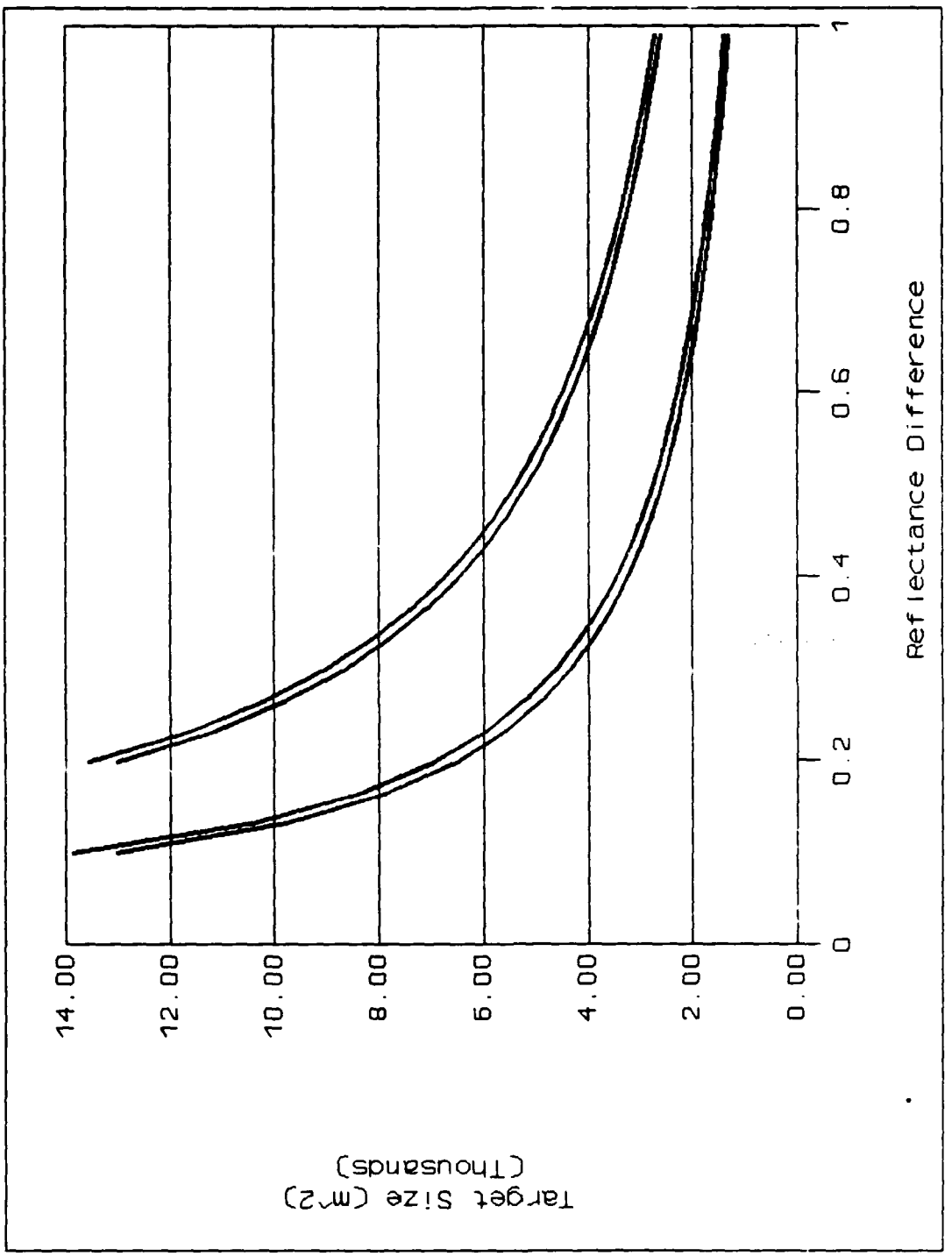

Figure C17. NOAA K/L/M AVHRR Winter
(Top to bottom are Bands 3b, 3a, 1, and 2)

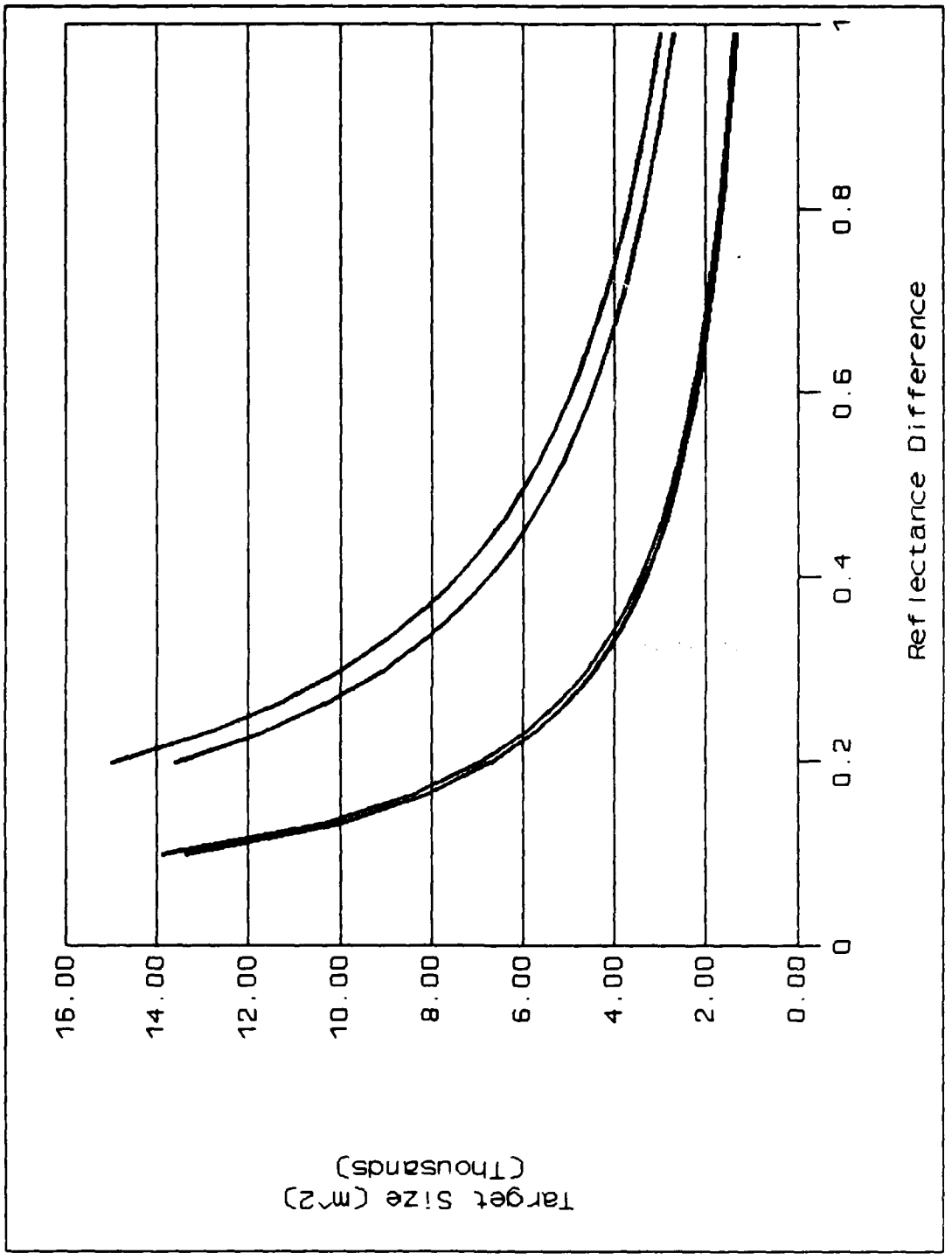

Figure C18. NOAA K/L/M AVHRR Summer
(Top to bottom are Bands 3b, 3a, 1, and 2)

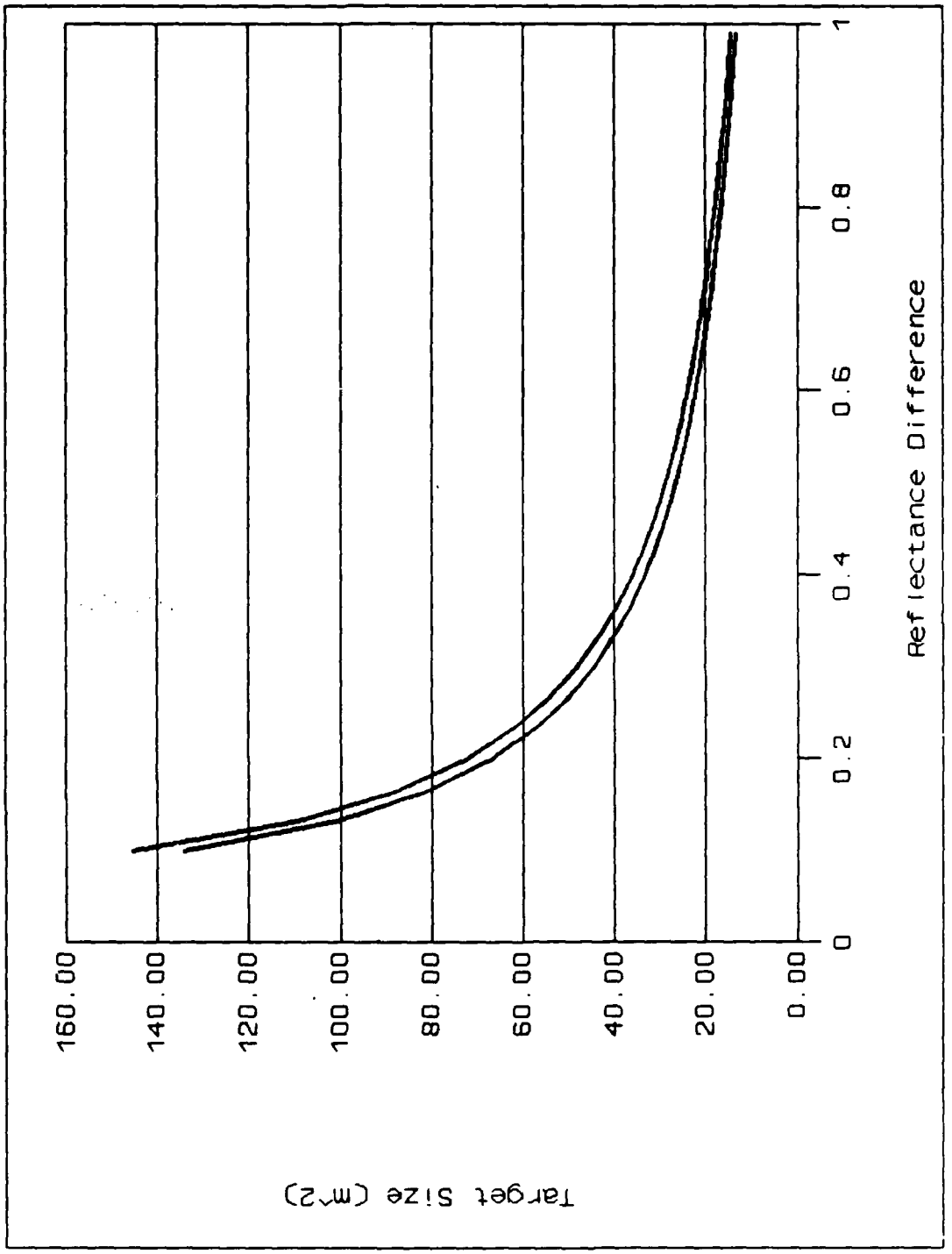

Figure C19. MOS-1 MESSR Winter
(Top curve is Band 1, bottom is Band 2, 3, or 4)

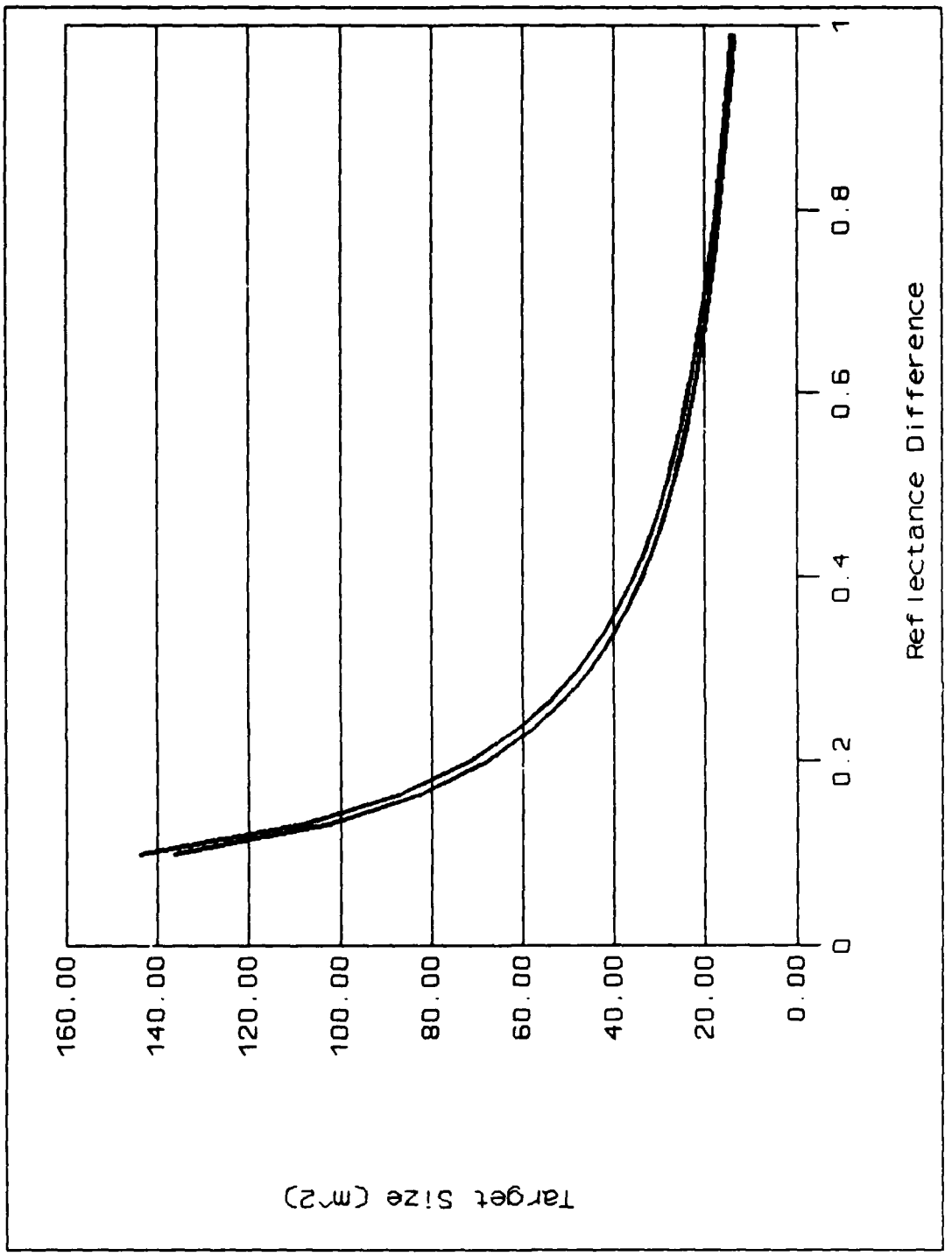

Figure C20. MOS-1 MESSR Summer
(Top curve is Band 1, bottom is Band 2, 3, or 4)

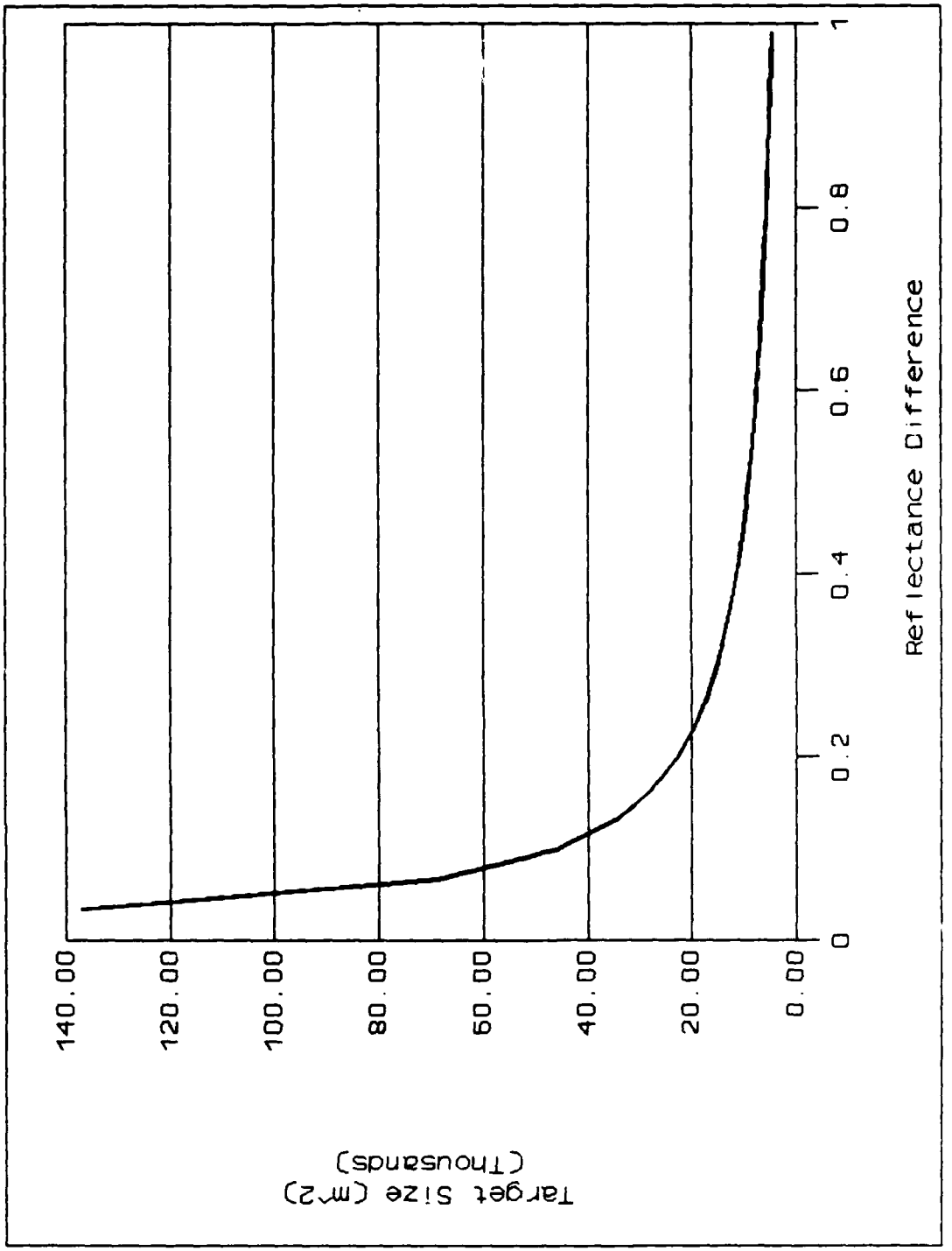

Figure C21. MOS-1 VTIR Summer

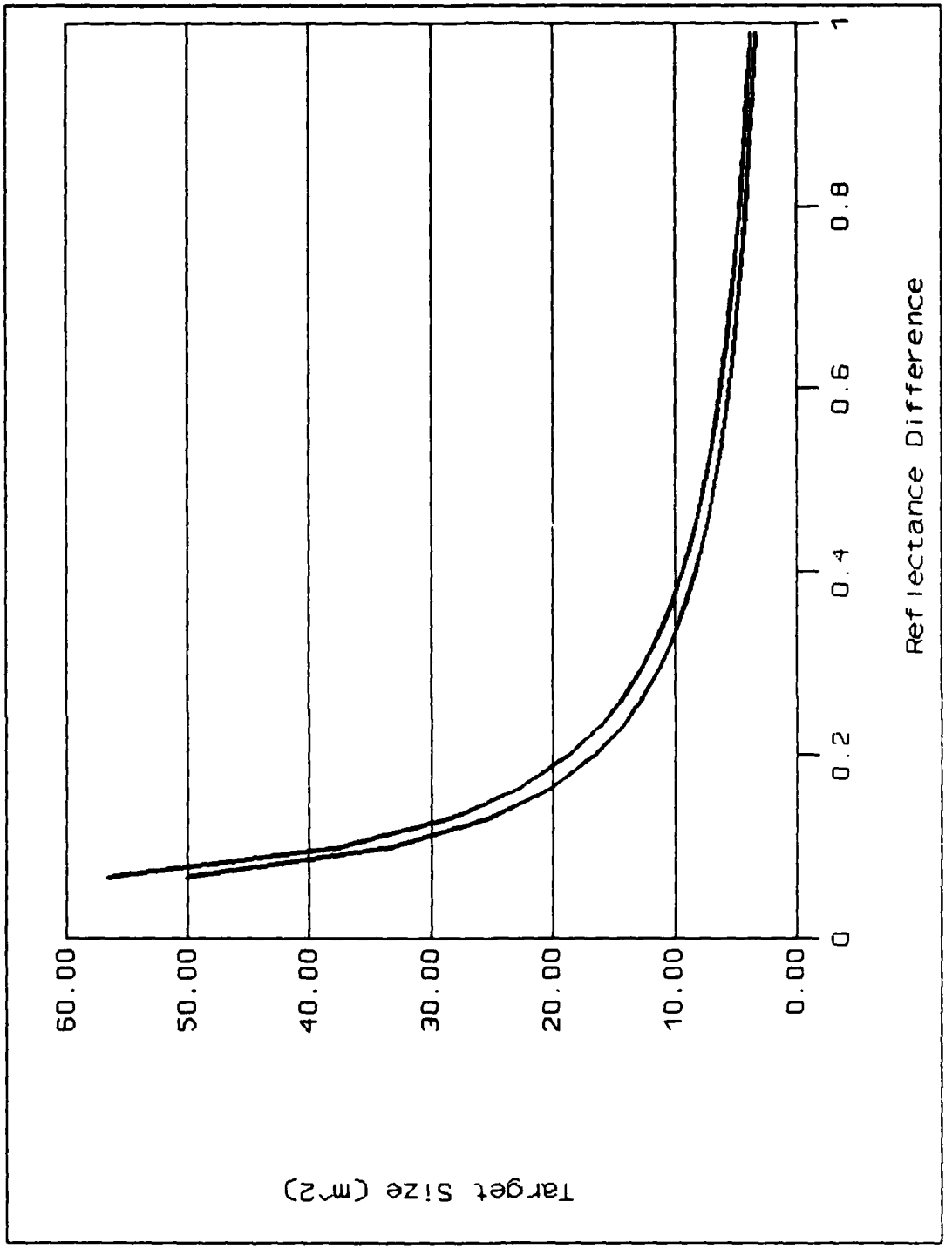

Figure C22. JERS-1 VNR Winter
(Top curve is Band 1, bottom is Band 4)

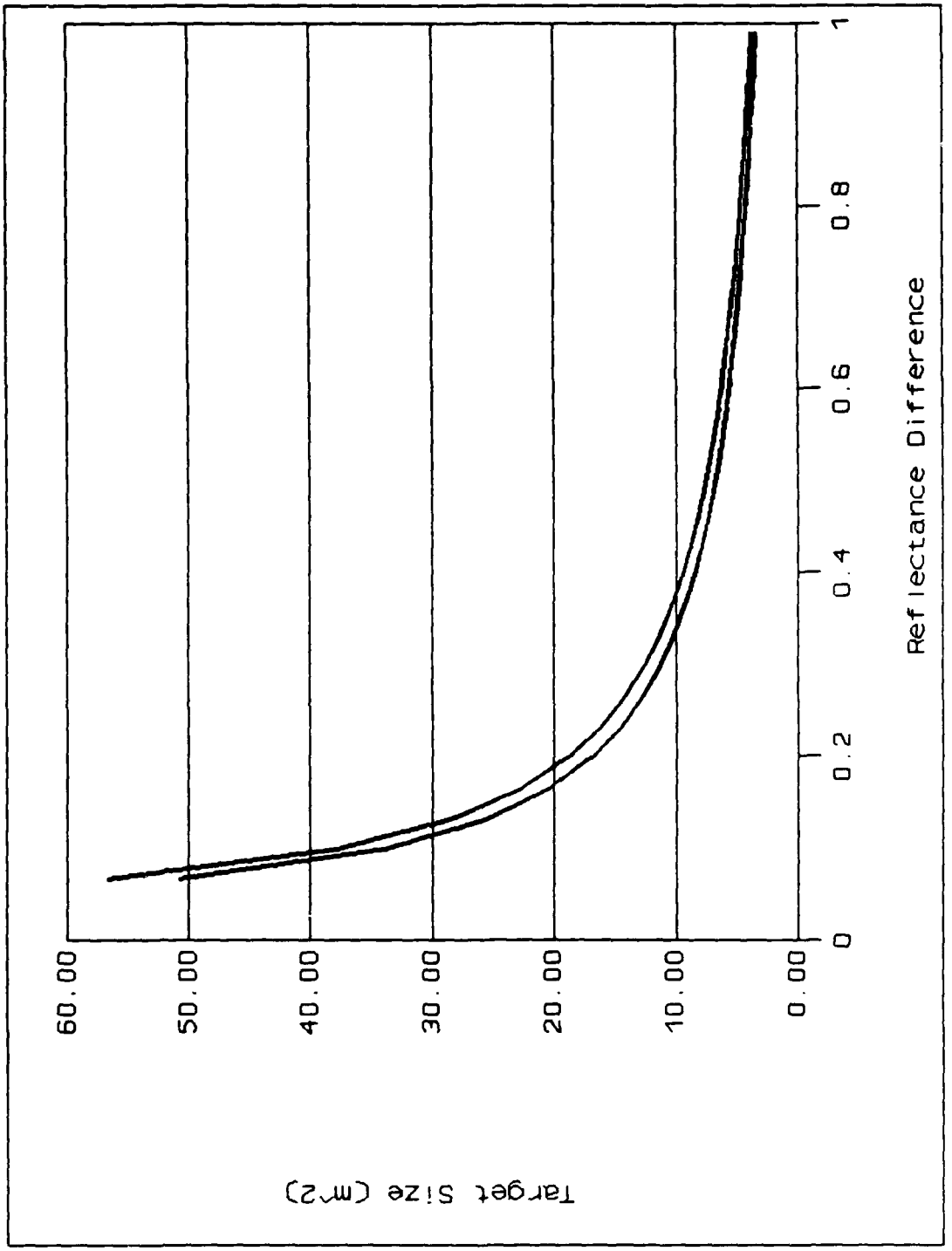

Figure C23. JERS-1 VNR Summer
(Top curve is Band 1, bottom is Band 3)

Appendix D: Target Description

A Canadian Government report, Satellites and Sovereignty, published in August 1977, identifies targets which would be subject to surveillance in the Canadian arctic. Two target types are of interest: survey parties on land or ice; and shipping. This appendix contains summaries of the target descriptions provided in the government report and representative coating reflectances taken from the TPRC Data Series, Volume 9, Thermal Radiative Properties -- Coatings.

Survey Party Description

General:

Survey parties are made up of clusters of vehicles and shelters. The vehicles can be expected to be metallic. The shelters can be made of a variety of materials. The number of vehicles and shelters will vary.

Spatial Characteristics:

Spatial characteristics will also vary. For analysis a representative party consisting of 10 vehicles and five shelters will be used. Vehicles are assumed to be pairs of 10, 20, 30, 40, and 50 square meters plan size when viewed from nadir. Shelters for analysis are tents 10 square meters plan size when viewed from nadir. When in camp all vehicles and shelters are assumed to be clustered within a 500 square meter area. When deployed vehicles are assumed to be in column and spaced by 100 meters.

These choices are arbitrary but within the guidelines established in the government report previously cited.

Spectral Characteristics:

Vehicles and shelters are assumed to be painted US Army olive drab in sufficient quantity to provide an optically thick coating. The reflectance of this paint, as a function of wavelength, is plotted in Figure D1.

It is assumed that 1/4 of vehicle plan size is 2°K warmer than the background while vehicles are operating.

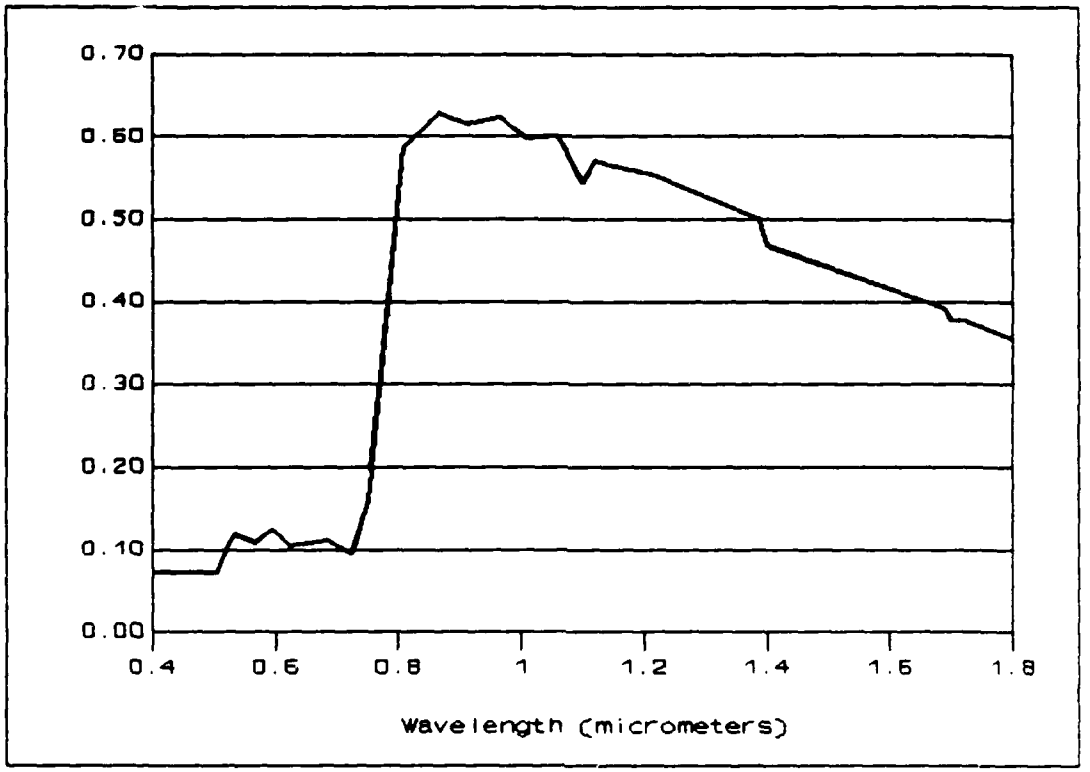

Figure D1. Reflectance of US Army Olive Drab vs Wavelength (TPRC:569)

Vehicles are assumed to be in constant operation. Shelters are assumed to be at ambient temperature.

Temporal Characteristics:

Base camps are assumed to be stationary but can be moved monthly.

Information Requirements:

Images are required daily and must be available within 12 hours of collection.

Shipping

General Description:

Targets of interest are single ships entering and travelling in Canadian arctic waters.

Spatial Characteristics:

Ships may be 10 to 200 meters in length. For this analysis ships will be a DDH class destroyer which is 115 meters long and 15 meters wide (37:73).

Spectral Characteristics:

Ships will be made of steel and painted wi ' aluminum

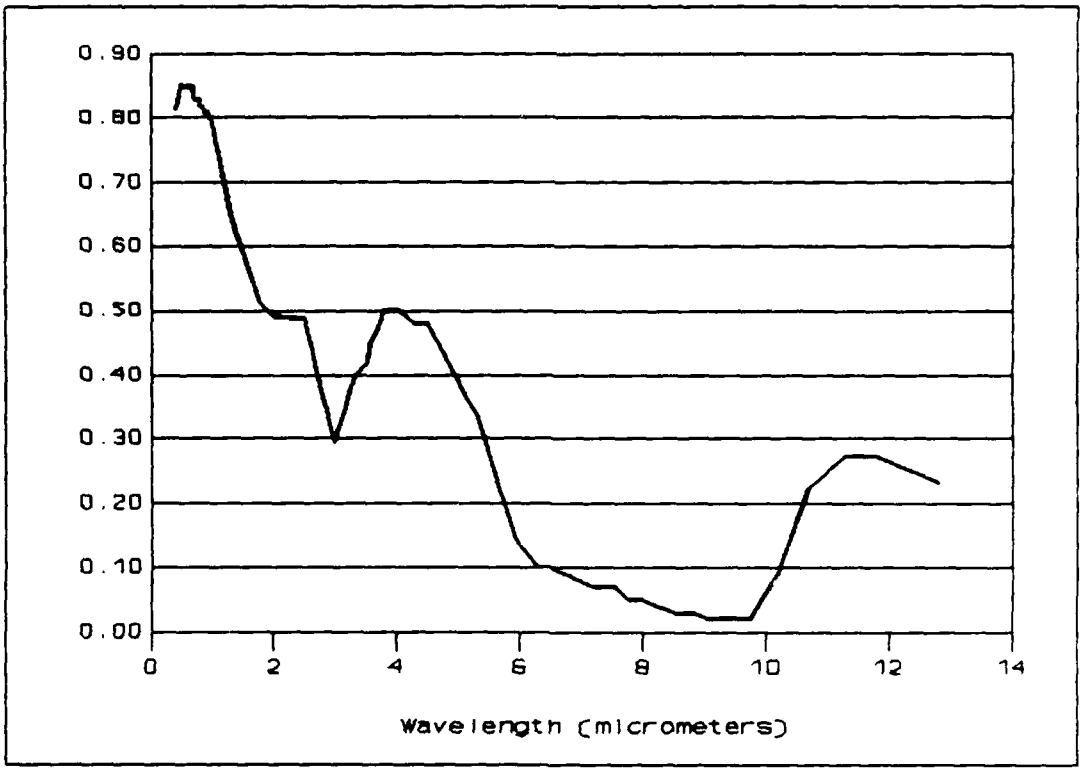

Figure D2. Reflectance of Aluminum Oxide on Steel vs Wavelength (70:795)

oxide contact coating. The reflectance of this paint, as a function of wavelength, is plotted in Figure D2.

One tenth of the plan size of the ship is assumed to be 2°K warmer than ambient temperature.

Temporal Characteristics:

The ship is assumed to travel at 20 knots in open water, and at 3 knots through ice.

Information Requirements:

Images are required every 12 hours and must be available within 12 hours of collection.

Appendix E: Threshold Longitudes for Landsat and SPOT

This appendix contains threshold longitude curves for overlap of the possible target area by Landsat and SPOT sensor swaths. If the sensor passes within the threshold longitude, the sensor's swath and the possible target area will overlap.

To determine the local crossing angle, the following equations are used:

$$\cos(90-q) = \cos(Long)\sin(i)$$

and

$$\sin(Long) = \tan(Lat)/\tan(i)$$

Where

q = local crossing angle
Long = longitude
i = inclination
Lat = latitude

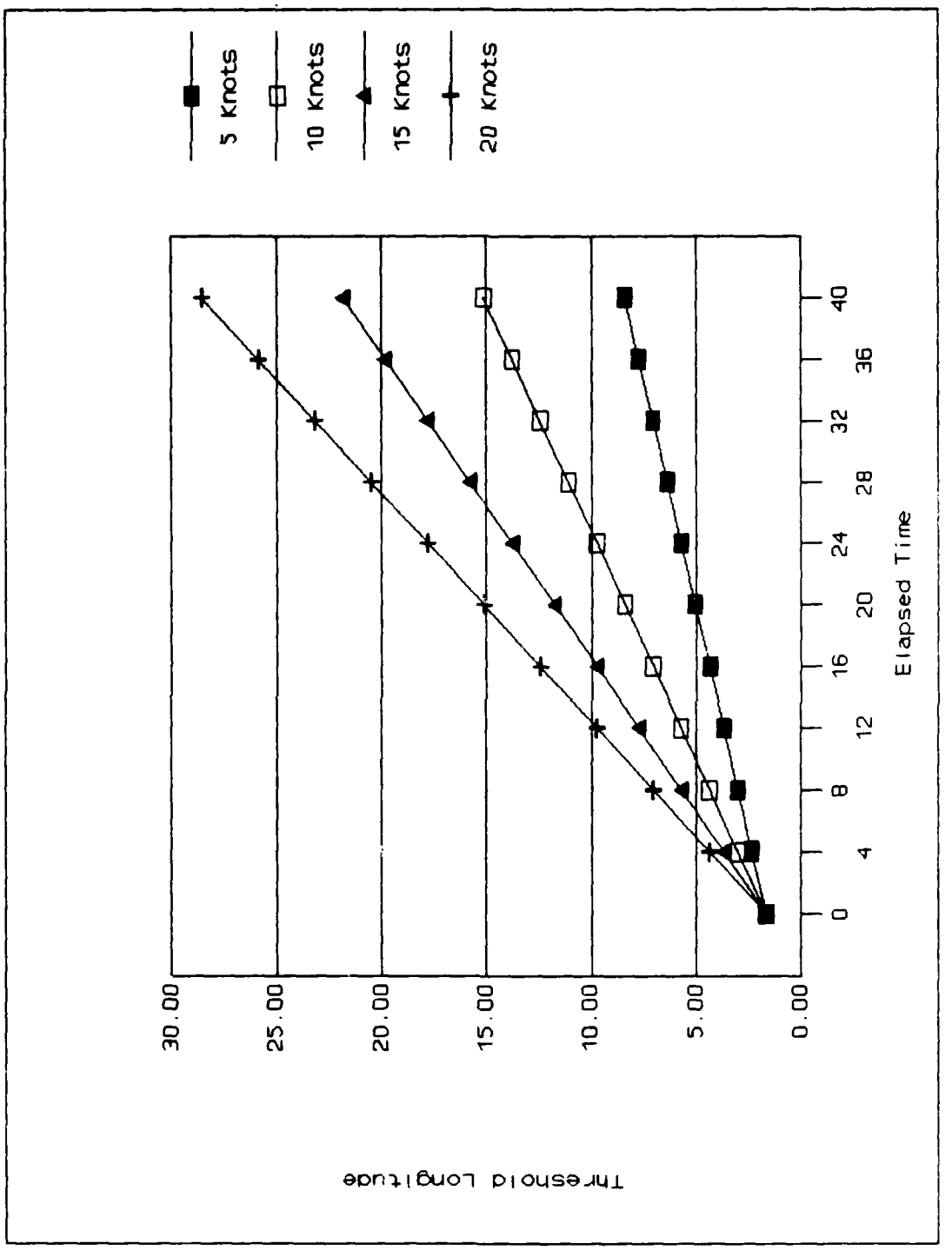

Figure E1. Threshold Longitude for Overlap
Landsat 5, 60°N Latitude

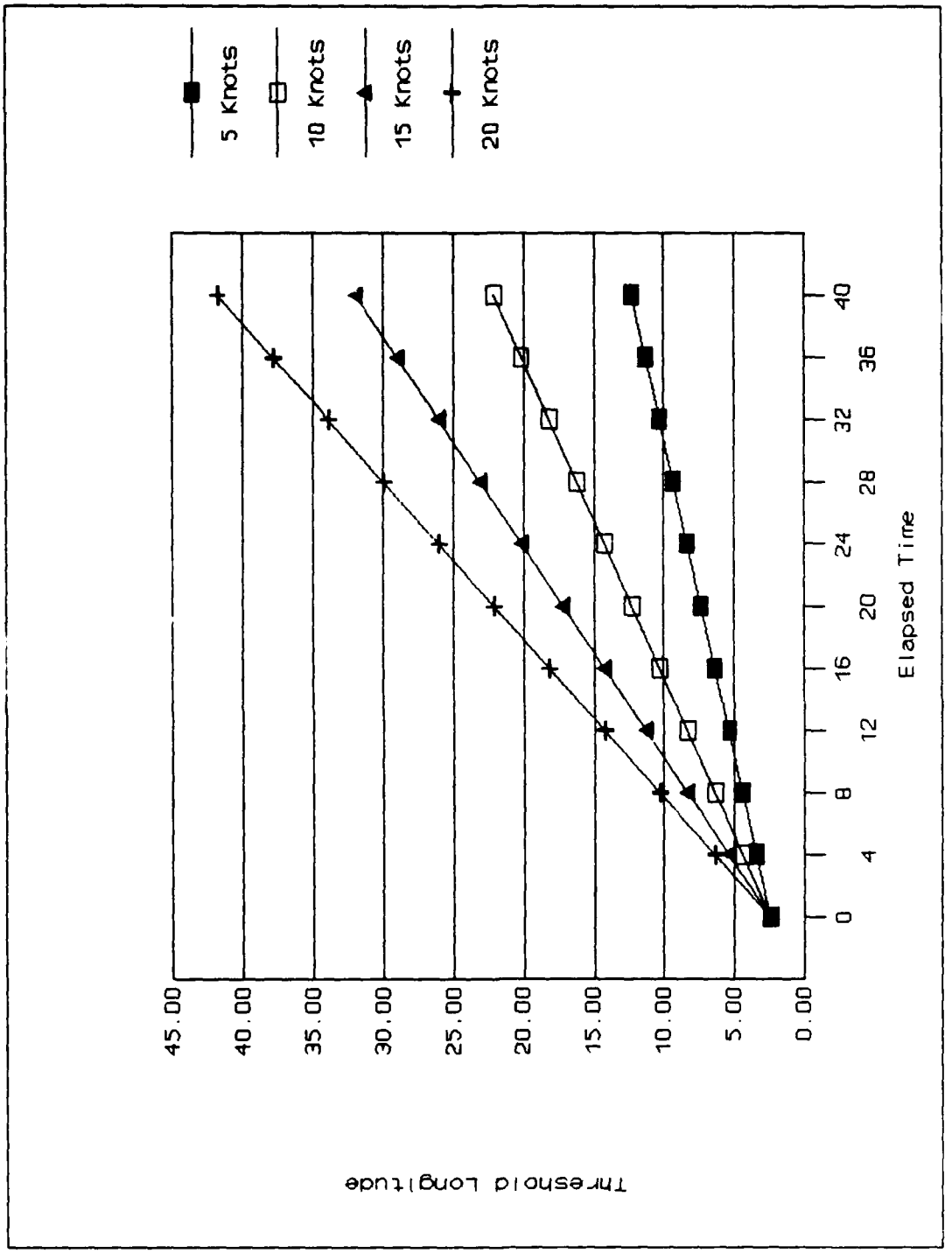

Figure E2. Threshold Longitude for Overlap
Landsat 5, 70°N Latitude

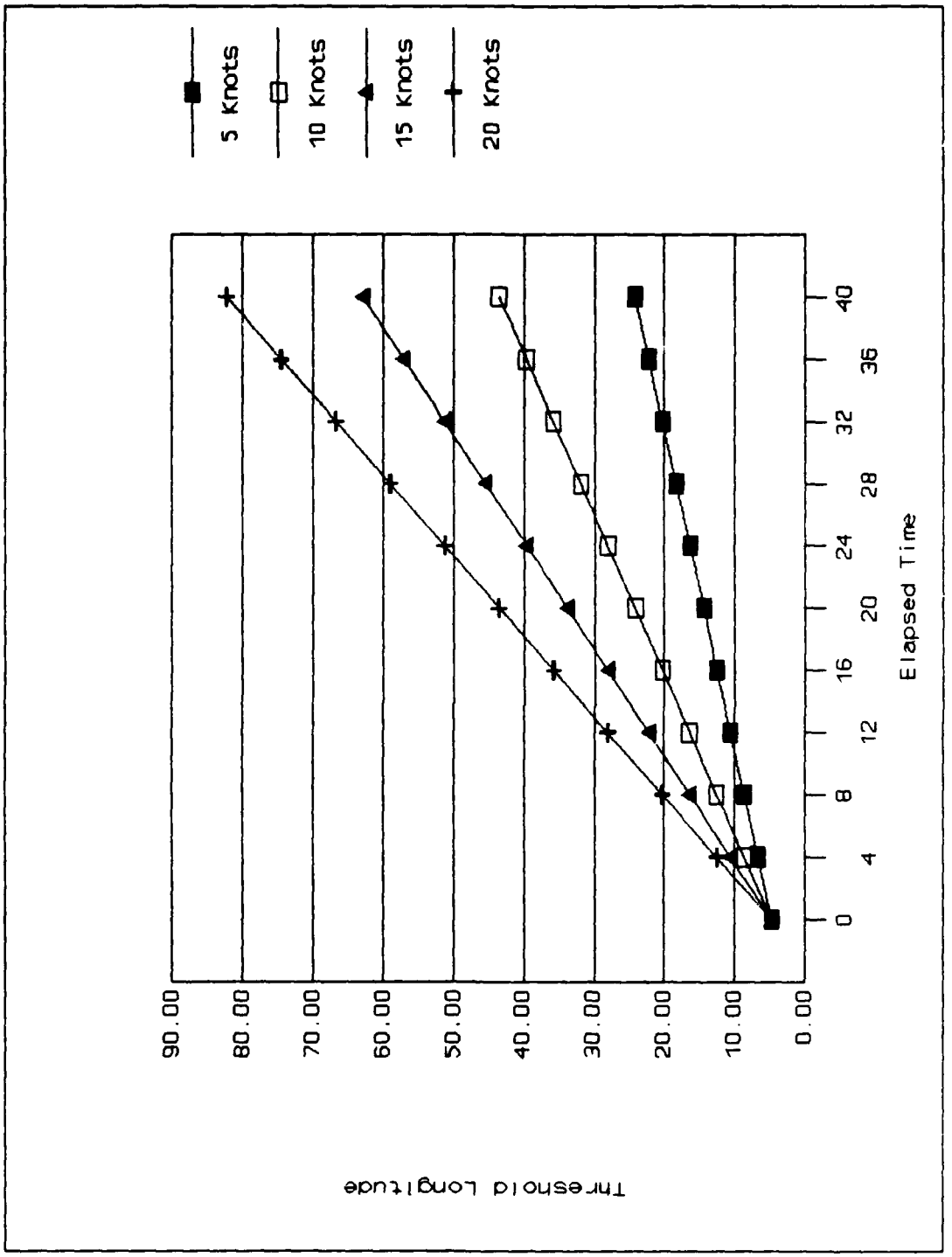

Figure E3. Threshold Longitude for Overlap
Landsat 5, 80°N Latitude

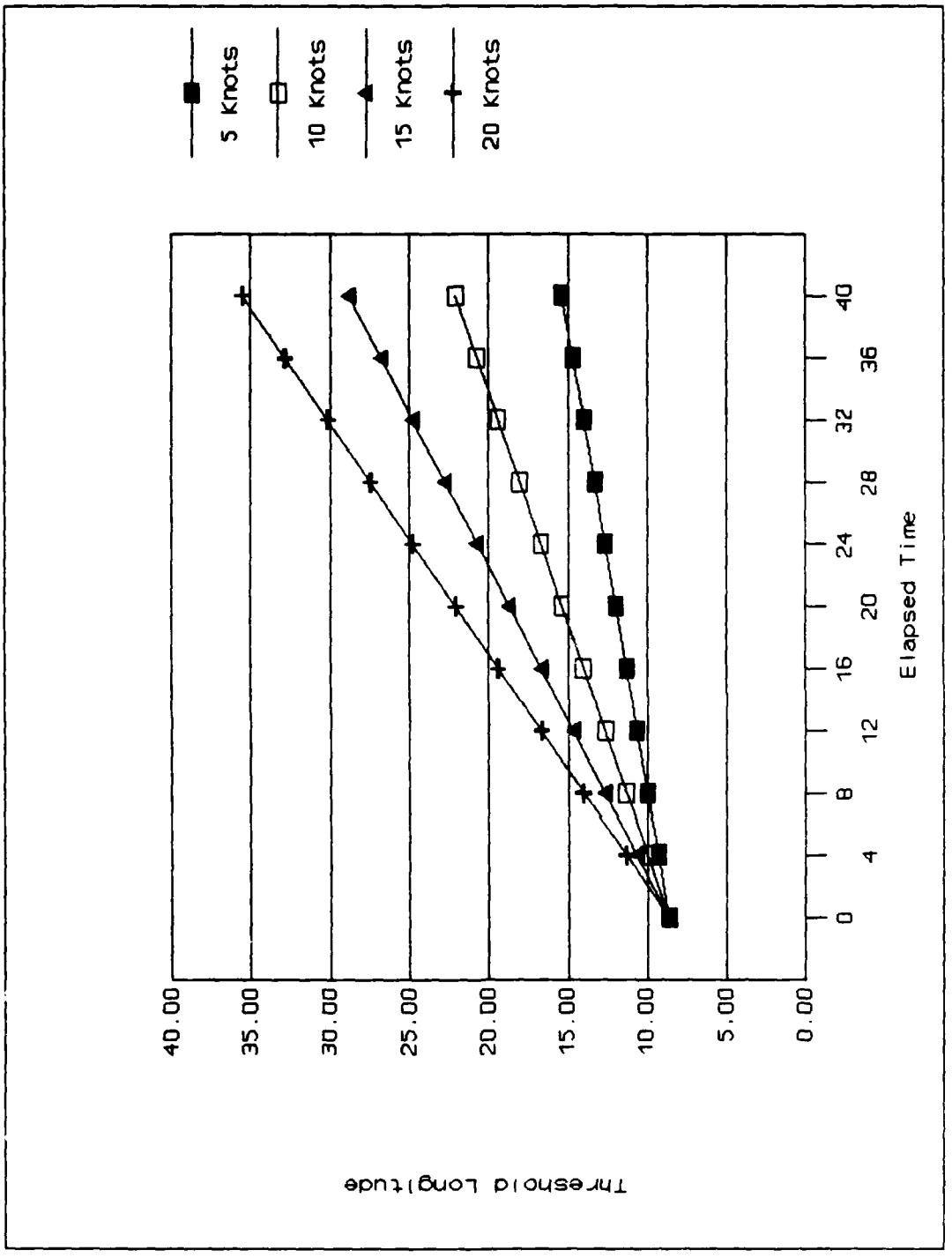

Figure E4. Threshold Longitude for Overlap SPOT 1, 60°N Latitude

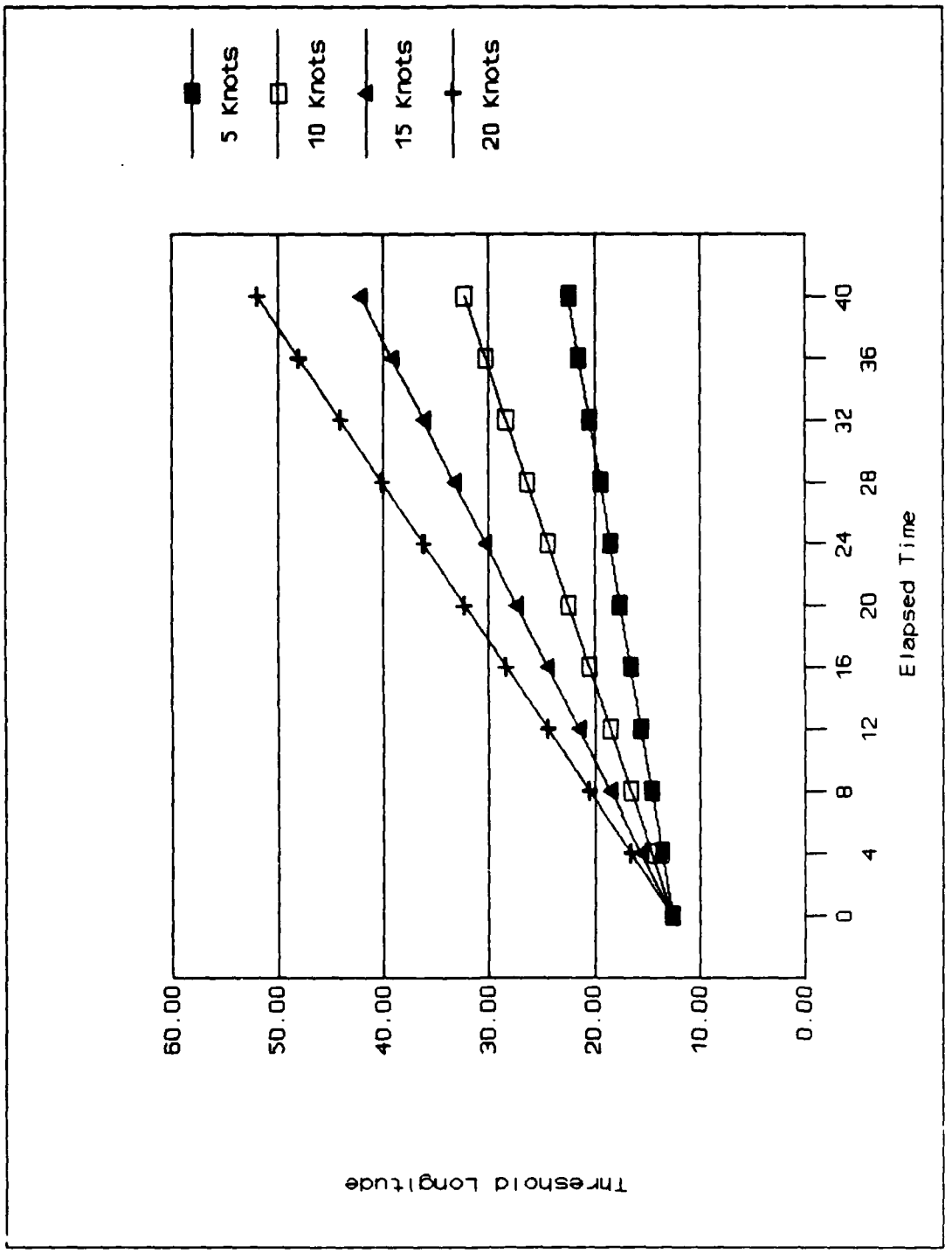

Figure E5. Threshold Longitude for Overlap SPOT 1, 70°N Latitude

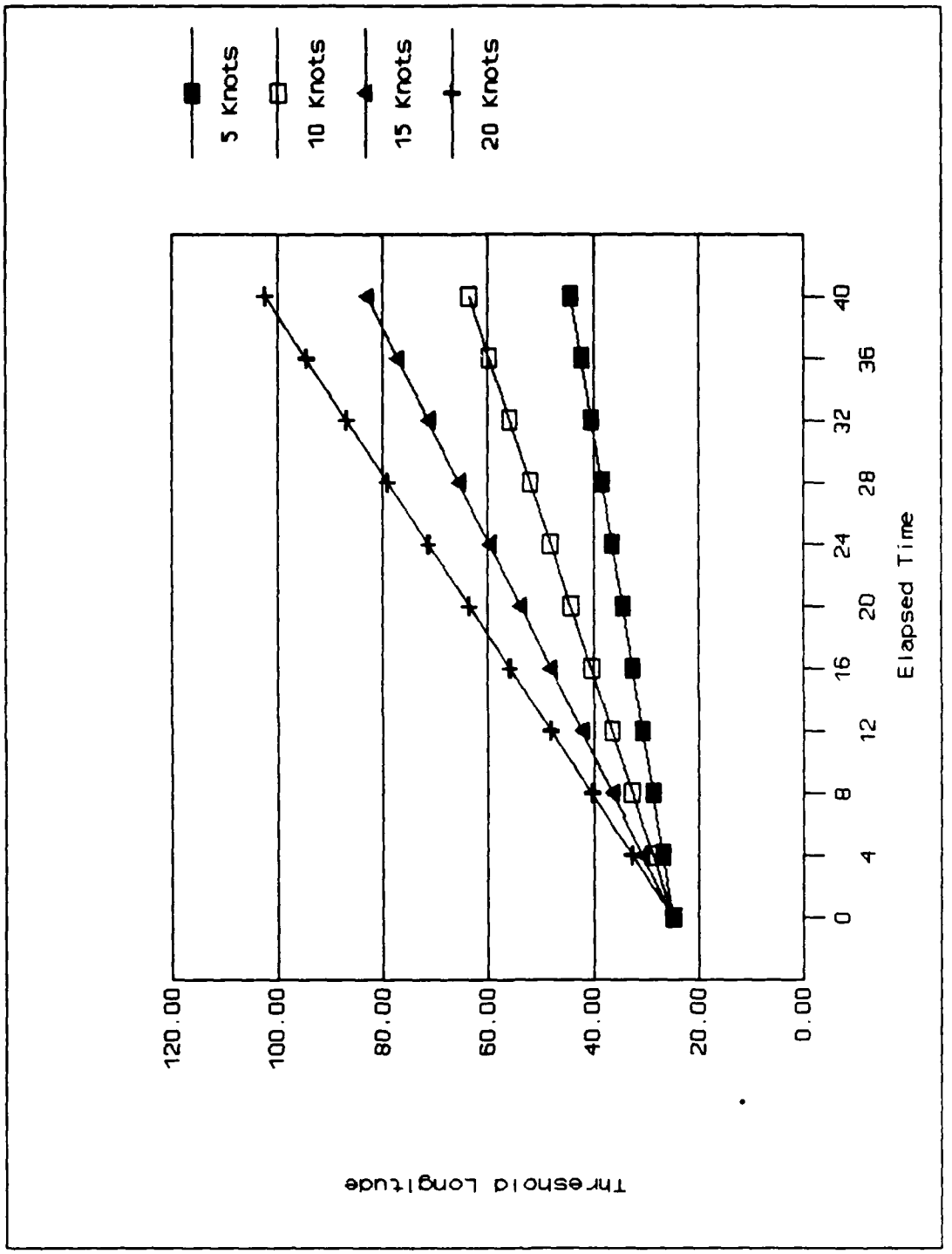

Figure E6. Threshold Longitude for Overlap SPOT 1, 80°N Latitude

Appendix F: Conditional Tracking Probabilities

This appendix contains plots of conditional tracking probabilities for Landsat 5 and SPOT sensors.

One anomaly of the spreadsheet used to generate these curves is that achieving a conditional tracking probability of 1.0 forces the software to expand the y axis to a maximum score of 1.2. Since a probability in excess of 1.0 is meaningless, conditional tracking probabilities exactly equal to 1.0 are restricted to a value of 0.99 in this appendix but should be taken to be 1.0.

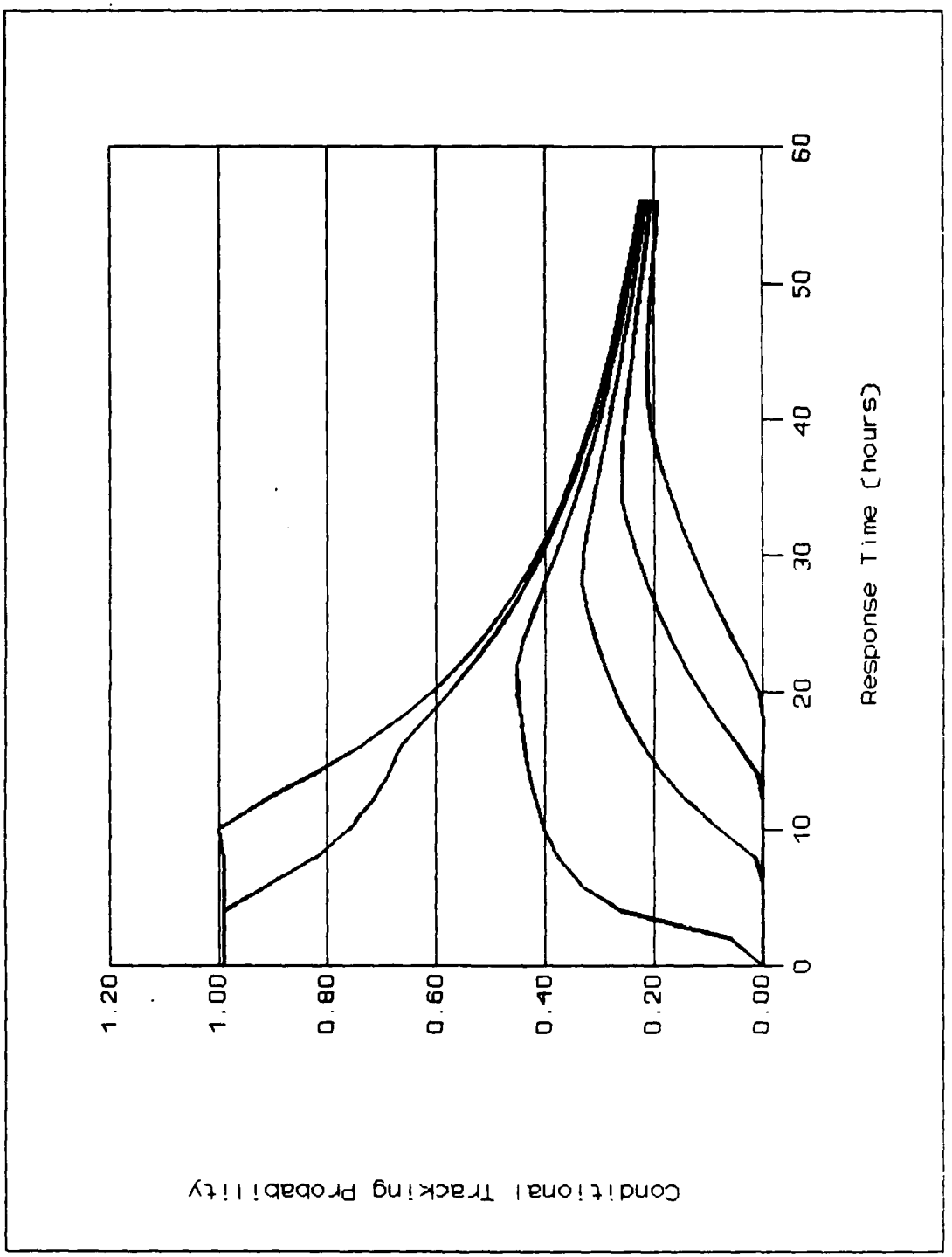

Figure F1. Landsat 5 Conditional Tracking Probability
60°N Latitude, 5 Knots
(Top to bottom are 0,1,2,3,4,5° Longitude Displacement)

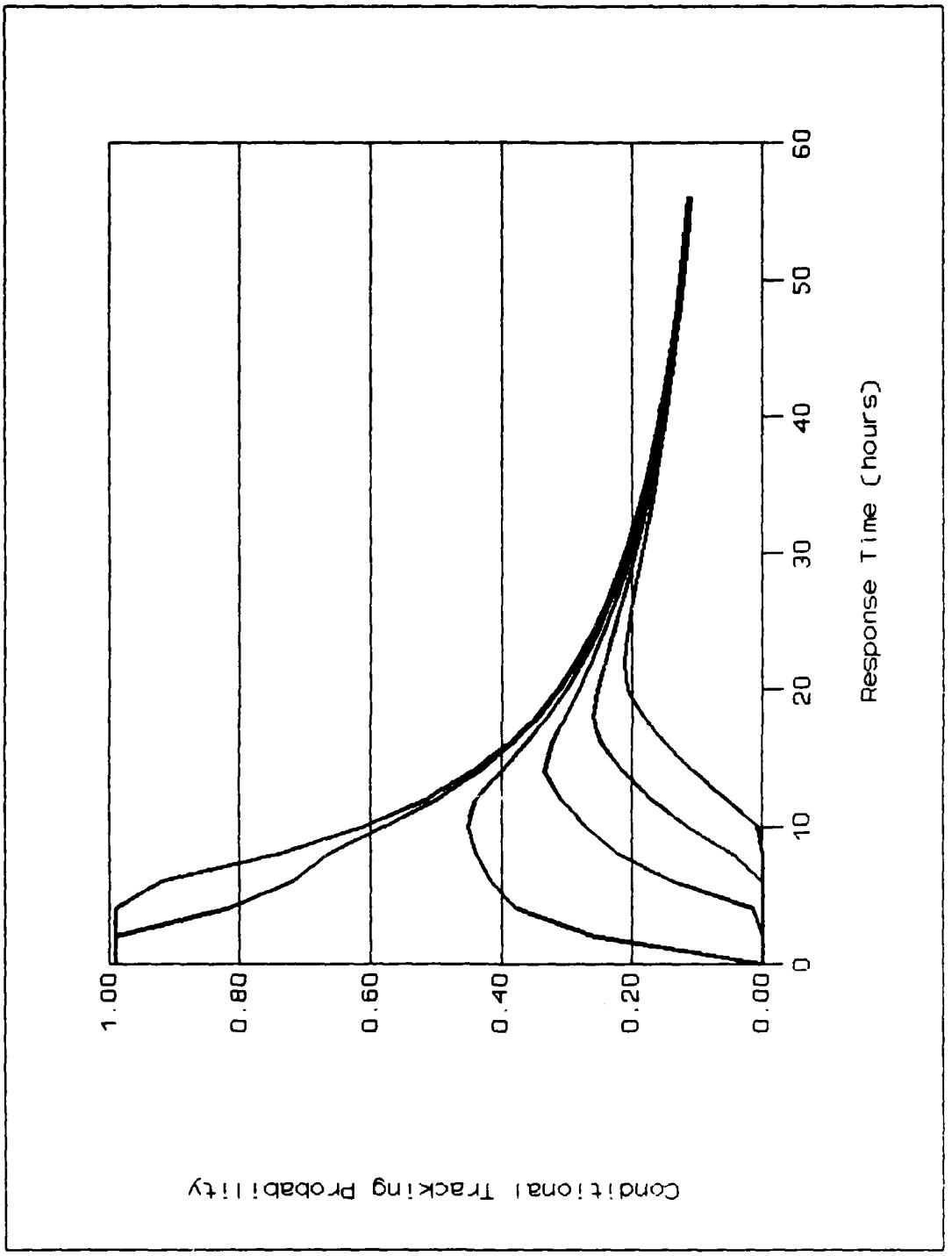

Figure F2. Landsat 5 Conditional Tracking Probability
60°N Latitude, 10 Knots
(Top to bottom are 0,1,2,3,4,5° Longitude Displacement)

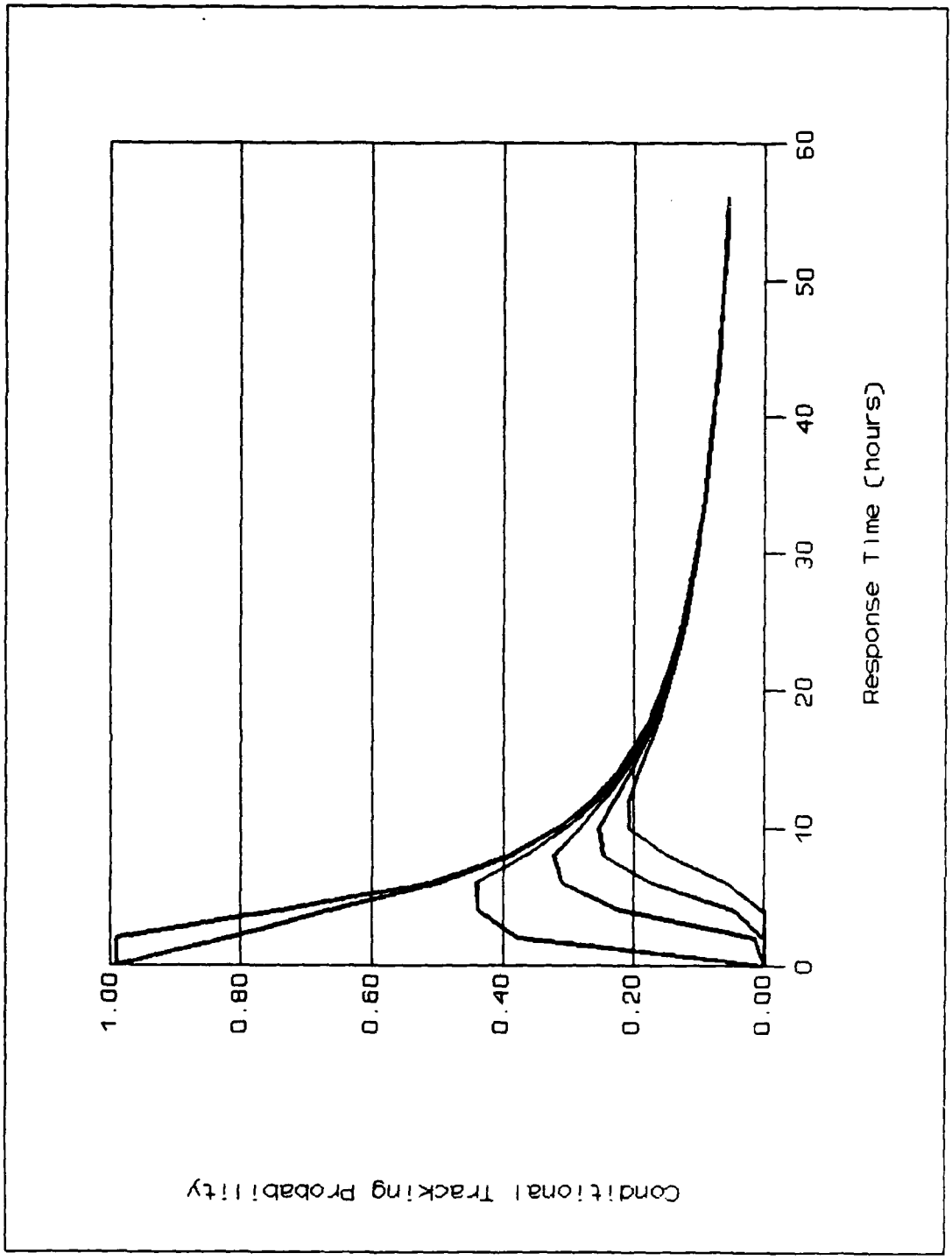

Figure F3. Landsat 5 Conditional Tracking Probability
60°N Latitude, 20 Knots
(Top to bottom are 0,1,2,3,4,5° Longitude Displacement)

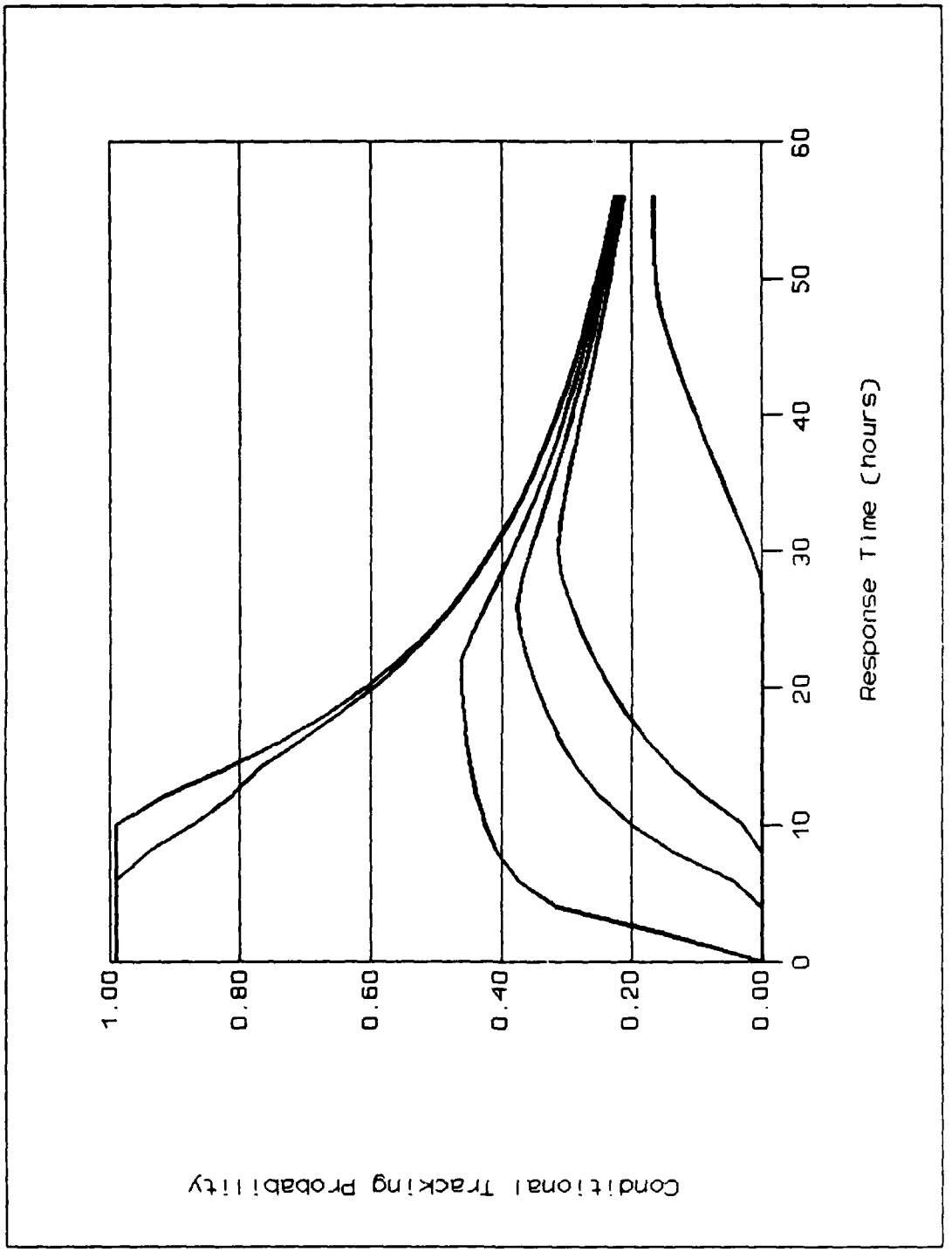

Figure F4. Landsat 5 Conditional Tracking Probability
70°N Latitude, 5 Knots
(Top to bottom are 0,1,3,4,5,10° Longitude Displacement)

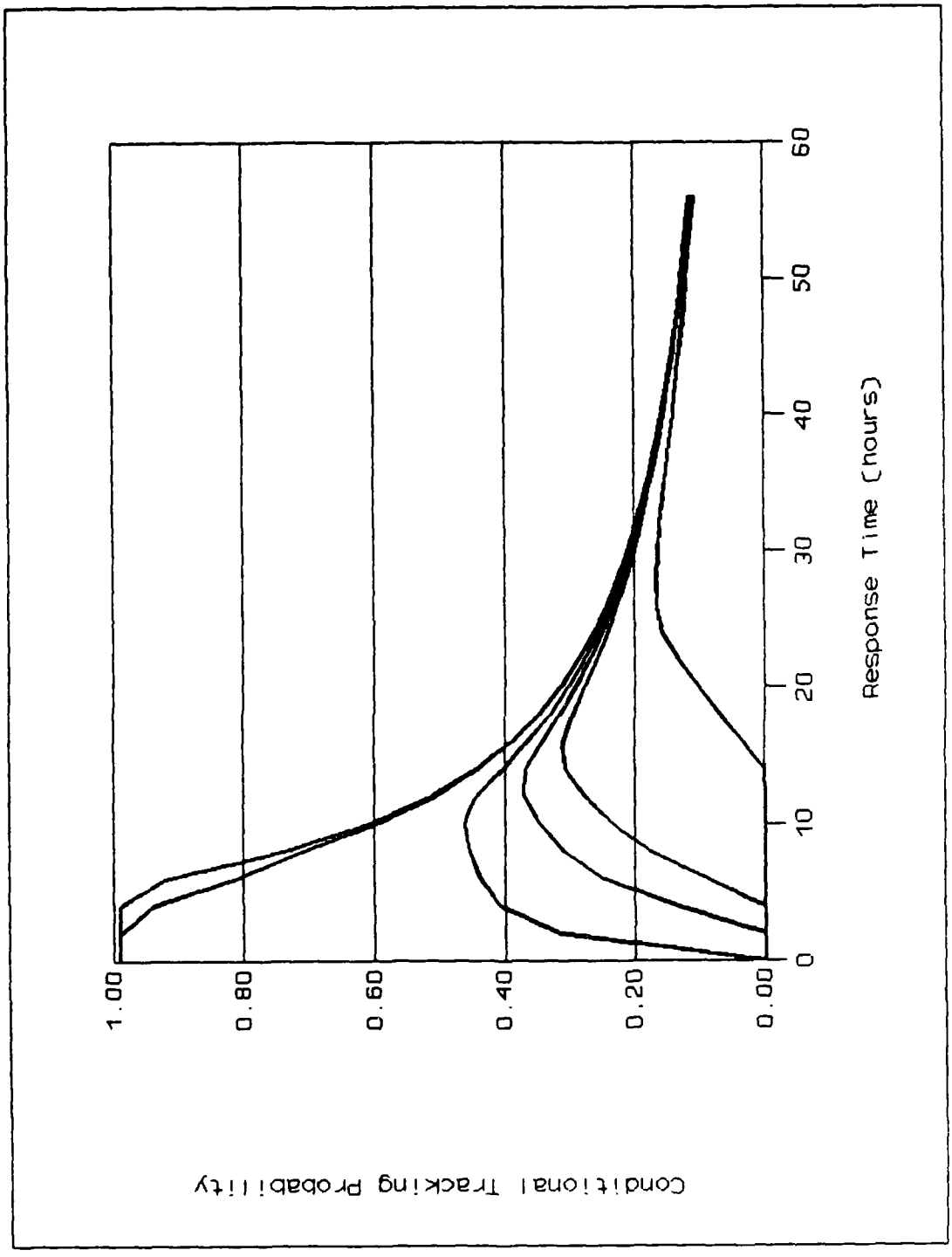

Figure F5. Landsat 5 Conditional Tracking Probability
70°N Latitude, 10 Knots
(Top to bottom are 0,1,3,4,5,10° Longitude Displacement)

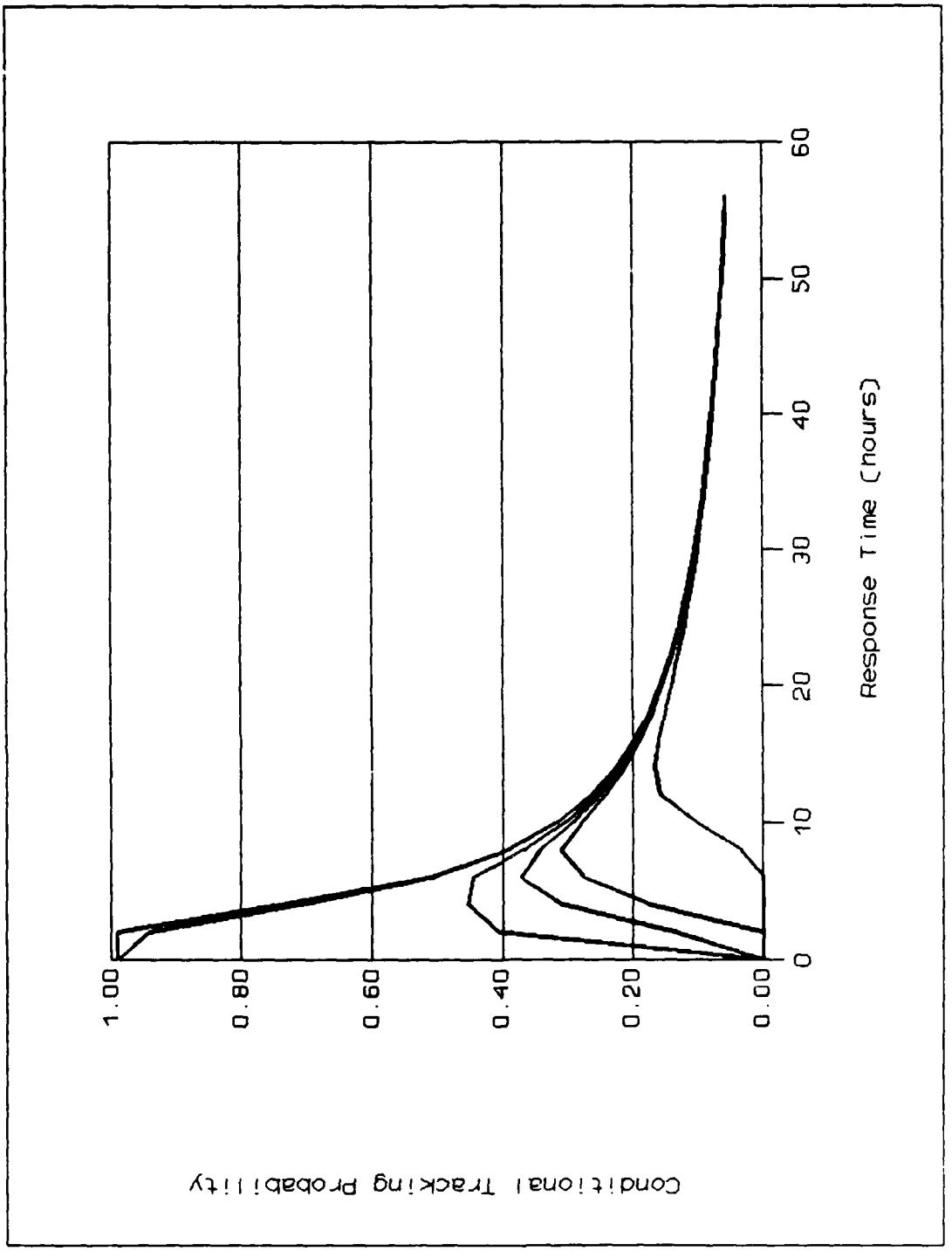

Figure F6. Landsat 5 Conditional Tracking Probability
70°N Latitude, 20 Knots
(Top to bottom are 0,1,3,4,5,10° Longitude Displacement)

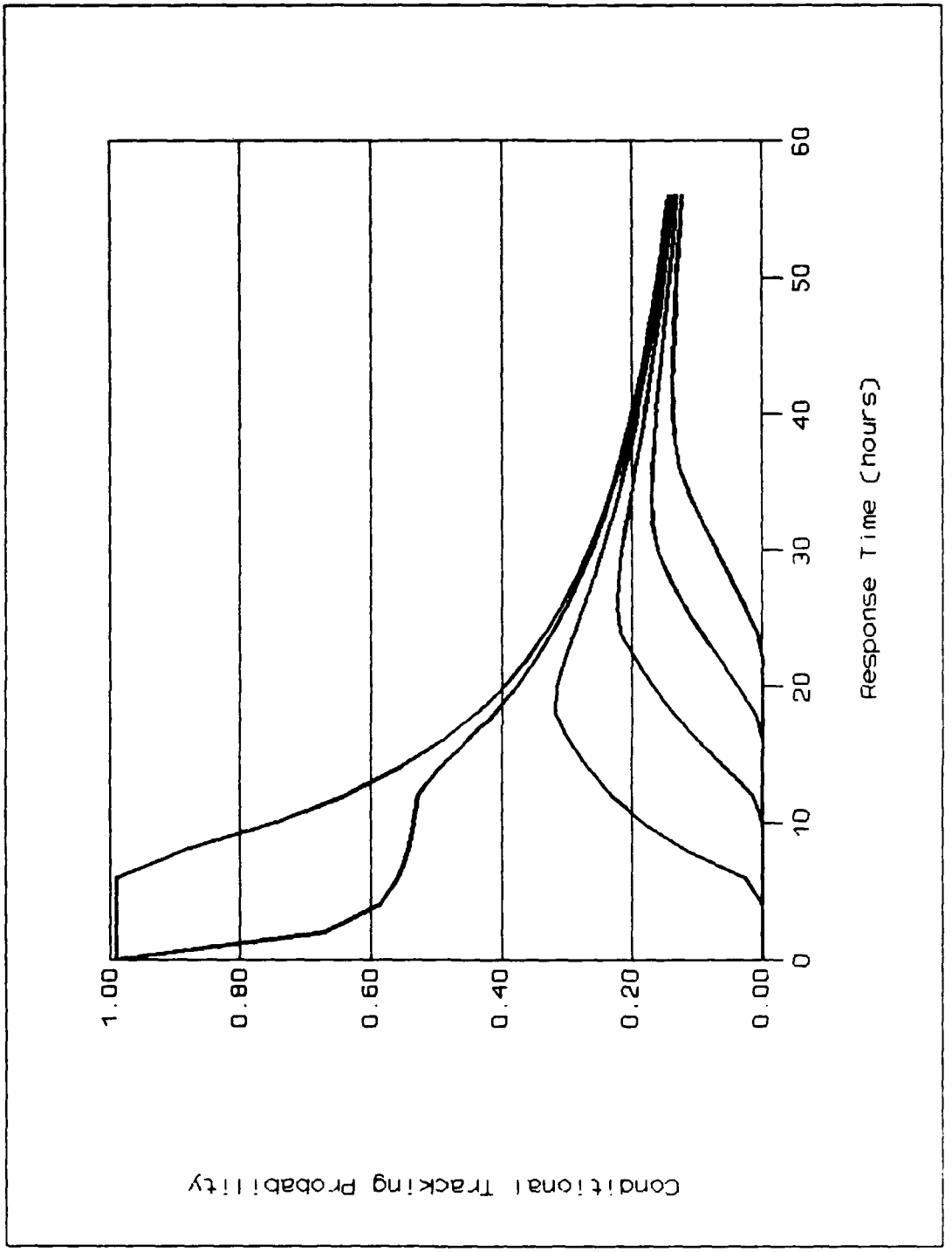

Figure F7. SPOT 1 Conditional Tracking Probability
60°N Latitude, 5 Knots
(Top to bottom are 0,1,2,3,4,5° Longitude Displacement)

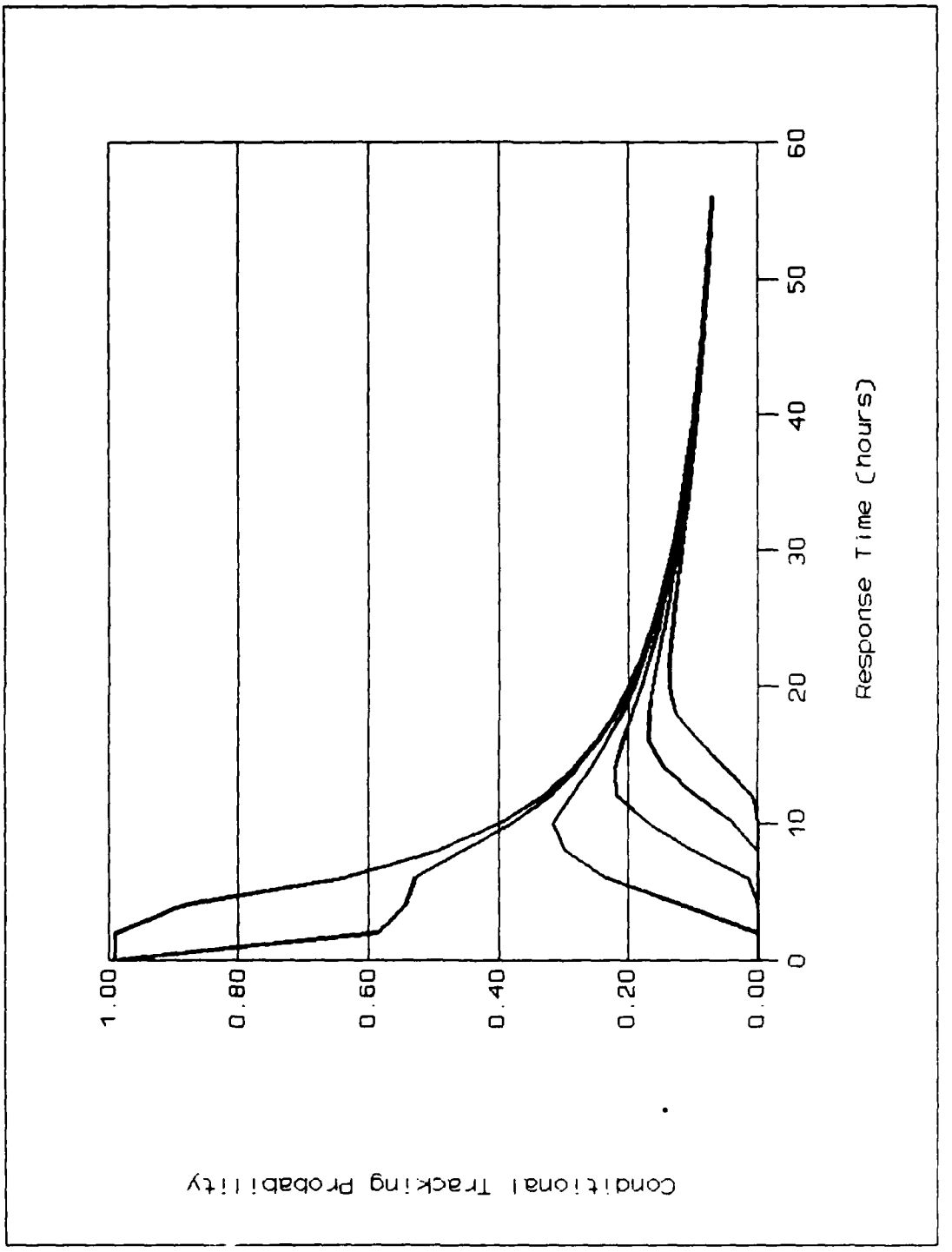

Figure F8. SPOT 1 Conditional Tracking Probability
60° N Latitude, 10 Knots
(Top to bottom are 0,1,2,3,4,5° Longitude Displacement)

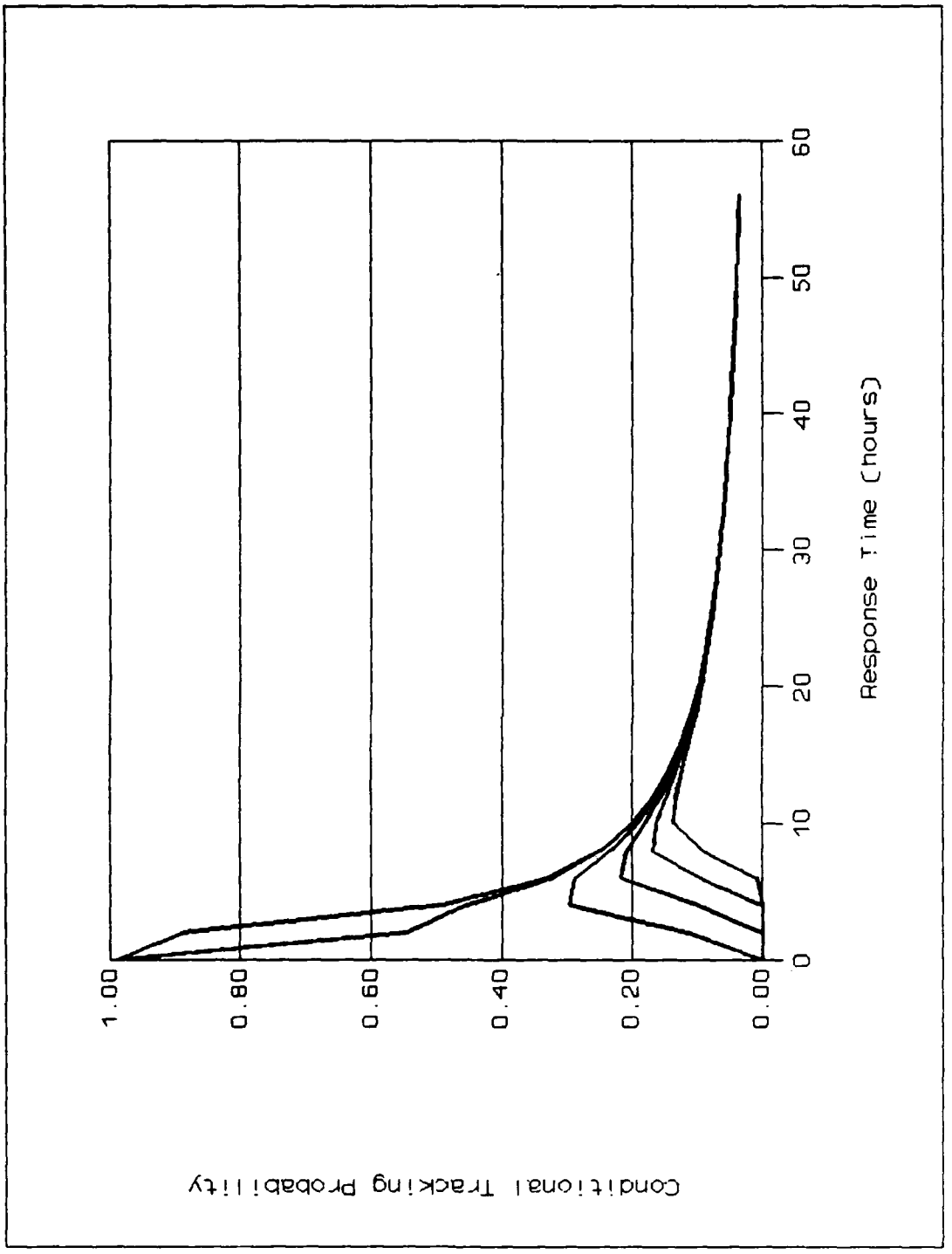

Figure F9. SPOT 1 Conditional Tracking Probability
60° N Latitude, 20 Knots
(Top to bottom are 0,1,2,3,4,5° Longitude Displacement)

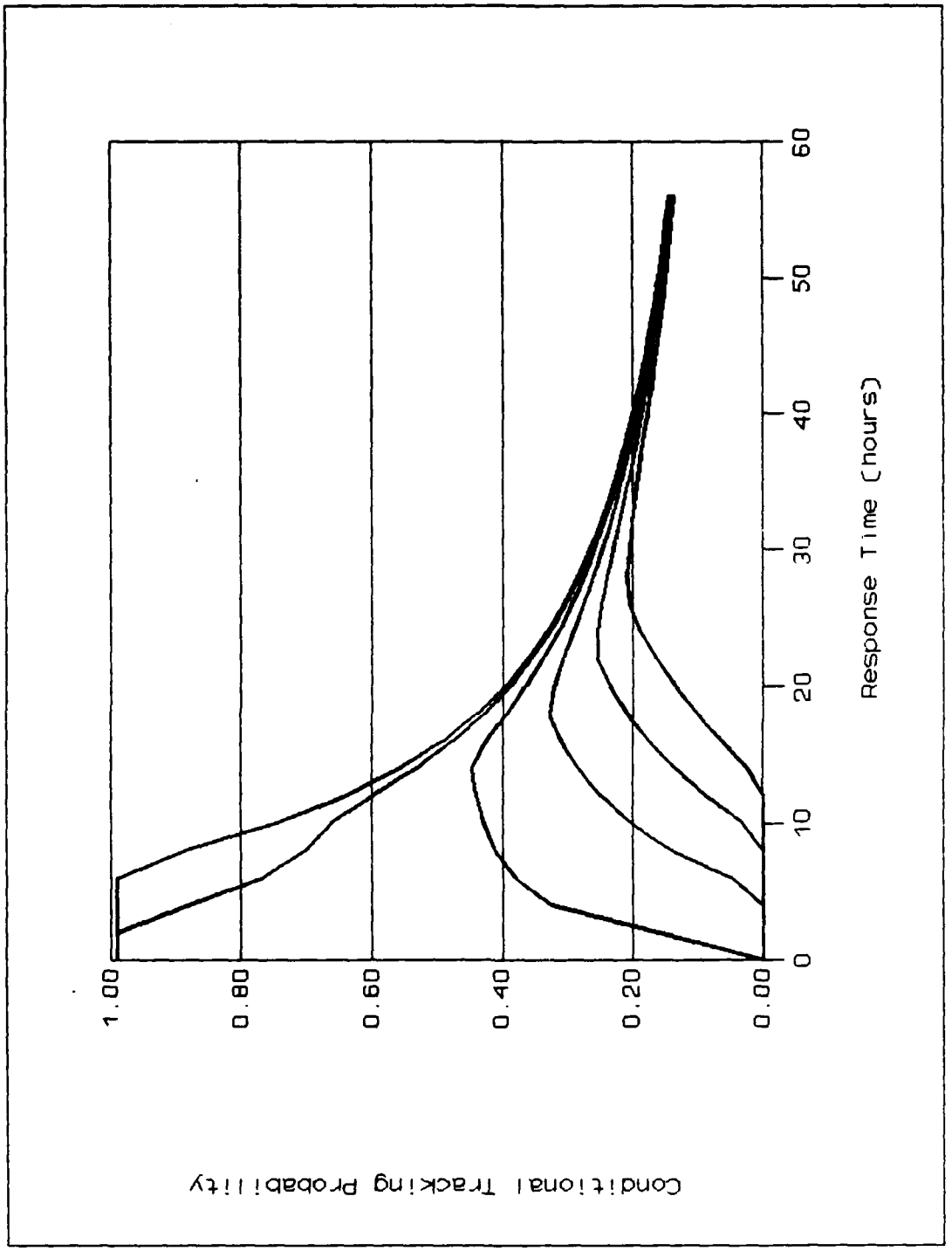

Figure F10. SPOT 1 Conditional Tracking Probability
70° N Latitude, 5 Knots
(Top to bottom are 0,1,2,3,4,5° Longitude Displacement)

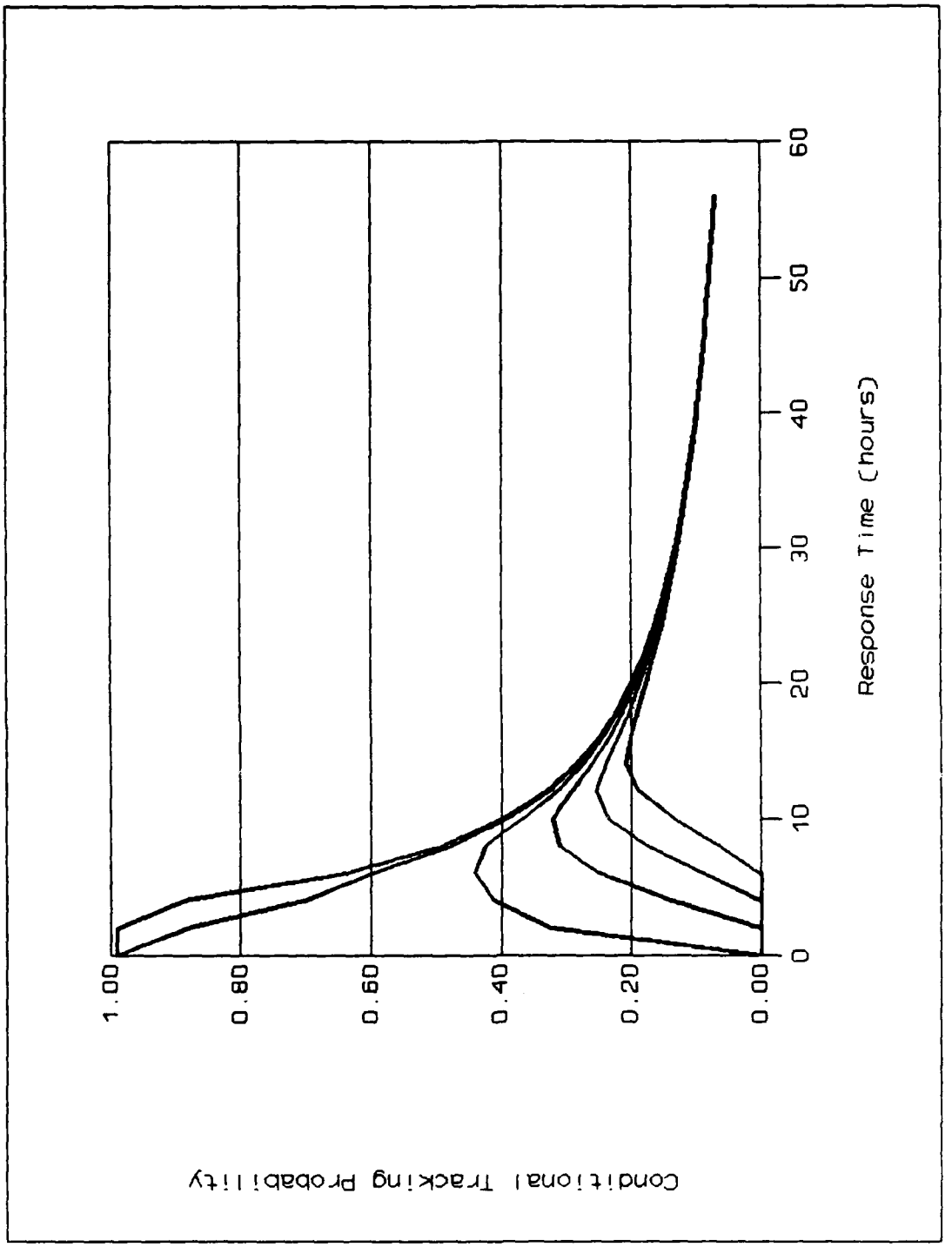

Figure F11. SPOT 1 Conditional Tracking Probability
70° N Latitude, 10 Knots
(Top to bottom are 0,1,2,3,4,5° Longitude Displacement)

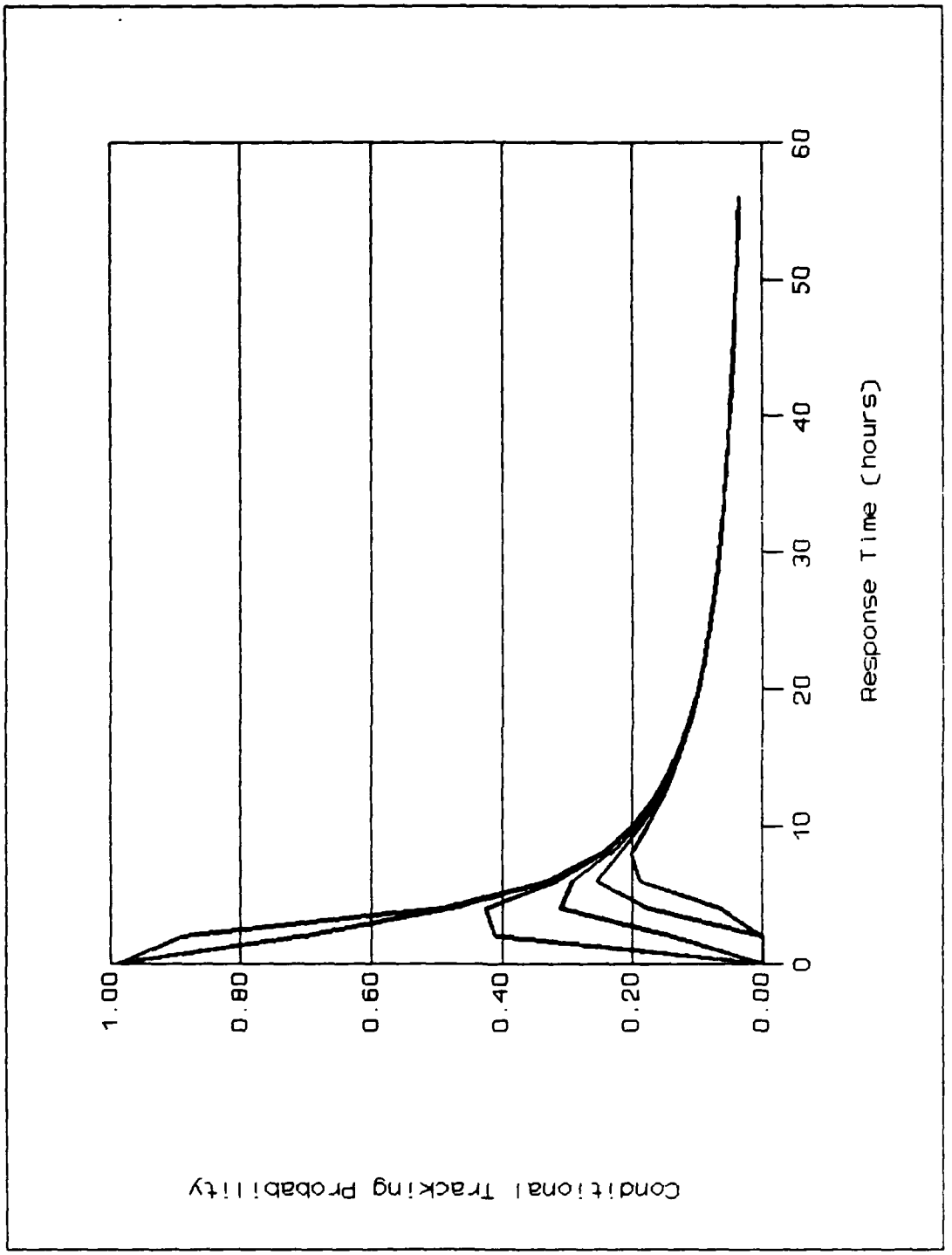

Figure F12. SPOT 1 Conditional Tracking Probability
70° N Latitude, 20 Knots
(Top to bottom are 0,1,2,3,4,5° Longitude Displacement)

Appendix G: Thermal Threshold Detection Curves

This appendix contains plots of threshold target sizes for detection as a function of target exitance for specific combinations of targets and background. Combinations of target exitance and area which fall below the threshold curve will not be detected by the sensor. Those that fall on or above the line will be detected by the sensor.

The conditions specified below each graph are important since the graphs only apply for the indicated target and background conditions.

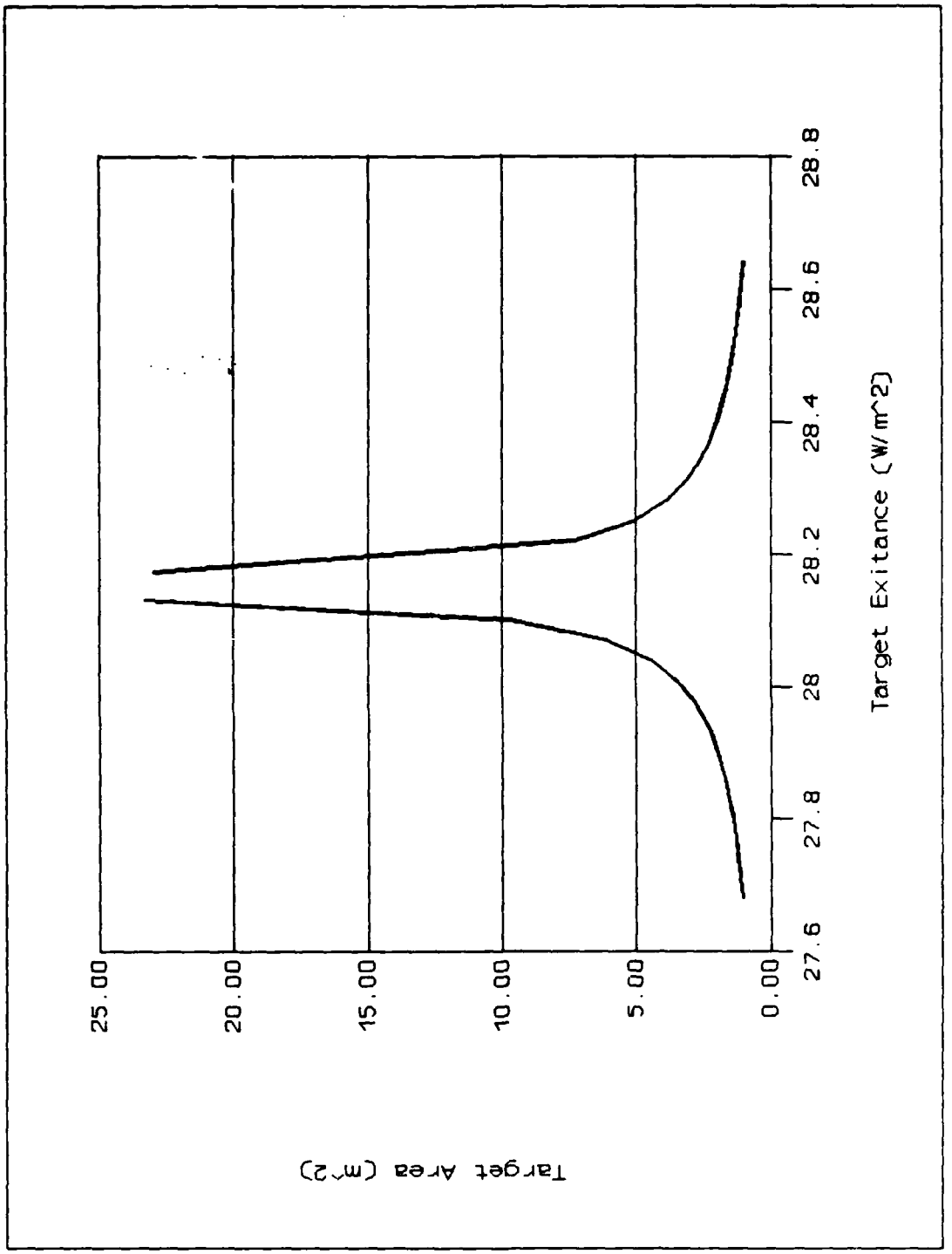

Figure G1. Threshold Target Area vs Target Exitance
Target Emissivity .92, Background Emissivity .94
Landsat 5 Band 6 Sensor, Background Temperature 253°K

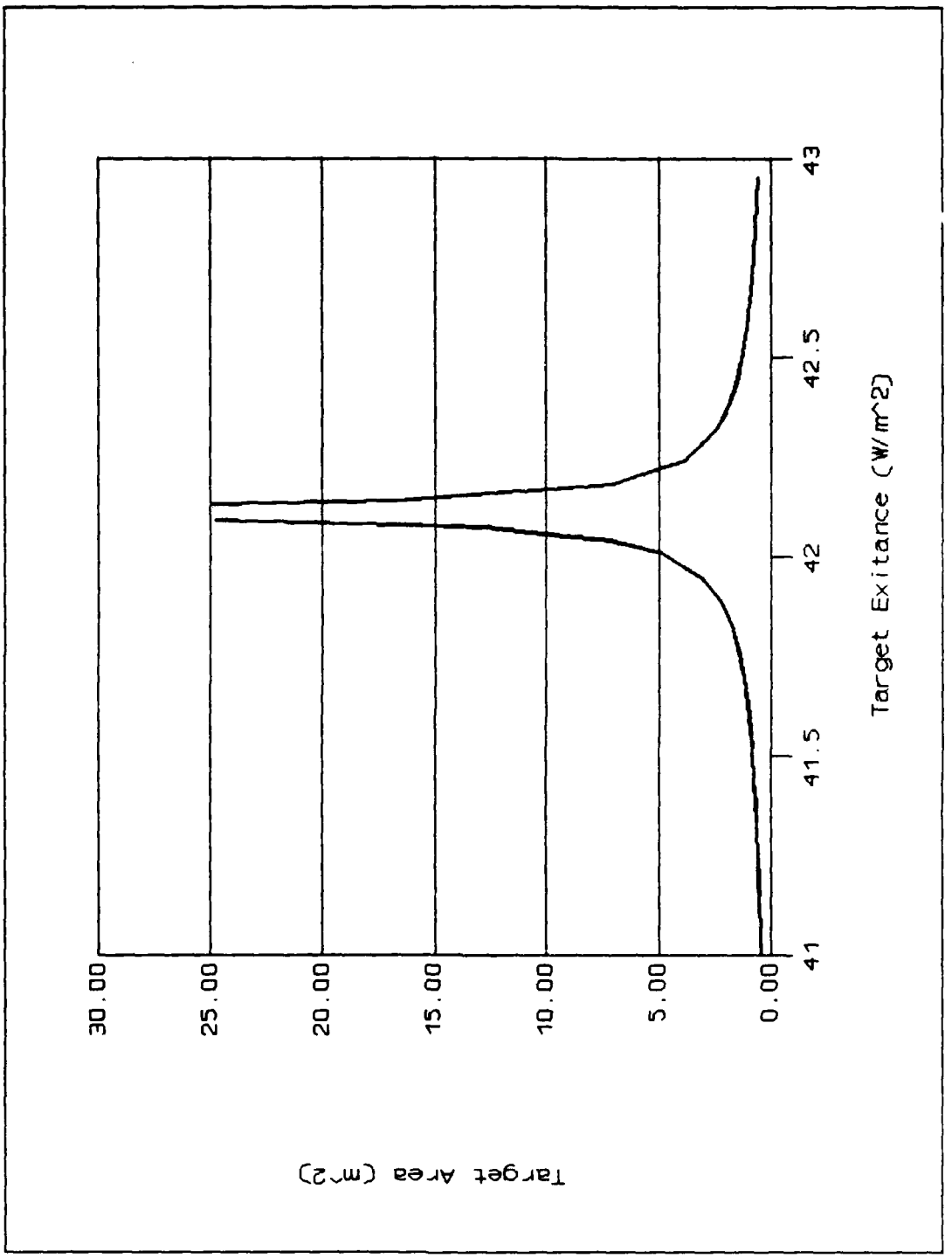

Figure G2. Threshold Target Area vs Target Exitance
Target Emissivity .92, Background Emissivity .94
Landsat 5 Band 6 Sensor, Background Temperature 275°K

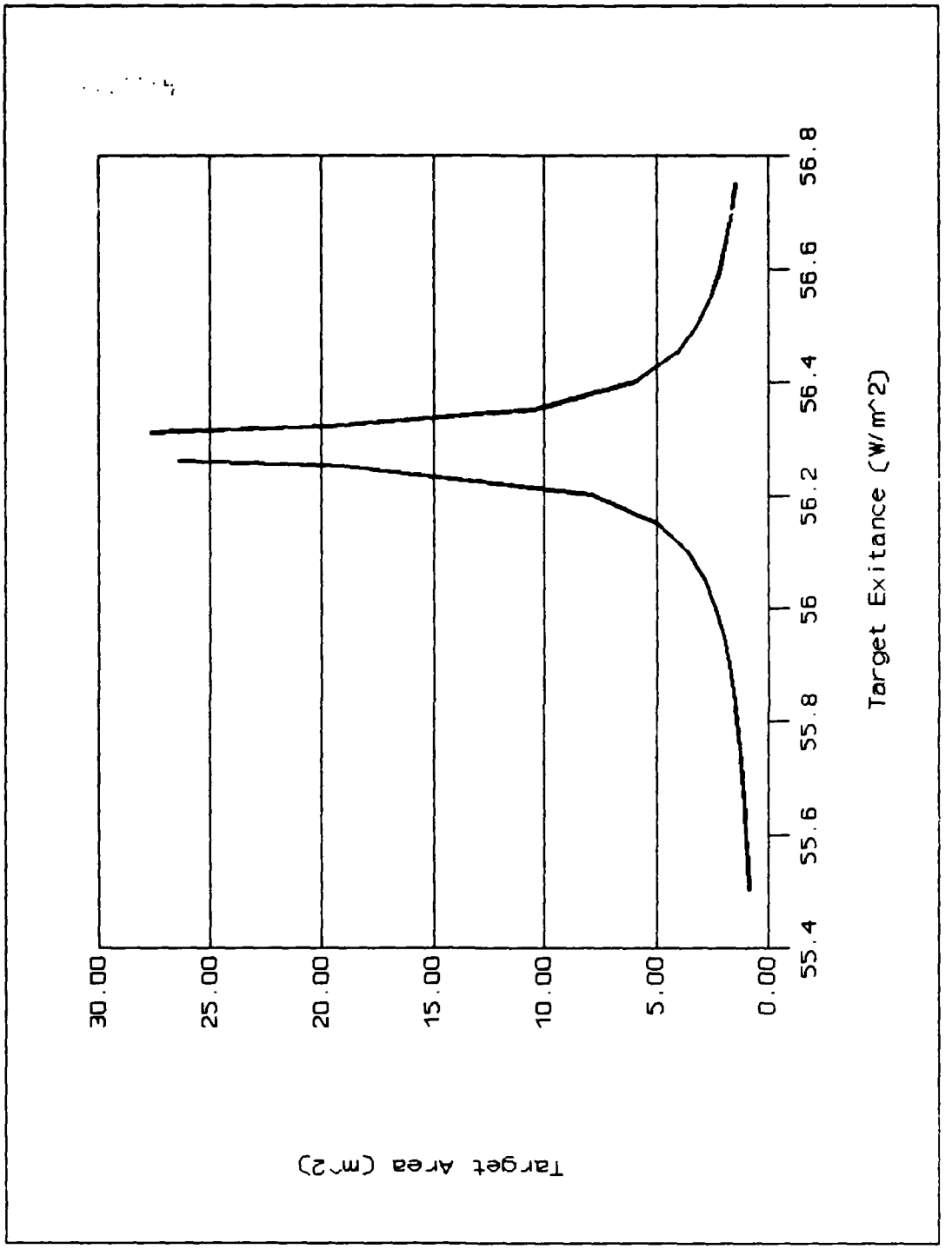

Figure G3. Threshold Target Area vs Target Exitance
Target Emissivity .92, Background Emissivity .94
Landsat 5 Band 6 Sensor, Background Temperature 293°K

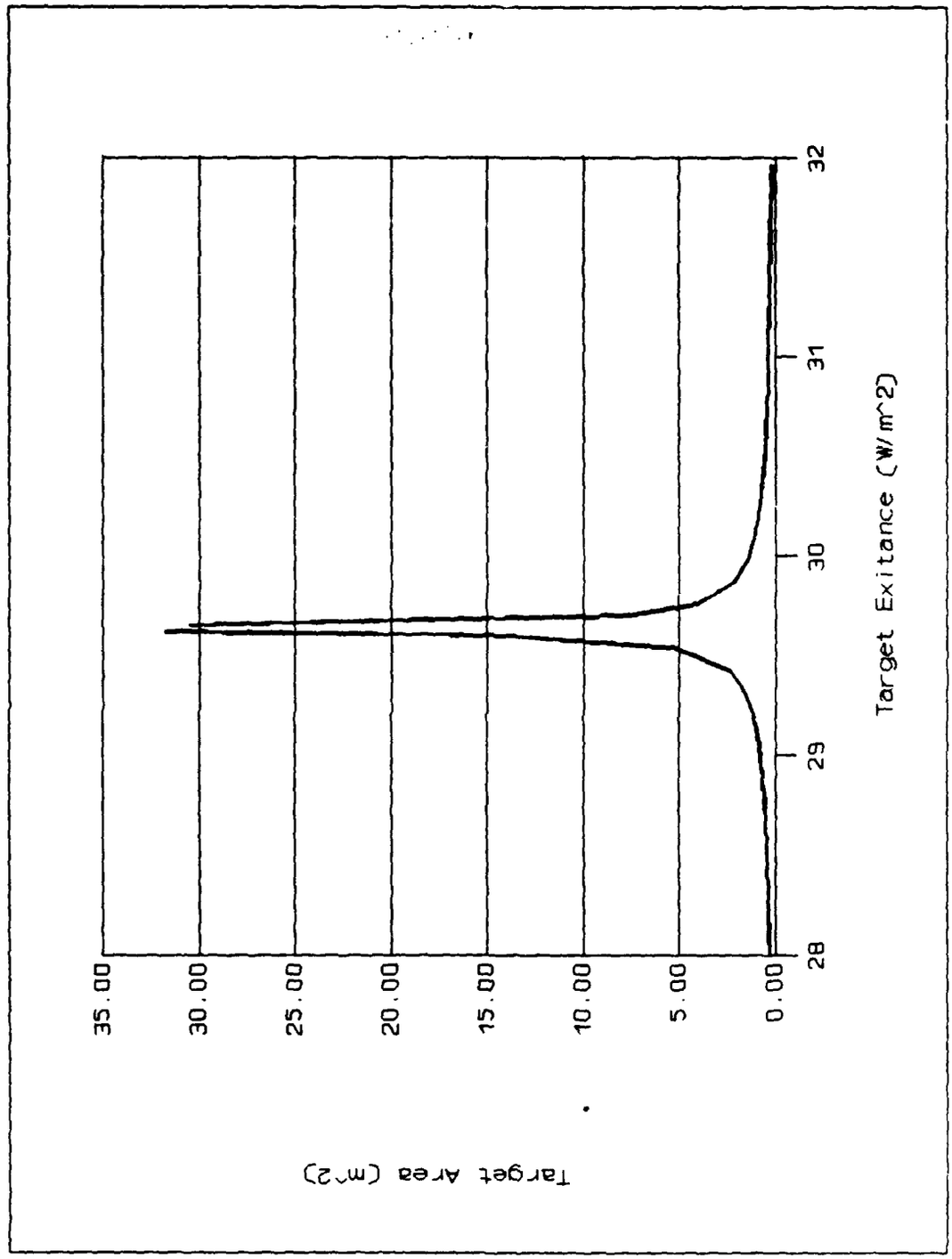

Figure G4. Threshold Target Area vs Target Exitance
Target Emissivity .92, Background Emissivity .985
Landsat 5 Band 6 Sensor, Background Temperature 253°K

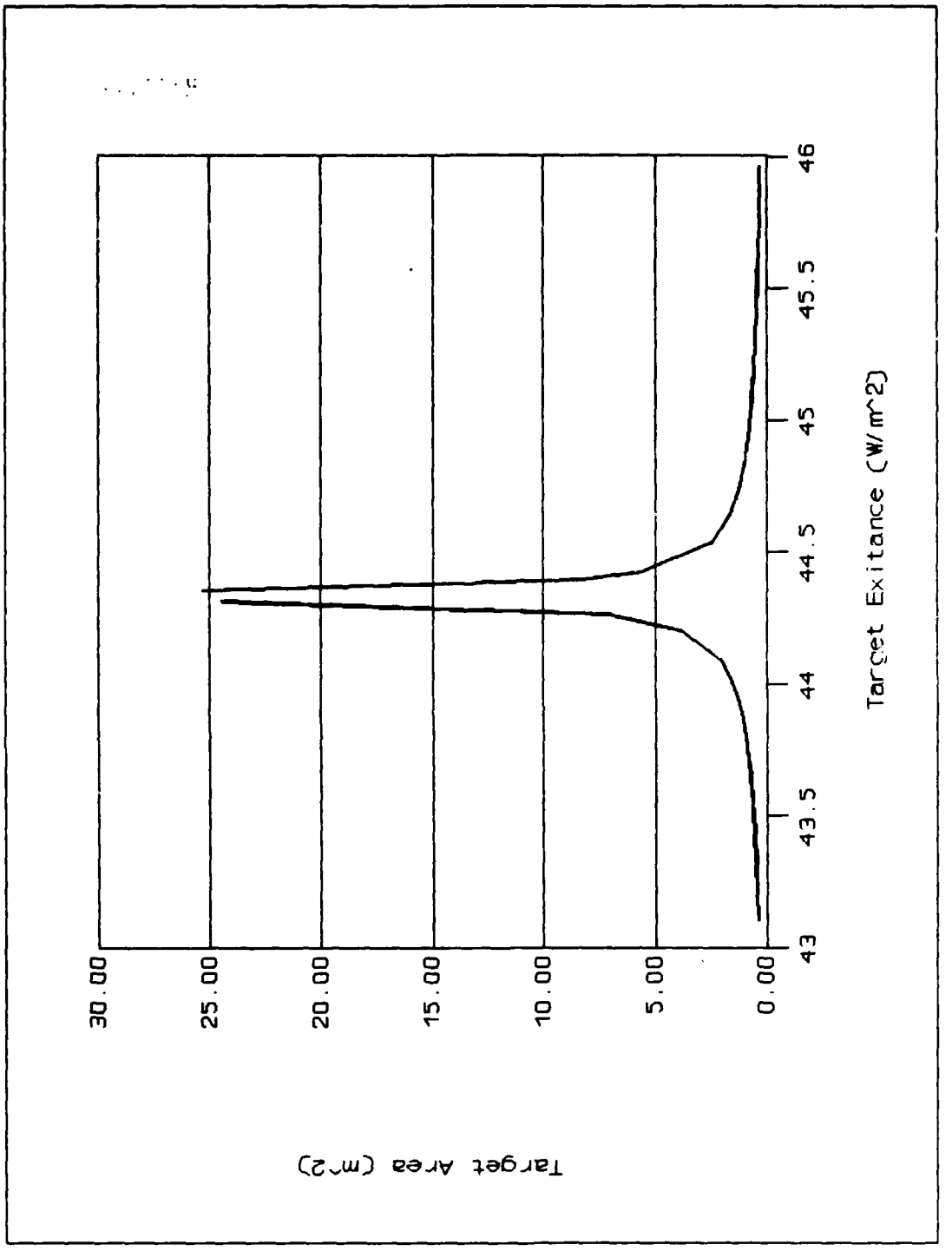

Figure G5. Threshold Target Area vs Target Exitance
Target Emissivity .92, Background Emissivity .985
Landsat 5 Band 6 Sensor, Background Temperature 275°K

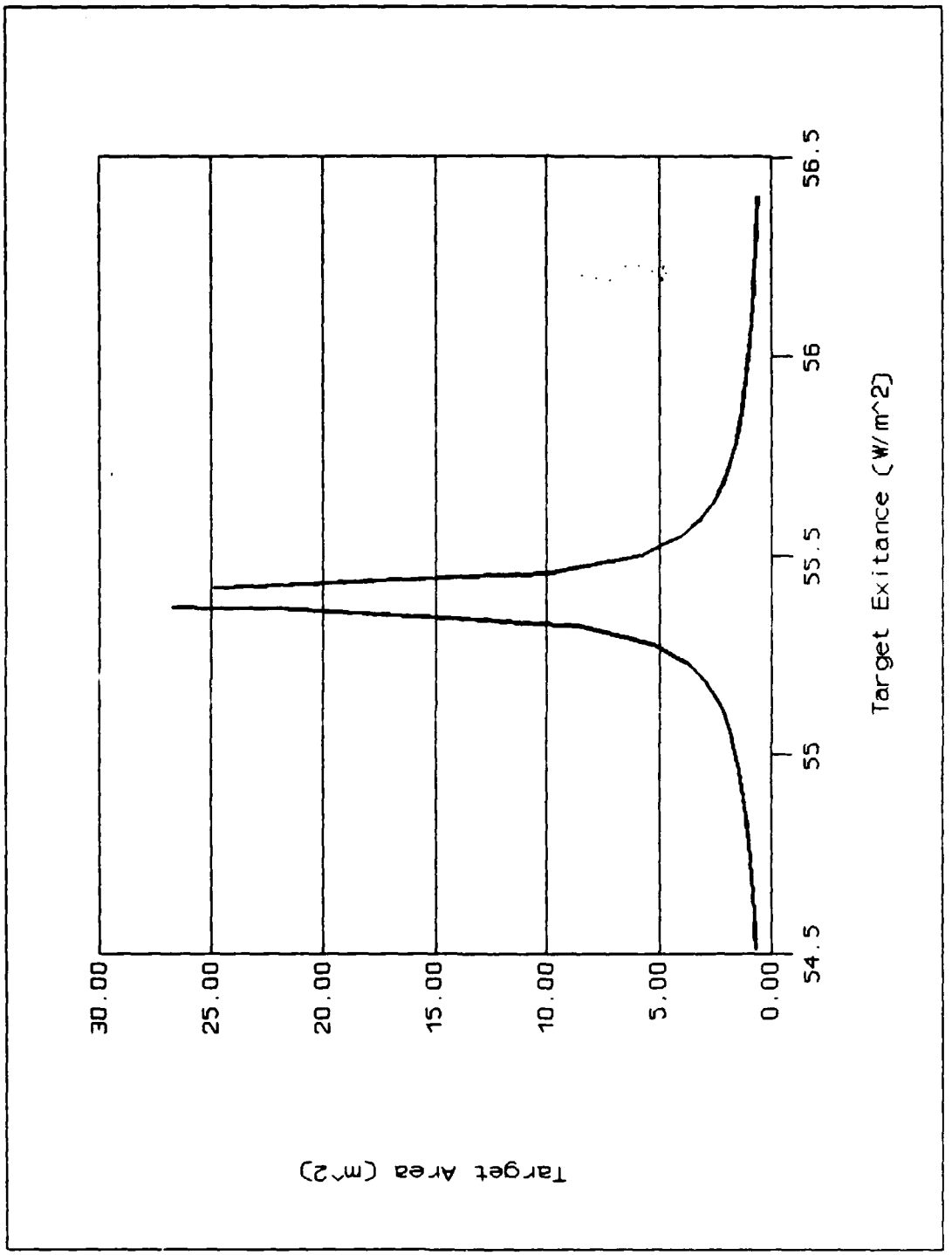

Figure G6. Threshold Target Area vs Target Exitance
Target Emissivity .74, Background Emissivity .99
Landsat 5 Band 6 Sensor, Background Temperature 275°K

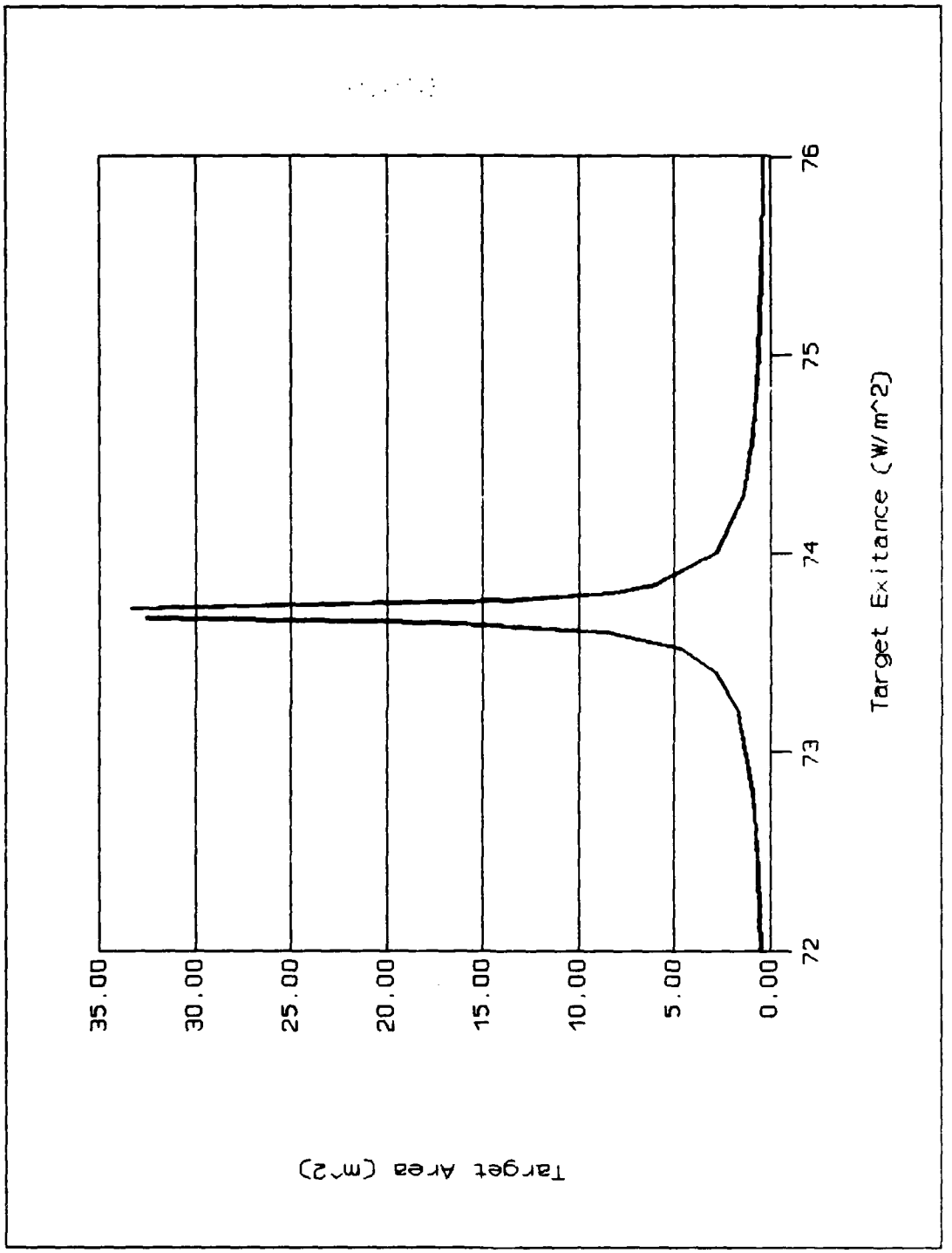

Figure G7. Threshold Target Area vs Target Exitance
Target Emissivity .74, Background Emissivity .99
Landsat 5 Band 6 Sensor, Background Temperature 293°K

Appendix H: Analysis Checklists

This appendix contains the checklists used to calculate individual remote sensing passive sensors' probabilities of detection and tracking, and to optimize system use of these sensors.

Checklist 1 -- Start

1. Specify mission, target(s) of interest, and timeframe.
2. Define area of interest.
3. Identify backgrounds possible in area of interest during timeframe.
4. Describe background's spatial, spectral, and temporal characteristics.
5. Describe target's spatial, spectral, and temporal characteristics.
6. Identify sensors available during timeframe.
7. Calculate P_{det} for each combination of sensor, target, and background using Equations 10 or 24. (See Appendices C and G)
8. Discard all combinations with $P_{det} = 0$.
9. Go to mission checklist.

Checklist 2 -- Non-Cued Detection of Stationary Targets

1. Calculate P_{det} considering array geometry using Equations 26, 27, 28 and 29.
2. Partition area of interest into areas of common obscuration.
3. For each zone, target, background, and sensor calculate the P_{det*} using Equations 35 or 36.
4. Discard all combinations with $P_{det*} = 0$.
5. Calculate each combination's P_{dot1} using Equation 41.
6. Specify if the probability of detection is to be maximized or if the cost is to be minimized.
7. IF goal is to maximize P_{dsys}:
   A. Equation 42 used as objective function; and
   B. Equations 43, 44, 45 and specification that each area must return similar P_{dsys} make up the constraint set.
8. ELSE goal is to minimize cost:
   A. Equation 43 is the objective function; and
   B. Equations 42, 44, 45 and specification that each area must return similar P_{dsys} make up the constraint set.
9. Solve the linear program.

Checklist 3 -- Non-Cued Detection of Moving Targets

1. Calculate P_{det} considering array geometry using Equations 26, 27, 28 and 29.
2. Partition area of interest into areas of common obscuration.
3. For each zone, target, background, and sensor calculate the P_{det*} using Equations 35 or 36.
4. Discard all combinations with $P_{det*} = 0$.
5. Calculate each combination's P_{dot1} using Equation 41.
6. Specify if the probability of detection is to be maximized or if the cost is to be minimized.
7. IF goal is to maximize $P_{d\geq 1}$:
   - A. Equation 47 used as objective function; and
   - B. Equations 43, 45 and specification that each area must return similar $P_{d\geq 1}$ make up the constraint set.
   - C. Solve using non-linear programming.
8. ELSE goal is to minimize cost:
   - A. Equation 43 is the objective function; and
   - B. Equations 45, 47 and specification that each area must return similar $P_{d\geq 1}$ make up the constraint set.
   - C. Solve using non-linear programming.

Checklist 4 -- Cued Detection of Stationary Targets

1. Identify sensors which will have imaging opportunity in timeframe.
2. Calculate P_{det} considering array geometry using Equations 26, 27, 28 and 29.
3. Calculate P_{det^*} using Equations 35 or 36.
4. Specify if the probability of detection is to be maximized or if the cost is to be minimized.
5. IF goal is to maximize $P_{d\geq 1}$:
   A. Equation 48 used as objective function; and
   B. Equations 43, and 45 make up the constraint set.
   C. Solve using non-linear programming.
6. ELSE goal is to minimize cost:
   A. Equation 43 is the objective function; and
   B. Equations 45, and 48 make up the constraint set.
   C. Solve using non-linear programming.

Checklist 5 -- Second Contact

1. Determine longitude and time of crossing of last known target latitude for all sensors throughout timeframe.
2. Determine if overlap of swath and possible target area overlap using Equation 53. (or see Appendix E)
3. Calculate P_{det} considering array geometry using Equations 26, 27, 28 and 29.
4. Calculate P_{det*} using Equations 35 and 36.
5. Discard options with $P_{det*} = 0$.
6. IF sensor is Landsat 5 or SPOT 1:
   A. See Appendix F to determine P_{trkcon}.
   ELSE
   A. Determine value of Y using Equations 54 and 55.
   B. IF Y < half the swath width of the sensor:
      1. Determine A_{SWC} using Equations 57, 58, 59, 60, 61, 62, 63 and 64.
      2. Determine A_{pos} using Equation 73.
      ELSE Y > half the sensor's swath width:
      1. Determine A_{SWC} using Equations 65, 66, 67, 68, 69, 70, 71 and 72.
      2. Determine A_{pos} using Equation 73.
      ALWAYS
      3. Determine P_{trkcon} using Equation 74.
7. Determine P_{tim} using Equation 75.
8. Determine P_{track1} using Equation 76.
9. IF available swaths do not overlap:
   A. Specify if P_{track} to be maximized or cost minimized.
   B. IF P_{track} to be maximized:
      1. Equation 77 is the objective function.
      2. Equations 78 and 79 are the constraint set.
   C. IF cost to be minimized:
      1. Equation 78 is the objective function.

2. Equations 77 and 79 are the constraint set.

D. Solve using linear programming.

10. IF available swaths do overlap:

A. Specify if P_{track} to be maximized or cost minimized.

B. IF P_{track} to be maximized:

1. Equation 81 is the objective function.

2. Equations 82 and 83 are the constraint set.

3. Solve using non-linear programming.

C. IF cost to be minimized:

1. Equation 82 is the objective function.

2. Equations 81 and 83 are the constraint set.

3. Solve using non-linear programming.

Checklist 6 -- Follow-on Contact

1. Determine longitude and time of crossing of last known target latitude for all sensors throughout timeframe.
2. Determine earliest target penetration of swath and swath transit time using Equations 84 and 85.
3. Identify all imaging opportunities in timeframe.
4. Calculate P_{det*} using Equations 35 and 36.
5. Specify if $P_{d\geq 1}$ to be maximized or cost minimized.
   A. IF $P_{d\geq 1}$ to be maximized:
      1. Equation 86 is the objective function.
      2. Equations 87 and 88 are the constraint set.
      3. Solve using non-linear programming.
   B. IF cost to be minimized:
      1. Equation 87 is the objective function.
      2. Equations 86 and 88 are the constraint set.
      3. Solve using non-linear programming.

Bibliography

1. Ahmed, S. and others. "RADARSAT -- Canada's First Earth Observation Satellite," Canadian Aeronautics and Space Journal, 34: 4-12 (1988).

2. Allen, P.G. "Real Time Revisited," Airborne Reconnaissance IX, edited by F. LaGesse and P. Henkel. Proc. SPIE 561, 141-148 (1986).

3. Archer, P. "SPOT Data Distribution," Spaceflight, 28: 362-364 (Sep/Oct 1986)

4. Astronomical Almanac for 1986, edited by C. Roberts and A. Boksenberg. Washington: Government Printing Office, 1985.

5. Bartolucci, L.A. and others. "Atmospheric Effects on Landsat TM Thermal IR Data," IGARSS '87 Remote Sensing: Understanding the Earth as a System, edited by M. Dobson. New York: IEEE Press, 1988.

6. Begni, G. and others. "Results of SPOT 1 Images: Quality Assessment Program," Space: New Opportunities for All People, edited by L. Napolitano. Acta Astronautica, 207-212 (1987).

7. Bernstein, R. "Remote Sensing from Space: An Overview," Space Science and Applications: Progress and Potential, edited by J.H. McElroy. New York: IEEE Press, 1986.

8. Bescond, P. "The SPOT Program: Commercialization of Remote Sensing," IGARSS '87 Remote Sensing: Understanding the Earth as a System, edited by M. Dobson. New York: IEEE Press, 1988.

9. Bodin, P. and J-F. Reulet. "A New Channel for SPOT Satellite in the SWIR Band," Focal Plane Arrays: Technology and Applications, edited by Jean-Pierre Chartard. Proc. SPIE 865, 142-149 (1987).

10. Burrows, W.E. Deep Black, Space Espionage and National Security. New York: Random House, 1986.

11. Campbell, J.B. Introduction to Remote Sensing. New York and London: The Guilford Press, 1987.

12. Canada Relief Map (MCR 4097). The National Atlas of Canada (Fifth edition). Ottawa: Energy Mines and Resources Canada, 1986.

13. Canada Year Book 1978-79, edited by B.E. Pearson. Ottawa: The Bryant Press Limited, 1978.

14. Canadian Government Report. Satellites and Sovereignty. Ottawa: Canadian Government Publishing Centre 1977.

15. Carter, A.B. "Satellites and Anti-Satellites: The Limits of the Possible," International Security, 10: 46-98 (1986).

16. Chen, H.S. Space Remote Sensing: An Introduction. New York: Academic Press, Inc., 1985.

17. Cimino, J. and D. Held. "The Earth Observing System (EOS) Synthetic Aperture Radar (SAR)," Remote Sensing, edited by Robert T. Menzies. Proc. SPIE 644, 97-105 (1986).

18. Climatic Atlas Climatique -- Canada. AES Map Series 3. Ottawa: Canadian Government Publishing Centre, 1987.

19. Colwell, R. "Land Applications for Remote Sensing from Space," Space Science and Applications: Progress and Potential, edited by J.H. McElroy. New York: IEEE Press, 1986.

20. Courtois, M. "The SPOT Satellite System," Monitoring Earth's Ocean, Land, and Atmosphere from Space-- Sensors, Systems, and Applications. Volume 97, edited by Abraham Schnapf. New York: American Institute of Aeronautics and Astronautics, Inc., 1985.

21. Demathieu, P. "Localization, Mapping, Intelligence and Mission Planning with SPOT Data," Airborne Reconnaissance XI, edited by F. LaGesse, P. Henkel, and W. Schurter. Proc. SPIE 833, 3-6 (1987).

22. Devore, J.L. Probability and Statistics for Engineering and the Sciences (Second Edition). Monterey: Brooks/Cole Publishing Company, 1987.

23. Donohoe, M.J. and D. Vane. "Earth Resources Instrumentation for the Space Station Polar Platform," Remote Sensing, edited by Robert T. Menzies. Proc. SPIE 644, 76-81 (1986).

24. Doyle, F.J. "Paper 1. The Utility of Civil Remote Sensing Satellites for Arms Control Monitoring," Satellites for Arms Control and Crisis Monitoring, edited by B. Jasani and T. Sakata. New York: Oxford University Press, 1987.

25. Duchossois, G. "ERS-1: Mission Objectives and System Description," Monitoring Earth's Ocean, Land, and Atmosphere from Space--Sensors, Systems, and Applications. Volume 97, edited by Abraham Schnapf. New York: American Institute of Aeronautics and Astronautics, Inc., 1985.

26. Elachi, C. and others. "Remote Sensing of the Earth with Spaceborne Imaging Radars," Monitoring Earth's Ocean, Land, and Atmosphere from Space--Sensors, Systems, and Applications. Volume 97, edited by Abraham Schnapf. New York: American Institute of Aeronautics and Astronautics, Inc., 1985.

27. Engel, J. "The Land Satellite (Landsat) System Earth Observation Satellite Company (EOSAT's) Plans for Landsat-6 and Beyond," Earth Remote Sensing Using the Landsat Thematic Mapper and SPOT Sensor Systems, edited by P.N. Slater. Proc. SPIE 660, 169-174 (1986).

28. -----. "The Landsat Sensors: EOSAT's Plans for Landsat 6 and 7," Acta Astronautica, 15: 879-885 (1987).

29. Evans, H. Class handout distributed in PHYS 521, Space Surveillance. School of Engineering, Air Force Institute of Technology (AU), Wright-Patterson AFB OH, October 1987.

30. Fusco, L. and A. Hsu. "Different Scanning Instruments Comparison: MOMS and TM," Earth Remote Sensing Using the Landsat Thematic Mapper and SPOT Sensor Systems, edited by P.N. Slater. Proc. SPIE 660, 159-168 (1986).

31. Goetz, A. and M. Herring. "The High Resolution Imaging Spectrometer (HIRIS) for EOS," IGARSS '87 Remote Sensing: Understanding the Earth as a System, edited by M. Dobson. New York: IEEE Press, 1988.

32. Guignard, J.P. "ERS-1 Fast Delivery Processing and Products," IGARSS '86 Remote Sensing: Today's Solutions for Tomorrow's Information Needs, edited by T. Guyenne and J. Hunt. New York: IEEE Press, 1986.

33. Harris, R. Satellite Remote Sensing. London and New York: Routledge & Kegan Paul, 1987.

34. Herring, M. "Conceptual Design of the High Resolution Imaging Spectrometer (HIRIS) for EOS," Remote Sensing, edited by Robert T. Menzies. Proc. SPIE 644, 82-89 (1986).

35. Hord, R.M. Remote Sensing: Methods and Applications. New York: John Wiley & Sons, 1986.

36. Horikawa, Y. "Studies on Japanese Earth Resources Satellite 1," Monitoring Earth's Ocean, Land, and Atmosphere from Space--Sensors, Systems, and Applications. Volume 97, edited by Abraham Schnapf. New York: American Institute of Aeronautics and Astronautics, Inc., 1985.

37. Hussey, W.J. "The Economic Benefit of Operational Environmental Satellites," Monitoring Earth's Ocean, Land, and Atmosphere from Space--Sensors, Systems, and Applications. Volume 97, edited by Abraham Schnapf. New York: American Institute of Aeronautics and Astronautics, Inc., 1985.

38. Jane's Fighting Ships: 1987-1988, edited by J. Moore. New York, 1987.

39. Jasani, B. "Satellite Monitoring -- Programs and Prospects," Satellites for Arms Control and Crisis Monitoring, edited by B. Jasani and T. Sakata. New York: Oxford University Press, 1987.

40. Jasani, B. and P. Creasey. "Outer Space and International Security," RUSI Research Program Report.

41. Jensen, J.R. Introductory Digital Image Processing. New Jersey: Prentice-Hall, 1986.

42. Kasturirangan, K. "The Evolution of Satellite-Based Remote-Sensing Capabilities in India," Remote Sensing Yearbook 1986, edited by A. Cracknell and L. Hayes. London and Philadelphia: Taylor & Francis, 1986.

43. Konecny, G. "Alternatives for Mapping from Satellite Imagery," Acta Astronautica, 17: 355-358 (1988).

44. Kusanagi, M. and others. "Marine Observation Satellite MOS-1," Monitoring Earth's Ocean, Land, and Atmosphere from Space--Sensors, Systems, and Applications. Volume 97, edited by Abraham Schnapf. New York: American Institute of Aeronautics and Astronautics, Inc., 1985.

45. Langham, E.J. "RADARSAT--Canada's Program for Operational Remote Sensing," Canadian Journal of Remote Sensing, 8: 31-36 (July 1982).

46. -----. "RADARSAT Enters Phase B," Monitoring Earth's Ocean, Land, and Atmosphere from Space--Sensors, Systems, and Applications. Volume 97, edited by Abraham Schnapf. New York: American Institute of Aeronautics and Astronautics, Inc., 1985.

47. Langham, E.J. and others. "Canadian Plans for Operational Demonstration of Satellite Imaging Radar Applications," IGARSS '86 Remote Sensing: Today's Solutions for Tomorrow's Information Needs, edited by T. Guyenne and J. Hunt. New York: IEEE Press, 1986.

48. Lillesand, T. and R. Kiefer. Remote Sensing and Image Interpretation. New York: John Wiley & Sons, 1979.

49. Maeda, K. and others. "Geometric and Radiometric Performance Evaluation Methods for Marine Observation Satellite-1 (MOS-1) Verification Program (MVP)," Acta Astronautica, 15: 297-304 (1987).

50. Malila, W.A. "Components and Comparisons of Potential Information from Several Imaging Satellites," IGARSS '86 Remote Sensing: Today's Solutions for Tomorrow's Information Needs, edited by T. Guyenne and J. Hunt. New York: IEEE Press, 1986.

51. Markland, R.E. Topics in Management Science (Second Edition). New York: John Wiley & Sons, 1983.

52. Marshall, E. "A Spy Satellite for the Press ?," Science, 238: 1346-1348 (1987).

53. Matsumae, T. and others. "Paper 2. Technological Requirements of a Satellite Monitoring System," Satellites for Arms Control and Crisis Monitoring, edited by B. Jasani and T. Sakata. New York: Oxford University Press, 1987.

54. McElroy, J.H. "Earthview--Remote Sensing of the Earth from Space," Monitoring Earth's Ocean, Land, and Atmosphere from Space--Sensors, Systems, and Applications. Volume 97, edited by Abraham Schnapf. New York: American Institute of Aeronautics and Astronautics, Inc., 1985.

55. Molette, P. and J. Jouan. "JEOS: The JANUS Earth Observation Satellite," Acta Astronautica, 13: 607-621 (1986).

56. Mowle, E.W. "Landsat-D and -D'--The Operational Phase of Land Remote Sensing from Space," Monitoring Earth's Ocean, Land, and Atmosphere from Space--Sensors, Systems, and Applications. Volume 97, edited by Abraham Schnapf. New York: American Institute of Aeronautics and Astronautics, Inc., 1985.

57. Needham, B. "Operational Instruments on the Space Station -- Polar Platforms: Contributions by NOAA and the International Community," IGARSS '87 Remote Sensing: Understanding the Earth as a System, edited by M. Dobson. New York: IEEE Press, 1988.

58. Ohring, G. "NOAA Plans for Remote Sensing of the Earth, Oceans and Atmosphere," IGARSS '85 Remote Sensing Instrumentation: Technology for Science and Applications, edited by K. Carver. New York: IEEE Press, 1985.

59. Rajan, Y.S. "Remote Sensing Activities in India--Past, Present and Future," Monitoring Earth's Ocean, Land, and Atmosphere from Space--Sensors, Systems, and Applications. Volume 97, edited by Abraham Schnapf. New York: American Institute of Aeronautics and Astronautics, Inc., 1985.

60. Rajan, Y.S. and J. Ninan. "Remote Sensing--International Status and Trends," Remote Sensing Yearbook 1986, edited by A. Cracknell and L. Hayes. London and Philadelphia: Taylor & Francis, 1986.

61. Rao, U.R. and S. Chandreshekar. "An International Regime for Remote Sensing--Problems and Prospects," Remote Sensing Yearbook 1986, edited by A. Cracknell and L. Hayes. London and Philadelphia: Taylor & Francis, 1986.

62. Salomonson, V. and others. "MODIS: Advanced Facility Instrument for Studies of the Earth as a System," IGARSS '87 Remote Sensing: Understanding the Earth as a System, edited by M. Dobson. New York: IEEE Press, 1988.

63. Schnapf, A. "The TIROS Meteorological Satellites--Twenty-Five Years: 1960-1985," Monitoring Earth's Ocean, Land, and Atmosphere from Space--Sensors, Systems, and Applications. Volume 97, edited by Abraham Schnapf. New York: American Institute of Aeronautics and Astronautics, Inc., 1985.

64. Slater, P.N. Remote Sensing: Optics and Optical Systems. Reading: Addison-Wesley Publishing Company, Inc., 1980.

65. -----. "Survey of Multispectral Imaging Systems for Earth Observations," Remote Sensing of the Environment, 17: 85-102 (1985)

66. Sloup, G.P. "Arms Control Verification -- The Poor Person's Approach," Colloquium on the Laws of Outer Space. New York: AIAA, 1987.

67. Stares, P.B. Space and National Security. Washington, D.C.: The Brookings Institution, 1987.

68. Strahler, A.H. and others. "On the Nature of Models in Remote Sensing," Remote Sensing of the Environment, 20: 121-139 (1986)

69. Townshend, J. "The Spatial Resolving Power of Earth Resources Satellites: A Review," NASA-TM-82020, 1980.

70. TPRC Data Series 9: Thermal Radiative Properties: Coatings, edited by Y.S. Touloukian.

71. Watkins, A.H. and J.M. Thormodsgard. "Higher Resolution Satellite Remote Sensing and the Impact on Image Mapping," IAF International Astronautical Congress, 37th: 86-98 (1986).

72. Williams, C.P. "Space Remote Sensing," Spaceflight, 28: 359-360 (Mar 1986)

VITA

Major Bob Chekan was born on [redacted] He graduated from high school in [redacted] in 1972 and attended the University of Guelph and Carleton University. He completed his Bachelor of Science in Biology in May, 1977. Upon graduation he enrolled in the Canadian Armed Forces and was commissioned. He has served as an air weapons controller in North Bay, Ontario, and in Cold Lake, Alberta. He has served as a staff officer in Fighter Group Headquarters in North Bay from 1982 to 1987. In May 1987 Major Chekan entered the School of Engineering, Air Force Institute of Technology.

[redacted]

REPORT DOCUMENTATION PAGE

Form Approved
OMB No. 0704-0188

1a. REPORT SECURITY CLASSIFICATION Unclassified	1b. RESTRICTIVE MARKINGS
2a. SECURITY CLASSIFICATION AUTHORITY	3. DISTRIBUTION/AVAILABILITY OF REPORT Approved for public release; distribution unlimited.
2b. DECLASSIFICATION/DOWNGRADING SCHEDULE	
4. PERFORMING ORGANIZATION REPORT NUMBER(S) AFIT/GSO/ENS/88D-4	5. MONITORING ORGANIZATION REPORT NUMBER(S)
6a. NAME OF PERFORMING ORGANIZATION School of Engineering 6b. OFFICE SYMBOL (If applicable) AFIT/ENS	7a. NAME OF MONITORING ORGANIZATION
6c. ADDRESS (City, State, and ZIP Code) Air Force Institute of Technology Wright-Patterson AFB, Ohio 45433-6583	7b. ADDRESS (City, State, and ZIP Code)
8a. NAME OF FUNDING/SPONSORING ORGANIZATION 8b. OFFICE SYMBOL (If applicable)	9. PROCUREMENT INSTRUMENT IDENTIFICATION NUMBER
8c. ADDRESS (City, State, and ZIP Code)	10. SOURCE OF FUNDING NUMBERS PROGRAM ELEMENT NO. / PROJECT NO. / TASK NO / WORK UNIT ACCESSION NO.

11. TITLE (Include Security Classification)
USE OF COMMERCIAL SATELLITE IMAGERY FOR SURVEILLANCE OF THE CANADIAN NORTH BY THE CANADIAN ARMED FORCES

12. PERSONAL AUTHOR(S)
Robert J. Chekan, Maj CAF

13a. TYPE OF REPORT	13b. TIME COVERED	14. DATE OF REPORT (Year, Month, Day)	15. PAGE COUNT
MS Thesis	FROM _____ TO _____	1988, DEC	261

16. SUPPLEMENTARY NOTATION

17. COSATI CODES			18. SUBJECT TERMS (Continue on reverse if necessary and identify by block number)
FIELD	GROUP	SUB-GROUP	Satellite Photography, Images, Space Surveillance Systems
08	02		

19. ABSTRACT (Continue on reverse if necessary and identify by block number)

This thesis examines the utility of commercial satellite-acquired imagery for the surveillance of the Canadian North. Analytical performance models are developed for visible and thermal wavelength sensors. These models form the basis for evaluation of an individual sensor's potential contribution to surveillance. The mission of surveillance is sectioned into five separate missions. For each mission, sensor system evaluation algorithms, which combine individual sensor's probabilities of detection and tracking, are proposed and optimization techniques identified. Sample algorithms, using a representative target set, are provided for each mission. Analysis shows that the selection of specific sensors is mission and situation specific.

20. DISTRIBUTION/AVAILABILITY OF ABSTRACT	21. ABSTRACT SECURITY CLASSIFICATION
☒ UNCLASSIFIED/UNLIMITED ☐ SAME AS RPT. ☐ DTIC USERS	Unclassified
22a. NAME OF RESPONSIBLE INDIVIDUAL LtCol J. Robinson, Phd.	22b. TELEPHONE (Include Area Code) (513) 255-3362 22c. OFFICE SYMBOL AFIT/ENS